MATRIX-ASSISTED LASER DESORPTION/IONIZATION TIME-OF-FLIGHT MASS SPECTROMETRY FOR CHARACTERIZING PROANTHOCYANIDINS: AUTHENTICITY, STANDARDIZATION, AND EFFICACY

by

Daniel Alfredo Esquivel Alvarado

a dissertation submitted in partial fulfillment of the requirements for the degree of

Doctor of Philosophy

(Food Sciences)

at the

UNIVERSITY OF WISCONSIN-MADISON

2020

Date of final oral examination: 10/23/2020

The dissertation is approved by the following members of the Final Oral Committee:

Jess D. Reed, Ph.D., Professor, Animal Science, Food Science
Bradley W. Bolling, Ph.D., Associated Professor, Food Science
Jan Peter van Pijkeren, Ph.D., Assistant Professor, Food Science
Martha M. Vestling, Ph.D., Senior Scientist, Chemistry

A Dios,

A mi madre Daisy Alvarado Porras

y mi padre Alfredo Esquivel Rivera (q.e.p.d.)

ACKNOWLEDGMENTS

I would like to express my deep and sincere gratitude to my advisor Prof. Jess D. Reed, for giving me the opportunity to conduct research in his group and providing invaluable guidance during my doctoral studies. Also, I would like to thank Prof. Reed for his friendship, empathy, patience, and support during these years. Prof. Reed is one of the most important scientists in polyphenol science, and his knowledge is immeasurable. It was a great privilege and honor for me to work and learn from him. Prof. Reed taught me to think, write, and work as a scientist, and for this, I always will be thankful. From Prof. Reed, I admire his curiosity, creativity, vision, skilled oratory, and problem-solving personality, that have inspired me to become a better scientist. In addition, I am always going to be grateful to Dr. Reed for helping improve my English. I will miss the conversations in his office talking about science and consistently encouraging me to think. However, I blame myself for not taking those opportunities that Prof. Reed offered me to talk about science earlier in my doctoral studies. Thank you for everything; you pushed me to become a better person and scientist.

Thanks to Christian G. Krueger, who always gave me positive inputs during these years in the Reed Research Group. The knowledge of Mr. Krueger of business management helped me think outside academia. Mr. Krueger taught me how to think like an entrepreneur and the opportunities that might arise from an idea. I appreciate that Mr. Krueger always had his office doors open for when I needed advice. I will always be grateful for your friendship.

I must also give thanks to Mr. Michael A. Polewski. It was a great pleasure working with you and I appreciate your ideas, help, and good humor. I appreciate that Mr. Polewski always helped me proof-read my manuscripts. Mr. Poleswki supported me during these years, he was like a psychologist to me. The long

hours talking about science, family, and sports, amongst others, were invaluable to me. Mike, Mike, Mike, Mike, Mike. Mi gringo favorito ☺.

I would like to thank my dissertation committee. Dr. Martha M. Vestling, Dr. Bradley W. Bolling, and Dr. Jan Peter van Pijkeren, who have each provided helpful feedback and have been great professors. Special thanks to Dr. Vestling for allowing me to use the mass spectrometers at the Chemistry Building. Dr. Vestling always had a smile, greeting, and a positive comment when I arrived at her laboratory. I really appreciate that Dr. Vestling never had no as a respond when I asked for a training on her instruments. The help provide by Dr. Vestling was invaluable for the development of this dissertation.

I also want to thank my friends Dr. Gerardo Rodríguez Rodríguez and Dr. Sergio Madrigal Carballo. Both Dr. Rodriguez and Dr. Madrigal were a very important pillars in my beginnings as researcher. They showed me the fascinating world of the phytochemistry and polyphenols. I really thank the opportunity that Dr. Rodriguez gave me to work at Phytochemistry Laboratory, and subsequently, the opportunity that Dr. Madrigal gave me to work at National Center for Biotechnological Innovations. I never will forget our soccer games in Costa Rica (Gerardo and Sergio) and USA (Sergio). I love you guys.

I would like to thank the undergraduate students from the Reed Research Group, whose assisted me during my dissertation research; Tommy Ollmann, Turner Schmidt, Nicholas Wedde, Pilar Gonzalez, Erica Gullickson, and Roberto Sapienza.

A mis amigos Omar Iván Santana, Jorge Barrientos Blanco, Liliana Fadul Pacheco, Andrey Vega Alfaro y Mariola Grez Capdeville. No puedo expresar el agradecimiento que tengo con todos ustedes. Cada una de las conversaciones que tuvimos fueron un aprendizaje. Ustedes hicieron mi vida mas fácil al distraerme de mis labores curriculares. De ustedes voy a recodar las largas charlas hablando de rumiantes (hasta entendí que los cuatro estomagos de las vacas no son cutro estomagos individuales), los asados, y los juegos de mesa. Se les va a extrañar.

A mi compañera de aventuras Emilia Alfaro Viquez. Se que para ambos esta aventura no fue fácil pero juntos pudimos superarlo con creces. Gracias por su apoyo incondicional. Durante estos años fuiste mi soporte, muchas de las técnicas que se usted me las enseño. Eso si tuve que soportar sus berrinches, no todo es color de rosas.

Quiero expresar mi agradecimiento al Ministerio de Ciencia, Tecnología y Telecomunicaciones (MICITT), al Programa de Innovación y Capital Humano (PINN), y al Consejo Nacional para Investigaciones Científicas y Tecnológicas (CONICIT) por la beca otorgada según el contrato PED-056-2015-I.

TABLE OF CONTENTS

LIST OF FIGURES

APPENDIX I

LIST OF TABLES

CHAPTER 1

CHAPTER 3

LIST OF ABBREVIATIONS

Numbers	
^{1}H	Proton
^{13}C	Carbon-13
1D	One-dimensional
2D	Two-dimensional
A	
a-PAC	apple proanthocyanidins
ACS	American Chemical Society
AOAC	Association of Official Analytical Chemists
A_{max}	Maximum absorbance
ATR-FTIR	Attenuated total reflectance Fourier transform infrared
C	
c-PAC	cranberry proanthocyanidins
C3G	Cyanidin-3-glucoside
CFU	Colony-forming unit
CIN	cinnamaldehyde
CON	4-hydroxy-3-methoxycinnamaldehyde
CONICIT	National Council for Scientific and Technology Research
CPS	Complete Phytochemical Solutions
D	
DD	Double distilled
DHB	2,5-dihydroxybenzoic acid
DIC	Differential interference contrast

DM	Dry matter
DMAC	4-(dimethylamino)cinnamaldehyde
DP	Degree of polymerization
DPPH	2,2-diphenyl-1-picrylhydrazyl
DTAF	5-([4,6-dichlorotriazin-2-yl]amino)fluorescein
	E
ESI	Electrospray ionization
ExPEC	Extra-intestinal pathogenic *Escherichia coli*
	G
GAE	Gallic acid equivalent
GFP	Green fluorescent protein
	H
HCl	Hydrochloric acid
HILIC	Hydrophilic interaction liquid chromatography
$HorRat_R$	Hortwitz ratio
HPLC	High-performance liquid chromatography
HRMS	High-resolution mass spectrometry
	I
IAA	*trans*-3-indolacrylic acid
	K
KDa	Kilodalton
	L
LDA	Linear discriminant analysis
LOOCV	Leave-one-out cross-validation

LOQ	Limit of quantification
LSD	Least significant difference
	M
m/z	Mass-to-charge
MALDI	Matrix-assisted laser desorption/ionization time-of-flight
MICITT	Ministry of Science, Technology, and Telecommunications
MS	Mass spectrometry
	N
NMR	Nuclear magnetic resonance
NOE	Nuclear overhauser effect
NP-	Normal-phase
	P
p-PAC	peanut skins proanthocyanidins
PAC	Proanthocyanidins
PC	Procyanidin
PCA	Principal component analysis
PCPP	Proanthocyanidin-cinnamaldehyde pyrylium products
PD	Prodelphinidin
PINN	Innovation and Human Capital Program for Competitiveness
PPO	Polyphenol oxidase
ProA2	procyanidin A2
ProB2	procyanidin B2

	Q
QE	Quercetin equivalent
	R
RP-	Reverse-phase
RSD_r	Relative standard deviation of repeatability
	S
s-PAC	Soluble proanthocyanidins
S/N	Signal-to-noise
SEM	Scanning electron microscopy
SIN	4-hydroxy-3,5-dimethoxycinnamaldehyde
SMPR	Standard method performance requirements
	T
T1	Spin-lattice
TAC	Total anthocyanin content
TFC	Total flavonoid content
TMS	tetramethylsilane
TOL	4-methylcinnamaldehyde
TPC	Total polyphenol content
TVS	Tropical *Vaccinium* species
	U
UHPLC	Ultra-high-performance liquid chromatography
USDA	United States Department of Agricultural
UTI	Urinary tract infection
UW	University of Wisconsin-Madison

ABSTRACT

Cranberry (*Vaccinium macrocarpon* Aiton) is a native fruit crop of northeastern North America. In 2017, cranberry production in the United States was estimated at $251 million, resulting in annual sales of fresh and marketed cranberry products that exceeded $3.5 billion dollars. These sales come as a result of the putative health benefits associated with the consumption of cranberry products, specifically the proanthocyanidins (PAC) with A-type interflavan bonds. This increased demand for healthy products on the part of consumers combined with the expensive cost of cranberry compared to other botanical sources and lack of regulatory policies on the part of the Food and Drug Administration (FDA) have resulted in unethical manufacturers to adulterate cranberry products. The lack of standardization and authentication undermines the market of cranberry products and erodes consumer confidence and the perception of health benefits. For this reason, there is a need for rapid, precise, and accurate analytical methods capable of providing reliable quantification and characterization of cranberry proanthocyanidins (c-PAC). However, current analytical methods used by the industry are obsolete and time-consuming. Thus, cranberry products marketed to consumers may lack A-type PAC, contain lower quantities, or contain adulterants, which results in ineffective products.

In this dissertation, c-PAC standard isolated from cranberry fruit, which reflects the structural heterogeneity and complexity of PAC, was used for an inter-laboratory validation of 4-(dimethylamino)cinnamaldehyde (DMAC) assay for quantification of soluble PAC (**Chapter 1**). Commercial standards such as procyanidin A2 and B2 lead to an underestimation of the PAC content because the heterogeneity and complexity of PAC are not reflected in these commercial

standards. c-PAC exists not only as simple oligomers or polymers of flavan-3-ols but also contains anthocyanin-flavan-3-ol oligomers, which may introduce analytical error due to the change in the stoichiometry and kinetics of reaction. Results indicate that the use of both procyanidin A2 and c-PAC standards meets the standard method performance requirements (SMPR) 2017.003 established by the Association of Official Analytical Chemist (AOAC). Nevertheless, the use of procyanidin A2 standard underestimates the PAC content by at least 3.14-fold compared to c-PAC standard. Despite the DMAC assay providing reliable information on the PAC content, it is not selective and does not differentiate between A- and B-type interflavan bonds. Thus, a complementary technique such as matrix-assisted laser desorption/ionization time-of-flight mass spectrometry (MALDI-TOF MS) that differentiates A- and B-type interflavan bonds is needed.

MALDI-TOF MS has demonstrated that the structural heterogeneity and complexity of PAC can be characterized without the problem arising from the formation of multiply charged molecular ions that occurs when electrospray ionization mass spectrometry (ESI-MS) is used. Spectra analysis is less cumbersome in MALDI-TOF MS compared to ESI-MS, because this technique detects single-charged molecular ions. MALDI-TOF MS and the deconvolution method were used for identifying A-type PAC in cranberry products from other botanical sources containing B-type PAC (**Chapter 2**). Results indicate that both MALDI-TOF MS and the deconvolution method were able to identify the presence of A-type PAC in cranberry products from other botanical sources with a probability greater than 90% and a confidence of 95%. Classification models can be built based on the percentage of A- and B-type PAC because deconvolution of the overlapping

isotope pattern of MALDI-TOF MS spectra determines the percentage of A- and B-type PAC at each degree of polymerization (DP).

The growing demand for cranberry products and the lack of policies by regulatory organizations has caused some companies to adulterate their cranberry products with cheaper sources of PAC. MALDI-TOF MS spectra data combined with multivariate analysis was used to build classification models capable of determining authenticity in mixtures of c-PAC with apple-PAC (a-PAC) or peanut skins-PAC (p-PAC) (**Chapter 3**). Results indicate that MALDI-TOF MS spectra data combined with principal component analysis (PCA) and linear discriminant analysis (LDA) offer the possibility to differentiate and to discriminate amongst sources of PAC. The method is able to determine the adulteration of mixtures of c-PAC with a-PAC or p-PAC, within 5% (w/w) with a confidence level of 95%. Overall, our two previous studies demonstrated that MALDI-TOF MS has the capability to characterize PAC from different botanical sources.

Previous studies have indicated that 96% of PAC from *V. macrocarpon* contain one or more A-type interflavan bonds. However, the *Vaccinium* genus contains about 450 species, most of which have unknown PAC composition. The PAC composition from three tropical *Vaccinium* species (*V. consanguineum*, *V. floribundum*, and *V. poasanum*) from Costa Rica were characterized by MALDI-TOF MS, nuclear magnetic resonance (NMR), and attenuated total reflection Fourier transform infrared spectroscopy (ATR-FTIR) (**Chapter 4**). Results indicate that PAC from the three tropical *Vaccinium* species are mainly composed of procyanidins with a *cis* configuration. In

addition, results indicate that B- and not A-type interflavan bonds are the predominant bonds but greater than 74% of the oligomer contain one or more A-type interflavan bonds.

As previously mentioned, PAC analysis is constrained by the lack of analytical methods. In addition, an understanding of the interaction between PAC and their putative health benefits is still lacking. Previously, PAC was fluorescently labeled with 5-([4,6-dichlorotriazin-2-yl]amino) fluorescein (DTAF). However, auto-fluorescence at the excitation wavelength of fluorescein creates difficulties in distinguishing signal-to-noise in fluorescent microscopy using DTAF tagged PAC. We were able to synthesis PAC with cinnamaldehyde and four cinnamaldehyde derivatives, which produced fluorescent proanthocyanidins-cinnamaldehydes pyrylium products (PCPP) for microscopic detection of interaction with extra-intestinal pathogenic *Escherichia coli* (**Chapter 5**). Synthesized PCPP were detected and characterized by MALDI-TOF MS. Fluorescent microscopy showed that PCPP exhibited higher excitation and emission wavelengths than PAC and each cinnamaldehyde condensation product exhibited different fluorescent properties, providing a useful tool to trace the fate of PAC and study the interaction between PAC and their putative health benefits.

Overall, this dissertation presents research on the development and use of analytical tools to quantify and characterize PAC that help solve problems associated with the lack of authenticity, standardization, and efficacy of products from cranberries and other sources of PAC.

KEYWORDS

Proanthocyanidins (PAC); A- and B-type interflavan bonds; 4-(dimethylammino)cinnamaldeyde (DMAC); matrix-assisted laser desorption/ionization time-of-flight mass spectrometry (MALDI-TOF MS); electrospray ionization mass spectrometry (ESI-MS); degree of polymerization (DP); fluorescence, extra-intestinal pathogenic *Escherichia coli* (ExPEC).

INTRODUCTION

Overview

Cranberry (*Vaccinium macrocarpon* Aiton) is one of the most popular fruits in North America. The putative active compounds in cranberries are proanthocyanidins (PAC), specifically PAC with A-type interflavan bonds. Consumption of cranberry PAC is associated with preventing recurrent urinary tract infections and relieving associated symptoms. Because of the health benefits associated with cranberry, there is a growing demand for cranberry products such as botanical dietary supplements, sweetened fruit, and juices. However, the continued demand for cranberry products and the high price of cranberry raw material compared to other botanical sources containing PAC has caused unscrupulous companies to adulterate cranberry for economic reasons, which has become a challenge for regulatory organizations in the monitoring and compliance of quality control and manufacturing. Recent works have reported the existence of cranberry products that are mislabeled, contaminated, and adulterated with dangerous and unknown components. Thus, robust, precise, and accurate analytical methods are needed to authenticate and standardize cranberry products and provide reliable information to consumers.

Cranberry

Cranberry is a native fruit of northeastern North America that belongs to the *Ericaceae* family. Cranberry is a perennial trailing woody vine that grows in acidic, sandy bogs, swamps, shorelines, and streambanks. Cranberry blooms during June and July and is harvested from mid-September to early-November (Sinha, Sidhu, Barta, Wu, & Cano, 2012). Cranberries are harvested using two

methods: dry and wet harvesting. Dry harvesting is the method used to harvest firm cranberries that are sold as fresh fruit, while wet harvesting is used for cranberries that are sold for producing processed foods. Because cranberries have an acidic taste, 95% of cranberries are processed to produce juices, jam, jellies, and purees, amongst other processed foods, and the remaining 5% are consumed as fresh fruit (USDA, 2020a).

In 2018, the worldwide production of cranberries accounted for 722,683 metric tons, of which the United States was the leading producer with 56%, followed by Canada with 27%, and Chile with 15% of the total global production (FAO, 2020). According to the National Agricultural Statistics Service of the United States Department of Agricultural (USDA), in 2017, the national production of cranberry was 377,434 metric tons. This cranberry crop was valued at $251 million dollars (USDA, 2020b), producing annual sales of fresh and marketed cranberry products that exceeded $3.55 billion dollars (USDA, 2017). In the United States, Wisconsin is the leading producer with 64%, followed by Massachusetts with 23% of the national production of cranberry (USDA, 2020b).

Cranberries are sources of vitamins, essential amino acids, minerals, organic acids, sugars, dietary fibers, and phenolic compounds (Dorofejeva, Rakcejeva, Kviesis, & Skudra, 2011; Phillips, Pehrsson, Agnew, Scheett, Follett, Lukaski, et al., 2014; Llorent-Martínez, Spínola, & Castilho, 2017; Nemzer, Vargas, Xia, Sintara, & Feng, 2018). There is substantial interest in cranberries because of the composition of phenolic compounds. Specifically, proanthocyanidins (PAC), a group of phenolic compounds in the flavonoid family, because of their putative health benefits.

Previous studies suggest that PAC prevent urinary tract infections, decrease the risk of cardiovascular, gastrointestinal, and kidney diseases, improve the gut mucus layer morphology and homeostasis, and demonstrate anticancer activities in colon, prostate, ovaries, and lung cancer cell lines, amongst others (Porter, Krueger, Wiebe, Cunningham, & Reed, 2001; Pierre, Heneghan, Feliciano, Shanmuganayagam, Roenneburg, Krueger, et al., 2013; Feliciano, Meudt, Shanmuganayagam, Krueger, & Reed, 2014; Weh, Clarke, & Kresty, 2016; Joshi, Howell, & D'Souza, 2016; de Almeida Alvarenga, Borges, Moreira, Teixeira, Carraro-Eduardo, Dai, et al., 2019).

Phenolic compounds

Phenolic compounds are a diverse and bioactive category of secondary metabolites that play an essential role in the human diet due to their biological properties. Quideau et al., (2011) indicated that the terms "phenolic compounds" and "polyphenolic compounds" should be used to define secondary metabolites derived from the shikimate-derived phenylpropanoid, and/or the polyketide pathways (Quideau, Deffieux, Douat-Casassus, & Pouysegu, 2011). Polyphenolic compounds are composed of more than one benzene ring and devoid of any nitrogen-based functional group, whereas phenolic compounds are composed of one benzene ring bearing one or more hydroxyl groups, as well as, naturally derivatives such as methyl phenyl ether and *O*-phenyl glycosides (Quideau, Deffieux, Douat-Casassus, & Pouysegu, 2011).

Flavonoids are the largest group of naturally-occurring plant polyphenolic compounds, which are found both as glycosides or aglycones. Flavonoids are biosynthesized by the phenylpropanoid pathway, transforming phenylalanine into *p*-coumaroyl-CoA. Following this transformation, one molecule of *p*-coumaroyl-CoA is condensed with three molecules of malonyl-CoA to produce chalcone through a chalcone synthase. Next, chalcone is isomerized by chalcone flavanone isomerase to flavanone (Winkel-Shirley, 2002). From this flavanone skeleton, the pathway diverges into seven groups, according to differences in the pyran ring. These groups are flavones (e.g. luteolin), isoflavones (e.g. genistein), flavonols (e.g. fisetin), flavanones (e.g. butin), flavanonols (e.g. taxifolin), anthocyanidins (e.g cyanidin), and flavanols (e.g. catechin) (**Figure 1**). Flavonoids have two aromatic rings (A- and B-ring), joined by a three-carbon bridge, in the form of a heterocyclic ring (C-ring), which results in 15-carbons, sharing a common C_6-C_3-C_6 skeleton.

Flavones (**1**), the first group, contain an oxo group at C_4, a double bond between C_2 and C_3, and the B-ring attached to C_2. Flavones, which are predominant in herbs and vegetables and in some fruits, include apigenin, luteolin, chrysin, and their glycosides. The second group, isoflavones (**2**), is structurally similar to flavones, but the B ring is attached to C_3 instead of C_2. Isoflavones, which are abundant in soybeans and soy products and in a lesser amount in legumes and beans, include daidzein, genistein, and biochanin A. The third group, called flavonols (**3**), is similar to flavones but contains a hydroxyl group at C_3. Flavonols, which are the most abundant in fruits and vegetables, include kaempferol, myricetin, and quercetin. The fourth and fifth groups, flavanones (**4**) and flavanonols (**5**), do not present the double bond between C_2 and C_3. Flavanones differ from

flavanonols because the latter contains a hydroxyl group at C_3. Thus, flavanones present only one chiral center on the C-ring leading two diastereoisomers, while flavanonols present two chiral centers on the C-ring leading four diastereoisomers. Both flavanones and flavanonols, which are not abundant in nature compared to other flavonoids, include butin, naringenin, hesperetin, taxifolin, and aromadendrin. The sixth group, called anthocyanidins (**6**), does not contain the oxo group at C_4, but possesses two double bonds in the C-ring, a hydroxyl group attached to C_3, the B-ring attached to C_2, and a positive charge, which produces the resonant structures of the flavylium ion.

Anthocyanidins are the aglycone form of anthocyanins. Anthocyanins are water-soluble pigments responsible for the color of flowers, fruits, and vegetables, amongst others. There are at least 31 anthocyanidins, but the six most common are cyanidin, delphinidin, malvidin, pelargonidin, peonidin, and petunidin. Finally, the seventh group, flavanols (flavan-3-ols) (**7**), does not contain the oxo group at C_4 and double bonds in the C-ring but possesses a hydroxyl group attached to C_3 and the B-ring attached to C_2. Thus, flavanols present two chiral centers in the C-ring leading to four diastereoisomers. For instance, the chiral center at C_3 results in two isomers called catechin and epicatechin. The most common flavanols are (epi)-catechin, (epi)-afzelechin, (epi)-gallocatechin, and their gallates. In addition, flavan-3-ols can link to each other to form oligomeric or polymeric structures called PAC.

Proanthocyanidins

Chemistry

Proanthocyanidins (PAC) are oligomeric and polymeric structures composed of repeating flavan-3-ol monomers (polyflavan-3-ols), while 3-deoxyproanthocyanidins are oligomeric and polymeric structures composed of repeating flavan monomers (polyflavan) (Gujer, Magnolato, & Self, 1986; Reed, Krueger, & Vestling, 2005). PAC constitute one of the most ubiquitous polyphenolic groups in plants; however, the exact mechanism of how PACs are biosynthesized is uncertain. There are two hypotheses claiming that PAC are biosynthesized by an enzymatic pathway or by a stereospecific nucleophilic condensation mechanism. Nevertheless, enzymes that catalyze the polymerization reaction of PAC have not been detected. Hence, the stereospecific nucleophilic condensation mechanism is the most accepted hypothesis, although this hypothesis also fails in the stereochemistry of the extension unit. For instance, polymerization of PAC involves a reaction through an electrophilic attack of the C_4 of an extension unit (2,3-*trans* leucoanthocyanidin) to a nucleophilic carbon C_6 or C_8 of a terminal unit (flavan-3-ol). However, the problem is that majority of extension units in PAC are 2,3-*cis* but leucoanthocyanidins are 2,3-*trans* (Stafford, 1990; Oliveira, Mateus, & de Freitas, 2013). PAC are structurally differentiated according to the patterns of hydroxylation of the flavan-3-ol (A and B-ring), the nature of the interflavan bonds (A- versus B- type), the stereochemistry (*R*, *S*) at the C_2 and C_3 positions, the substituents at the C_3 and C_5 positions, and the degree of polymerizations (DP) (Monagas, Quintanilla-Lopez, Gomez-Cordoves, Bartolome, & Lebron-Aguilar, 2010; Wang, Singh, Hurst, Glinski, Koo, & Vorsa, 2016).

Based on the patterns of hydroxylation of the flavan-3-ol, PAC are classified into at least sixteen classes (Bladé, Arola-Arnal, Crescenti, Suárez, Bravo, Aragonès, et al., 2017). However, this classification implies that PAC are composed of homo-oligomers, whereas in nature, PAC are composed of hetero-oligomers. Therefore, caution should be exercised when it comes to PAC composition. Amongst these classes, the most abundant PAC that occur naturally are procyanidins, propelargonidins, and prodelphinidins, named after the resulting anthocyanidin from the acid depolymerization of PAC, proposed by Bate-Smith (Hummer & Schreier, 2008). For instance, after acid depolymerization of a PAC sample and subsequent analysis by reversed-phase high performance liquid chromatographic electrospray ionization mass spectrometry (RP-HPLC-ESI-MS), procyanidins which are oligomers of (epi)catechin yield cyanidin, propelargonidins which are oligomers of (epi)afzelechin yield pelargonidin, and prodelphinidins which are oligomers of (epi)gallocatechin yield delphinidin.

PAC are also classified based on the nature of the interflavan bonds, such as A- or B-type. PAC containing single interflavan bonds through C_4-C_8 or C_4-C_6 are called B-type PAC, whereas PAC containing an additional interflavan bond linked through C_2-O-C_7 bonds or C_2-O-C_5 are called A-type PAC (**Figure 2**) (Foo, Lu, Howell, & Vorsa, 2000). The additional interflavan bond, in addition to the structural difference, confers a difference in the molecular weight due to the loss of two mass units. Likewise, the additional interflavan bond confers conformational rigidity to PAC, which in turn may play a role in increasing extra-intestinal pathogenic *Escherichia coli* (ExPEC) agglutination and decreasing ExPEC epithelial cell invasion (Feliciano, Meudt, Shanmuganayagam, Krueger, & Reed, 2014). A-type PAC are less abundant in nature than B-type

PAC. Gu, et al., (2003) indicated that A-type PAC are found in fruits, legumes, and spices such as plums, cranberries, avocados, peanut skins, curry, and cinnamon (Gu, Kelm, Hammerstone, Beecher, Holden, Haytowitz, et al., 2003). Kondo et al., (2000) and Tanaka et al., (2000) described that B-type dimers are converted to A-type dimers in an alkaline/hydrogen peroxide medium and in presence of a stable radical such as 2,2-diphenyl-1-picrylhydrazyl (DPPH), respectively (Kondo, Kurihara, Fukuhara, Tanaka, Suzuki, Miyata, et al., 2000; Tanaka, Kondou, & Kouno, 2000). Chen et al., (2014) studied the conversion of B-type trimers to A-type trimers when subjected to temperature, pH, and four catalysts (two free radicals and two oxidases). Results indicated that temperature is the predominant factor in the conversion of B- to A-type trimers, while pH is detrimental in the conversion of B- to A-type trimers. For instance, under acid conditions conversion of B- to A-type trimers does not occur, while under basic conditions B-type trimers were unstable, producing oxy-polymerization. On the other hand, catalysts [1,1-diphenyl-2-picrylhydrazyl radical ($DPPH^{\bullet}$), superoxide anion radical ($O_2^{\bullet-}$), polyphenol oxidase (PPO), and xanthine oxidase (XO)] increase the conversion rate but do not increase the conversion ratio (Chen, Yuan, Chen, Jia, & Li, 2014). Finally, Poupard et al., (2011) and Chen et al., (2014) suggested that the conversion of B- to A-type PAC in *in vitro* models are driven by free-radicals or an enzyme-catalyzed free-radicals through a quinone methide mechanism (Poupard, Sanoner, Baron, Renard, & Guyot, 2011; Chen, Yuan, Chen, Jia, & Li, 2014). However, it is unclear how the conversion of B- to A-type PAC occur in plants because if this happens A-type PAC would be more abundant and present in all plants.

Additionally, the two chiral centers at the C_2 and C_3 positions in the flavan-3-ol monomers of PAC that produce four diastereoisomers can be used to differentiate PAC. For instance, flavan-3-ol monomers with a 2*R*,3*S* configuration are called (+)-catechin and with a 2*S*,3*R* configuration are called (-)-catechin, whereas flavan-3-ol monomers with a 2*R*,3*R* configuration are called (-)-epicatechin and with a 2S,3S configuration are called (+)-epicatechin. On the other hand, the substituents at the C_3 and C_5 positions in the flavan-3-ol monomers of PAC can be useful for differentiating PAC. For instance, PAC from grape skins and seeds contain galloyl moieties at the C_3 position, whereas 3-deoxyproanthocyanidins from sorghum contain glycosides at the C_5 position with a flavanone, eriodictyol or eriodictyol-5-O-β-glucoside in the terminal unit (Gujer, Magnolato, & Self, 1986; Reed, Krueger, & Vestling, 2005). Apart from the previous structural features, direct reactions between anthocyanins and PAC or indirect condensation reactions between anthocyanins and PAC mediated by glyoxylic acid or acetaldehyde also increase the structural heterogeneity and complexity of PAC. Products resulting from these direct and indirect reactions are commonly found in fermented beverages such as red wine and rose cider (made with red-fleshed apples), although condensation of anthocyanin and PAC through an ethyl bridge, arising from acetaldehyde has been described in cranberry fruits (Reed, Krueger, & Vestling, 2005). In fermented beverages, acetaldehyde is attributable to microbial by-products or oxidation of ethanol. However, the presence of acetaldehyde in cranberry fruits is attributed to fruit ripening, processing, and storage. (Krueger, Vestling, & Reed, 2004) indicated that the initial step in cranberry harvesting involves the flooding of the cranberry bog, which causes a reduction in the oxygen concentration. The change from aerobic to anaerobic metabolism causes a shift in the means of generating adenosine triphosphate, which results in the production of acetaldehyde via pyruvate decarboxylase (Krueger, Vestling, & Reed, 2004). Studies on apple and pear fruits under

a controlled atmosphere showed accumulation of both ethanol and acetaldehyde due to a fermentative metabolism (Neuwald, Saquet, & Klein, 2019).

Finally, the degree of polymerization (DP), which indicates the size of PAC based on the number of flavan-3-ol monomers attached to each other, is also used to differentiate PAC as oligomers or polymers. Depolymerization using thiolysis with subsequent analysis with high-performance liquid chromatography (HPLC) from two apple fruits (*Malus domestica* var.; Guillevic and Avrolles) detected average DP between 40 to 50, which correspond to an average molecular weight from 11 to 15 KDa (Sanoner, Guyot, Marnet, Molle, & Drilleau, 1999). Although, the thiolysis method is accepted and used by the scientific community, it suffers from serious problems, which will be discussed in the chromatography section. In cranberry fruits (*Vaccinium macrocarpon* Aiton) DP range from DP2 to DP36 was detected by matrix-assisted laser desorption/ionization time-of-flight mass spectrometry (MALDI-TOF MS) in linear mode (Alfaro-Viquez, Esquivel-Alvarado, Madrigal-Carballo, Krueger, & Reed, 2019). Taken together, the structural heterogeneity and complexity of PAC, and the number of PAC isomers increases exponentially as the DP increases. Thus, methods of extraction, purification, and analysis of PAC present considerable challenges.

Methods of extraction and purification

PAC have the ability to bind spontaneously to plant cell-wall protein and polysaccharides, when cell-walls are ruptured during grinding, pressing, or mastication. Hazak et al., (2004) indicated that

PAC extraction from berries is incomplete because only 22% of available PAC were recovered. In addition, they reported that extractable PAC had lower DP, while non-extractable PAC had higher DP, which suggests that the structural composition of extractable and non-extractable PAC are different (Hazak, Harbertson, Lin, Ro, & Adams, 2004). Because PAC extractability from plant materials is a challenge due to its binding properties, different parameters for extracting PAC have been studied; such as the extraction solvent, particle size, sample to solvent ratio, time and temperature of extraction, and number of extractions. Among these parameters, the solvent(s) used for extracting PAC is the most important. The solvent(s) affect the amount of PAC extracted, the DP distribution, and therefore the biological activity and functional attributes of PAC. Although there are methodologies for extracting PAC, there is no consensus among the methodologies for generating PAC fractions. PAC extraction from plant materials is mostly performed by solid/liquid extraction using acetone-water, methanol-water, and methanol. Mitchell et al., (2017) indicated that the use of acetone-water (7:3 v/v) at a sample to solvent ratio of 3g/15 mL is optimal for the extraction of PAC.(Mitchell, Robertson, & Koh, 2017) Another alternative method to extract PAC is using imidazolium-based ionic liquids (IL), an organic salt in the liquid state containing an organic cation paired with an organic or inorganic anion, such as 1-ethyl-3-methylimidazolium bromide, 1-butyl-3-methylimidazolium bromide, 1-pentyl-3-methylimidazolium bromide, and 1-(4-sulfobutyl)-3-methylimidazolium hydrogen sulfate. Ćurko et al., (2017) reported that these imidazolium-based IL at a concentration of 2.5 mol/L significantly (p-value < 0.05) increase PAC extraction than acetone-water (7:3 v/v). Despite the fact that IL are recognized as an eco-friendly alternative to organic solvents, they have some drawbacks, such as the toxicity for humans and that they are 5 to 20 times more expensive than organic solvent (Kunz & Häckl, 2016; Ćurko, Tomašević, Cvjetko-Bubalo, Gracin, Radojčić-Redovniković, & Kovačević-Ganić, 2017).

PAC extraction using organic solvents such as acetone-water, methanol-water, or methanol provides a wide range of solubility and selective properties. However, in fact, each solvent is not specific for a class of compounds. Therefore, different resin beds are used to purify PAC. Sephadex® LH-20, a crosslinked dextran that has been hydroxypropylated to have both lipophilic and hydrophilic properties, is the most widely used resin to purify PAC (Porter, Krueger, Wiebe, Cunningham, & Reed, 2001; Krueger, Vestling, & Reed, 2004; Pierre, et al., 2013; Feliciano, Meudt, Shanmuganayagam, Krueger, & Reed, 2014; Luca, Bujor, Miron, Aprotosoaie, Skalicka-Woźniak, & Trifan, 2019). Efficient purification of PAC fractions by Sephadex® LH-20 involves a step-wise elution with solvents of different polarities (Luca, Bujor, Miron, Aprotosoaie, Skalicka-Woźniak, & Trifan, 2019). For instance, in a four-step elution, water, which is the first solvent used has a relative polarity of 1.0. Ethanol, which is the second solvent used has a relative polarity of 0.654. Ethanol:methanol (1:1 v/v), which is the third solvent used has a relative polarity of 0.708. Finally, acetone:water (7:3 v/v), which is the fourth solvent used has a relative polarity of 0.482. Feliciano et al., (2012) indicated that using this four-step elution on Sephadex® LH-20, the purity obtained from the acetonic fraction, which contain PAC, is higher than 95% (Feliciano, Shea, Shanmuganayagam, Krueger, Howell, & Reed, 2012). Even though PAC elution appears to be driven by the solvent polarity, dehydration of the Sephadex® LH-20, which causes the shrink of the Sephadex® LH-20, is the main factor that influences the interaction of PAC and other flavonoids with the Sephadex® LH-20.

Other resins used to purify PAC are Toyopearl TSK HW-40 and Toyopearl TSK HW-50F (Brandão, Silva, García-Estévez, Mateus, de Freitas, & Soares, 2017; Ganeko, Kato, Watanabe,

Bastian, Miyake, & Ito, 2019). Toyopearl, a hydroxylated methacrylic polymer, is usually used as a size exclusion chromatography. However, because PAC contain hydroxyl groups, the separation of PAC based on the molecular sieve is affected by the interactions that results from hydrogen bonding and hydrophobic adsorptions between the resin and PAC. Because of this interaction, the separation of PAC is adsorption rather than size-exclusion chromatographic (Luca, Bujor, Miron, Aprotosoaie, Skalicka-Woźniak, & Trifan, 2019). Brown, et al., (2017) compared both Sephadex® LH-20 and Toyopearl TSK HW-50F for their ability to separate PAC. Results indicated that when Sephadex® LH-20 and Toyopearl TSK HW-50F resins are eluted with acetone, higher yields are obtained using Sephadex® LH-20 (94%) compared to Toyopearl TSK HW-50F (71%). Conversely, when Sephadex® LH-20 and Toyopearl TSK HW-50F are eluted with acetone, higher mean DP are obtained using Toyopearl TSK HW-50F (45.8) compared to Sephadex® LH-20 (14.9). Brown, et al., (2017) also indicated that although Toyopearl TSK HW-50F resin generate fractions with higher DP, it needs more time for purification and gave lower yields of recovery compared to Sephadex® LH-20 (Brown, Mueller-Harvey, Zeller, Reinhardt, Stringano, Gea, et al., 2017). This suggests that Toyopearl TSK HW-50F forms interactions with PAC, causing high DP to attach to the surface of the gel beads, resulting in an increase in the mean DP on the Toyopearl TSK HW-50F. Finally, Amberlite XAD and Diaion HP (copolymers of styrene/divinylbenzene), Sepabeads SP (copolymer of divinylbenzene/ethylvinylbenzene), and C_{18} (octadecylsilane; reversed-phase silica gel) resins are used as pre-purification steps to remove sugar and other polar compounds prior to Sephadex® LH-20. Overall, it is suggested that the heterogeneity and complexity of PAC affect the extraction and purification of PAC. Therefore, the analysis of PAC by reliable gravimetry, colorimetry, chromatography, and spectrometry methods are required.

Methods of analysis

Gravimetric methods

The ability of PAC to binds and precipitate proteins and polysaccharides can be applied for quantifying PAC. Makkar et al., (1993) described a gravimetric modification of precipitation of PAC with polyvinylpyrrolidone. This gravimetric method quantifies total PAC and avoids problems of standards associated with colorimetry methods (Harinder Makkar, Blümmel, Borowy, & Becker, 1993). Even though gravimetric methods do not require the use of standard, they are time-consuming, complicated, less sensitive, and do not provide qualitative information. Because of these drawbacks, colorimetry methods, which are cheaper, simpler, and faster than gravimetric methods, are commonly used in research and commercial laboratories for quantifying PAC.

Colorimetric methods

Three specific colorimetric methods to quantify PAC are the vanillin assay (Price, Van Scoyoc, & Butler, 1978), the acid-butanol assay and its modifications, and the 4-(dimethylamino)cinnamaldehyde (DMAC) assay. The vanillin assay is based on the ability of vanillin to react with PAC to form colored complexes that are measured at 500 nm. Currently, the vanillin assay is not extensively used due to its limitations. (Makkar & Becker, 1993) reported that the solvents used for the extraction of PAC alter the quantification and kinetic of reaction in the vanillin assay. For instance, when methanol is used to extract PAC, the absorbance value increases as the concentration of methanol in the sample increases. On the other hand, when acetone is used to extract PAC, the kinetics of the reaction are affected by the concentration of acetone in the

sample. Bae et al., (1993) reported that the water content in the vanillin assay reduces the extent of its chromophore development, which causes low reproducibility (Bae, McAllister, Muir, Yanke, Bassendowski, & Cheng, 1993). Hagerman & Butler, (1994) indicated that although the vanillin assay has been used to quantify PAC, the reaction is not specific to PAC. Monomers, such as catechin, also react to produce the colored complex. Thus, although both PAC and catechin react with vanillin, the reaction kinetics are different, resulting in lower absorbance intensities for catechin than for PAC. Furthermore, PAC extracted from quebracho tree (*Schinopsis* sp), which contain 5-deoxy-proanthocyanidins, provides low PAC content (Hagerman & Butler, 1994). This is because the vanillin assay reacts only with meta-substituted flavonoids.

The butanol-HCl assay and its modifications, which are simpler and more reliable than the vanillin assay, are based on the oxidative depolymerization of PAC in acid medium with the consequent conversion of flavan-3-ol monomers into anthocyanidins. Because the butanol-HCl assay produces anthocyanidins resulting from the oxidative cleavage of the interflavan bonds of PAC, native anthocyanins in the samples, which have similar absorption spectra to anthocyanidins, need to be subtracted from the final results. As in the vanillin assay, the butanol-HCl assay also presents some drawbacks. First, Porter et al., (1985) reported that the anthocyanidins color yields are dependent on the PAC profile, the age of the sample, and the dry treatment of the sample (Porter, Hrstich, & Chan, 1985). Second, Giner-Chavez et al., (1997) reported that when cyanidin, delphinidin, and quebracho PAC were used as external standards for quantifying the content of PAC in three plant species, the PAC content in the three plant species was under- or over-estimated compared to customized PAC standards (Giner-Chavez, Van Soest, Robertson, Lascano, Reed, & Pell, 1997).

In addition, Stewart et al., (2000) reported that *Calliandra calothyrsus* collected from different two locations resulted in differences in color yield in the butanol-HCl assay, which results from differences in the PAC composition (Stewart, Mould, & Mueller-Harvey, 2000). *C. calothyrsus* from one location was composed mainly of (epi)catechin, while the other one was composed mainly of (epi)gallocatechin. Overall, this suggest that PAC from different sources and locations may have different stoichiometry of reactions and reaction products (molar absorption coefficients), although the PAC were extracted from the same species. Third, Dalzell & Kerven, (1998) reported that when the water content increases from 2 to 6% in the sample/reagent matrix, the color formation is suppressed by 0.250 absorbance units. Fourth, although the butanol-HCl assay is used for quantifying soluble and insoluble PAC, previous studies indicate that during the oxidative cleavage of the interflavan bonds of PAC, the extractability of insoluble PAC is not complete (Makkar, Gamble, & Becker, 1999). Grabber et al., (2013) reported that the use of butanol-HCl-acetone iron (HBAI) assay increased total PAC content by up to 3.2 fold over the conventional butanol-HCl assay (Grabber, Zeller, & Mueller-Harvey, 2013). However, the increase in the total PAC content using the HBAI assay is due to the fact that is was applied directly to whole tissues and not to extracts. Therefore, the increase in the total PAC content is the result of a higher amount of PAC extracted from the whole tissue and not of insoluble PAC that remains unextractable. Later, Grabber & Zeller, (2020) compared the use of direct and sequential analysis for quantifying PAC by the HBAI assay. Sequential analysis of acetone:water (7:3 v/v) extracts and insoluble residues provided more robust estimates and recoveries of total PAC than the direct analysis (whole tissue) when the HBAI assay was used. This suggests that to obtain reliable total PAC contents, samples should be quantified into soluble PAC, which are extracted using acetone:water (7/3 v/v), and insoluble PAC, which is the insoluble residue remaining after the

solvent extraction, by using the butanol-HCl or HBAI assays. An alternative for quantifying soluble PAC from samples containing native anthocyanins is using the DMAC assay.

The DMAC assay is based on the ability of the DMAC reagent to react with the C_8 position of the A-ring of PAC terminal units in acid medium. The chromophore resulting from the reaction between PAC and DMAC has a maximum wavelength of 640 nm, eliminating the interferences caused by anthocyanins, which affect the vanillin and butanol-HCl assays. Currently, the DMAC assay is the most used assay to quantify soluble PAC (Payne, Hurst, Stuart, Ou, Fan, Ji, et al., 2010; Prior, Fan, Ji, Howell, Nio, Payne, et al., 2010). Even though the DMAC assay has gained popularity as a reliable assay for quantifying soluble PAC over the vanillin and butanol-HCl assays, the three colorimetric methods all lack a suitable standard that reflects the structural heterogeneity and complexity of PAC. In addition, colorimetric methods do not provide qualitative information such as the patterns of hydroxylation, nature of the interflavan bonds, substituents at the C3 and C5 positions, and DP. In order to address the lack of a suitable standard, Feliciano et al., (2012) developed a cranberry PAC (c-PAC) standard to be used in the DMAC assay for quantifying PAC in cranberry products. This c-PAC standard, isolated from cranberry press cake, reflects the structural heterogeneity and complexity of PAC, thus, increasing the accuracy of the DMAC assay (Feliciano, Shea, Shanmuganayagam, Krueger, Howell, & Reed, 2012). For instance, when c-PAC was used for quantifying soluble PAC by the DMAC assay, the PAC content was 2.2-fold higher using the c-PAC standard (isolated from cranberry press cake) compared to the commercial standard (procyanidin A2). However, because the PAC composition may differ amongst fruits, juices, and press cake, (Krueger, et al., 2016) developed a c-PAC standard isolated

from cranberry fruit. This c-PAC standard isolated from cranberry fruit indicates that the PAC content was 3.6-fold higher using the c-PAC (isolated from cranberry fruit) compared to procyanidin A2 (Krueger, Chesmore, Chen, Parker, Khoo, Marais, et al., 2016). Later, Gullickson et al., (2019) found that the c-PAC standard (isolated from cranberry fruit) may be used for quantifying insoluble PAC by the BuOH-HCl assay (Gullickson, Krueger, Birmingham, Maranan, & Reed, 2019). Taken together, these results highlight the importance of using customized standards for quantifying PAC in order to avoid the underestimation of PAC when colorimetric assays are used.

Because of the need for obtaining accurate PAC quantification in cranberry food and dietary supplements that allows associating the PAC content with its putative health benefits, the Association of Official Analytical Chemists (AOAC) opened a call for submitting methods that are able to quantify soluble PAC (Schaneberg, Brown, Bzhelyansky, Chang, Cunningham, Gu, Haesaerts, Howell, Johnson, & Konings, 2017). Our group, in collaboration with Complete Phytochemical Solutions, responded to this call with an inter-laboratory validation of the DMAC assay using the c-PAC standard isolated from cranberry fruit and procyanidin A2 standard. Results of this study support the previous studies and demonstrate the utility of the c-PAC standard in comparison to the procyanidin A2 standard and the advantage of using a microplate reader for the accurate quantification of PAC in cranberry foods and dietary supplements (Birmingham, Esquivel-Alvarado, Maranan, Krueger, & Reed, 2020).

Chromatographic methods

As an alternative to gravimetric and colorimetric methods, some researchers use chromatographic methods for the analysis of PAC. These chromatographic methods are carried out using HPLC with reversed or normal phases coupled with diode array, fluorescence, or mass spectrometry detectors. Ultra-high-performance liquid chromatography (UHPLC) provides shorter run times, lower solvent consumption, and higher resolution in comparison to HPLC. The analysis of PAC by chromatographic methods are classified into those that analyze PAC after acid-catalyzed cleavage (quantitative) and those that analyze intact PAC oligomers (qualitative/quantitative). The analysis of PAC after acid-catalyzed cleavage in the presence of nucleophilic reagents such as phloroglucinol, toluene α-thiol, cysteamine, or menthofuran are carried out using reverse-phase columns. Gao et al., (2018) described a thiolysis HPLC method for the analysis of c-PAC using cysteamine, which is able to quantify total PAC, DP_n, and ratios of A-type interflavan bonds (Gao, Cunningham, Liu, Khoo, & Gu, 2018). However, this method has some drawbacks, which include 1) incomplete depolymerization during thiolysis (cleavage of the interflavan bond is assumed to be complete and follows a 1:1 stoichiometry, which is not true), 2) lack of commercial standards for thiolysis products (flavan-3-ol benzyl thioethers have the same molar absorptivity's as their respective flavan-3-ol monomers), and 3) PAC with two or more A-type interflavan bonds cannot be quantified (thiolysis is depended on cleavage through auto-oxidation of the interflavan bonds). Overall, separation and quantification of low molecular weight phenolic compounds are carried out using RP columns. Conversely, because of the heterogeneity and complexity of PAC, the separation of intact PAC using RP columns are not achieved and they are eluted as a single hump (Feliciano, Shea, Shanmuganayagam, Krueger, Howell, & Reed, 2012; Esquivel-Alvarado, Muñoz-Arrieta, Alfaro-Viquez, Madrigal-Carballo, Krueger, & Reed, 2020).

In order to enhance the separation of PAC, normal-phase (NP) columns have also been used for the analysis of PAC. Rigaud et al., (1993) reported that good separation of PAC oligomers up to DP5 in cacao bean extract and a poor separation of PAC oligomers in grape seed extract were obtained when a LiChrospher silica 100 column and a mobile phase composed of solvents A (dichloromethane:methanol:formic acid:water, 5:43:1:1 v/v/v/v) and B (dichloromethane:methanol:formic acid:water, 41:7:1:1 v/v/v/v) were used (Rigaud, Escribano-Bailon, Prieur, Souquet, & Cheynier, 1993). This difference in the separation occurred because cacao bean PAC are composed of (epi)catechin with all B-type interflavan bonds, while grape seed PAC are composed of (epi)catechin and (epi)gallocatechin monomers in the same oligomer with all B-type interflavan bonds and galloyl substitutions. Similarly, Hammerstone et al., (1999) reported separation of PAC oligomers up to DP10 in cocoa and chocolate when a Luna silica column and the same mobile phase proposed by Rigaud et al., (1993) were used (Hammerstone, Lazarus, Mitchell, Rucker, & Schmitz, 1999). This suggests that silica-based columns differ among manufacturers, resulting in different PAC oligomers distribution. Kelm et al., (2006) reported separation of PAC oligomers up to DP14 in cacao when a Develosil diol column and a mobile phase composed of solvents A (acetonitrile:acetic acid, 99:1 v/v) and B (methanol:water:acetic acid, 95:4:1 v/v) were used (Kelm, Johnson, Robbins, Hammerstone, & Schmitz, 2006). (Robbins, et al., 2009) modified the chromatographic conditions to that proposed by Kelm et al., (2006) and assessed five diol-based columns (Develosil Diol, Lichrosorb Diol, Inertsil WP300 Diol, Lichrospher, and Cosmosil) (Robbins, Leonczak, Johnson, Li, Kwik-Uribe, Prior, et al., 2009). The modification of the chromatographic conditions enhanced baseline separation, while the use of a fluorescence detector increased signal intensity by a factor of up to 25 in comparison to a diode array detector. From this study, we also concluded that the separation

of PAC oligomers using diol-based columns differs among manufacturers and that DP higher than 10 were not obtained. Hummer & Schreier, (2008) indicated that PAC with high DP tend to bind irreversibly to silica-based NP columns, whereas PAC with high DP attach reversibly to diol-based columns, providing an alternative for separating PAC. The binding differs because hydrogen bonding in the hydroxyl groups with diol-based columns is not as strong as those with the silica-based columns, which provides selectivity without excessive retention of PAC.

Currently, a variant of the NP for the analysis of PAC is the hydrophilic interaction liquid chromatography (HILIC). HILIC employs hydrophilic stationary phases (bare silica, aminopropyl, amide, diol, or cyano phases) with RP type eluents. Hollands, et al., (2017) hypothesized that the chromatographic resolution of PAC oligomers would be better if HILIC-based columns were used instead of diol-based columns (Hollands, Voorspoels, Jacobs, Aaby, Meisland, Garcia-Villalba, et al., 2017). This hypothesis was confirmed when a Develosil diol column was compared to a Luna HILIC column and a better resolution was obtained with a Luna HILIC column. HILIC-based columns are composed of cross-linked diol groups, which add functionality and robustness in comparison to diol-based columns. Despite the fact that NP- and HILIC-based columns are used for the analysis of PAC oligomers up to DP10, the peaks that represent DP do not consist of only one PAC monomer, but rather of PAC monomers with the same molecular mass (multiple isomeric structures) and hetero-oligomers. Furthermore, caution is required when samples containing A-type interflavan bonds such as cranberry, cinnamon, and plums amongst others are analyzed by NP- and HILIC-based columns. Previous studies indicated that samples containing A-type interflavan bonds show poor sensitivity and difficulties in separating PAC oligomers, especially

as the DP increase due to the overlapping of A- and B-type interflavan bonds (Sintara, Wang, Li, Liu, Cunningham, Prior, et al., 2020). In addition to this limitation, the analysis of PAC oligomers up to DP10 by NP- and HILIC-based columns is restricted only to the analysis of samples containing B-type interflavan bonds without substituents such as cacao and apples. Thus, other methods, such as nuclear magnetic resonance and mass spectrometry, are more reliable for the analysis of complex and heterogeneous intact PAC.

Nuclear magnetic resonance

Nuclear magnetic resonance (NMR) is a powerful theoretical/practical method, wherein a sample is placed in a constant magnetic field, irradiated, and a magnetic signal is detected. PAC are analyzed via proton (^{1}H) and carbon-13 (^{13}C) NMR spectroscopy using one-dimensional (1D) and two-dimensional (2D) methods. Early studies suggested that the procyanidin (PC) and prodelphinidin (PD) ratio, the stereochemistry (*R*, *S*) at the C_2 and C_3 positions, the number-average molecular weight, and the presence of A- and B-type interflavan bonds may be deduced by ^{13}C NMR using 1D methods (Czochanska, Foo, Newman, & Porter, 1980). The PC and PD ratio is determined by direct integration of the signals at δ145 ppm and at δ146 ppm, respectively. The stereochemistry (*R*, *S*) at the C_2 and C_3 positions is determined from the region between δ65-80 ppm by direct integration. The number-average molecular weight is deduced by the direct integration of the ratio of C_3 terminal units (δ67-68 ppm) and C_3 extension units (δ72-73 ppm). Direct integration of these signals is allowed because these signals have identical spin-lattice (T1) and steady-state nuclear Overhauser effect (NOE). The presence of the C_4-C_8 linkages shows signals at δ37-38 ppm due to the chemical shifts of C_4 and signals at δ106-107 ppm due to the

chemical shifts of C_8. While, the presence of the C_6-C_8 shows signals at δ97-98 ppm due to the chemical shifts of C_6 and signals at δ106-107 ppm due to the chemical shifts of C_8. In addition, the presence of A-type interflavan bonds is deduced by the occurrence of signals at δ148-153 (C_8q) and a quaternary carbon signal at δ104.9 ppm (C_2q). Even though ^{1}H NMR reveals information on PAC composition, it does not provide a total PAC characterization. For instance, the presence of C_4-C_8 or C_6-C_8 linkages is difficult to determine because of the atropisomerism caused by the hindrance of rotation about the single bond, which prevents rotation to the extent that would allow for the isolation of individual conformers (Harborne, 2013). This suggests that the spin-spin relaxation (T2) values are small, and, therefore the detection of cross-peak in ^{1}H NMR 2D methods at room temperature is impossible. In order to solve the problem of atropisomerism, Shoji et al., (2003) acquired spectra at low temperature (-20 and -40°C). Despite NMR spectra resulting in sharper signals at low temperatures, structural elucidation was carried out for isolate monomers [(-)-catechin and (+)-epicatechin], procyanidin dimers (procyanidin B1 and B2), and six procyanidin trimers and not for a mixture of naturally occurring PAC oligomers (Shoji, Mutsuga, Nakamura, Kanda, Akiyama, & Goda, 2003). Overall, ^{1}H and ^{13}C NMR spectroscopy have been used to elucidate isolated monomer, dimers, and trimers, but suffer from broad and unresolved signals, long acquisition times, low signal-to-noise ratios, large sample requirements, and a barrier due to the expertise necessary to interpret the spectra.

Mass spectrometry

The analysis of PAC by mass spectrometry (MS) is carried out by electrospray ionization (ESI) or by matrix-assisted laser desorption/ionization (MALDI). ESI is a soft ionization technique, in

which a high voltage is applied to assist the transfer of ions from solution into a gas-phase with the subsequent analysis using a mass detector. PAC are ionized by losing a proton to form $[M-H]^-$ ions or by gaining a proton to form $[M+H]^+$ ions. Despite the fact that ESI-MS is one of the most common methods for the characterization and quantification of low molecular weight phenolic compounds, ESI-MS is not suitable for the analysis of PAC. During PAC analysis, multiply-charged ions ($[M-2H]^{2-}$ and $[M-3H]^{3-}$) of high DP are stacked with singly-charged ions. For instance, triple-charged ions of B-type nonamers ($[M-3H]^{3-}$; 864.1902 amu), double-charged ions of B-type hexamers ($[M-2H]^{2-}$; 864.6941 amu), and single-charged ions of B-type trimers ($[M-H]^-$; 865.1980 amu) are stacked, which may result in difficult interpretation or misinterpretation of PAC spectra. Additionally, during PAC analysis, equal masses resulting from the contribution of carbon, oxygen, and hydrogen isotopes of PAC oligomers may overlap. For instance, the mass of single-charged ions of trimers containing all B-type interflavan bonds (865.1980 amu), which represents the contribution of ^{12}C, ^{16}O, and ^{1}H isotopes, is equal to the isotope mass of single-charged ions of trimers containing one A-type interflavan bond or the double-charged ions of hexamers with all B-type interflavan bonds, which represents the contribution of two ^{13}C, or one ^{13}C and one ^{2}H, or one ^{18}O, or two ^{2}H isotopes. Taken together, the interpretation of PAC by using ESI-MS spectra is cumbersome and time-consuming. Zhang et al., (2017) developed an algorithm using MATLAB for processing ESI-MS data capable of identifying and quantifying PAC, deconvoluting the isotope patterns of A- and B-type interflavan bonds and the multi-charged ions of PAC. Despite the fact that this algorithm process ESI-MS spectra in less than one minute, it does not replace human expertise because it cannot provide positive confirmation of PAC structures, especially when chromatographic peaks of PAC and non-PAC overlap (Zhang, Sun, & Chen, 2017). Because ESI-MS has limitations arising from the formation of multiply-charged ions,

MALDI-TOF MS is preferable to ESI-MS for the analysis of PAC. In addition, MALDI-TOF MS offers greater tolerance for impurities than ESI-MS and allows the possibility to re-analyze the same sample (Monagas, Quintanilla-Lopez, Gomez-Cordoves, Bartolome, & Lebron-Aguilar, 2010).

MALDI is a soft ionization technique that occurs in two steps. In the first step, the sample analyzed is dissolved into a solution containing low molecular weight organic molecules. These low molecular weight organic molecules are called matrices and must have strong absorption of radiation at the laser wavelength, good mixing and solvent compatibility with the sample, good vacuum stability and low vapor pressure, and participate in a photochemical reaction (Monagas, Quintanilla-Lopez, Gomez-Cordoves, Bartolome, & Lebron-Aguilar, 2010). Examples of matrices used for the analysis of PAC are 2,5-dihydroxybenzoic acid (DHB), *trans*-3-indolacrylic acid (IAA), *R*-cyano-4-hydroxycinnamic acid, and sinapinic acid. The mixture containing the sample and the matrix is placed on a target plate and allowed to dry, which produces sample-doped matrix crystals. In the second step, which occurs inside the mass spectrometer, the sample-doped matrix crystals are irradiated by the laser, which causes rapid heating of the crystals and subsequent sublimation and expansion of the matrix into the gas phase without fragmentation of the sample. After desorption, the ionization of the intact sample occurs which is accelerated by an electrostatic field towards the time-of-flight (TOF) analyzer. Because the sample is analyzed without fragmentation, MALDI-TOF MS provides a rapid, accurate, and inexpensive alternative for PAC analysis, eliminating the problem of multiply-charged ions produced by ESI-MS.

MALDI-TOF MS has emerged as the MS method of choice for PAC analysis because it has the ability to resolve the heterogeneity and complexity of PAC (Krueger, Dopke, Treichel, Folts, & Reed, 2000; Reed, Krueger, & Vestling, 2005). Ohnishi-Kameyama et al., (1997) were the first researchers to demonstrate the capacity of MALDI-TOF MS to characterize PAC from apples, showing (epi)catechin oligomers from DP2 to DP15 (Ohnishi-Kameyama, Yanagida, Kanda, & Nagata, 1997). Later, Krueger et al., (2000) used MALDI-TOF MS to characterize for the first time PAC with galloyl moieties from grape seed extract (Krueger, Dopke, Treichel, Folts, & Reed, 2000). Foo et al., (2000) also used MALDI-TOF MS to characterize cranberry PAC, and demonstrated that MALDI-TOF MS was able to determine A- and B-type interflavan bonds (Foo, Lu, Howell, & Vorsa, 2000). Taken together, these early studies that used MALDI-TOF MS to characterize PAC from different natural sources indicate that it is a useful and attractive tool for elucidating the heterogeneity and complexity of PAC by predicting the nature of the monomer unit, interflavan linkage, DP, and other substitutions on the flavan-3-ol oligomers (Esquivel-Alvarado, Alfaro-Viquez, Krueger, Vestling, & Reed, 2021). These structural features of PAC can be determined because MALDI-TOF MS provides mass resolution from 5000 to 20000 with mass accuracy from 10 to 200 ppm, which allows MALDI-TOF MS to obtain baseline resolution of one atomic mass and interpret the isotope patterns (de Hoffmann & Stroobant, 2007).

Reed et al., (2005) hypothesized that the isotope abundance of carbon, oxygen, and hydrogen within PAC structures and the use of MALDI-TOF MS could be used to determine the percentage of A- and B-type interflavan bonds in PAC for each DP (Reed, Krueger, & Vestling, 2005). Feliciano et al., (2012) validated this hypothesis for binary mixtures of procyanidin A2 (Pro A2)

and procyanidin B2 (Pro B2) and subsequently applied it to c-PAC from DP2 to DP11. Results indicated that the deconvolution of overlapping isotope pattern of MALDI-TOF MS spectra was repeatable, robust, accurate, and precise for the binary mixtures ProA2 and ProB2. Likewise, MALDI-TOF MS demonstrated that the isotope cluster for c-PAC was repeatable at each DP, which suggests that the isotope patterns are unique to individual samples and are not an artifact of the spectrometer, which allows estimating the percentage of A- and B-type interflavan bonds when using the deconvolution method (Feliciano, Krueger, Shanmuganayagam, Vestling, & Reed, 2012). Because MALDI-TOF MS provides unique isotope patterns for each source of PAC, the deconvolution of overlapping isotope patterns of MALDI-TOF MS can be applied for standardization and authentication of c-PAC. The use of both MALDI-TOF MS and the deconvolution method were widely used in this dissertation in order to determine standardization, authentication, and efficacy. In addition, the use of both MALDI-TOF MS and the deconvolution method was discussed in appendix I, which was accepted for publication in the book Recent Advances in Polyphenol Research Volume 7 published by Wiley.

The increasing demand for cranberry foods, dietary supplements, and beverages and the high price of cranberry compared to other less expensive botanical sources of PAC, has caused unscrupulous, profit-motivated companies to adulterate their cranberry products. Brendler & Gafner, (2017) detailed a pricelist that varied based on the percentage of c-PAC. For instance, dried cranberry press cake containing from 0.8 to 1.5% (w/w) PAC ranged from $50-75/kg. Berry extracts and blends of juice extracts and berry extracts containing from 3 to 5% (w/w) PAC ranged from $150-300/kg, while pure juice extracts containing from 12 to 24% (w/w) PAC ranged from $400-600/kg.

On the other hand, the other botanical sources containing PAC, which are used to adulterate cranberry products, have a much lower cost. For instance, the price for peanut skin extracts in 2017 containing from 80 to 90% (w/w) PAC ranged from $30-50/kg, while proprietary grape seed extracts are sold for up to $110/kg (Kupina & Gafner, 2016; Brendler & Gafner, 2017). In order to prevent adulteration and address the lack of a standardized method able to identify A-type interflavan bonds in cranberry based foods and dietary supplements, an AOAC stakeholder panel composed of regulatory organizations, academic institutions, industry, and contract laboratories solicited for methods to detect A-type interflavan bonds in cranberry based foods and dietary supplements, by analytical techniques that meet the minimum method performance requirements. The analytical technique had to evaluate at least 33 samples known to contain A-type interflavan bonds and at least 33 samples that do not contain A-type interflavan bonds and with 90% probability of identification with 95% confidence (Schaneberg, Brown, Bzhelyansky, Chang, Cunningham, Gu, Haesaerts, Howell, Johnson, Konings, et al., 2017).

In order to meet these requirements, we used MALDI-TOF MS and the deconvolution method (**Chapter 2**). MALDI-TOF MS parameters were optimized for obtaining high-resolution spectra. These optimized parameters were matrix selection and matrix-to-sample ratio, cationization element, pulsed ion extraction, and laser power. Our analysis of the MALDI-TOF MS spectra showed that, for 35 samples known to contain A-type interflavan bonds and 36 samples that do not contain A-type interflavan bonds, the predominant mass for each DP was representative of PAC structure with (epi)catechin oligomers that have either A- or B-type interflavan bonds. Visual inspection of MALDI-TOF MS spectra by experts in the field of PAC was sufficient to

differentiate samples with structural variation in the nature of the interflavan bonds. However, identification and authentication of A-type interflavan bonds in cranberry based foods and dietary supplements were confirmed by the deconvolution method, which may be presented in the form of a bar graph to facilitate interpretation. Deconvolution of overlapping isotope patterns of MALDI-TOF MS spectra for the 35 samples known to contain A-type interflavan bonds was able to identify the presence of 1 A-type interflavan bond with a probability of 95.6% and 95% confidence, while for the 36 samples that do not contain A-type interflavan bonds it was able to confirm the absence of A-type interflavan bonds (all B-type interflavan bonds) with a probability of 93.4% and 95%. Principal component analysis (PCA) was applied to reduce the dimensionality of the deconvolution of overlapping isotope patterns of MALDI-TOF MS data. PCA was able to differentiate the 35 samples known to contain A-type interflavan bonds from the 36 samples that do not contain A-type interflavan bonds. Overall, our results indicate that authentication and standardization of c-PAC using both MALDI-TOF and the deconvolution method for identifying the presence of A-type interflavan bonds and for estimating the percentage of A- and B-type interflavan bonds in cranberry based foods and dietary supplements was achieved (Esquivel-Alvarado, Alfaro-Viquez, Krueger, Vestling, & Reed, 2020).

Because AOAC requirements did not include the analysis of other PAC sources containing A-type interflavan bonds such as peanut skins, we hypothesized that MALDI-TOF MS and the deconvolution method could differentiate and discriminate amongst unmixed and mixed PAC sources containing either A- or B-type interflavan bonds using multivariate analysis. The hypothesis was evaluated by analyzing 28 unmixed apple PAC (a-PAC), 24 unmixed peanut skins

PAC (p-PAC), 34 unmixed c-PAC, 70 samples of c-PAC mixed with a-PAC, and 70 samples of c-PAC mixed with p-PAC, for a total of 226 samples. These c-PAC mixed either with a-PAC and p-PAC were prepared at the following percentages of c-PAC by weight: 5%, 10%, 15%, 20%, 25%, 50%, and 75%. Our results indicated that the relative intensity of the isotopic patterns varies based on the percentage of c-PAC mixed either with a-PAC or p-PAC. In addition, when PCA and linear discriminant analysis (LDA) were applied to the auto-scaled MALDI-TOF MS spectra data of the 226 samples, visualization of the PCA score plot indicated that the variation in the PAC profile obtained by the auto-scaled MALDI-TOF MS spectra data is sufficient for the differentiation of a-PAC, c-PAC, and p-PAC, and that c-PAC mixed either with a-PAC or p-PAC were classified into fourteen groups according to their percentages. On the other hand, the predictive classification model constructed using LDA was able to discriminate the seventeen groups. The classification accuracy, specificity, and sensitivity were evaluated using RStudio software. The auto-scaled MALDI-TOF MS spectra data were randomly split into a training set (70%) and a testing set (30%). The training set was used to build the model, whereas the testing set was used to evaluate the final model. Validation of the LDA classification was assessed using leave-one-out cross-validation. Results indicate that LDA models correctly classified 99.4% of the training set, 100% of the testing set, and 94.2% of the validation set, suggesting that MALDI-TOF MS combined with multivariate analysis allows the determination of c-PAC, either with a-PAC or p-PAC, within 5% (w/w) with a confidence level of 95% (Esquivel-Alvarado, Alfaro-Viquez, Krueger, Vestling, & Reed, 2021). Overall, our recent publications support that MALDI-TOF MS and the deconvolution methodology combined with multivariate analysis can be used to determinate the authenticity, standardization, and efficacy of cranberry products. Information

about the percentage of A- and B-type interflavan bonds at each DP allows determining a PAC fingerprint that is specific to each PAC source.

REFERENCES

Alfaro-Viquez, E., Esquivel-Alvarado, D., Madrigal-Carballo, S., Krueger, C., & Reed, J. (2019). Proanthocyanidin-chitosan composite nanoparticles prevent bacterial invasion and colonization of gut epithelial cells by extra-intestinal pathogenic *Escherichia coli*. *International Journal of Biological Macromolecules*, 630-636. doi:10.1016/j.ijbiomac.2019.04.170.

Bae, H., McAllister, T., Muir, A., Yanke, L., Bassendowski, K., & Cheng, K. (1993). Selection of a method of condensed tannin analysis for studies with rumen bacteria. *Journal of agricultural and food chemistry, 41*(8), 1256-1260. doi:10.1021/jf00032a018.

Birmingham, A., Esquivel-Alvarado, D., Maranan, M., Krueger, C., & Reed, J. (2020). Inter-laboratory validation of 4-(dimethylamino)cinnamaldehyde (DMAC) assay using cranberry proanthocyanidin standard for quantification of soluble proanthocyanidins in cranberry foods and dietary supplements, First Action Method: 2019.06. *Journal of AOAC International*. doi:10.1093/jaoacint/qsaa084.

Bladé, C., Arola-Arnal, A., Crescenti, A., Suárez, M., Bravo, F., Aragonès, G., Muguerza, B., & Arola, L. (2017). Proanthocyanidins and Epigenetics. In V. Patel & V. Preedy (Eds.), *Handbook of Nutrition, Diet, and Epigenetics*, (pp. 1-24). Cham: Springer International Publishing.

Brandão, E., Silva, M., García-Estévez, I., Mateus, N., de Freitas, V., & Soares, S. (2017). Molecular study of mucin-procyanidin interaction by fluorescence quenching and saturation transfer difference (STD)-NMR. *Food chemistry, 228*, 427-434. doi:10.1016/j.foodchem.2017.02.027.

Brendler, T., & Gafner, S. (2017). Adulteration of cranberry (*Vaccinium macrocarpon*). *Botanical Adulterants Bulletin*, 1-8.

Brown, R., Mueller-Harvey, I., Zeller, W., Reinhardt, L., Stringano, E., Gea, A., Drake, C., Ropiak, H., Fryganas, C., & Ramsay, A. (2017). Facile purification of milligram to gram quantities of condensed tannins according to mean degree of polymerization and flavan-3-ol subunit composition. *Journal of agricultural and food chemistry, 65*(36), 8072-8082. doi:10.1021/acs.jafc.7b03489.

Chen, L., Yuan, P., Chen, K., Jia, Q., & Li, Y. (2014). Oxidative conversion of B-to A-type procyanidin trimer: Evidence for quinone methide mechanism. *Food chemistry, 154*, 315-322. doi:10.1016/j.foodchem.2014.01.018.

Ćurko, N., Tomašević, M., Cvjetko-Bubalo, M., Gracin, L., Radojčić-Redovniković, I., & Kovačević-Ganić, K. (2017). Extraction of proanthocyanidins and anthocyanins from grape skin by using ionic liquids. *Food technology and biotechnology, 55*(3), 429-437. doi:10.17113/ftb.55.03.17.5200.

Czochanska, Z., Foo, L., Newman, R., & Porter, L. (1980). Polymeric proanthocyanidins. Stereochemistry, structural units, and molecular weight. *J Chem Soc Perkin Trans 1*, 2278-2286. doi:10.1039/P19800002278.

Dalzell, S., & Kerven, G. (1998). A rapid method for the measurement of *Leucaena* spp proanthocyanidins by the proanthocyanidin (butanol/HCl) assay. *Journal of the Science of Food and Agriculture, 78*(3), 405-416. doi:10.1002/(SICI)1097-0010(199811)78:3<405::AID-JSFA133>3.0.CO;2-G.

de Almeida Alvarenga, L., Borges, N., Moreira, L., Teixeira, K., Carraro-Eduardo, J., Dai, L., Stenvinkel, P., Lindholm, B., & Mafra, D. (2019). Cranberries - Potential benefits in patients with chronic kidney disease. *Food & function, 10*(6), 3103-3112. doi:10.1039/c9fo00375d.

de Hoffmann, E., & Stroobant, V. (2007). *Mass Spectrometry: Principles and Applications* (Third ed.): Wiley.

Dorofejeva, K., Rakcejeva, T., Kviesis, J., & Skudra, L. (2011). Composition of vitamins and amino acids in Latvian cranberries. In *6-th Baltic Conference on Food Science and Technology "Innovations for food science and production" Foodbalt*, (pp. 153-158).

Esquivel-Alvarado, D., Alfaro-Viquez, E., Krueger, C., Vestling, M., & Reed, J. (2020). Identification of A-type proanthocyanidins in cranberry-based foods and dietary supplements by matrix-assisted laser desorption/ionization time-of-flight mass spectrometry, First Action Method: 2019.05. *Journal of AOAC International*. doi:10.1093/jaoacint/qsaa106.

Esquivel-Alvarado, D., Alfaro-Viquez, E., Krueger, C., Vestling, M., & Reed, J. (2021). Classification of proanthocyanidin profiles using matrix-assisted laser desorption/ionization time-of-flight mass spectrometry (MALDI-TOF MS) spectra data combined with multivariate analysis. *Food chemistry, 336*. doi:10.1016/j.foodchem.2020.127667.

Esquivel-Alvarado, D., Muñoz-Arrieta, R., Alfaro-Viquez, E., Madrigal-Carballo, S., Krueger, C., & Reed, J. (2020). Composition of anthocyanins and proanthocyanidins in three tropical *Vaccinium* species from Costa Rica. *Journal of agricultural and food chemistry, 68*(10), 2872-2879. doi:10.1021/acs.jafc.9b01451.

FAO. (2020). Food and Agriculture Organization of the United Nations. In). http://www.fao.org/faostat/en/#data/QC.

Feliciano, R., Krueger, C., Shanmuganayagam, D., Vestling, M., & Reed, J. (2012). Deconvolution of matrix-assisted laser desorption/ionization time-of-flight mass spectrometry isotope patterns to determine ratios of A-type to B-type interflavan bonds in cranberry proanthocyanidins. *Food chemistry, 135*(3), 1485-1493. doi:10.1016/j.foodchem.2012.05.102.

Feliciano, R., Meudt, J., Shanmuganayagam, D., Krueger, C., & Reed, J. (2014). Ratio of "A-type" to "B-type" proanthocyanidin interflavan bonds affects extra-intestinal pathogenic *Escherichia coli* invasion of gut epithelial cells. *Journal of agricultural and food chemistry, 62*(18), 3919-3925. doi:10.1021/jf403839a.

Feliciano, R., Shea, M., Shanmuganayagam, D., Krueger, C., Howell, A., & Reed, J. (2012). Comparison of isolated cranberry (*Vaccinium macrocarpon* Ait.) proanthocyanidins to catechin and procyanidins A2 and B2 for use as standards in the 4-(dimethylamino)cinnamaldehyde assay. *Journal of agricultural and food chemistry, 60*(18), 4578-4585. doi:10.1021/jf3007213.

Foo, L., Lu, Y., Howell, A., & Vorsa, N. (2000). The structure of cranberry proanthocyanidins which inhibit adherence of uropathogenic P-fimbriated *Escherichia coli in vitro*. *Phytochemistry, 54*(2), 173-181. doi:10.1016/S0031-9422(99)00573-7.

Ganeko, N., Kato, N., Watanabe, S., Bastian, F., Miyake, M., & Ito, H. (2019). Proanthocyanidin and anthocyanins from the hulls and beards of red-kerneled rice and their antiglycation

properties. *Bioscience, biotechnology, and biochemistry, 83*(4), 605-608. doi:10.1080/09168451.2018.1553609.

Gao, C., Cunningham, D., Liu, H., Khoo, C., & Gu, L. (2018). Development of a Thiolysis HPLC Method for the Analysis of Procyanidins in Cranberry Products. *Journal of agricultural and food chemistry, 66*(9), 2159-2167. doi:10.1021/acs.jafc.7b04625.

Giner-Chavez, B., Van Soest, P., Robertson, J., Lascano, C., Reed, J., & Pell, A. (1997). A method for isolating condensed tannins from crude plant extracts with trivalent ytterbium. *Journal of the Science of Food and Agriculture, 74*(3), 359-368. doi:10.1002/(SICI)1097-0010(199707)74:3<359::AID-JSFA811>3.0.CO;2-C.

Grabber, J., & Zeller, W. (2020). Direct versus sequential analysis of procyanidin- and prodelphinidin-based condensed tannins by the HCl-butanol-acetone-iron assay. *Journal of agricultural and food chemistry, 68*(10), 2906-2916. doi:10.1021/acs.jafc.9b01307.

Grabber, J., Zeller, W., & Mueller-Harvey, I. (2013). Acetone enhances the direct analysis of procyanidin- and prodelphinidin-based condensed tannins in *Lotus* species by the butanol-HCl-iron assay. *Journal of agricultural and food chemistry, 61*(11), 2669-2678. doi:10.1021/jf304158m.

Gu, L., Kelm, M., Hammerstone, J., Beecher, G., Holden, J., Haytowitz, D., & Prior, R. (2003). Screening of foods containing proanthocyanidins and their structural characterization using LC-MS/MS and thiolytic degradation. *Journal of agricultural and food chemistry, 51*(25), 7513-7521. doi:10.1021/jf034815d.

Gujer, R., Magnolato, D., & Self, R. (1986). Glucosylated flavonoids and other phenolic compounds from sorghum. *Phytochemistry, 25*(6), 1431-1436. doi:10.1016/S0031-9422(00)81304-7.

Gullickson, E., Krueger, C., Birmingham, A., Maranan, M., & Reed, J. (2019). Development of a cranberry standard for quantification of insoluble cranberry (Vaccinium macrocarpon Ait.) proanthocyanidins. *Journal of agricultural and food chemistry, 68*(10), 2900-2905. doi:10.1021/acs.jafc.9b03696.

Hagerman, A., & Butler, L. (1994). Assay of condensed tannins or flavonoid oligomers and related flavonoids in plants. In *Methods in enzymology*, vol. 234 (pp. 429-437): Elsevier.

Hammerstone, J., Lazarus, S., Mitchell, A., Rucker, R., & Schmitz, H. (1999). Identification of procyanidins in cocoa (*Theobroma cacao*) and chocolate using high-performance liquid chromatography/mass spectrometry. *Journal of agricultural and food chemistry, 47*(2), 490-496. doi:10.1021/jf980760h.

Harborne, J. (2013). *The flavonoids: advances in research since 1980* (Vol. 3): Springer.

Hazak, J., Harbertson, J., Lin, C., Ro, B., & Adams, D. (2004). The phenolic components of grape berries in relation to wine composition. In *VII International Symposium on Grapevine Physiology and Biotechnology*, (pp. 189-196).

Hollands, W., Voorspoels, S., Jacobs, G., Aaby, K., Meisland, A., Garcia-Villalba, R., Tomas-Barberan, F., Piskula, M., Mawson, D., & Vovk, I. (2017). Development, validation and evaluation of an analytical method for the determination of monomeric and oligomeric procyanidins in apple extracts. *Journal of Chromatography A, 1495*, 46-56. doi:10.1016/j.chroma.2017.03.030.

Hummer, W., & Schreier, P. (2008). Analysis of proanthocyanidins. *Mol Nutr Food Res, 52*(12), 1381-1398. doi:10.1002/mnfr.200700463.

Joshi, S., Howell, A., & D'Souza, D. (2016). Reduction of enteric viruses by blueberry juice and blueberry proanthocyanidins. *Food and environmental virology, 8*(4), 235-243. doi:10.1007/s12560-016-9247-3.

Kelm, M., Johnson, J., Robbins, R., Hammerstone, J., & Schmitz, H. (2006). High-performance liquid chromatography separation and purification of cacao (*Theobroma cacao* L.) procyanidins according to degree of polymerization using a diol stationary phase. *Journal of agricultural and food chemistry, 54*(5), 1571-1576. doi:10.1021/jf0525941.

Kondo, K., Kurihara, M., Fukuhara, K., Tanaka, T., Suzuki, T., Miyata, N., & Toyoda, M. (2000). Conversion of procyanidin B-type (catechin dimer) to A-type: evidence for abstraction of C-2

hydrogen in catechin during radical oxidation. *Tetrahedron letters, 41*(4), 485-488. doi:10.1016/S0040-4039(99)02097-3.

Krueger, C., Chesmore, N., Chen, X., Parker, J., Khoo, C., Marais, J., Shanmuganayagam, D., Crump, P., & Reed, J. (2016). Critical reevaluation of the 4-(dimethylamino)cinnamaldehyde assay: cranberry proanthocyanidin standard is superior to procyanidin A2 dimer for accurate quantification of proanthocyanidins in cranberry products. *Journal of functional foods, 22*, 13-19. doi:10.1016/j.jff.2016.01.017.

Krueger, C., Dopke, N., Treichel, P., Folts, J., & Reed, J. (2000). Matrix-assisted laser desorption/ionization time-of-flight mass spectrometry of polygalloyl polyflavan-3-ols in grape seed extract. *Journal of agricultural and food chemistry, 48*(5), 1663-1667. doi:10.1021/jf990534n.

Krueger, C., Vestling, M., & Reed, J. (2004). Matrix-Assisted Laser Desorption-Ionization Time-of-Flight Mass Spectrometry of Anthocyanin-poly-flavan-3-ol Oligomers in Cranberry Fruit (*Vaccinium macrocarpon*, Ait.) and Spray-Dried Cranberry Juice. In *Red Wine Color*, vol. 886 (pp. 232-246): ACS Symposium Series.

Kunz, W., & Häckl, K. (2016). The hype with ionic liquids as solvents. *Chemical Physics Letters, 661*, 6-12. doi:10.1016/j.cplett.2016.07.044.

Kupina, S., & Gafner, S. (2016). Adulteration of grape seed extract. *Botanical Adulterants Bulletin*, 1-6.

Llorent-Martínez, E., Spínola, V., & Castilho, P. (2017). Evaluation of the inorganic content of six underused wild berries from Portugal: Potential new sources of essential minerals. *Journal of Food Composition and Analysis, 59*, 153-160. doi:10.1016/j.jfca.2017.02.016.

Luca, S., Bujor, A., Miron, A., Aprotosoaie, A., Skalicka-Woźniak, K., & Trifan, A. (2019). Preparative separation and bioactivity of oligomeric proanthocyanidins. *Phytochemistry Reviews*, 1-48. doi:10.1007/s11101-019-09611-5.

Makkar, H., & Becker, K. (1993). Vanillin-HCl method for condensed tannins: Effect of organic solvents used for extraction of tannins. *J Chem Ecol, 19*(4), 613-621. doi:10.1007/BF00984996.

Makkar, H., Blümmel, M., Borowy, N., & Becker, K. (1993). Gravimetric determination of tannins and their correlations with chemical and protein precipitation methods. *Journal of the Science of Food and Agriculture, 61*(2), 161-165. doi:10.1002/jsfa.2740610205.

Makkar, H., Gamble, G., & Becker, K. (1999). Limitation of the butanol–hydrochloric acid–iron assay for bound condensed tannins. *Food chemistry, 66*(1), 129-133. doi:10.1016/S0308-8146(99)00043-6.

Mitchell, A., Robertson, D., & Koh, E. (2017). Optimizing the extraction of procyanidins oligomers through decamer. *Nutrition & Food Science International Journal, 4*(2), 61-67. doi:10.19080/NFSIJ.2017.04.555636.

Monagas, M., Quintanilla-Lopez, J. E., Gomez-Cordoves, C., Bartolome, B., & Lebron-Aguilar, R. (2010). MALDI-TOF MS analysis of plant proanthocyanidins. *Journal of Pharmaceutical and Biomedical Analysis, 51*(2), 358-372. doi:10.1016/j.jpba.2009.03.035.

Nemzer, B., Vargas, L., Xia, X., Sintara, M., & Feng, H. (2018). Phytochemical and physical properties of blueberries, tart cherries, strawberries, and cranberries as affected by different drying methods. *Food chemistry, 262*, 242-250. doi:10.1016/j.foodchem.2018.04.047.

Neuwald, D., Saquet, A., & Klein, N. (2019). Disorders During Storage of Fruits and Vegetables. In *Postharvest Physiological Disorders in Fruits and Vegetables*, (pp. 89-110): CRC Press.

Ohnishi-Kameyama, M., Yanagida, A., Kanda, T., & Nagata, T. (1997). Identification of catechin oligomers from apple (*Malus pumila* cv. Fuji) in matrix-assisted laser desorption/ionization time-of-flight mass spectrometry and fast-atom bombardment mass spectrometry. *Rapid Communications in Mass Spectrometry, 11*(1), 31-36. doi:10.1002/(SICI)1097-0231(19970115)11:1<31::AID-RCM784>3.0.CO;2-T.

Oliveira, J., Mateus, N., & de Freitas, V. (2013). Flavanols: catechins and proanthocyanidins. In *Natural products: phytochemistry, botany and metabolism of alkaloids, phenolics and terpenes.*, (pp. 1755-1788). New Delhi: Springer-Verlag.

Payne, M., Hurst, W., Stuart, D., Ou, B., Fan, E., Ji, H., & Kou, Y. (2010). Determination of total procyanidins in selected chocolate and confectionery products using DMAC. *J AOAC Int, 93*(1), 89-96. doi:10.1093/jaoac/93.1.89.

Phillips, K., Pehrsson, P., Agnew, W., Scheett, A., Follett, J., Lukaski, H., & Patterson, K. (2014). Nutrient composition of selected traditional United States Northern plains native American plant foods. *Journal of Food Composition and Analysis, 34*(2), 136-152. doi:10.1016/j.jfca.2014.02.010.

Pierre, J., Heneghan, A., Feliciano, R., Shanmuganayagam, D., Roenneburg, D., Krueger, C., Reed, J., & Kudsk, K. (2013). Cranberry proanthocyanidins improve the gut mucous layer morphology and function in mice receiving elemental enteral nutrition. *JPEN J Parenter Enteral Nutr, 37*(3), 401-409. doi:10.1177/0148607112463076.

Porter, L., Hrstich, L., & Chan, B. (1985). The conversion of procyanidins and prodelphinidins to cyanidin and delphinidin. *Phytochemistry, 25*(1), 223-230. doi:10.1016/S0031-9422(00)94533-3.

Porter, M., Krueger, C., Wiebe, D., Cunningham, D., & Reed, J. (2001). Cranberry proanthocyanidins associate with low-density lipoprotein and inhibit in vitro Cu2+-induced oxidation. *Journal of the Science of Food and Agriculture, 81*(14), 1306-1313. doi:10.1002/jsfa.940.

Poupard, P., Sanoner, P., Baron, A., Renard, C., & Guyot, S. (2011). Characterization of procyanidin B2 oxidation products in an apple juice model solution and confirmation of their presence in apple juice by high-performance liquid chromatography coupled to electrospray ion trap mass spectrometry. *Journal of Mass Spectrometry, 46*(11), 1186-1197. doi:10.1002/jms.2007.

Price, M., Van Scoyoc, S., & Butler, L. (1978). A critical evaluation of the vanillin reaction as an assay for tannin in sorghum grain. *Journal of agricultural and food chemistry, 26*(5), 1214-1218. doi:10.1021/jf60219a031.

Prior, R., Fan, E., Ji, H., Howell, A., Nio, C., Payne, M., & Reed, J. (2010). Multi-laboratory validation of a standard method for quantifying proanthocyanidins in cranberry powders. *Journal of the Science of Food and Agriculture, 90*(9), 1473-1478. doi:10.1002/jsfa.3966.

Quideau, S., Deffieux, D., Douat-Casassus, C., & Pouysegu, L. (2011). Plant polyphenols: Chemical properties, biological activities, and synthesis. *Angewandte Chemie International Edition, 50*(3), 586-621. doi:10.1002/anie.201000044.

Reed, J., Krueger, C., & Vestling, M. (2005). MALDI-TOF mass spectrometry of oligomeric food polyphenols. *Phytochemistry, 66*(18), 2248-2263. doi:10.1016/j.phytochem.2005.05.015.

Rigaud, J., Escribano-Bailon, M., Prieur, C., Souquet, J., & Cheynier, V. (1993). Normal-phase high-performance liquid chromatographic separation of procyanidins from cacao beans and grape seeds. *Journal of Chromatography A, 654*(2), 255-260. doi:10.1016/0021-9673(93)83368-3.

Robbins, R., Leonczak, J., Johnson, J., Li, J., Kwik-Uribe, C., Prior, R., & Gu, L. (2009). Method performance and multi-laboratory assessment of a normal phase high pressure liquid chromatography–fluorescence detection method for the quantitation of flavanols and procyanidins in cocoa and chocolate containing samples. *Journal of Chromatography A, 1216*(24), 4831-4840. doi:10.1016/j.chroma.2009.04.006.

Sanoner, P., Guyot, S., Marnet, N., Molle, D., & Drilleau, J. (1999). Polyphenol profiles of french cider apple varieties (*Malus domestica* sp.). *Journal of agricultural and food chemistry, 47*(12), 4847-4853. doi:10.1021/jf990563y.

Schaneberg, B., Brown, P., Bzhelyansky, A., Chang, T., Cunningham, D., Gu, L., Haesaerts, G., Howell, A., Johnson, H., & Konings, E. (2017). AOAC SMPR® 2017.003. *J AOAC Int, 100*(4), 1208-1209. doi:10.5740/jaoacint.SMPR2017_003.

Schaneberg, B., Brown, P., Bzhelyansky, A., Chang, T., Cunningham, D., Gu, L., Haesaerts, G., Howell, A., Johnson, H., Konings, E., Krueger, C., Liu, H., Merkh, K., Phillips, M., Phillips, T., Reed, J., Rimmer, C., Szpylka, J., Yadlapalli, S., & Coates, S. (2017). AOAC SMPR® 2017.004. *J AOAC Int, 100*(4), 1210-1211. doi:10.5740/jaoacint.SMPR2017_004.

Shoji, T., Mutsuga, M., Nakamura, T., Kanda, T., Akiyama, H., & Goda, Y. (2003). Isolation and structural elucidation of some procyanidins from apple by low-temperature nuclear magnetic resonance. *Journal of agricultural and food chemistry, 51*(13), 3806-3813. doi:10.1021/jf0300184.

Sinha, N., Sidhu, J., Barta, J., Wu, J., & Cano, M. (2012). *Handbook of fruits and fruit processing* (Second ed.): John Wiley & Sons.

Sintara, M., Wang, Y., Li, L., Liu, H., Cunningham, D., Prior, R., Chen, P., Chang, T., & Wu, X. (2020). Quantification of cranberry proanthocyanidins by normal-phase high-performance liquid chromatography using relative response factors. *Phytochemical Analysis*. doi:10.1002/pca.2952.

Stafford, H. (1990). *Flavonoid metabolism*: CRC press.

Stewart, J., Mould, F., & Mueller-Harvey, I. (2000). The effect of drying treatment on the fodder quality and tannin content of two provenances of Calliandra calothyrsus Meissner. *Journal of the Science of Food and Agriculture, 80*(10), 1461-1468. doi:10.1002/1097-0010(200008)80:10<1461::AID-JSFA672>3.0.CO;2-R.

Tanaka, T., Kondou, K., & Kouno, I. (2000). Oxidation and epimerization of epigallocatechin in banana fruits. *Phytochemistry, 53*(2), 311-316. doi:10.1016/s0031-9422(99)00533-6.

USDA. (2017). United States Department of Agricultural - *Vaccinium* crop vulnerability statement part 2: Cranberries small fruit crop germplasm committee. In). https://www.ars-grin.gov/npgs/cgc_reports/cranberry_vulnerability_statement_2017.pdf.

USDA. (2020a). United States Department of Agricultural - Agricultural marketing resource center. In).

USDA. (2020b). United States Department of Agricultural - National agricultural statistics service - Cranberries. In).

Wang, Y., Singh, A., Hurst, W., Glinski, J., Koo, H., & Vorsa, N. (2016). Influence of degree-of-polymerization and linkage on the quantification of proanthocyanidins using 4-dimethylaminocinnamaldehyde (DMAC) assay. *Journal of agricultural and food chemistry, 64*(11), 2190-2199. doi:10.1021/acs.jafc.5b05408.

Weh, K., Clarke, J., & Kresty, L. (2016). Cranberries and cancer: An update of preclinical studies evaluating the cancer inhibitory potential of cranberry and cranberry derived constituents. *Antioxidants, 5*(3), 27. doi:10.3390/antiox5030027.

Winkel-Shirley, B. (2002). Biosynthesis of flavonoids and effects of stress. *Current opinion in plant biology, 5*(3), 218-223. doi:10.1016/S1369-5266(02)00256-X.

Zhang, C., Sun, J., & Chen, P. (2017). A computational tool for accelerated analysis of oligomeric proanthocyanidins in plants. *Journal of Food Composition and Analysis, 56*, 124-133. doi:10.1016/j.jfca.2016.11.014.

FLAVONES
(1)

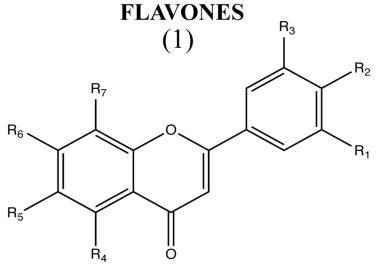

	R_1	R_2	R_3	R_4	R_5	R_6	R_7
Apigenin	H	OH	H	OH	H	OH	H
Luteolin	OH	OH	H	OH	H	OH	H
Tricetin	OH	OH	OH	OH	H	OH	H
Primuletin	H	H	H	OH	H	H	H
Chrysin	H	H	H	OH	H	OH	H
Baicalein	H	H	H	OH	OH	OH	H
Hypolaetin	OH	OH	H	OH	H	OH	OH

ISOFLAVONES
(2)

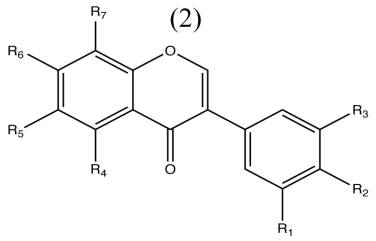

	R_1	R_2	R_3	R_4	R_5	R_6	R_7
Daidzein	H	OH	H	H	H	OH	H
Genistein	H	OH	H	OH	H	OH	H
Glycitein	H	OH	H	H	OCH_3	OH	H
Biochanin A	H	OCH_3	H	OH	H	OH	H
Formononetin	H	OCH_3	H	H	H	OH	H

FLAVONOLS
(3)

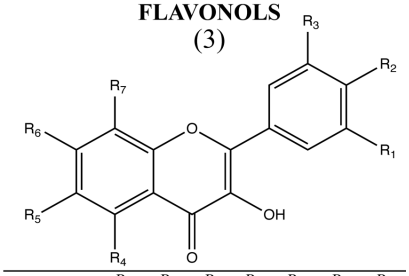

	R_1	R_2	R_3	R_4	R_5	R_6	R_7
Fisetin	OH	OH	H	H	H	OH	H
Galangin	H	H	H	OH	H	OH	H
Gossypetin	OH	OH	H	OH	H	OH	OH
Kaempferol	H	OH	H	OH	H	OH	H
Myricetin	OH	OH	OH	OH	H	OH	H
Quercetin	OH	OH	H	OH	H	OH	H

FLAVANONES
(4)

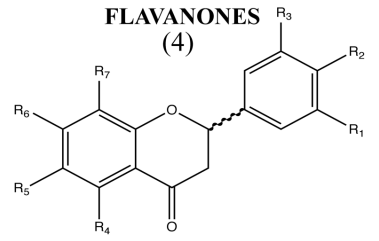

	R_1	R_2	R_3	R_4	R_5	R_6	R_7
Naringenin	H	OH	H	OH	H	OH	H
Pinocembrin	H	H	H	OH	H	OH	H
Butin	OH	OH	H	H	H	OH	H
Eriodictyol	OH	OH	H	OH	H	OH	H
Hesperetin	OH	OCH_3	H	OH	H	OH	H
Sterubin	OH	OH	H	OH	H	OCH_3	H

FLAVANONOLS
(5)

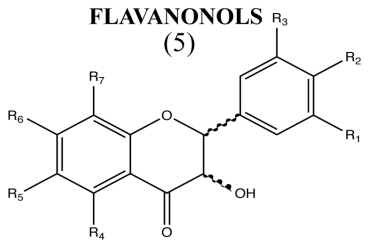

	R_1	R_2	R_3	R_4	R_5	R_6	R_7
Pinobanksin	H	H	H	OH	H	OH	H
Garbanzol	H	OH	H	H	H	OH	H
Aromadedrin	H	OH	H	OH	H	OH	H
Fustin	OH	OH	H	H	H	OH	H
Taxifolin	OH	OH	H	OH	H	OH	H
Ampelopsin	OH	OH	OH	OH	H	OH	H

ANTHOCYANIDINS
(6)

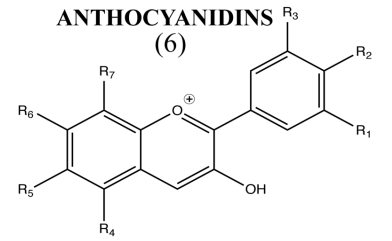

	R_1	R_2	R_3	R_4	R_5	R_6	R_7
Cyanidin	OH	OH	H	OH	H	OH	H
Delphinidin	OH	OH	OH	OH	H	OH	H
Pelargonidin	H	OH	H	OH	H	OH	H
Peonidin	OCH_3	OH	H	OH	H	OH	H
Petunidin	OCH_3	OH	OH	OH	H	OH	H
Malvidin	OCH_3	OH	OCH_3	OH	H	OH	H

FLAVANOLS
(7)

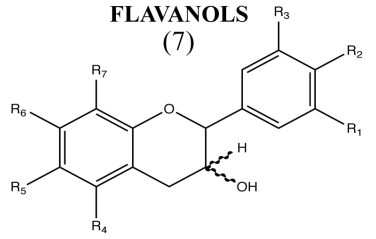

	R_1	R_2	R_3	R_4	R_5	R_6	R_7
Catechin	OH	OH	H	OH	H	OH	H
Afzelechin	H	OH	H	OH	H	OH	H
Gallocatechin	OH	OH	OH	OH	H	OH	H
Fisetinidol	OH	OH	H	H	H	OH	H
Guibourtinidol	H	OH	H	H	H	OH	H
Robinetinidol	OH	OH	OH	H	H	OH	H

Figure 1. Chemical structures of flavonoids.

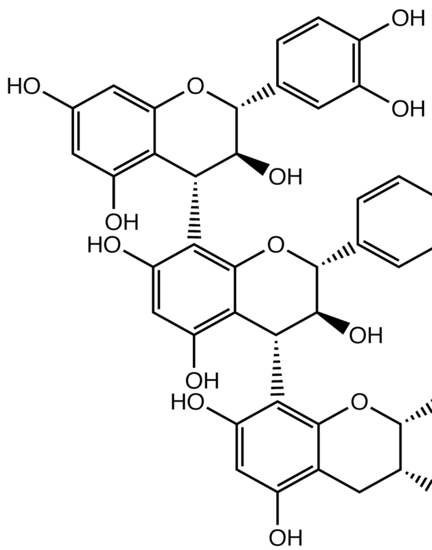

(8)

(+)-catechin-(4β→8)-(+)-catechin-(4β→8)-(-)-epicatechin

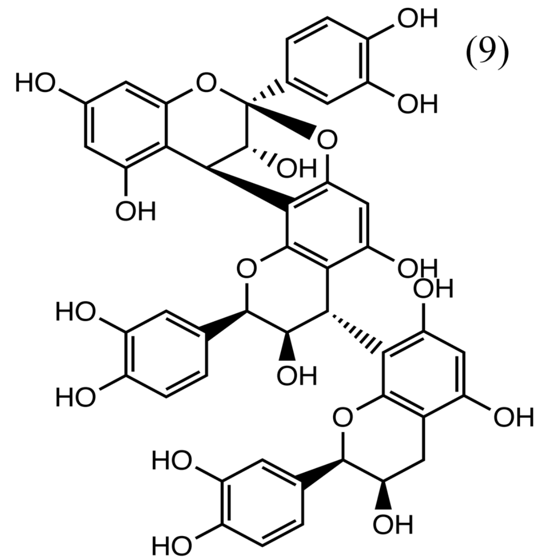

(9)

(-)-epicatechin-(2β→O→7, 4β→8)-(+)-epicatechin-(4β→8)-(+)-epicatechin

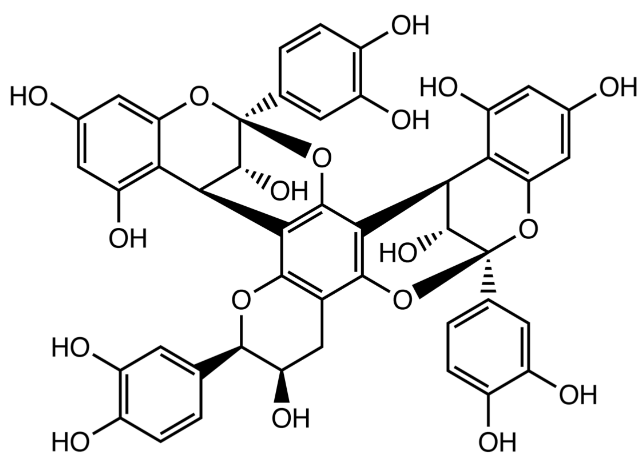

(10)

(-)-epicatechin-(2β→O→7, 4β→8)-(+)-epicatechin-(5→O→2β, 6→4β)-(-)-epicatechin

Figure 2. Chemical structures of PAC trimers with all B-type interflavan bonds (8), one A-type and one B-type interflavan bond (9), and all A-type interflavan bonds (10).

CHAPTER 1: Inter-laboratory validation of 4-(dimethylamino)cinnamaldehyde (DMAC) assay using cranberry proanthocyanidin standard for quantification of soluble proanthocyanidins in cranberry foods and dietary supplements, First Action Method: 2019.06

Andrew D. Birmingham[†], Daniel Esquivel-Alvarado[§], Michael Maranan[†], Christian G. Krueger[†,§,*,] and Jess D. Reed[†,§]

[†] Complete Phytochemical Solutions LLC, 3619 Hwy O, Cambridge, WI 53523, USA.

[§] University of Wisconsin-Madison, Reed Research Group, Dept. Animal Sciences, 1675 Observatory Drive, Madison, WI 53706, USA.

This chapter is published as-is in the *Journal of AOAC International, 2020*,

https://doi: 10.1093/jaoacint/qsaa084

ABSTRACT

Background: Proanthocyanidins (PAC) are oligomers and polymers of flavan-3-ols with putative health benefits. PAC are prevalent in a wide variety of natural products and dietary supplements. ***Objective:*** A inter-laboratory study was conducted to validate the 4-(dimethylamino)cinnamaldehyde (DMAC) colorimetric assay using a 96-well plate spectrophotometer for the accurate quantification of proanthocyanidins (PAC) in cranberry products and to evaluate the comparison of the procyanidin A2 (ProA2) dimer and cranberry PAC (c-PAC) reference standards. ***Methods:*** Four test materials analyzed in this study included cranberry fiber powder, cranberry extract powder, concentrated cranberry juice, and a purified cranberry PAC juice. The samples were homogenized, extracted, sonicated, centrifuged, and analyzed using a 96 well plate spectrophotometer. ***Results:*** The linearity for both ProA2 and c-PAC standards were determined from 4.053 to 50.666 µg/mL and from 13.520 to 135.95 µg/mL, respectively. The relative standard deviation of repeatability (RSD_r) values for the four materials analyzed using both ProA2 and c-PAC standards met the SMPR requirements. The inter-laboratory precision using the Hortwitz ratio (HorRat) values for the four materials analyzed using both ProA2 and c-PAC standards satisfies the acceptance range in Appendix K of the Official Methods of Analysis (2003): Guidelines for Dietary Supplements and Botanicals. The limit of quantification (LOQ) was estimated to be 3.16 µg/mL. The mean recovery for both ProA2 and c-PAC standards ranged from 98.0 to 102% and 100 to 103% respectively. ***Conclusions:*** The results produced from this study demonstrate the utility of the c-PAC standard over the ProA2 standard and the advantages of using a 96-well plate spectrophotometer for the accurate quantification of PAC.

INTRODUCTION

Proanthocyanidins (PAC), a class of polyphenols also referred to as condensed tannins, are oligomers and polymers of flavan-3-ols such as epicatechin and catechin (Reed, Krueger, & Vestling, 2005). PAC are named based on the conversion of the monomeric unit to the corresponding anthocyanidin during acid catalyzed autooxidation (Hummer & Schreier, 2008). Thus, the (epi)catechin oligomers yield cyanidin and are called procyanidins, (epi)gallocatechin yield delphinidin and are called prodelphinidins, and (epi)afzelechin yield pelargonidin and are called propelargonidins. PAC are also classified by the type of interflavan bonds. B-type PAC are linked by C_4-C_6 or C_4-C_8. A-type PAC are linked by C_4-C_8 and contain an additional ether interflavan bond C_2-O-C_7 (Foo, Lu, Howell, & Vorsa, 2000a, 2000b). Cranberry PAC are associated with the prevention of urinary tract infections. However, the exact mechanism of how this happens is not fully understood. Previous research suggests that this effect is related to the ability of PAC to adhere and attach to the virulence factors expressed by Extra-intestinal *Escherichia coli* (ExPEC) (Foo, Lu, Howell, & Vorsa, 2000a, 2000b; Alfaro-Viquez, Esquivel-Alvarado, Madrigal-Carballo, Krueger, & Reed, 2018; Alfaro-Viquez, Esquivel-Alvarado, Madrigal-Carballo, Krueger, & Reed, 2019). Feliciano *et al*., (2014) showed that A-type PAC have greater bioactivity than B-type PAC for increasing ExPEC agglutination and decreasing ExPEC invasion (Feliciano, Meudt, Shanmuganayagam, Krueger, & Reed, 2014;).

Cranberries are used to produce a variety of products such as: fresh and frozen whole fruit, beverages, sauces, sweetened dried cranberries, and nutritional supplements. The 4-(dimethylamino)cinnamaldehyde (DMAC) assay is used for the quantification of soluble PAC

(Hummer & Schreier, 2008; Krueger, Reed, Feliciano, & Howell, 2013). However, commercial standards based on dimers such as procyanidin A2 (ProA2) and procyanidin B2 (ProB2) are not accurate for the quantification of PAC (Feliciano, Shea, Shanmuganayagam, Krueger, Howell, & Reed, 2012). The use of dimers leads to the underestimation of cranberry PAC content because the complexity and heterogeneity of naturally occurring PAC leads to large differences in the reaction kinetics and extent of reaction of the dimers in comparison the PAC of higher degrees of polymerization and variations in interflavan bonds and patterns of substitution (Krueger, Chesmore, Chen, Parker, Khoo, Marais, et al., 2016). Previously, cranberry PAC (c-PAC) were derived from fresh cranberries and were developed as a customized reference standard in order to represent the complex heterogeneity of c-PAC containing products in the marketplace (Feliciano, Shea, Shanmuganayagam, Krueger, Howell, & Reed, 2012).

The DMAC assay is usually performed using a single absorbance measurement for each reaction at a single, specific time-point (Prior, Fan, Ji, Howell, Nio, Payne, et al., 2010). A 96-well plate absorbance reader is an alternative tool that allows for the observation of the results from the reaction kinetics of each sample and standard in real time. Products containing cranberry PAC are used in research and sold in the marketplace may have varied kinetics based on their production protocols, and/or source material. Maximum absorbance (A_{max}) measurements across unknown samples and standards over a sufficient period of time allow for a more accurate estimation of PAC to overcome these differences.

The 96-well plate DMAC assay is an improvement over the traditional single cuvette method. The 96-well plate method incorporates automated analyses leading to greater accuracy and precision. The 96-well plate method is also less costly to perform as it requires fewer personnel hours and less volume of reagents. The goals of this study were (a) to demonstrate the validity of the high-throughput method using two laboratories [Complete Phytochemical Solutions, LLC (CPS) and the University of Wisconsin-Madison (UW)] and two analysts for the quantification of soluble PAC (following the AOAC standard method performance requirements (SMPR) 2017.003) (Schaneberg, Brown, Bzhelyansky, Chang, Cunningham, Gu, et al., 2017) and (b) to determine the utility of the c-PAC standard over the ProA2 standard for the accurate quantification of PAC in a variety of cranberry products.

MATERIAL AND METHODS

Caution: Refer to the Material Safety Data Sheets for all chemicals prior to use. This method includes the use of hydrochloric acid. Use all appropriate personal protective equipment and follow good laboratory practices.

A. Principle of Method

The 4-(dimethylamino)cinnamaldehyde (DMAC) assay is used for the quantification of soluble PAC (Hummer & Schreier, 2008; Krueger, Reed, Feliciano, & Howell, 2013).

B. Sample Materials

(a) *Cranberry fiber powder.* --Low concentration solid: Obtained commercially from a raw ingredient manufacturer (Fruit d'Or, Villeroy, QC, Canada).

(b) *Cranberry extract powder (soluble powder enriched in PAC).* --High concentration solid: Obtained commercially from a raw ingredient manufacturer (Fruit d'Or, Villeroy, QC, Canada).

(c) *Cranberry juice concentrate.* --Low concentration liquid: Obtained commercially from a raw ingredient manufacturer (Neil Jones Food Company, Vancouver, WA, USA).

(d) *Cranberry PAC liquid. --30% (w/v);* High concentration liquid: Produced at UW laboratory.

C. Apparatus

(a) *Volumetric flasks.*--Used for reagent and standard preparations.

(b) *UV-Vis microplate reader.*--Capable of measuring kinetic reactions at 640 nm in a 96-well plate.

(c) *96-well plate.*

(d) *Ultrasonic bath.*

(e) *Vortex mixer.*

(f) *Balance, analytical.*--Minimum weighing capacity of 0.01 mg.

(g) *Bottle-top dispenser.*--Capable of dispensing 15 mL.

(h) *Centrifuge.*

(i) *Centrifuge tubes.*--50 mL HDPE plastic with screw caps.

D. Reagents

(a) *Solvents and chemicals.*--ACS grade glacial acetic acid; ACS grade acetone; ACS grade ethanol; ACS grade methanol; ACS grade concentrated hydrochloric acid; ProA2 standard (Sigma-Aldrich, >98% purity, CAS 6203-18-5, Lot#BCBZ5168); and cranberry-PAC (c-PAC) standard (>99.0% purity by the formaldehyde-HCl precipitation assay, MALDI-TOF MS spectrum in linear mode showed that c-PAC had a degree of polymerization ranged from 3 to 26) (Feliciano, Shea, Shanmuganayagam, Krueger, Howell, & Reed, 2012).

(b) *Deionized water.*--Resistivity of ≥1 mega-ohm/cm.

(c) *Acetic acid solution.*--2% (v/v), prepared by adding 20 mL of acetic acid to a 1 L volumetric flask and dilute to volume with deionized water.

(d) *Dilution solution.*--75% (v/v) reagent alcohol: prepared by adding 750 mL of reagent alcohol to a 1 L volumetric flask and diluting to volume with deionized water.

(e) *Reaction Buffer*.--12.5% (v/v) concentrated hydrochloric acid, 75% reagent alcohol: prepared by adding 125 mL of concentrate hydrochloric acid and 125 mL of deionized water in a 1 L volumetric flask and diluting to volume with reagent alcohol.

(f) *4-(dimethylamino)cinnamaldehyde (DMAC) solution*.--0.1% (w/v): prepared by weighing 25 mg DMAC (Sigma-Aldrich, ≥97.5% purity, CAS 6203-18-5, Lot#BCBS7544V) in a 25 mL volumetric flask and dissolving to volume with reaction buffer.

(g) *ProA2 standard solutions.*--(1) *Stock solution.*--500 µg/mL: accurately weigh 5 mg ProA2 into a 10 mL volumetric flask and dilute to volume with methanol. Final calculated concentration of the stock solution may require adjustment based on manufacturer's claim of purity. (2) *Working standard solutions.*--Dilute stock standard to 4, 10, 20, 30, 40, and 50 µg/mL with dilution solution using volumetric flask.

(h) *cranberry PAC (c-PAC) standard solutions.*--(1) *Stock solution.* 0.9013 mg/mL: accurately weigh 9 mg c-PAC standard into a 10 mL volumetric flask and dilute to volume with methanol. (2) *Working standard solutions*.--Dilute stock standard to 13.5, 27.0, 54.0, 81.0, 108, and 135 µg/mL with dilution solution using volumetric flask.

E. Sample Extraction

(a) *Cranberry extract powder.*--Weigh 100 mg sample into 50 mL centrifuge tube and add 5 mL acetic acid solution. Vortex tube and sonicate for 10 minutes. Add 15 mL acetone, vortex, and sonicate for 30 minutes. Centrifuge tube at 1800g for 10 minutes at 20 °C. Dilute extracted solutions as necessary with dilution solution.

(b) *Cranberry fiber powder.*--Weigh 500 mg sample into 50 mL centrifuge tube and add 5 mL acetic acid solution. Vortex tube and bath sonicate for 10 minutes. Add 15 mL acetone, vortex, and sonicate for 30 minutes. Centrifuge tube at 1800g for 10 minutes at 20°C. Dilute extracted solutions as necessary with dilution solution.

(c) *Cranberry juice concentrate.*--Dilute juice as necessary with dilution solution.

(d) *30% (w/v) PAC laboratory produced cranberry liquid.*--SMPR 2017.003 calls for the evaluation of cranberry juice that contains >15% PAC (w/v) (Schaneberg, et al., 2017). There are no juice products in the commercial market that meet this criterion. Thus, we created a 30% (w/v) PAC laboratory based juice using purified PAC isolated from cranberry fruit by methods previously described by Feliciano *et al* 2012 (Feliciano, Shea, Shanmuganayagam, Krueger, Howell, & Reed, 2012). Weigh 300 mg isolated cranberry PAC into a microfuge tube and add 1 mL water. Vortex tube and sonicate to ensure PAC is completely solubilized. Dilute juice as necessary with dilution solution.

F. Analysis

Transfer 70 µL of dilution solution (blank), standards, and samples into desired wells of a 96-well plate. Transfer 210 µL of 0.1% (w/v) DMAC solution into each well. Plate is shaken for 10 seconds at 600 shakes per minute and read at an absorbance of 640 nm every 1 minute for 30 minutes at 25°C. The concentration is calculated at maximum absorbance (A_{max}) (SM 1).

G. Calculations

The results are calculated from the ProA2 standard curve and the c-PAC standard curve by plotting the absorbance values on a linear y-axis and the concentration of PAC on a linear x-axis. The PAC concentration for powder samples (w/w) is calculated using the following equation:

$$Total\ soluble\ PAC\ \left(\frac{mg}{g}\right) = \frac{\frac{y - A}{B} \times DV}{M}$$

where y is the maximum absorbance at 640 nm, A is the intercept, B is the slope, D is the dilution factor, V is the extraction volume (mL), and M is the sample mass (g).

The PAC concentration for liquid samples (w/v) is calculated using the following equation:

$$Total\ soluble\ PAC\ \left(\frac{mg}{mL}\right) = \frac{y - A}{B} \times D$$

where y is the maximum absorbance, A is the intercept, B is the slope, and D is the dilution factor.

H. Method Validation and Statistical Analysis

Validation of this method was conducted according to the ICH Harmonized Tripartite Guideline Validation of Analytical Procedures: Text and Methodology Q2(R1) (Guideline, 2005), following the acceptability criteria AOAC SMPR.003 shown in Table 1 (Schaneberg, et al., 2017). Statistical analysis was performed using RStudio (version 1.2.1335). The function lm() was used to create the regression model and the function plot() was used to evaluated the regression diagnostics plots.

RESULTS AND DISCUSSION

Linearity

Six concentrations of ProA2 standard (4.0530, 10.133, 20.266, 30.400, 40.533, and 50.666 µg/mL) and six concentrations of the c-PAC standard (13.520, 27.039, 54.078, 81.117, 108.16, and 135.95 µg/mL) were used. The absorbance at each concentration was determined to prepare the standard curves for both laboratories. The correlation coefficients, slopes, and intercepts for both ProA2 and c-PAC standards are shown in Figure 1 and Table 2. For both laboratories, the regression curves for ProA2 were greater than 0.9985, and for c-PAC the regression curves were greater than 0.9942. In addition, the linearity for the four standard curves were checked using four plots: residuals vs fitted, normal Q-Q, scale-location, and residuals vs leverage (SM 2-5).

Repeatability Precision

Each sample consisted of 3 different concentrations with 3 replicates per concentration were analyzed by each of the two laboratories. The cranberry fiber powder had relative standard deviation of repeatability (RSD_r) values less than 5.3% for the c-PAC standard and less than 5.7% for the ProA2 standard for both laboratories (Table 3). This satisfies the acceptance criteria of $RSD_r \leq 15\%$ for the low concentration powder (Table 1). The cranberry extract powder had RSD_r values less than 3.8% for the c-PAC standard and less than 4.1% for the ProA2 standard for both laboratories (Table 4). This satisfies the acceptance criteria of $RSD_r \leq 10\%$ for the high concentration powder (Table 1). The cranberry juice concentrate (liquid) had RSD_r values of less than 1.7% for the c-PAC standard and less than 1.9% for the ProA2 standard for both laboratories

(Table 5). This satisfies the acceptance criteria of $RSD_r \leq 10\%$ for the low concentration liquid (Table 1). The 30% (w/v) PAC laboratory produced liquid had RSD_r values of less than 3.2% for the c-PAC standard and less than 3.4% for the ProA2 standard for both laboratories (Table 6). This satisfies the acceptance criteria of $RSD_r \leq 5\%$ for the high concentration liquid (Table 1).

Inter-laboratory Precision

Inter-laboratory precision was evaluated by performing the analysis on two different days by two different laboratories, and by two different analysts. The inter-laboratory precision was evaluated following the Appendix K of the AOAC Official Methods of Analysis (2003): Guidelines for Dietary Supplements and Botanicals (AOAC, 2013). The inter-laboratory precision was assessed using the Horwitz ratio ($HorRat_R$) values. (Horwitz & Albert, 2006). The summarized results for the inter-laboratory precision are found in Table 7. The low concentration powder, the high concentration powder, the low concentration liquid, and the high concentration liquid had $HorRat_R$ values greater than 0.5 to less than 1.6. This satisfies the acceptance criteria for the $HorRat_R$ values, which are set from 0.5 to 2.0.

Accuracy

The accuracy of the method was evaluated by providing nine determinations at three different concentrations for each sample at each laboratory. The average recoveries of all the concentrations for the samples were between 98.0 and 103.2% for both the ProA2 standard and the c-PAC standard (Table 8).

Limit of Quantitation

The limit of quantitation (LOQ) was determined by preparing and analyzing three separate low concentrations (1.58, 3.16, and 6.31 µg/mL) of c-PAC standard at both laboratories using 6 replicates at each laboratory. Table 9 shows that the 3.16 µg/mL and 6.31 µg/mL concentrations yielded absorbance values with an RSD of ≤10% at both laboratories. The 1.58 µg/mL concentration yielded absorbance values with an RSD of >10% at the CPS laboratory. Therefore, the LOQ was estimated to be 3.16 µg/mL.

CONCLUSION

Accurate quantification of soluble PAC in cranberry products is crucial to the nutritional supplement industry to enable them to meet regulatory requirements and design well informed clinical studies that support structure / function claims. Results of this study show that the use of both ProA2 and c-PAC standards meet the SMPR 2017.003 acceptance criteria (Schaneberg, et al., 2017). However, as previously reported (Feliciano, Shea, Shanmuganayagam, Krueger, Howell, & Reed, 2012; Krueger, Reed, Feliciano, & Howell, 2013) the use of ProA2 standard as a means of quantifying PAC results in an underestimation when compared to the more accurate c-PAC standard when using the DMAC assay. Additionally, the use of 96-well plate reader is an improvement over the use of a single cuvette reader as it allows for the observation of the reaction kinetics of the samples and standards in an automated, high-throughput manner with greater accuracy and precision.

Our inter-laboratory, multiple analyst approach validated the use and efficiency of the 96-well plate as well as the utility of the c-PAC standard over the ProA2 standard for the accurate quantification of soluble PAC. These improvements to the DMAC method conform to the repeatability precision, inter-laboratory precision, recovery, and LOQ requirements of SMPR 2017.003 (Schaneberg, et al., 2017). The high concentrated liquid has been identified as problematic in that no known liquid product in the 15-55% (w/v) PAC range exists in the marketplace and had to be laboratory produced in an attempt to meet the requirements of SMPR 2017.003 (Schaneberg, et al., 2017). We conclude that the use of the 96-well plate method and the

use of the c-PAC reference standard are suitable and advantageous improvements to the current methods of soluble PAC.

CONFLICT OF INTEREST

The authors declare the following competing financial interest(s): Christian G. Krueger and Jess D. Reed have ownership interest in Complete Phytochemical Solutions, LLC, and acknowledge their affiliation with this company.

ACKNOWLEDGMENTS

The authors acknowledge financial support from the Ministry of Science, Technology and Telecommunications (MICITT), Innovation and Human Capital Program for Competitiveness (PINN), and the National Council for Scientific and Technology Research (CONICIT) (Grant number PED-056-2015-I) at Costa Rica. The authors thank Fruit d'Or and Neil Jones Food Company for their help in supplying the samples.

AUTHORSHIP CONTRIBUTION STATEMENT

Andrew D. Birmingham: Conceptualization, Methodology, Formal Analysis, Writing – original draft, Writing – review & editing. **Daniel Esquivel-Alvarado:** Conceptualization, Methodology, Formal analysis, Investigation, Data curation, Writing - original draft, Writing - review & editing, Visualization. **Michael Maranan:** Investigation. **Christian G. Krueger:** Conceptualization,

Writing - review & editing, Funding acquisition. **Jess D. Reed:** Conceptualization, Writing - review & editing, Supervision, Funding acquisition.

REFERENCES

Alfaro-Viquez, E., Esquivel-Alvarado, D., Madrigal-Carballo, S., Krueger, C., & Reed, J. (2018). Cranberry proanthocyanidin-chitosan hybrid nanoparticles as a potential inhibitor of extra-intestinal pathogenic *Escherichia coli* invasion of gut epithelial cells. *International Journal of Biological Macromolecules*, 111, 415-420. doi:10.1016.j.ijbiomac.2018.01.033

Alfaro-Viquez, E., Esquivel-Alvarado, D., Madrigal-Carballo, S., Krueger, C., & Reed, J. (2019). Proanthocyanidin-chitosan composite nanoparticles prevent bacterial invasion and colonization of gut epithelial cells by extra-intestinal pathogenic *Escherichia coli*. *International Journal of Biological Macromolecules, 135, 630-636*. doi:10.1016/j.ijbiomac.2018.04.170

AOAC. (2013). Appendix K: Guidelines for Dietary Supplements and Botanicals. AOAC International.

Feliciano, R., Meudt, J., Shanmuganayagam, D., Krueger, C., & Reed, J. (2014). Ratio of "A-type" to "B-type" proanthocyanidin interflavan bonds affects extra-intestinal pathogenic *Escherichia coli* invasion of gut epithelial cells. *Journal of Agricultural and Food Chemistry, 62*(18), 3919-3925. doi:10.1021/jf403839a

Feliciano, R., Shea, M., Shanmuganayagam, D., Krueger, C., Howell, A., & Reed, J. (2012). Comparison of isolated cranberry (*Vaccinium macrocarpon* Ait.) proanthocyanidins to catechin and procyanidins A2 and B2 for use as standards in the 4-(dimethylamino)cinnamaldehyde assay. *Journal of Agricultural and Food Chemistry, 60*(18), 4578-4585. doi:10.1021/jf3007213

Foo, L., Lu, Y., Howell, A., & Vorsa, N. (2000a). The structure of cranberry proanthocyanidins which inhibit adherence of uropathogenic P-fimbriated *Escherichia coli in vitro*. *Phytochemistry, 54*(2), 173-181. doi:10.1016/s0031-9422(99)00573-3

Foo, L., Lu, Y., Howell, A., & Vorsa, N. (2000b). A-Type proanthocyanidin trimers from cranberry that inhibit adherence of uropathogenic P-fimbriated *Escherichia coli*. *Journal of Natural Products, 63*(9), 1225-1228. doi:10.1021/np000128u

Guideline, I. (2005). Validation of analytical procedures: text and methodology Q2(R1). *International Conference on Harmonization*, (pp. 1-13).

Horwitz, W., & Albert, R. (2006). The Horwitz ratio (HorRat): a useful index of method performance with respect to precision. *Journal of AOAC International, 89*(4), 1095-1109.

Hummer, W., & Schreier, P. (2008). Analysis of proanthocyanidins. *Molecular Nutrition & Food Research, 52*(12), 1381-1398. doi:10.1002/mnfr.200700463

Krueger, C., Chesmore, N., Chen, X., Parker, J., Khoo, C., Marais, J., Shanmuganayagam, D., Crump, P., & Reed, J. (2016). Critical reevaluation of the 4-(dimethylamino) cinnamaldehyde assay: cranberry proanthocyanidin standard is superior to procyanidin A2 dimer for accurate quantification of proanthocyanidins in cranberry products. *Journal of Functional Foods, 22*, 13-19. doi:10.1016/j.jff.2016.01.017

Krueger, C., Reed, J., Feliciano, R., & Howell, A. (2013). Quantifying and characterizing proanthocyanidins in cranberries in relation to urinary tract health. *Analytical and Bioanalytical Chemistry, 405*(13), 4385-4395. doi:10.1007/s00216-013-6750-3

Prior, R., Fan, E., Ji, H., Howell, A., Nio, C., Payne, M., & Reed, J. (2010). Multi-laboratory validation of a standard method for quantifying proanthocyanidins in cranberry powders. *Journal of the Science of Food and Agriculture, 90*(9), 1473-1478. doi:10.1002/jsfa.3966

Reed, J., Krueger, C., & Vestling, M. (2005). MALDI-TOF mass spectrometry of oligomeric food polyphenols. *Phytochemistry, 66*(18), 2248-2263. doi:10.1016/j.phytochem.2005.05.015

Schaneberg, B., Brown, P., Bzhelyansky, A., Chang, T., Cunningham, D., Gu, L., Haesaerts, G., Howell, A., Johnson, H., & Konings, E. (2017). AOAC SMPR® 2017.003. *Journal of AOAC International, 100*(4), 1208-1209. doi:10.5740/jaoacint.SMPR2017_003

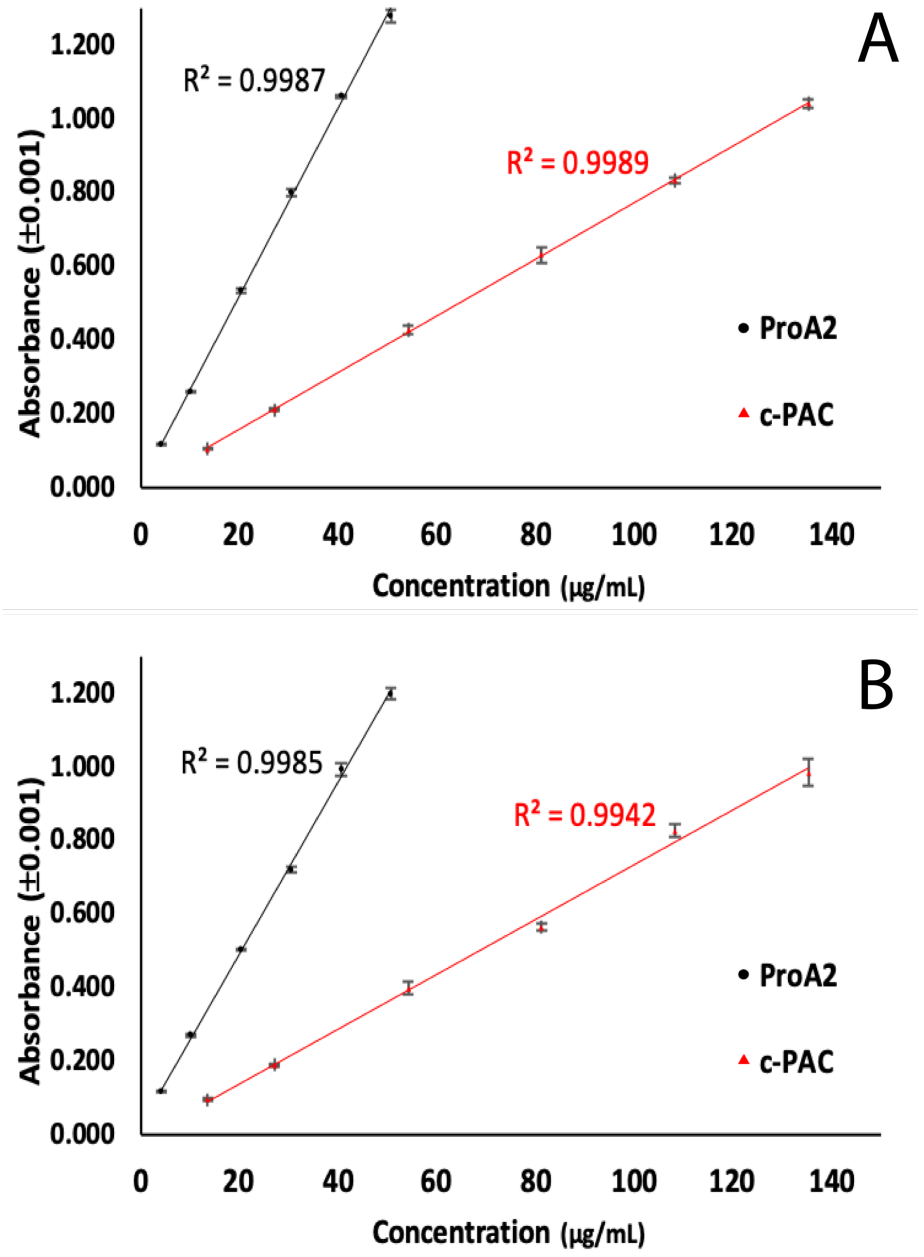

Figure 1. Regression curves for ProA2 and c-PAC after reaction with 4-(dimethylamino)cinnamaldehyde for CPS laboratory (A) and UW laboratory (B). The slope of the ProA2 standard at CPS laboratory and UW laboratory is higher than the c-PAC slope by 3.14 and 3.28 fold, respectively. This results in an underestimation of PAC by ProA2 in comparison to c-PAC.

Table 1. Acceptance criteria for method performance criteria (AOAC SMPR 2017.003).

	Liquids (w/v)		Solids (w/w)	
Range, %	0.03-15	>15-55	0.03-15	>15-55
Rec., %	97-103	97-103	90-107	97-103
RSD_r, %	≤10	≤5	≤15	≤10
RSD_R, %	≤15	≤8	≤20	≤15

Table 2. Calibration curves of ProA2 and c-PAC standards.

Standard	Laboratory	Adjusted-R^2	Slope	Intercept
Pro A2	CPS	0.9987	0.0253	0.0166
	UW	0.9985	0.0233	0.0277
c-PAC	CPS	0.9989	0.0077	0.0053
	UW	0.9942	0.0074	-0.0082

Table 3. Repeatability precision using ProA2 and c-PAC standards for the quantification of PAC from cranberry fiber powder (Range, 0.03-15% (w/w)).

Replicate	Dilution Factor	CPS Laboratory			UW Laboratory		
		Absorbance	ProA2 Standard, mg/g	c-PAC Standard, mg/g	Absorbance	ProA2 Standard, mg/g	c-PAC Standard, mg/g
A		0.852	33.0	110.3	0.817	33.5	110.2
B	25	0.875	33.9	113.3	0.840	34.5	113.3
C		0.860	33.3	111.4	0.805	33.0	108.6
Mean			33.4	111.7		33.7	110.7
RSD_r, %			1.4	1.4		2.2	2.1
D		0.515	31.5	106.2	0.500	32.1	108.6
E	40	0.511	31.3	105.4	0.535	34.5	116.1
F		0.513	31.4	105.8	0.557	36.0	120.8
Mean			31.4	105.8		34.2	115.2
RSD_r, %			0.4	0.4		5.7	5.3
G		0.213	31.1	108.2	0.218	32.3	120.8
H	100	0.212	30.9	107.7	0.215	31.8	119.2
I		0.214	31.2	108.8	0.224	33.4	124.0
Mean			31.1	108.2		32.5	121.3
RSD_r, %			0.5	0.5		2.4	2.0

Table 4. Repeatability precision using ProA2 and c-PAC standards for the quantification of PAC from cranberry extract powder (Range, >15-55% (w/w)).

		CPS Laboratory			UW Laboratory		
Replicate	Dilution Factor	Absorbance	ProA2 Standard, mg/g	c-PAC Standard, mg/g	Absorbance	ProA2 Standard, mg/g	c-PAC Standard, mg/g
A		0.743	112.9	377.8	0.693	112.0	370.9
B	20	0.725	110.1	368.6	0.682	110.1	365.1
C		0.710	107.8	360.9	0.728	117.9	389.4
Mean			110.3	369.1		113.4	375.1
RSD_r, %			2.3	2.3		3.6	3.4
D		0.409	122.0	413.5	0.345	106.8	373.7
E	40	0.411	122.6	415.6	0.352	109.2	381.1
F		0.418	124.8	422.8	0.367	114.2	396.9
Mean			123.1	417.3		110.1	383.9
RSD_r, %			1.2	1.2		3.4	3.1
G		0.166	116.1	411.5	0.154	106.3	429.0
H	100	0.157	109.1	388.5	0.152	104.6	423.7
I		0.155	107.6	383.4	0.155	107.1	431.6
Mean			110.9	394.5		106.0	428.1
RSD_r, %			4.1	3.8		1.2	0.9

Table 5. Repeatability precision using ProA2 and c-PAC standards for the quantification of PAC from cranberry juice concentrate (Range, 0.03-15% (w/v)).

		CPS Laboratory			UW Laboratory		
Replicate	Dilution Factor	Absorbance	ProA2 Standard, mg/mL	c-PAC Standard, mg/mL	Absorbance	ProA2 Standard, mg/mL	c-PAC Standard, mg/mL
A		0.712	5.5	18.4	0.677	5.6	18.5
B	200	0.709	5.5	18.3	0.681	5.6	18.6
C		0.711	5.5	18.4	0.691	5.7	18.9
Mean			5.5	18.4		5.6	18.6
RSD_r, %			0.2	0.2		1.1	1.0
D		0.373	5.6	19.2	0.349	5.5	19.3
E	400	0.361	5.4	18.5	0.348	5.5	19.2
F		0.370	5.6	19.0	0.338	5.3	18.7
Mean			5.6	18.9		5.4	19.1
RSD_r, %			1.8	1.7		1.9	1.7
G		0.189	5.5	19.1	0.179	5.2	20.2
H	800	0.187	5.4	18.9	0.176	5.1	19.9
I		0.188	5.4	19.0	0.178	5.2	20.1
Mean			5.4	19.0		5.2	20.1
RSD_r, %			0.6	0.5		1.0	0.8

Table 6. Repeatability precision using ProA2 and c-PAC standards for the quantification of PAC from 30% (w/v) PAC laboratory liquid (Range, 15-55% (w/v)).

		CPS Laboratory			UW Laboratory		
Replicate	Dilution Factor	Absorbance	ProA2 Standard, mg/mL	c-PAC Standard, mg/mL	Absorbance	ProA2 Standard, mg/mL	c-PAC Standard, mg/mL
A		0.876	84.9	283.5	0.798	82.7	271.9
B	2500	0.858	83.1	277.6	0.848	88.0	288.7
C		0.850	82.4	275.0	0.841	87.3	286.4
Mean			83.5	278.7		86.0	282.3
RSD_r, %			1.6	1.6		3.4	3.2
D		0.623	95.9	321.8	0.527	85.7	288.8
E	4000	0.624	96.0	322.3	0.521	84.7	285.5
F		0.601	92.4	310.3	0.534	86.9	292.5
Mean			94.8	318.1		85.8	288.9
RSD_r, %			2.2	2.1		1.3	1.2
G		0.299	89.3	306.0	0.259	79.4	288.3
H	8000	0.301	89.9	308.1	0.262	80.4	291.6
I		0.314	94.0	321.6	0.266	81.8	295.9
Mean			91.1	311.9		80.6	291.9
RSD_r, %			2.8	2.7		1.5	1.3

Table 7. Inter-laboratory precision using ProA2 and c-PAC standards for the quantification of PAC from cranberry fiber powder (Range, 0.03-15% (w/w)), cranberry extract powder (Range, >15-55% (w/w)), cranberry juice concentrate (Range, 0.03-15% (w/v)), and 30% (w/v) PAC laboratory liquid (Range, 15-55% (w/v)).

Cranberry Fiber Powder Range, 0.03-15% (w/w))			Cranberry Extract Powder (Range, >15-55% (w/w))			Cranberry Juice Concentrate (Range, 0.03-15% (w/v))			PAC Laboratory Liquid (Range, 15-55% (w/v))		
Dilution Factor	ProA2	c-PAC	Dilution Factor	ProA2	c-PAC	Dilution Factor	ProA2	c-PAC	Dilution Factor	ProA2	c-PAC
	$HorRat_{(R)}$			$HorRat_{(R)}$			$HorRat_{(R)}$			$HorRat_{(R)}$	
25	1.2	1.2	20	1.0	1.3	200	1.5	0.9	2500	1.0	0.6
40	1.2	1.2	40	1.0	1.2	400	1.6	0.8	4000	1.0	0.6
100	1.2	1.0	100	1.0	1.0	800	1.6	0.7	8000	1.0	0.5

Table 8. Accuracy of inter-laboratory and analyst's analysis.

	Cranberry fiber powder		Cranberry extract powder		Cranberry juice concentrate		Purified cranberry PAC juice	
Standard	Pro A2	c-PAC	Pro A2	c-PAC	Pro A2	c-PAC	Pro A2	c-PAC
Average CPS recovery %	100.0	100.0	102.0	103.2	100.0	101.1	100.0	100.0
Average UW recovery %	99.7	102.2	98.4	102.6	98.0	101.6	98.9	100.9

Table 9. Determination of the limit of quantitation (LOQ) based on six replicates of each concentration at each laboratory.

	CPS Laboratory			UW Laboratory		
Concentration (µg/mL)	6.31	3.16	1.58	6.31	3.16	1.58
RSD, %	2.67	4.57	20.9	5.30	2.50	3.96

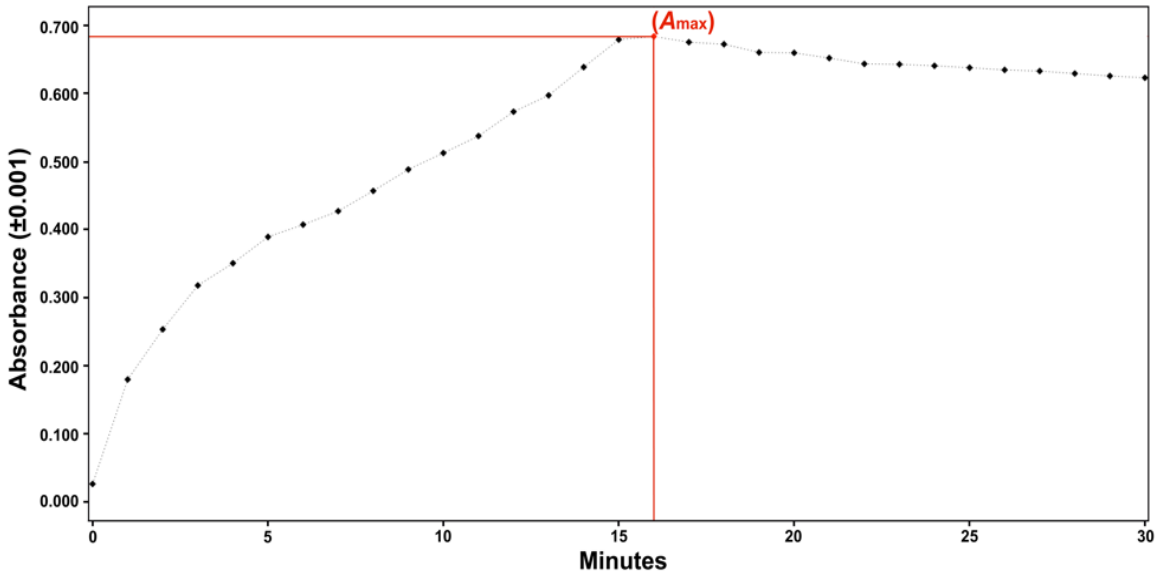

SM 1. Representative reaction kinetic of a cranberry PAC sample measured with the 4-(dimethylamino)cinnamaldehyde (DMAC) assay. Quantification of soluble proanthocyanidins is based on the maximum absorbance (A_{max}) during the 30 min time period.

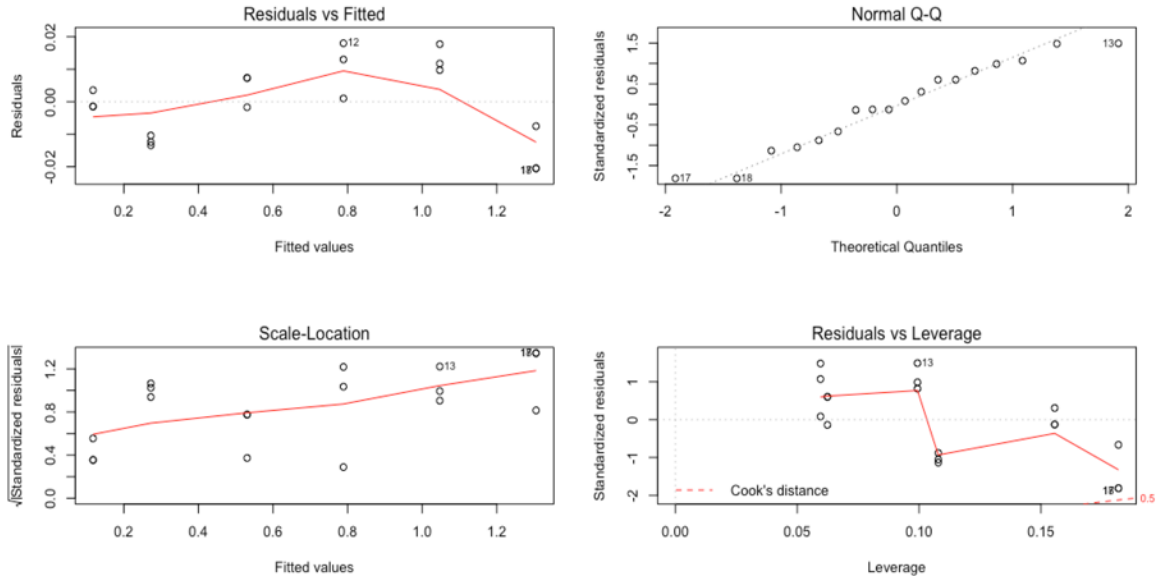

SM 2. Diagnostic plots for the standard curve of ProA2 standard at Complete Phytochemical Solutions, LLC. The residuals vs fitted plot shows if residuals have non-linear patterns. The Normal Q-Q plot shows if residuals are normally distributed. The scale-location plot shows if residuals are spread equally (homoscedasticity). The residuals vs leverage plot shows if influential data points are present in our model.

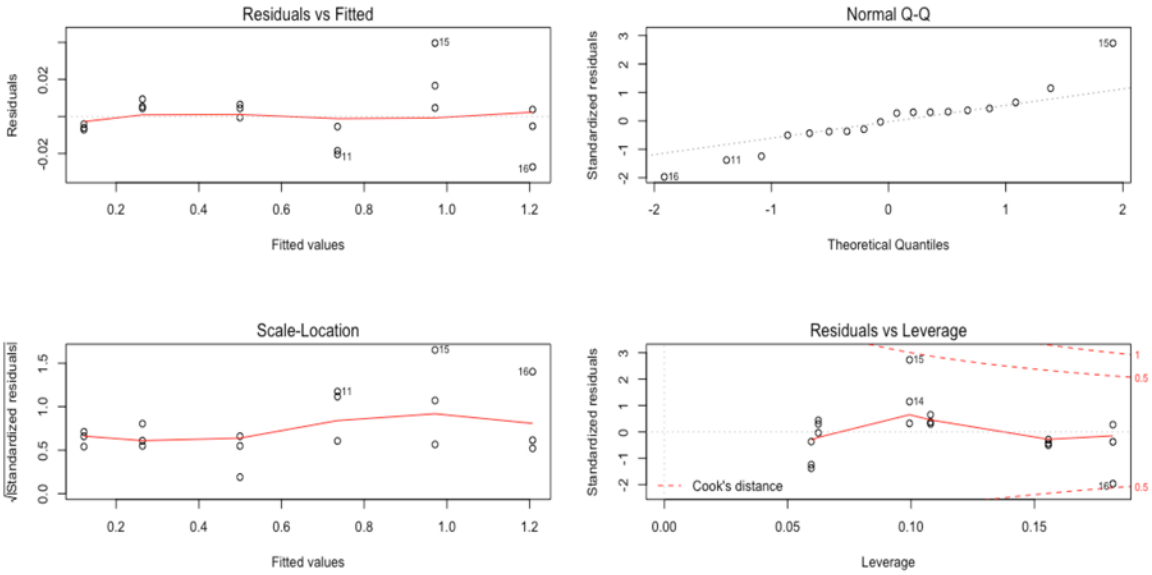

SM 3. Diagnostic plots for the standard curve of ProA2 standard at University of Wisconsin-Madison. The residuals vs fitted plot shows if residuals have non-linear patterns. The Normal Q-Q plot shows if residuals are normally distributed. The scale-location plot shows if residuals are spread equally (homoscedasticity). The residuals vs leverage plot shows if influential data points are present in our model.

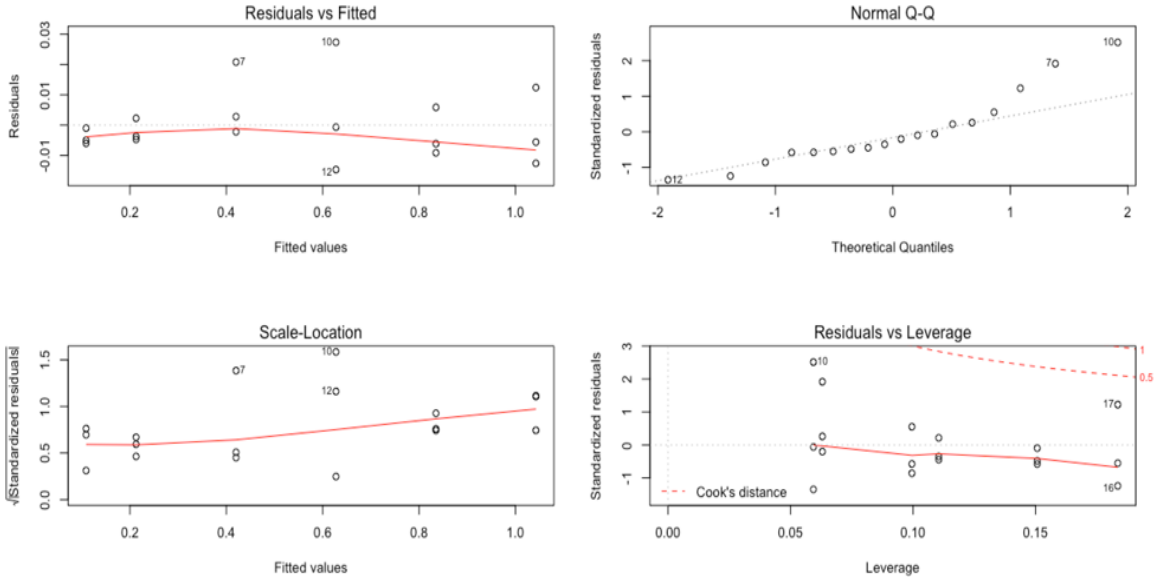

SM 4. Diagnostic plots for the standard curve of c-PAC standard at Complete Phytochemical Solutions, LLC. The residuals vs fitted plot shows if residuals have non-linear patterns. The Normal Q-Q plot shows if residuals are normally distributed. The scale-location plot shows if residuals are (homoscedasticity). The residuals vs leverage plot shows if influential data points are present in our model.

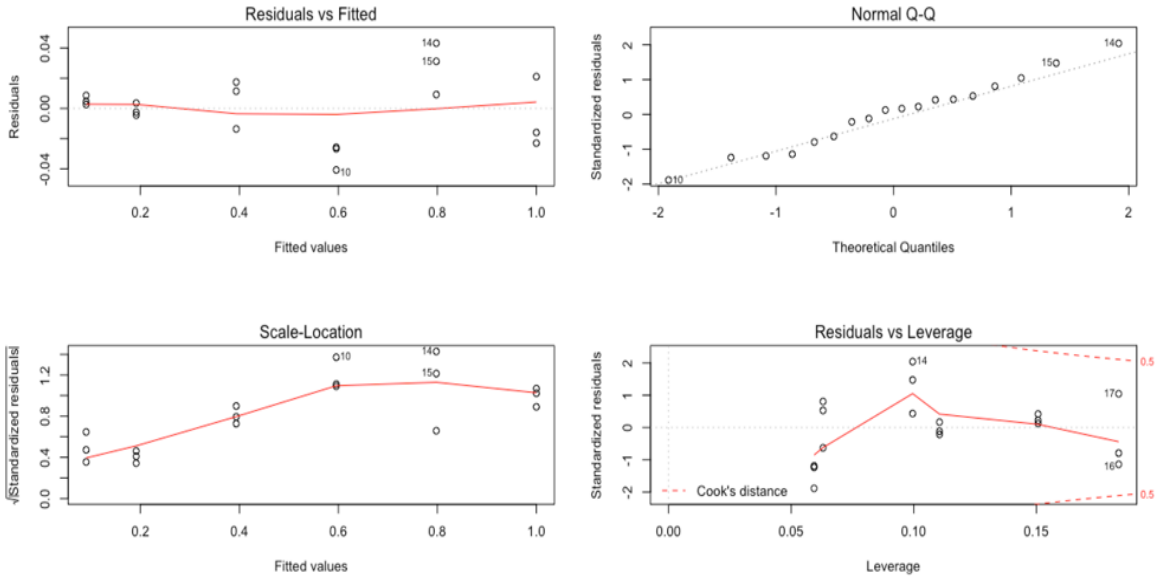

SM 5. Diagnostic plots for the standard curve of c-PAC standard at University of Wisconsin-Madison. The residuals vs fitted plot shows if residuals have non-linear patterns. The Normal Q-Q plot shows if residuals are normally distributed. The scale-location plot shows if residuals are spread equally (homoscedasticity). The residuals vs leverage plot shows if influential data points are present in our model.

CHAPTER 2: Identification of A-type proanthocyanidins in cranberry-based foods and dietary supplements by matrix-assisted laser desorption/ionization time-of-flight mass spectrometry, First Action Method: 2019.05

Daniel Esquivel-Alvarado[§], Emilia Alfaro-Viquez[§], Christian G. Krueger[§,†], Martha M. Vestling[π], Jess D. Reed[§,†]

[§] University of Wisconsin-Madison, Department of Animal Sciences, Reed Research Group, 1675 Observatory Drive, Madison, WI 53706

[†] Complete Phytochemical Solutions, LLC, 275 Rodney Road, Cambridge, WI 53523; University

[π] University of Wisconsin-Madison, Department of Chemistry, 1101 University Avenue, Madison, WI, 53706

This chapter is published as-is in the *Journal of AOAC International, 2020*

https://doi: 10.1093/jaoacint/qsaa106

ABSTRACT

Background: Cranberry proanthocyanidins (c-PAC) are oligomeric structures of flavan-3-ol units, which possess A-type interflavan bonds. c-PAC differs from other botanical sources because other PAC mostly have B-type interflavan bonds. Cranberry products used to alleviate and prevent urinary tract infections may suffer from adulteration, where c-PAC are replaced with less expensive botanical sources of PAC that contain B-type interflavan bonds. ***Objective:*** Identifying the presence of A-type interflavan bonds in cranberry fruit and dietary supplements. ***Methods:*** Thirty-five samples reported to contain A-type PAC (cranberry fruit and cranberry products) and thirty-six samples reported to contain B-type PAC (other botanical sources) were identified and differentiated using MALDI-TOF MS, deconvolution of overlapping isotope patterns, and principal component analysis (PCA). ***Results:*** Our results show that both MALDI-TOF MS and deconvolution of overlapping isotope patterns were able to identify the presence of A-type interflavan bonds with a probability greater than 90% and a confidence of 95%. Deconvolution of MALDI-TOF MS spectra also determined the ratio of A-type to B-type interflavan bonds at each degree of polymerization in cranberry fruit and cranberry products, which is a distinguishing feature of c-PAC in comparison to other botanical sources of PAC. PCA shows clear differences based on the nature of the interflavan bonds. ***Conclusions:*** MALDI-TOF MS, deconvolution of overlapping isotope patterns of MALDI-TOF MS spectra, and PCA allow the identification, estimation, and differentiation of A-type interflavan bonds in cranberry-based foods and dietary supplements among other botanical sources containing mostly B-type interflavan bonds.

INTRODUCTION

Cranberries (*Vaccinium macrocarpon* Aiton) grown in North America are mostly processed into products such as juice, sauce, sweetened dried cranberries, and dietary supplements. In the United States, cranberry production for 2018 was estimated to be 9.72 million barrels (one barrel is equivalent to 45.4 kg of cranberries) (Cranberry Institute, 2019). Cranberry fruit and cranberry products are sources of proanthocyanidins (PAC), which are widely researched because of their putative health benefits (Feliciano, Meudt, Shanmuganayagam, Metzger, Krueger, & Reed, 2014; Feliciano, Krueger, & Reed, 2015). The consumption of cranberry PAC (c-PAC) has been associated with the prevention of urinary tract infections. Recent studies suggest that c-PAC agglutinate extra-intestinal pathogenic *Escherichia coli* (ExPEC) and inhibit ExPEC adhesion and invasion of epithelial cells (Feliciano, Meudt, Shanmuganayagam, Krueger, & Reed, 2014; Feliciano, Krueger, & Reed, 2015; Alfaro-Viquez, Esquivel-Alvarado, Madrigal-Carballo, Krueger, & Reed, 2019). The bioactivity of c-PAC against *E. coli* is greater than other PAC because c-PAC contains one or more A-type interflavan bonds (Foo, Lu, Howell, & Vorsa, 2000a; Feliciano, Meudt, Shanmuganayagam, Krueger, & Reed, 2014; Feliciano, Krueger, & Reed, 2015; Alfaro-Viquez, Esquivel-Alvarado, Madrigal-Carballo, Krueger, & Reed, 2019).

PAC are oligomeric structures composed of repeating flavan-3-ol units (Monagas, Quintanilla-Lopez, Gomez-Cordoves, Bartolome, & Lebron-Aguilar, 2010). PAC are structurally differentiated according to the stereochemistry, the pattern of hydroxylation of flavan units (B-ring), the degree of polymerization (DP), and the nature of the interflavan bonds (A- versus B-type) (Reed, Krueger, & Vestling, 2005; Monagas, Quintanilla-Lopez, Gomez-Cordoves,

Bartolome, & Lebron-Aguilar, 2010; Esquivel-Alvarado, Muñoz-Arrieta, Alfaro-Viquez, Madrigal-Carballo, Krueger, & Reed, 2020). In B-type interflavan bonds, PAC form bonds between C4-C8; in A-type interflavan bonds, PAC have an additional bond between C2-O-C7 (Foo, Lu, Howell, & Vorsa, 2000b; Monagas, Quintanilla-Lopez, Gomez-Cordoves, Bartolome, & Lebron-Aguilar, 2010; Esquivel-Alvarado, Muñoz-Arrieta, Alfaro-Viquez, Madrigal-Carballo, Krueger, & Reed, 2020).

Cranberry products used to alleviate and prevent urinary tract infections may suffer from adulteration, where cranberries are replaced with less expensive botanical sources of PAC that contain B-type interflavan bonds (Pardo-Mates, Vera, Barbosa, Hidalgo-Serrano, Nunez, Saurina, et al., 2017; Barbosa, Pardo-Mates, Hidalgo-Serrano, Saurina, Puignou, & Núñez, 2018). Manufacturers are able to adulterate cranberry products while still claiming high PAC content because the majority of claims are based on results from a colorimetric assay, such as the 4-(dimethylamino)cinnamaldehyde (DMAC) reaction to produce a chromophore that is detected at 640nm (Feliciano, Shea, Shanmuganayagam, Krueger, Howell, & Reed, 2012; Pardo-Mates, et al., 2017; Barbosa, Pardo-Mates, Hidalgo-Serrano, Saurina, Puignou, & Núñez, 2018). While useful for quantifying PAC, the DMAC assay is unable to differentiate and authenticate the source of PAC (Prior, Fan, Ji, Howell, Nio, Payne, et al., 2010; Birmingham, Esquivel-Alvarado, Maranan, Krueger, & Reed, 2020).

Current methodologies for identification, classification, and authentication of PAC are inadequate and time consuming due to the structural heterogeneity and complexity of PAC, posing a challenge

for qualitative and quantitative analysis (Feliciano, Krueger, & Reed, 2015). The goals of this study were (1) to develop a methodology to identify the presence of A-type interflavan bonds in cranberry fruit and cranberry products (following the AOAC standard method performance requirements (SMPR) 2017.004) (Schaneberg, Brown, Bzhelyansky, Chang, Cunningham, Gu, et al., 2017) and (2) to differentiate amongst other botanical sources containing mostly B-type interflavan bonds. The proposed methodology could be used to support manufacturers' claims of the presence of A-type interflavan bonds in cranberry products.

MATERIAL AND METHODS

Caution: Refer to Material Safety Data Sheets (MSDS) for all chemicals prior to use. Use all appropriate personal protective equipment and follow good laboratory practices.

A. Principle of Method

Proanthocyanidins (PAC) in samples are extracted with 70% v/v acetone, purified by chromatography on LH-20 column, and analyzed by matrix-assisted laser desorption/ionization time-of-flight mass spectrometry (MALDI-TOF MS). The deconvolution of overlapping isotopic patterns of MALDI-TOF MS spectra are used for the identification of A-type interflavan bonds in PAC.

B. Sample Materials

(a) Cranberry fruit (*Vaccinium macrocarpon* Aiton).--Varieties Scarlet Knight, BenLear A2, G1 A57, G2A20, and Stevens A10 (Habelman Bros. Company, Tomah, WI, USA).

(b) Cranberry products.--capsules

(c) Apple fruit (*Malus pumila*).--Varieties Cameo, Honeycrisp, Jazz, Ambrosia, SnapDragon, RubyFrost, SweeTango, Kanzi, Eve, Kiku, Red Delicious, McIntosh, Golden Delicious, Braeburn , Cripps Pink, Pink Lady, Fuji, Gala ,Granny Smith, and Paula Red.

(d) Cocoa (*Threobroma cacao* L).--powder cans

(e) Grape Skins (*Vitis sp*).-- Cotton Candy, Summer Royal, Autumm King, Crimson Seedless, Thompson Seedless, and Flame Seedless.

(f) Black chokeberry fruit (*Aronia melanocarpa* Michx).

C. Apparatus

(a) Bruker UltraFlex® III MALDI TOF/TOF mass spectrometer equipped with a SmartBeam™ laser (Billerica, MA, USA). MALDI-TOF MS conditions: ion source 1 (25.0 kV), ion source 2 (20.6kV), lens voltage (9.5 kV), reflector 1 (26.5 kV), reflector 2 (14.41 kV), pulsed ion extraction (130 ns), detector gain (2.64x; 1548V), preamplifier filter bandwidth (small), and digitizer sampling frequency (100 Hz). Spectra are the sum of different locations in each well, accumulating a total of 2000 shots with deflection set at 900 Da. FlexControl, and Flex Analysis software (Bruker Daltonik GmbH, Bremen, Germany) are used for data acquisition and data processing, respectively.

(b) Balance, analytical.--Minimum weighing capacity of 0.01 mg.

(c) Bench-top Dewar flask.

(d) High speed blender

(e) Ultrasonic bath.

(f) Centrifuge.

(g) Rotary vacuum evaporator**.**

(h) Centrifuge tubes.--50 mL HDPE plastic with screw caps.

(i) Pipetters.--with disposable tips.

(j) Strong cation resin tips PureSpeed IEX 1 mL/20 μL (Rainin, Oakland, CA, USA).

D. Reagents

(a) 2,5-dihydrobenzoic acid (DHB) – Sigma-Aldrich (St. Louis, Missouri, USA).

(b) 2-propanol - Sigma-Aldrich (St. Louis, Missouri, USA).

(c) Acetone – Fisher Scientific (Fair Lawn, New Jersey, USA).

(d) Bradykinin – Sigma-Aldrich (St. Louis, Missouri, USA).

(e) Cesium trifluoroacetate – Sigma-Aldrich (St. Louis, Missouri, USA).

(f) Ethanol – Decon Laboratories, Inc. (King of Prussia, Pennsylvania, USA).

(g) Glucagon – Sigma-Aldrich (St. Louis, Missouri, USA).

(h) Liquid nitrogen

(i) Methanol – Fisher Scientific (Fair Lawn, New Jersey, USA).

(j) Sephadex LH-20™ - GE Healthcare, 18-111 μm (Uppsala, Sweden).

E. Reagent Preparations

(a) Acetone solution.--(1) 70% v/v. Place 700 mL acetone into 1 L volumetric flask, dilute to volume with deionized water. (2) 80% v/v. Place 800 mL acetone into 1 L volumetric flask, dilute to volume with deionized water.

(b) Ethanol:methanol solution.--1:1 v/v. Place 500 mL ethanol into 1 L volumetric flask, dilute to volume with methanol.

(c) 2,5-dihydroxybenzoic acid (DHB) solution.--1.30 M in methanol. Dissolve 400 mg of 2,5-dihydroxybenzoic acid in methanol and dilute to 2 mL with methanol.

Note: Prepare ≤ 1 h before use.

(d) Cesium trifluoroacetate solution.--(1) Stock solution.--5 millimolar (mM) in methanol. Dissolve 2.46 mg of cesium trifluoroacetate in methanol and dilute to 2 mL. (2) Working solution.--Dispense 50 μL stock solution into 1 mL volumetric flask, dilute to volume with methanol

(e) Bradykinin solution.--(1) Stock solution.--100 micromolar (μM) in water. Dissolve 0.21 mg of bradykinin in water and bring to 2 mL. (2) Working solution.--Dispense 40 μL stock solution into 1 mL volumetric flask, bring to final volume with water.

(f) Glucagon solution.--(1) Stock solution.--100 micromolar **(**μM) in water. Dissolve 0.69 mg of glucagon in water and dilute to 2 mL. (2) Working solution.--Dispense 40 μL stock solution into 1 mL volumetric flask, dilute to water.

F. Column Preparation

(a) Chromatographic tube.-- Use 25 mm id and 250 length chromatographic tube with medium porosity fritted glass.

(b) Preparation, wash, and activation of Sephadex LH-20^{TM} resin.--weigh 25 g Sephadex LH-20^{TM} resin into 600 mL beaker and add 200 mL deionized water. Mix by swirling vigorously. Let settle and decant upper layer. Wash slurry with three times with 100 mL of deionized water, decanting upper layer each time.

(c) Preparation of column.-- Add an aqueous slurry of LH-20^{TM} to 10 cm bed depth (wet resin). Wash column with 100 mL deionized water and equilibrate the column with 100 mL ethanol. Maintain head of 1 cm liquid on column throughout assay.

G. Sample Preparation

(a) Whole fruits.--Cut the whole fruits into small pieces of approximately 1 cm^3. Weigh 200 g of the pieces of fruits and transfer into a 2 L bench-top Dewar flask. Add 1 L liquid nitrogen into the 2 L bench-top Dewar flask (Caution: perform under good ventilation and wear insulated gloves and face shield to protect against liquid nitrogen). Decant the frozen pieces of fruits into

a blender and grind the sample thoroughly. Let evaporate the remaining liquid nitrogen from the sample powder.

(b) Capsules.--Open at least 25 capsules and collect the powder. Discard the capsule shells.

(c) Powders.--Preparation is not required.

(d) Grape Skins.--Peel by hand 0.5 kg of grapes. Weight 40 g of the grape skins and transfer into a 1 L bench-top Dewar flask. Add 300 mL liquid nitrogen into the 1 L bench-top Dewar flask. (Caution: perform under good ventilation and wear insulated gloves and face shield to protect against liquid nitrogen). Decant the frozen grape skins into a blender and grind the sample thoroughly. Let evaporate the remaining liquid nitrogen from the sample powder.

H. Sample Extraction

Weigh 20 g of the powder into a 250 mL Erlenmeyer flask. Add 100 mL 70% (v/v) acetone solution into the 250 mL Erlenmeyer flask. Swirl the Erlenmeyer flask and sonicate for 15 min. Decant the extract into two 50 mL centrifuge tube. Centrifuge the extract at 1800 g for 10 min at 15°C and pooled together the supernatant from both tubes. Evaporate the supernatant to dryness by rotary vacuum evaporation at 35°C. Solubilize the extract in 10 mL of ethanol. Load 5 mL of the ethanolic extract onto the prepared chromatographic column. Sequentially elute the column with 150 mL ethanol, 150 mL ethanol:methanol solution, and 200 mL 80% (v/v) acetone solution. Evaporate the acetone fraction to dryness using a rotary evaporator at 35°C. Solubilize the PAC extract in 1.5 mL methanol.

I. Sample deionization, DHB solution deionization, deionized DHB solution/cesium trifluoroacetate solution, and bradykinin/glucagon solution procedures

(a) Sample deionization.--Pipette 500 μL of the PAC extract into a 1.5 mL transparent chromatography vial. Pipette the 500 μL of the PAC extract into the strong cation resin tip PureSpeed IEX 1mL/20μL. Maintain the tip inside the 1.5 mL transparent chromatography vial and mix the PAC extract by pipetting a minimum of 5 times up and down in the pipette tip. Dispense the deionized sample into a new 1.5 mL transparent chromatography vial.

(b) DHB solution deionization.--Pipette 500 μL of the DHB solution into a 1.5 mL transparent chromatography vial. Pipette the 500 μL of the DHB solution into the strong cation resin tip PureSpeed IEX 1mL/20μL. Maintain the tip inside the 1.5 mL transparent chromatography vial and mix the DHB solution by pipetting a minimum of 5 times up and down in the pipette tip. Dispense the deionized DHB solution into a new 1.5 mL transparent chromatography vial.

(c) Deionized DHB solution/cesium trifluoroacetate solution.--Mix 400 μL deionized DHB solution with 400 μL cesium trifluoroacetate working solution.

(d) Bradykinin/glucagon solution.--Mix 400 μL bradykinin working solution with 400 μL glucagon working solution

J. MALDI-TOF MS Spectra

(a) MALDI-TOF MS stainless steel target plate cleaning procedure.--Place the MALDI-TOF MS stainless steel target plate into a suitable container and pour in enough 2-propanol to cover the target surface. Sonicate the MALDI-TOF MS stainless steel target plate for 15 min. Remove the MALDI-TOF MS stainless steel target plate and rinse it thoroughly under deionized water.

Rinse the MALDI-TOF MS stainless steel target plate with ethanol. Let the MALDI-TOF MS stainless steel target plate dry completely at room temperature. Store the clean MALDI-TOF MS stainless steel target plate in the container provided.

(b) Bradykinin/glucagon external standard procedure.--Pipette 0.5 μL of the bradykinin/glucagon solution onto five wells of the MALDI-TOF MS stainless steel target plate. Let the bradykinin/glucagon solution dry completely at room temperature. Overlay each bradykinin/glucagon solution position with 0.6 μL deionized DHB solution/cesium trifluoroacetate solution by pipetting a minimum of 10 times up and down in the pipette tip. Let the mix bradykinin/glucagon solution and deionized DHB/cesium trifluoroacetate solution dry completely at room temperature.

(c) Sample Preparation procedure.--Pipette 0.5 μL of the deionized sample (0.05-0.5 mg c-PAC equivalents) onto five wells of the MALDI-TOF MS stainless steel target plate. Let the deionized sample dry completely at room temperature. Overlay each deionized sample position with 0.6 μL deionized DHB solution/cesium trifluoroacetate solution by pipetting a minimum of 10 times up and down in the pipette tip. Let the mix deionized sample and deionized DHB/cesium trifluoroacetate solution dry completely at room temperature. The sample MALDI-TOF MS stainless steel target plate is now ready for use.

Notes: (1).--For the quantification of c-PAC, refer to the Inter-laboratory validation of 4-(dimethylamino)cinnamaldehyde (DMAC) assay using cranberry proanthocyanidin standard for quantification of soluble proanthocyanidins in cranberry foods and dietary supplements, First Action Method: 2019.06 (Birmingham, Esquivel-Alvarado, Maranan, Krueger, & Reed, 2020). (2).--Use a new pipette tip to add the deionized DHB solution/cesium trifluoroacetate solution to each well of the MALDI-TOF MS stainless steel target plate.

K. Calculations

(a) Deconvolution of overlapping isotope patterns of A- to B-type interflavan bonds in PAC.--The absolute intensity (ai) of each PAC peak in the positive reflectron mode MALDI-TOF MS spectra data set is obtained using mMass software. Spectral data are excluded from deconvolution analysis when the signal-to-noise (S/N) ratio is lower than 3. The percentage of A- to B-type interflavan bonds in PAC is solved using the following algebraic matrix: $A^{-1} \times b = c$, where A-1 represents the inverse coefficient matrix of the relative intensity (ri) of the isotope patterns for each DP, b represents the constant matrix of ai from the spectra, and c represents the variable matrix of linear combinations that solve the simultaneous equation. The linear combinations obtained from $A^{-1} \times b$ are divided by the sum of all possible iterations and multiplied by 100 to obtain the percentage of A- to B-type interflavan bonds.

RESULTS AND DISCUSSION

MALDI-TOF MS spectra of PAC show masses $[M+Cs]^+$ that correspond to cesium adducts of (epi)catechin oligomeric units, which can be explained according to the equation $m/z = 290 + 288d - 2A + c$, where 290 represents the molecular weight of the terminal (epi)catechin unit, d is the DP, A is the number of A-type interflavan bonds, and c is the atomic weight of cesium cation (Reed, Krueger, & Vestling, 2005). Analysis of the MALDI-TOF MS spectra showed that, for the 71 samples (30 cranberry fruits, 5 cranberry products, 25 apples, 6 grape skins, 1 black chokeberry, and 4 cocoa powders), the predominant mass at each DP (Δ288 amu) is representative of a PAC structure with (epi)catechin oligomeric units that have either predominantly A-type or B-type interflavan bonds (Figures 1-4) (Feliciano, Meudt, Shanmuganayagam, Krueger, & Reed, 2014). The molecular weight difference between A-type and B-type interflavan bonds is due to the formation of an ether bond that results in the loss of two hydrogen atoms (Δ2 amu) (Krueger, Dopke, Treichel, Folts, & Reed, 2000; Reed, Krueger, & Vestling, 2005; Feliciano, Krueger, Shanmuganayagam, Vestling, & Reed, 2012). Visual inspection of MALDI-TOF MS spectra suggests that cranberry fruit, cranberry products, apple, black chokeberry, and cocoa powders have mainly (epi)catechin oligomeric units with structural variation in the nature of the interflavan bonds (Figure 1-3). In contrast, visual inspection of MALDI-TOF MS spectra of grape skins presented additional peaks that correspond to galloyl groups (Figure 4) (Krueger, Dopke, Treichel, Folts, & Reed, 2000).

Visual inspection alone of the MALDI-TOF MS spectra is sufficient to differentiate samples such as grape skins due to the presence of the additional peaks that are galloyl units (Krueger, Dopke,

Treichel, Folts, & Reed, 2000). A detailed inspection of the isotope patterns of MALDI-TOF MS spectra for all samples revealed that for cranberry fruit and cranberry products, the most predominant (epi)catechin oligomer units contain at least 1 A-type bond, with peaks corresponding to 0 A-type, 2 A-type, and 3 A-type interflavan bonds also present (Figure 5A). In contrast, spectra from the other botanical sources revealed that the most predominant linkage corresponds to 0 A-type, with 1 A-type interflavan bonds in lesser abundance (Figure 5B-D). As shown in Figure 5, the overlapping peaks for the hexamer cesium adducts suggest that peak patterns differ only in the A- and B-type interflavan bonds (e.g., for the hexamer cesium adducts, the isotope patterns are visible at m/z 1857.3 [3A-type:2B-type], m/z 1859.3 [2A-type:3B-type], m/z 1861.3 [1A-type:4B-type], and m/z 1863.3 [0A-type:5B-type]).

A- and B-type interflavan bonds can be identified visually by the isotope patterns of MALDI-TOF MS spectra. However, the identification and authentication were confirmed by deconvolution of overlapping isotope patterns (Feliciano, Krueger, Shanmuganayagam, Vestling, & Reed, 2012). The ability to deconvolute overlapping isotope patterns for each individual oligomer of PAC allowed for the estimation of the percentage of A- to B-type interflavan bonds for all samples. Median values from the deconvoluted data indicated that 95.6% of PAC from cranberry fruit and cranberry products contain at least one A-type interflavan bond and that 20.8% of PAC from cranberries and cranberry products contain two or more A-type interflavan bonds. In contrast, median values from the deconvoluted data indicated that only 6.6% of PAC from the other botanical sources contain at least one A-type interflavan bond and that only 0.5% of PAC from the other botanical sources contain two or more A-type interflavan bonds.

Deconvoluted MALDI-TOF MS spectra data are presented as a bar graph, providing a visual representation of A-type and B-type 'PAC fingerprints' (Figure 6). Previous research reports similar profiles for the percentage of A-type interflavan bonds in cranberries (Feliciano, Meudt, Shanmuganayagam, Krueger, & Reed, 2014; Feliciano, Meudt, Shanmuganayagam, Metzger, Krueger, & Reed, 2014; Feliciano, Krueger, & Reed, 2015; Polewski, Krueger, Reed, & Leyer, 2016; Alfaro-Viquez, Esquivel-Alvarado, Madrigal-Carballo, Krueger, & Reed, 2018). Moreover, our findings indicated that the established method determining relative percentages of A-type to B-type interflavan bonds is valid not only for cranberry fruit, but also for cranberry products (Figure 6A-B). Typically, in cranberry fruit and cranberry products, as the DP increases, the percentage of 2 A-type and 3-type interflavan bonds increases, whereas the percentage of 1 A-type interflavan bonds decreases (Feliciano, Krueger, Shanmuganayagam, Vestling, & Reed, 2012; Alfaro-Viquez, Esquivel-Alvarado, Madrigal-Carballo, Krueger, & Reed, 2018). In contrast, in the other botanical sources, as the DP increases, the percentage of B-type interflavan bonds is either consistently high or increases (>90%) (Figure 3C-D) (Feliciano, Meudt, Shanmuganayagam, Krueger, & Reed, 2014).

The existing literature has not confirmed the presence of A-type interflavan bonds in apples, black chokeberries, grape skins, and cocoa powders (Bhagwat, Haytowitz, Prior, Gu, Hammerstone, Gebhardt, et al., 2004; Prior & Gu, 2005). Thus, although the MALDI-TOF MS spectra detected masses above our threshold S/N ratio for the overlapping of isotope patterns that correspond to 1 A-type or 2 A-type interflavan bonds, these masses may result from the presence of low quantities of A-type bonds (not previously described) and/or polyphenol oxidase (PPO) (Cheynier &

Ricardo-da-Silva, 1991; Poupard, Sanoner, Baron, Renard, & Guyot, 2011; Feliciano, Meudt, Shanmuganayagam, Krueger, & Reed, 2014). PPO modifies the hydroxyl groups of the flavan units (B-ring) and produces quinones that alter the PAC structure, resulting in compounds that are 2 amu lighter than the all B-type PAC oligomeric series. This finding has been reported for MALDI-TOF MS analysis of apples and apple juice (Poupard, Sanoner, Baron, Renard, & Guyot, 2011; Feliciano, Meudt, Shanmuganayagam, Krueger, & Reed, 2014). Overall, MALDI-TOF MS spectra and the deconvolution method were able to identify the presence of at least 1 A-type interflavan bond in cranberry fruit and cranberry products with a probability of 95.6% and 95% confidence. In contrast, MALDI-TOF MS spectra and the deconvolution method were able to confirm the absence of A-type interflavan bonds (all B-type) in the other botanical sources with a probability of 93.4% and 95% confidence.

MALDI-TOF MS has some drawbacks such as low shot-to-shot reproducibility and dependence on the sample preparation method. For instance, each laser shot ablates a layer of the sample/matrix, producing variation in the shot-by-shot spectrum. In addition, the position of the laser shot on the sample/matrix leads to spectral variation (de Hoffmann & Stroobant, 2007). In order to prevent these limitations, we used the adaptation of the dried method and controlled the inter- and intra-well variability proposed by Feliciano et al., (2012) (Feliciano, Krueger, Shanmuganayagam, Vestling, & Reed, 2012). The inter-well variability was decreased by spotting the sample onto five wells of the MALDI-TOF MS stainless target plate, while intra-well variability was decreased by shooting 2000 times in 10 different locations in each well of the MALDI-TOF MS stainless target plate. Once the sample/matrix deposition, and inter- and intra-

well variability were addressed, precise ai were obtained for each m/z of interest. Deconvolution by matrix algebra was applied to ai for each m/z of interest and this data set was used to evaluate repeatability (Feliciano, Krueger, Shanmuganayagam, Vestling, & Reed, 2012). By definition repeatability refers to the degree of agreement of results when conditions are maintained as constant as possible with the same analyst, reagents, equipment, and instruments performed within a short period of time (AOAC, 2013), In order to evaluate repeatability, each sample analyzed in triplicate was evaluated at different times during the same day. Our results indicate that the coefficient of variation across PAC with DP3-8 was <5.0, demonstrating that our method is repeatable. Previously published research from our laboratory showed similar coefficient of variation across PAC with DP3-8 when c-PAC and apple PAC were extracted using 70% (v/v) acetone solution and when c-PAC were extracted using supercritical fluid extraction (Feliciano, Meudt, Shanmuganayagam, Krueger, & Reed, 2014). Because results from our previous research and the results reported here have a coefficient of variation of less than 5%, the "intermediate or large" within-laboratory precision was also satisfied (AOAC, 2013). In addition, our previous study on the deconvolution of overlapping isotope patterns of MALDI-TOF MS to determine the percentage of A- to B-type interflavan bonds in c-PAC reported that when eleven ratios of procyanidins A2 and B2 (commercial dimers) were analyzed, the observed percentages were within 3.6% of the predicted percentages, which suggest that the method is accurate (Feliciano, Krueger, Shanmuganayagam, Vestling, & Reed, 2012). Also, the coefficient of determination was >0.995, which suggest linearity. Finally, the standard deviation among series was ≤3.5 and the standard error of the mean was <0.8, which suggest that the method is precise (Feliciano, Krueger, Shanmuganayagam, Vestling, & Reed, 2012).

MALDI-TOF MS spectra of PAC suggests that four optimized parameters described in Section C, I, and J resulted in high-resolution spectra. First, because the MALDI-TOF is a desorption-ionization technique that requires mixing the matrix solution with the sample, the matrix selection and matrix:sample ratio are crucial, as the S/N ratio differs depending on the matrix (Wetzel, Guttman, Flynn, & Filliben, 2006). Both DHB and trans-3-indoleacrylic acid (IAA) matrices have been used for the detection of PAC by MALDI-TOF MS (Reed, Krueger, & Vestling, 2005). However, DHB was chosen because it is soluble in the same solvent as the sample, provides the widest mass range, and produces a suitable S/N ratio. Second, the PAC cationization with sodium $[M+Na]^+$ and potassium $[M+K]^+$ was addressed by deionizing both the matrix and the sample using a strong cation resin tip and adding cesium trifluoroacetate to the matrix solution. This produced PAC with cesium $[M+Cs]^+$ adduct ions, which solved the problem of distinguishing between (a) the formation of both $[M+Na]^+$ and $[M+K]^+$ adduct ions from one species and (b) the presence of two species with an additional hydroxyl group (Reed, Krueger, & Vestling, 2005). The molecular weight difference by one additional hydroxyl group substitution is equal to the atomic mass of oxygen (15.9949 amu) which is similar to the difference between the monoisotope of Na^+ (22.9900 amu) and the monoisotope of K^+ (39.0980 amu) which is 15.9739 amu (Reed, Krueger, & Vestling, 2005). Third, the pulsed ion extraction was changed from default values to correct the energy dispersion of the ions leaving the source with the same m/z ratio. This modification produced sharper peaks because the ions with the same m/z ratio reached the detector at the same time. For MALDI-TOF MS spectra of PAC, the optimal pulsed ion extraction was 130 ns at a detector gain of 1548 V. Fourth, the laser power used to desorb and ionize the sample also affected the MALDI-TOF MS spectra. Low laser powers are desired over high laser powers because the latter can fragment the sample, which are not desirable in MALDI-TOF MS spectra (Wetzel,

Guttman, Flynn, & Filliben, 2006). In addition, high laser powers are detrimental to the resolution of MALDI-TOF MS spectra. For MALDI-TOF MS spectra of PAC, the optimal laser power was between 45-60%. These parameters, as well as sample preparation and the location of the laser on the target, were the most influential parameters for obtaining high-resolution PAC spectra.

The deconvoluted MALDI-TOF MS spectra data of the 71 samples (30 cranberry fruits, 5 cranberry products, 25 apples, 6 grape skins, 1 black chokeberry, and 4 cocoa powders) were classified by principal component analysis (PCA) (Figure 7). PCA was used to reduce the dimensionality of the data and distinguish between samples with A- and B-type interflavan bonds. The first two components (PC1 and PC2) accounted for 90.50% of the total variance. PC1 (x-axis) compares the relative percentage of all B-type bonds (no A-type bonds) to 1 A-type bond across PAC with DP3-8 and contributes 86.1% of the total variance. The samples with 1 A-type interflavan bond were grouped along the positive values of PC1, whereas the samples with all B-type interflavan bonds were grouped along the negative values of PC1. A clear separation between samples with A-type interflavan bonds and samples with B-type interflavan bonds was obtained. Thus, the PCA score plot can be divided into two zones: (a) the cranberry fruit and cranberry products on the right and (b) the other botanical sources on the left. PC2 (y-axis) compares the relative percentage of 1 A-type bond to 2 A-type bonds and contributes 4.4% of the total variance. As expected there is greater variability in the cranberry products in this dimension because cranberry PAC have been reported to contain one or more A-type interflavan bonds at each DP. In the case of cranberry fruits this variability may be due to differences in variety and/or harvest date. In the case of the cranberry products this variability may be due differences in cranberry fruit,

harvest, post harvest storage, and/or processing (extraction, milling, and encapsulation, amongst others). Confidence ellipses with a 95% confidence interval are included for each set of samples in the PCA score plot; no outlier was detected. Overall, these results show that PCA correctly classifies samples as either A-type or B-type interflavan bonds using the deconvoluted MALDI-TOF MS spectra data.

CONCLUSION

The results of this study show that deconvolution of MALDI-TOF MS spectra distinguishes the A-type PAC in cranberry fruit and cranberry products from other botanical sources containing mostly B-type interflavan bonds with a probability greater than 90% and a confidence of 95%. In addition, information obtained by MALDI-TOF MS spectra allows for other aspects of the data set to be inspected and used as a metric of authentication (e.g. galloyl units in grape skins). The results also demonstrate that the deconvoluted MALDI-TOF MS spectra data in combination with PCA allowed a better understanding of the chemical profile of PAC. Therefore, PCA show that classification models can be built accurately based on the nature of the interflavan bonds (A- versus B-type) for cranberries and cranberries products and other botanical sources. Finally, the results of this study showed that MALDI-TOF MS is a powerful tool for structural characterization and identification of PAC.

CONFLICT OF INTEREST

The authors declare the following competing financial interest(s): Christian G. Krueger and Jess D. Reed have ownership interest in Complete Phytochemical Solutions, LLC, and acknowledge their affiliation with this company.

ACKNOWLEDGMENTS

The authors acknowledge financial support from the Ministry of Science, Technology and Telecommunications (MICITT), Innovation and Human Capital Program for Competitiveness (PINN), and the National Council for Scientific and Technology Research (CONICIT) (Grant

number PED-056-2015-I) at Costa Rica. The Authors acknowledge use of the Bruker UltraFlex® III MALDI TOF/TOF MS supported by NIH thought the University of Wisconsin, Department of Chemistry, Mass Spectrometry facility (NCRR 1S10RR024601-01).

AUTHORSHIP CONTRIBUTION STATEMENT

Daniel Esquivel-Alvarado: Conceptualization, Methodology, Formal analysis, Investigation, Data curation, Writing - original draft, Writing - review & editing, Visualization. **Emilia Alfaro-Viquez:** Conceptualization, Writing - review & editing, Visualization. **Christian G. Krueger:** Conceptualization, Writing - review & editing, Funding acquisition. **Martha M. Vestling:** Writing -review & editing. **Jess D. Reed:** Conceptualization, Writing - review & editing, Supervision, Funding acquisition.

REFERENCES

Alfaro-Viquez, E., Esquivel-Alvarado, D., Madrigal-Carballo, S., Krueger, C., & Reed, J. (2018). Cranberry proanthocyanidin-chitosan hybrid nanoparticles as a potential inhibitor of extra-intestinal pathogenic *Escherichia coli* invasion of gut epithelial cells. *International Journal of Biological Macromolecules*, *111*, 415-420. doi:10.1016/j.ijbiomac.2018.01.033

Alfaro-Viquez, E., Esquivel-Alvarado, D., Madrigal-Carballo, S., Krueger, C. G., & Reed, J. D. (2019). Proanthocyanidin-chitosan composite nanoparticles prevent bacterial invasion and colonization of gut epithelial cells by extra-intestinal pathogenic *Escherichia coli*. *International Journal of Biological Macromolecules*, *135*, 630-636. doi:10.1016/j.ijbiomac.2019.04.170

AOAC. (2013). Appendix K: Guidelines for Dietary Supplements and Botanicals, AOAC International.

Barbosa, S., Pardo-Mates, N., Hidalgo-Serrano, M., Saurina, J., Puignou, L., & Núñez, O. (2018). Detection and Quantitation of Frauds in the Authentication of Cranberry-Based Extracts by UHPLC-HRMS (Orbitrap) Polyphenolic Profiling and Multivariate Calibration Methods. *Journal of Agricultural and Food Chemistry, 66*(35), 9353-9365. doi:10.1021/acs.jafc.8b02855

Bhagwat, S., Haytowitz, D., Prior, R., Gu, L., Hammerstone, J., Gebhardt, S., Kelm, M., Cunningham, D., Beecher, G., & Holden, J. (2004). USDA database for proanthocyanidin content of selected foods. *US Department of Agriculture*.

Birmingham, A., Esquivel-Alvarado, D., Maranan, M., Krueger, C., & Reed, J. (2020). Inter-laboratory validation of 4-(dimethylamino) cinnamaldehyde (DMAC) assay using cranberry proanthocyanidin standard for quantification of soluble proanthocyanidins in cranberry foods and dietary supplements, First Action Method: 2019.06. *Journal of AOAC International*. doi:10.1093/jaoacint/qsaa084

Cheynier, V., & Ricardo-da-Silva, J. (1991). Oxidation of grape procyanidins in model solutions containing trans-caffeoyltartaric acid and polyphenol oxidase. *Journal of Agricultural and Food Chemistry, 39*(6), 1047-1049. doi:10.1021/jf00006a008

Cranberry Institute. Crop Statistics. (2019).Crop Statistics. https://www.cranberryinstitute.org/about_cran/Cropstatistics_about.html (accessed 2019)

de Hoffmann, E., & Stroobant, V. (2007). *Mass Spectrometry: Principles and Applications*, Wiley, New York.

Esquivel-Alvarado, D., Muñoz-Arrieta, R., Alfaro-Viquez, E., Madrigal-Carballo, S., Krueger, C., & Reed, J. (2020). Composition of anthocyanins and proanthocyanidins in three tropical *Vaccinium* species from Costa Rica. *Journal of Agricultural and Food Chemistry, 68*(10), 2872-2879. doi:10.1021/acs.jafc.9b01451

Feliciano, R., Krueger, C., & Reed, J. (2015). Methods to determine effects of cranberry proanthocyanidins on extraintestinal infections: relevance for urinary tract health. *Molecular Nutrition & Food Research, 59*(7), 1292-1306. doi:10.1002/mnfr.201500108

Feliciano, R., Krueger, C., Shanmuganayagam, D., Vestling, M., & Reed, J. (2012). Deconvolution of matrix-assisted laser desorption/ionization time-of-flight mass spectrometry isotope patterns to determine ratios of A-type to B-type interflavan bonds in cranberry proanthocyanidins. *Food Chemistry, 135*(3), 1485-1493. doi:10.1016/j.foodchem.2012.05.102

Feliciano, R., Meudt, J., Shanmuganayagam, D., Krueger, C., & Reed, J. (2014). Ratio of "A-type" to "B-type" proanthocyanidin interflavan bonds affects extra-intestinal pathogenic *Escherichia coli* invasion of gut epithelial cells. *Journal of Agricultural and Food Chemistry, 62*(18), 3919-3925. doi:10.1021/jf403839a

Feliciano, R., Shea, M., Shanmuganayagam, D., Krueger, C., Howell, A., & Reed, J. (2012). Comparison of isolated cranberry (*Vaccinium macrocarpon* Ait.) proanthocyanidins to catechin and procyanidins A2 and B2 for use as standards in the 4-(dimethylamino)cinnamaldehyde assay. *Journal of Agricultural and Food Chemistry, 60*(18), 4578-4585. doi:10.1021/jf3007213

Feliciano, R., Meudt, J., Shanmuganayagam, D., Metzger, B., Krueger, C., & Reed, J. (2014). Supercritical Fluid Extraction (SFE) of Cranberries Does Not Extract Oligomeric Proanthocyanidins (PAC) but Does Alter the Chromatography and Bioactivity of PAC Fractions Extracted from SFE Residues. *Journal of Agricultural and Food Chemistry, 62*(31), 7730-7737. doi:10.1021/jf502296b

Foo, L., Lu, Y., Howell, A., & Vorsa, N. (2000a). The structure of cranberry proanthocyanidins which inhibit adherence of uropathogenic P-fimbriated *Escherichia coli in vitro*. *Phytochemistry, 54*(2), 173-181. doi:10.1016/S0031-9422(99)00573-7

Foo, L., Lu, Y., Howell, A., & Vorsa, N. (2000b). A-Type proanthocyanidin trimers from cranberry that inhibit adherence of uropathogenic P-fimbriated *Escherichia coli*. *Journal of Natural Products, 63*(9), 1225-1228. doi:10.1021/np000128u

Krueger, C., Dopke, N., Treichel, P., Folts, J., & Reed, J. (2000). Matrix-assisted laser desorption/ionization time-of-flight mass spectrometry of polygalloyl polyflavan-3-ols in grape seed extract. *Journal of Agricultural and Food Chemistry, 48*(5), 1663-1667. doi:10.1021/jf990534n

Monagas, M., Quintanilla-Lopez, J. E., Gomez-Cordoves, C., Bartolome, B., & Lebron-Aguilar, R. (2010). MALDI-TOF MS analysis of plant proanthocyanidins. *Journal of Pharmaceutical and Biomedical Analysis, 51*(2), 358-372. doi:10.1016/j/jpba/2009.03.035

Pardo-Mates, N., Vera, A., Barbosa, S., Hidalgo-Serrano, M., Nunez, O., Saurina, J., Hernandez-Cassou, S., & Puignou, L. (2017). Characterization, classification and authentication of fruit-based extracts by means of HPLC-UV chromatographic fingerprints, polyphenolic profiles and chemometric methods. *Food Chemistry, 221*, 29-38. doi:10.1016/j.foodchem.2016.10.033

Polewski, M., Krueger, C., Reed, J., & Leyer, G. (2016). Ability of cranberry proanthocyanidins in combination with a probiotic formulation to inhibit in vitro invasion of gut epithelial cells by extra-intestinal pathogenic E. coli. *Journal of Functional Foods, 25*, 123-134. doi:10.1016/j.jff.2016.05.015

Poupard, P., Sanoner, P., Baron, A., Renard, C. M., & Guyot, S. (2011). Characterization of procyanidin B2 oxidation products in an apple juice model solution and confirmation of their presence in apple juice by high-performance liquid chromatography coupled to electrospray ion trap mass spectrometry. *Journal of Mass Spectrometry, 46*(11), 1186-1197. doi:10.1002/jms.2007

Prior, R., Fan, E., Ji, H., Howell, A., Nio, C., Payne, M., & Reed, J. (2010). Multi-laboratory validation of a standard method for quantifying proanthocyanidins in cranberry powders. *Journal of the Science of Food and Agriculture, 90*(9), 1473-1478. doi:10.1002/jsfa.3966

Prior, R. L., & Gu, L. (2005). Occurrence and biological significance of proanthocyanidins in the American diet. *Phytochemistry, 66*(18), 2264-2280. doi:10.1016/j.phytochem.2005.03.025

Reed, J., Krueger, C., & Vestling, M. (2005). MALDI-TOF mass spectrometry of oligomeric food polyphenols. *Phytochemistry, 66*(18), 2248-2263. doi:10.1016/j.phytochem.2005.05.015

Schaneberg, B., Brown, P., Bzhelyansky, A., Chang, T., Cunningham, D., Gu, L., Haesaerts, G., Howell, A., Johnson, H., Konings, E., Krueger, C., Liu, H., Merkh, K., Phillips, M., Phillips, T., Reed, J., Rimmer, C., Szpylka, J., Yadlapalli, S., & Coates, S. (2017). AOAC SMPR® 2017.004. *Journal of AOAC International, 100*(4), 1210-1211. doi:10.5740/jaoac-cin.SMPR2017_004

Wetzel, S., Guttman, C., Flynn, K., & Filliben, J. (2006). Significant parameters in the optimization of MALDI-TOF-MS for synthetic polymers. *Journal of the American Society for Mass Spectrometry, 17*(2), 246-252. doi:10.1016/j.jasms.2005.11.007

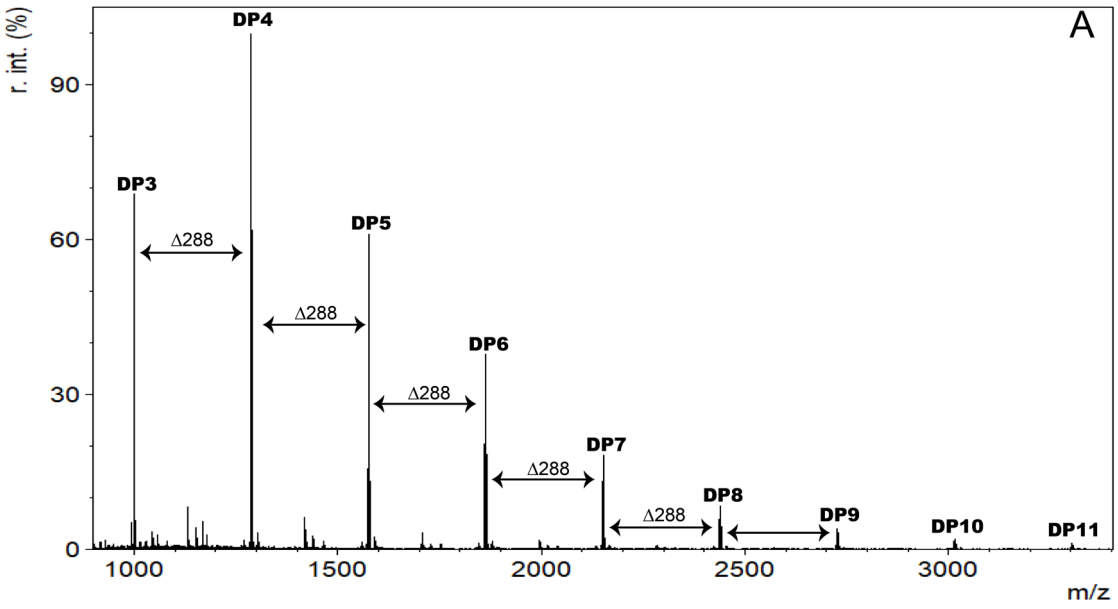

Figure 1. MALDI-TOF MS spectra in positive reflectron mode for cranberry fruit (A), which show (epi)catechin oligomeric units [M+Cs^+] from trimers to undecamers.

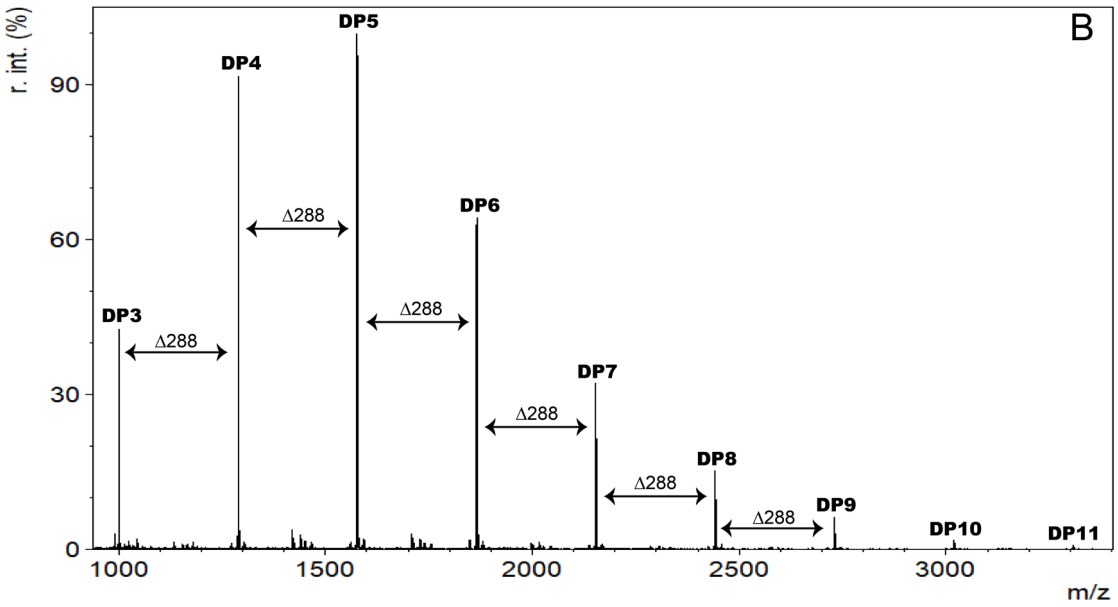

Figure 2. MALDI-TOF MS spectra in positive reflectron mode for apple (B), which show (epi)catechin oligomeric units [M+Cs^+] from trimers to undecamers.

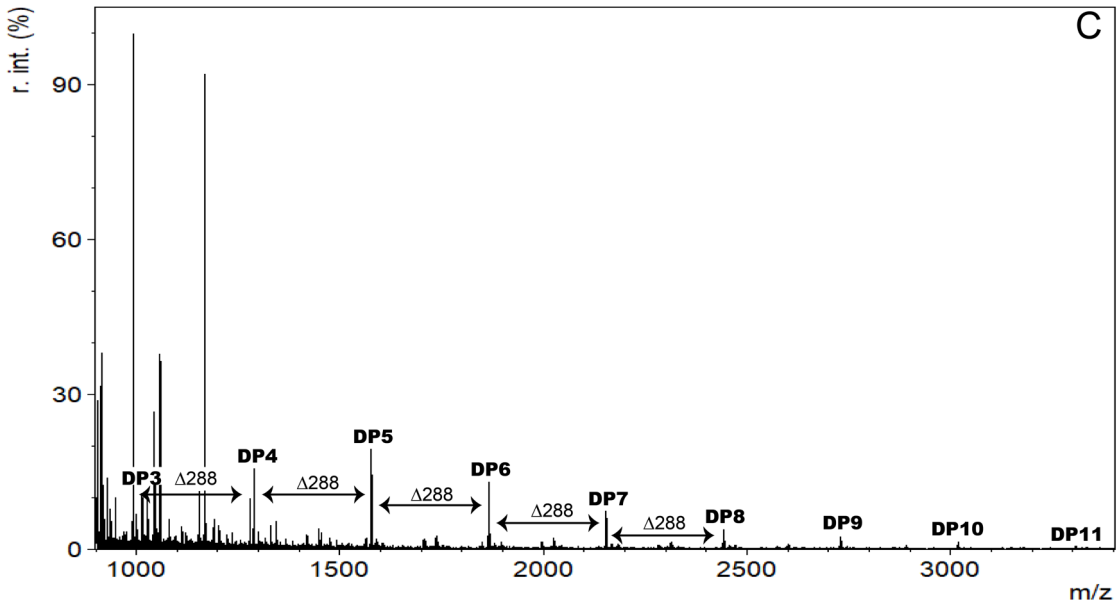

Figure 3. MALDI-TOF MS spectra in positive reflectron mode for black chokeberry (C), which show (epi)catechin oligomeric units [M+Cs^+] from trimers to undecamers.

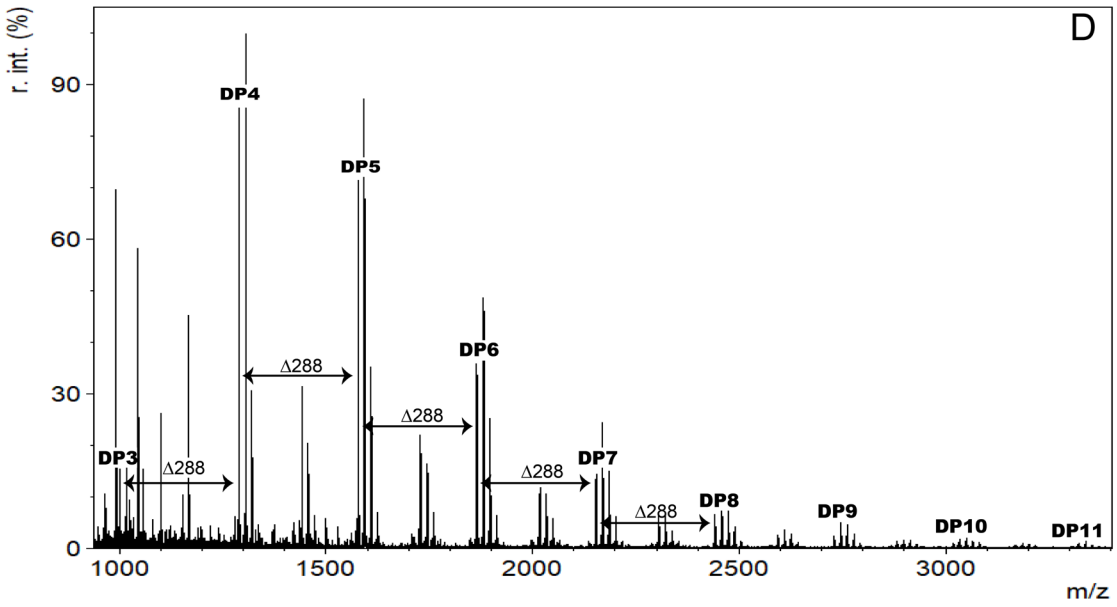

Figure 4. MALDI-TOF MS spectra in positive reflectron mode for grape skin (D), which show (epi)catechin oligomeric units [M+Cs^+] from trimers to undecamers.

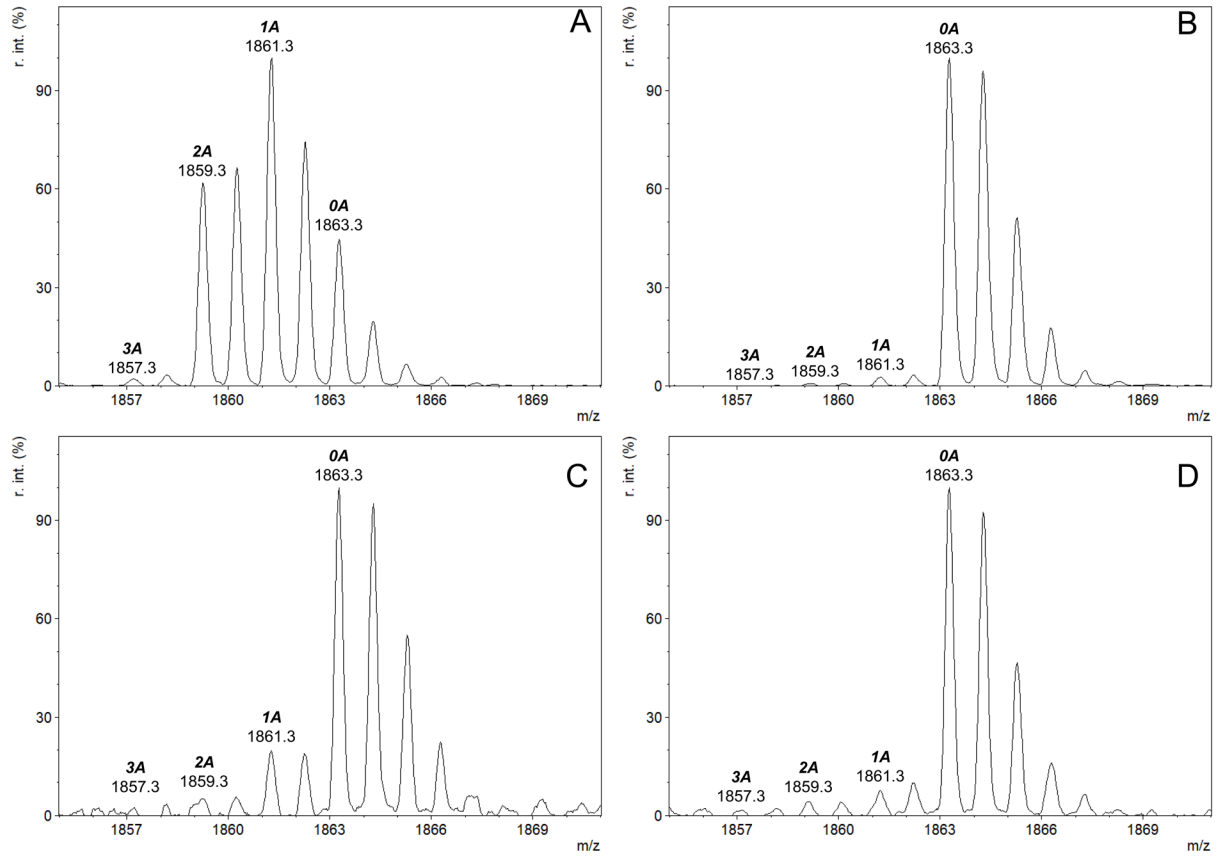

Figure 5. MALDI-TOF MS spectra in positive reflectron mode for cranberry fruit (A), apple (B), black chokeberry (C), and grape skin (D), which show the overlapping isotope patterns of PAC hexamers with cesium adducts.

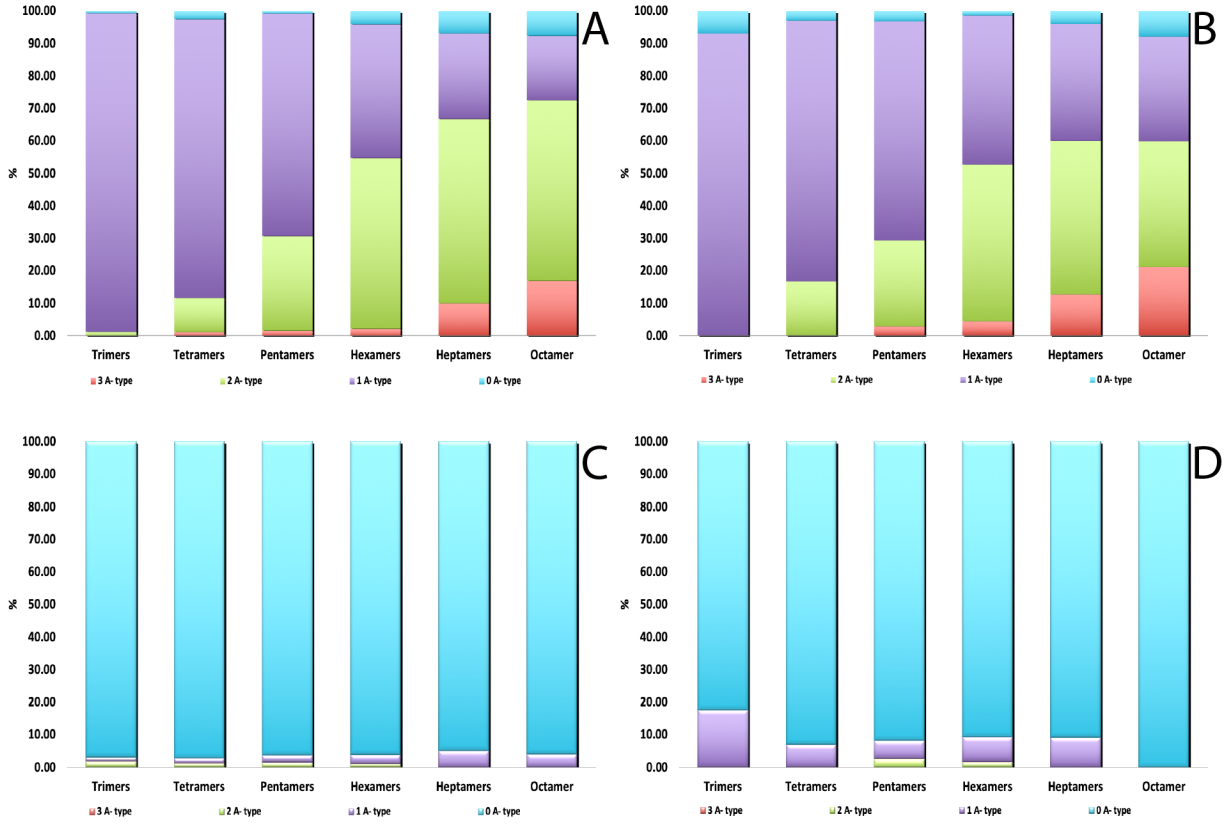

Figure 6. Percentage of A- and B-type interflavan bonds in cranberry fruit (A), cranberry products (B), apple (C), and grape skin (D)from trimers to octamers.

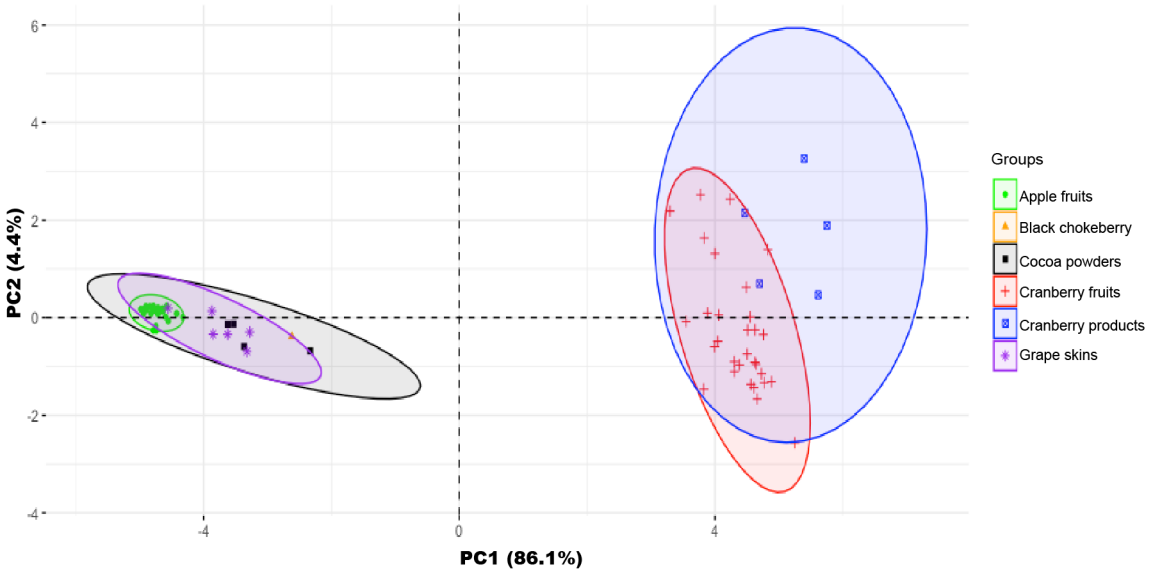

Figure 7. PCA score plot based on the deconvoluted MALDI-TOF MS spectra data, which show the PC1 (x-axis) and PC2 (y-axis) that accounted for 90.50% of the total variance.

CHAPTER 3: Classification of proanthocyanidin profiles using matrix-assisted laser desorption/ionization time-of-flight mass spectrometry (MALDI-TOF MS) spectra data combined with multivariate analysis

Daniel Esquivel-Alvarado[§], Emilia Alfaro-Viquez[§], Christian G. Krueger[§,†], Martha M. Vestling[π], Jess D. Reed[§,†]

[§] University of Wisconsin-Madison, Department of Animal Sciences, Reed Research Group, 1675 Observatory Drive, Madison, WI 53706, USA.

[†] Complete Phytochemical Solutions, LLC, 275 Rodney Road, Cambridge, WI 53523, USA.

[π] University of Wisconsin-Madison, Department of Chemistry, 1101 University Avenue, Madison, WI 53706, USA.

This chapter is published as-is in the *Journal of Food Chemistry, 336 (2021), 127667*

https://10.1016/j.foodchem.2020.127667

ABSTRACT

Proanthocyanidin (PAC) profiles of apples (a-PAC), cranberries (c-PAC), and peanut skins (p-PAC) were determined by matrix-assisted laser desorption/ionization time-of-flight mass spectrometry (MALDI-TOF MS). Deconvolution of overlapping isotopic patterns indicated that in apples, only 5% of the PAC oligomers contain one or more A-type bonds, whereas in cranberries and peanut skins, 96% of the PAC oligomers contain one or more A-type bonds. MALDI-TOF MS data combined with multivariate analysis, such as principal component analysis (PCA) and linear discriminant analysis (LDA), were used to differentiate and discriminate a-PAC, c-PAC, and p-PAC from one another. Mixtures of c-PAC with either a-PAC or p-PAC at different w/w ratios were evaluated by LDA modeling. The LDA model classified the training, testing, and validation sets with 99.4%, 100%, and 94.2% accuracy. Results suggest that MALDI-TOF MS and multivariate analysis are useful in determining authenticity of PAC from different sources and mixtures of PAC sources.

Keywords: cranberry; apples; peanut skins; adulteration; A-type interflavan bonds; B-type interflavan bonds; deconvolution of overlapping isotope patterns; principal component analysis; linear discriminant analysis.

INTRODUCTION

The American cranberry (*Vaccinium macrocarpon* Aiton) is an economically important fruit crop that is consumed as fresh fruit, juices, dried fruits, and dietary supplements. The putative health benefits of cranberry consumption is associated with the presence of proanthocyanidins (PAC) with A-type interflavan bonds (Feliciano, Krueger, & Reed, 2015). Previous work showed that cranberry PAC (c-PAC) inhibit cell adhesion and cell invasion by extra-intestinal pathogenic *Escherichia coli* (Feliciano, Meudt, Shanmuganayagam, Krueger, & Reed, 2014; Alfaro-Viquez, Esquivel-Alvarado, Madrigal-Carballo, Krueger, & Reed, 2018, 2019), a key factor associated with urinary tract infections. PAC are oligomers of flavan-3-ol units. The structural diversity of PAC depends on the nature of the monomer unit, interflavan linkage, degree of polymerization (DP), and other substitutions on the flavan-3-ol monomeric units (Reed, Krueger, & Vestling, 2005). B-type PAC contain a single interflavan carbon bond linked through C_4-C_8 or C_4-C_6, whereas A-type PAC contain an additional interflavan bond linked through C_2-O-C_7 bonds (Foo, Lu, Howell, & Vorsa, 2000).

Cranberry products are adulterated when less expensive sources of PAC are included in product and are not indicated on the label (Pardo-Mates, Vera, Barbosa, Hidalgo-Serrano, Nunez, Saurina, et al., 2017; Barbosa, Pardo-Mates, Hidalgo-Serrano, Saurina, Puignou, & Núñez, 2018). The most frequent adulterations are those carried out with sources containing B-type interflavan bonds, such as apple PAC (a-PAC). However, sources containing A-type interflavan bonds are also used, such as peanut skins PAC (p-PAC), a by-product of blanching and/or roasting peanuts, which are sold for $12-20 per ton (Sobolev & Cole, 2004). Adulteration of cranberry products by peanut skin poses a risk to public safety due to peanut allergens (van Boxtel, van den Broek, Koppelman,

Vincken, & Gruppen, 2007). There are several analytical methods to evaluate PAC (Feliciano, Krueger, & Reed, 2015). The 4-dimethylaminocinnamaldehyde (DMAC) assay is used to assess the content of PAC, but it is not selective and does not differentiate between A- and B-type interflavan bonds (Feliciano, Shea, Shanmuganayagam, Krueger, Howell, & Reed, 2012; Birmingham, Esquivel-Alvarado, Maranan, Krueger, & Reed, 2020). Matrix-assisted laser desorption/ionization time-of-flight mass spectrometry (MALDI-TOF MS) spectra data combined with multivariate analysis such as principal component analysis (PCA) and linear discriminant analysis (LDA) can be used to detect adulteration of cranberry products. Previous reports have used multivariate analysis to detect the adulteration of cranberry products, using targeted polyphenols (Pardo-Mates, Vera, Barbosa, Hidalgo-Serrano, Nunez, Saurina, et al., 2017; Barbosa, Pardo-Mates, Hidalgo-Serrano, Saurina, Puignou, & Núñez, 2018). For instance, Barbosa et al., 2018 indicate that the screening of 53-targeted polyphenol compounds using ultra-high-performance liquid chromatography-high resolution mass spectrometry (UHPLC-HRMS) and further assessed by partial-least square regression determined the percentage of adulteration in cranberry fruit extracts. However, there are no reports using multivariable analysis based on MALDI-TOF MS spectra of c-PAC to detect the adulteration of cranberry products. Thus, considering that cranberry is the second most-consumed nutritional supplement with an $800M/yr market in the United States (Leclair, 2016). The development of accurate approaches to verify the authenticity of cranberry products are needed.

The goals of this study were to use MALDI-TOF MS to determine the PAC fingerprints of apples, cranberries, and peanut skins and to use PCA and LDA modeling to differentiate and to discriminate amongst the PAC fingerprints of the samples. This information may be useful for

determining adulteration of cranberry products amongst other sources of PAC. To the best of our knowledge, this is the first time that MALDI-TOF MS spectra data combined with multivariate analysis such as PCA and LDA have been used to classified PAC profiles based on the percentage of A- and B-interflavan bonds.

MATERIAL AND METHODS

Chemicals and materials

Methanol and acetone were purchased from Fisher Scientific (Fair Lawn, NJ, USA). Ethanol (100%) was obtained from Decon's lab (King of Prussia, PA, USA). Sephadex LH-20® was purchased from GE Healthcare (Uppsala, Sweden). Bradykinin, glucagon, 2,5-dihydroxybenzoic acid (DHB; matrix), cesium trifluoroacetate were obtained from Sigma-Aldrich (St. Louis, MO, USA). Four raw peanut cultivars at six different batches of production (*Arachis hypogaea* L., cultivars Runner, Spanish, Virginia, and Valencia) for a total of 24 samples were obtained from nuts.com (Cranford, NJ, USA) and peeled by hand upon receipt. Peanuts skins were frozen immediately after removal and kept at -80°C for further processing. Three cranberry fruits cultivar at eight different harvest times and two cranberry fruits cultivar at five different harvest times (*Vaccinium macrocarpon* A., cultivars Ben Lear A2, Scarlet Knight, G1-A57, G2-A20, and Stevens A10) for a total of 34 samples were obtained from Habelman Bros. Company (Tomah, WI, USA). The harvest times for five cranberry fruits cultivar were comprised from July to September 2016. Twenty-four apple fruits cultivar at different sizes (*Malus pumila* Cv., Ambrosia, Aurora, Braeburn, Cameo, Cripps Pink (x2), Eve, Empire, Fuji, Gala (x2), Golden Delicious, Granny Smith, Honeycrisp (x2), Jazz, Jonagold, Kanzi (x2), Kiku, McIntosh, Paula Red, Pinata, Pink Lady, Red Delicious, RubyFrost, SnapDragon, and SweeTango) for a total of 28 samples were purchased from local markets (Madison, WI, USA). Cranberries and apples were frozen with liquid nitrogen, ground into a fine powder, and stored at -80°C until further use.

Extraction of Proanthocyanidins

The extraction of PAC was adapted from our previous work (Esquivel-Alvarado, Muñoz-Arrieta, Alfaro-Viquez, Madrigal-Carballo, Krueger, & Reed, 2020). Samples (2 g) were extracted with aqueous acetone (20 mL; 70% v/v) in an ultrasonic bath for 30 minutes at 25°C and then centrifuged at 1800g for 15 min. The supernatant was collected, and the extraction of the remaining insoluble material, was repeated twice. The supernatants were pooled and concentrated by rotary evaporation to dryness and then brought to 10 mL with double distilled (DD) water.

Purification of Proanthocyanidins

The crude extract previously prepared was loaded onto a glass column (Kontes, 4 cm internal diameter x 15 cm length). The glass column was packed with Sephadex LH-20 resin (GE Healthcare, 18-111 μm) that was previously equilibrated with DD water. PAC were purified by sequential elution with DD water (50 mL), ethanol (100 mL), ethanol/methanol (1:1 v/v; 100 mL), and acetone (80% v/v; 150 mL). The acetone fraction containing PAC was dried via rotary evaporation, weighted, and resuspended in 100% methanol. After purification of PAC, 10 c-PAC from different cultivars and harvest times were mixed either with 10 a-PAC from different cultivars or 10 p-PAC from different cultivars and batches of production (Table SI 1-2). These c-PAC were mixed with the other source of PACs to obtain these percentages of c-PAC by weight: 5%, 10%, 15%, 20%, 25%, 50%, and 75%. Therefore, the total number of samples analyzed by MALDI-TOF MS consisted of 226 samples (28 unmixed a-PAC samples, 34 unmixed c-PAC samples, 24 unmixed p-PAC samples, 70 samples of c-PAC mixed with a-PAC, and 70 samples c-PAC mixed with p-PAC).

Characterization of Proanthocyanidins by Matrix-Assisted Laser Desorption-Ionization Time-of-Flight Mass Spectrometry (MALDI-TOF MS) Analysis

MALDI-TOF MS spectra of the samples were collected on a Bruker UltraFlex III mass spectrometer (Billerica, MA, USA) equipped with a SmartBeam^{TM} laser (Esquivel-Alvarado, Alfaro-Viquez, Krueger, Vestling, & Reed, 2020). Analyses were performed in positive reflectron mode, with pulsed ion extraction set at 130 nm, detector gain at 1548 V, preamplifier filter bandwidth at small, and digitizer sampling frequency at 100 Hz. Deflection was set at 900 Da. Samples and matrix (DHB; 1.30 M in methanol) were deionized using PureSpeed IEX strong cation resin tips (Rainin, CA, USA). The deionized matrix was mixed with cesium trifluoroacetate (5mM) in a 1:1 volume ratio. Samples were spotted on the MALDI-TOF MS stainless steel target (0.5 μL), followed by the addition of the matrix (0.6 μL). Spectra were calibrated using bradykinin (1060.6 Da) and glucagon (3483.8 Da) as external standards. Spectra were the sum of different locations in each well to minimize intra-well variability. In addition, each sample was spotted at least six times in a separate well to minimize inter-well variability. FlexControl and FlexAnalysis (Bruker Daltonick GmbH, Bremen, Germany) were used for data acquisition and data processing, respectively.

Deconvolution of the overlapping isotope patterns of MALDI-TOF MS to determine percentage of A- and B-type interflavan bonds

Based on the natural abundance of carbon, hydrogen, and oxygen isotopes within PAC structures, the deconvolution of the overlapping isotope patterns of MALDI-TOF MS spectra was used to determine the percentage of A- and B-type interflavan bonds in PAC for each DP (Feliciano, Krueger, Shanmuganayagam, Vestling, & Reed, 2012). Feliciano et al., 2012 described three

methods to deconvolute MALDI-TOF MS spectra in positive reflectron mode. In our study, the third method based on matrix algebra was used. The relative intensity (ri) for each monoisotopic mass was determined using IsoPro 3.0, whereas the absolute intensity (ai) of each PAC peak was calculated using mMass software (version 5.5.0). Spectral data were excluded from deconvolution analysis when the signal-to-noise (S/N) ratio was lower than three. The percentage of A- and B-type interflavan bonds in PAC was calculated using the algebraic matrix: $A^{-1} \times b = c$, where A^{-1} represents the inverse coefficient matrix of the relative intensity (ri) of the isotope patterns for each DP, b represents the constant matrix of ai from the spectra, and c represents the variable matrix of linear combinations that solve the simultaneous equation. The linear combinations obtained from $A^{-1} \times b$ were divided by the sum of all possible iterations and multiplied by 100 to obtain the percentage of A- and B-type interflavan bonds. For example, the matrix that estimates the percentage of A- and B-type interflavan bonds in PAC trimers is shown in equation 1. An additional row and column will be added to the algebraic matrix for each additional DP.

$$A = \begin{bmatrix} ri_{(2A,995)} & ri_{(1A,995)} & ri_{(0A,995)} \\ ri_{(2A,997)} & ri_{(1A,997)} & ri_{(0A,997)} \\ ri_{(2A,999)} & ri_{(1A,999)} & ri_{(0A,999)} \end{bmatrix} A^{-1} \times \begin{bmatrix} x_{995} \\ y_{997} \\ z_{999} \end{bmatrix} = \begin{bmatrix} ai_{(T,995)} \\ ai_{(T,997)} \\ ai_{(T,999)} \end{bmatrix} (1)$$

Statistical analysis

All data were reported as the mean ± standard deviation of at least three replicates. Principal component analysis (PCA) and linear discriminant analysis (LDA) were performed on the MALDI-TOF MS spectra data using the RStudio software, version 1.2.1335 (2009-2019 RStudio, Inc.). PCA is an unsupervised pattern recognition method that maximizes variance among individual samples by reducing the dimensionality of multivariable data. The dimension reduction

is achieved by identifying the principal components (PCs) in which the data varies (Callao & Ruisánchez, 2018). The loading plot, which studies the distribution of variables, provided information dealing with the interflavan bonds. The score plot, which shows the distribution of the samples on the PCs, provides information dealing with the PAC source. LDA is a supervised pattern recognition method that maximizes variance among classes but minimizes the variance within classes (Callao & Ruisánchez, 2018). LDA was used to evaluate the potential of the autoscaled MALDI-TOF MS spectra data to discriminate PAC fingerprints. Before PCA and LDA analysis, all the MALDI-TOF MS spectra data were pretreated with the autoscaling method at each DP to provide similar weight to all of the samples. The data set for PCA and LDA consisted of a 226 x 45 matrix (10170 data altogether), in which rows represented samples, and columns represented mass charge ratios (m/z) determined by MALDI-TOF MS. Samples were randomly split into two subsets: the training set (70%) and testing set (30%). The performance of LDA was evaluated by the training set, testing set, and leave-one-out cross-validation method (LOOCV). The LOOCV is carried out by performing *N* repetitions of the data set, where *N* is the size of the data set. On each repetition, one of the observations serves as the test set, while the remaining observations (*N-1*) serve as the training set. This process is repeated until the data set is complete. The LOOCV method was used instead of k-fold cross-validation because the data set contained a large number of groups (17 groups) and a small number of samples by group. Indeed, when the number of groups is large and the number of samples is small, the LOOCV method has proven to be a suitable approach to test model prediction (Dias, Fernandes, Veloso, Machado, Pereira, & Peres, 2014).

RESULTS AND DISCUSSION

MALDI-TOF MS spectra were used to characterize the PAC profiles of apples, cranberries, and peanut skins. MALDI-TOF MS was used for the analysis of PAC because other MS techniques, such as electrospray ionization MS, have limitations in their ability to resolve the heterogeneity and complexity of PAC (Reed, Krueger, & Vestling, 2005; Krueger, Reed, Feliciano, & Howell, 2013). The MALDI-TOF MS spectra showed that the predominant mass at each DP for a-PAC, c-PAC, and p-PAC are typical of (epi)catechin (Δ288 Da) monomers corresponding to cesium adducts $[M+Cs]^+$ in positive reflectron mode. These (epi)catechin monomers can be explained according to the equation $m/z= 290 + 288d – 2A + 133$, where 290 represents the molecular weight of the terminal (epi)catechin monomer, d is the DP, A is the number of A-type interflavan bonds, and 133 represents the atomic weight of cesium cation (Figure 2A-C) (Neto, Krueger, Lamoureaux, Kondo, Vaisberg, Hurta, et al., 2006). MALDI-TOF MS detected oligomers with DP from trimers to dodecamers in a-PAC and c-PAC (Figure 2A-B), and oligomers with DP from trimers to decamers in p-PAC decamers (Figure 2C).

The mass spectral analysis for PAC tetramers indicates that a-PAC, c-PAC, and p-PAC have mainly (epi)catechin monomers with structural variation in the nature of the interflavan bonds (Figure 2D-F). For PAC tetramers, four molecules that differ in the number of A-type interflavan bonds are possible: m/z 1281.2 [3A-type:0B-type], m/z 1283.2 [2A-type:1B-type], m/z 1285.2 [1A-type:2B-type], and m/z 1287.2 [0A-type:3B-type]. This variation in the isotope patterns of MALDI-TOF MS spectra suggests that for tetramers of a-PAC, the most predominant linkage corresponds to zero A-type interflavan bonds (Figure 2D). Conversely, the isotope patterns of

MALDI-TOF MS spectra suggest that for tetramers of c-PAC, the most predominant linkage corresponds to one A-type interflavan bond, followed by no A-type interflavan bonds (Figure 2E). Furthermore, the isotope patterns of MALDI-TOF MS spectra suggest that for tetramers of p-PAC, the most predominant linkage corresponds to two A-type interflavan bonds, followed by one A-type interflavan bond (Figure 2F).

Previous research has demonstrated that procyanidin dimers and trimers with B-type interflavan bonds can be converted to A-type interflavan bonds as result of oxidative intramolecular reactions (Cheynier & Ricardo-da-Silva, 1991; Kondo, Kurihara, Fukuhara, Tanaka, Suzuki, Miyata, et al., 2000; Osman & Wong, 2007; Poupard, Sanoner, Baron, Renard, & Guyot, 2011). Poupard et al., 2011 described that when caffeoylquinic acid *o*-quinone was incubated with procyanidin B2 (578 Da) in an apple juice model, oxidation occurred, but polymerization was not detected. In addition, procyanidin A2 (576 Da) did not accumulate, but rather continued to react to form dimers with three linkages (574 Da). Our results indicate that when a-PAC were subjected to MALDI-TOF MS, evidence of extra linkages apart from the interflavan bonds were not detected. Consistency in all MALDI-TOF MS spectra from a-PAC were observed. Oxidative intramolecular reactions in a-PAC occur to a lesser extent in fresh apples than in apple juice PAC. Currently, no evidence of intramolecular oxidation reactions have been reported for c-PAC.

The complex isotopic patterns observed in a-PAC, c-PAC, and p-PAC across the MALDI-TOF MS spectra is due to the content of isotopes at each DP, which is related to the natural abundance of carbon, hydrogen and oxygen isotopes. This natural abundance makes it possible to apply a

deconvolution method to estimate the percentage of A- to B-type interflavan bonds (Feliciano, Krueger, Shanmuganayagam, Vestling, & Reed, 2012). Deconvolution of the overlapping isotopic patterns of MALDI-TOF MS spectra indicates that for a-PAC, c-PAC, and p-PAC the percentage of A- to B-type interflavan bonds varied based on the relative intensity of the isotopic patterns. Table 1 indicates that for apples at all DP, PAC with zero A-type interflavan bonds were the most abundant. On the other hand, table 1 indicates that for cranberries at DP between 3 to 6, PAC with one A-type interflavan bond were the most abundant oligomer; whereas for DP between 7 and 8 of c-PAC, PAC with two A-type interflavan bonds were the most abundant oligomers. Finally, table 1 indicates that for peanuts at DP3, PAC with one A-type interflavan bond were the most abundant oligomer; whereas for DP between 4 to 7 of p-PAC, PAC with two A-type interflavan bonds were the most abundant oligomers; and for DP8 of p-PAC, PAC with three A-type interflavan bonds were the most abundant oligomer.

Mean values from the deconvoluted data indicated that 95.08 ± 1.28% of PAC from apples contain zero A-type interflavan bonds. On the other hand, mean values from the deconvoluted data indicated that 4.47 ± 0.76% of PAC from cranberries contain zero A-type interflavan bonds. Finally, mean values from the deconvoluted data indicated that 3.90 ± 2.44% of PAC from peanut skins contain zero A-type interflavan bonds. This results for the distribution of A- and B-type PAC in a-PAC and c-PAC is similar to our previous publication and validate the use of MALDI-TOF MS for characterizing PAC (Feliciano, Meudt, Shanmuganayagam, Krueger, & Reed, 2014)

The auto-scaled MALDI-TOF MS spectra data of the 226 samples (28 a-PAC, 34 c-PAC, 24 p-PAC, 70 c-PAC mixed with a-PAC, and 70 c-PAC mixed with p-PAC) were analyzed by PCA. c-PAC were prepared at ratios of 5, 10, 15, 20, 25, 50, and 75% (w/w) either with a-PAC or p-PAC. The results showed that the two principal components (PC1 and PC2) explain 91.6% of total variance. PC1 explained 66.0% of total variance, whereas PC2 explained the additional 25.6% of the total variance. Figure 3A indicates that all PAC with zero A-type interflavan bonds and their subsequent peaks, which are one mass unit higher than their corresponding interflavan bond, between DP3 to DP8 are located on the negative part of PC1. All PAC with one A-type interflavan bond and their subsequent peaks between DP3 to DP8 are located on the positive part of PC1 and negative part of PC2. All PAC with two A-type interflavan bonds and their subsequent peaks are located on the positive part of PC1 and either positive or negative part of PC2. Specifically, PAC with two A-type interflavan bonds and their subsequent peaks between DP3 to DP8 are located on the positive parts of PC1 and PC2; however, the subsequent peaks of DP7 and DP8 are located on the positive part of PC1 and negative part of PC2. Finally, all three A-type interflavan bonds and their subsequent peaks between DP3 to DP8 are located on the positive parts of PC1 and PC2. This loading plot indicates that PC1 compares PAC with zero A-type interflavan bonds to PAC with one A-type interflavan bond across PAC between DP3 to DP8, whereas PC2 compares PAC with one A-type interflavan bond to PAC with two A-type interflavan bonds across PAC between DP3 to DP8.

Visualization of the score plot for PC1 and PC2 shows that a-PAC, c-PAC, and p-PAC were separated from each other (Figure 3B). a-PAC were located in the negative part of PC1 and positive part of PC2. c-PAC were located in the positive part of PC1 and negative part of PC2. p-PAC were

located on the positive parts of PC1 and PC2. The small confidence ellipses with a 95% confidence interval for the auto-scaled MALDI-TOF MS spectra data for a-PAC and c-PAC are related with minimal variance. Conversely, the large confidence ellipse with a 95% confidence interval for the auto-scaled MALDI-TOF MS spectra data for p-PAC is related with a high variance. These results indicate that the variation on the PAC profile obtained by the auto-scaled MALDI-TOF MS spectra data is sufficient for the differentiation of a-PAC, c-PAC, and p-PAC. In addition, c-PAC mixed either with a-PAC or p-PAC were classified into fourteen groups according to their percentage. These results indicate that PCA may be used in visualizing the variation in the percentage of c-PAC either with a-PAC or p-PAC. The percentage of c-PAC with a-PAC is scaled with PC1, whereas the percentage of c-PAC with p-PAC is scaled with PC2. The prediction in the mixture of c-PAC either with a-PAC or p-PAC was further studied by LDA.

The LDA model was constructed using the 226 samples (28 a-PAC, 34 c-PAC, 24 p-PAC, 70 c-PAC mixed with a-PAC, and 70 c-PAC mixed with p-PAC). LDA was applied in order to find a predictive classification model able to discriminate these 17 groups. The results showed that the two linear discriminants (LD1 and LD2) explain 93.9% of the total variance (Figure 4). LD1 explained 84.7% of total variance, whereas LD2 explained the additional 9.2% of the total variance. Visualization of the score plot showed that a-PAC, c-PAC, and p-PAC were separated from each other. a-PAC were located on the negative part of LD1 and positive part of LD2. c-PAC were located on the positive part of LD1 and negative part of LD2. p-PAC were located on the positive part of LD1 and LD2. The small confidence ellipses with a 95% confidence interval for the auto-scaled MALDI-TOF MS spectra data for a-PAC and c-PAC are related with minimal variance. Conversely, the large confidence ellipse with a 95% confidence interval for the auto-

scaled MALDI-TOF MS spectra data for p-PAC is related with a high variance. Mixed c-PAC with a-PAC show a decreasing trend on the x-axis as the ratio of a-PAC increased. Mixed c-PAC with p-PAC show an upward trend on the y-axis as the ratio of p-PAC increased.

Considering the data matrix of 45 m/z peaks and 226 samples, the classification accuracy was evaluated using the RStudio software. The data set was randomly split into the training set (70%) and the testing set (30%). The training set was used to build the model, whereas the testing set was used to provide an unbiased evaluation of the final model. Validation of the LDA classification was evaluated using the LOOCV method. The LOOCV method is a technique used for assessing the predictive ability of a model and is a re-sampling technique used for small data set. Table 2 shows the classification results obtained by LDA applied to the 17 groups. The results indicated that LDA models correctly classified 99.4% of the training set, 100% of the testing set, and 94.2% of the validation set (Table SI 3-5). These results suggest that our methods may determine the adulteration of c-PAC, either with a-PAC or p-PAC, within 5% (w/w) with a confidence level of 95%, across a large range of mixtures.

CONCLUSION

The results of this study indicate the feasibility of MALDI-TOF MS spectra to characterize the PAC profiles of apples, cranberries, and peanut skins. Deconvolution of the overlapping isotopic pattern of MALDI-TOF MS spectra indicates that for a-PAC, c-PAC, and p-PAC the percentage of A- to B-type interflavan bonds varied based on the relative intensity of the isotopic patterns. Results demonstrate that MALDI-TOF MS spectra data combined with PCA and LDA offer the possibility to differentiate and to discriminate amongst the different sources of PAC. Overall, MALDI-TOF MS combined with multivariate analysis is an effective tool for the determination of authenticity in mixtures of c-PAC with a-PAC or p-PAC. Future work should include the analysis of c-PAC from different growers, and evaluation of mixtures of cranberry and apple juices without prior purification of PAC.

CONFLICT OF INTEREST

The authors declare the following competing financial interest(s): Christian G. Krueger and Jess D. Reed have ownership interest in Complete Phytochemical Solution, LLC., and acknowledge their affiliation with this company.

ACKNOWLEDGMENTS

The authors acknowledge financial support from the Ministry of Science, Technology and Telecommunications (MICITT), the Innovation and Human Capital Program for Competitiveness (PINN), and the National Council for Scientific and Technology Research (CONICIT, Grant PED-056-2015-I) from Costa Rica. The authors thank Maria Kamenetsky and Liliana Fadul-Pacheco for their help with the R-code. Additionally, the authors gratefully acknowledge use of the Bruker

ULTRAFLEX III supported by NIH through the University of Wisconsin, Department of Chemistry, Mass Spectrometry facility (NCRR 1S10RR024601-01).

AUTHORSHIP CONTRIBUTION STATEMENT

Daniel Esquivel-Alvarado: Conceptualization, Methodology, Formal analysis, Investigation, Data curation, Writing - original draft, Writing - review & editing, Visualization. **Emilia Alfaro-Viquez:** Conceptualization, Writing - review & editing, Visualization. **Christian G. Krueger:** Conceptualization, Writing - review & editing, Funding acquisition. **Martha M. Vestling:** Writing -review & editing. **Jess D. Reed:** Conceptualization, Writing - review & editing, Supervision, Funding acquisition.

REFERENCES

Alfaro-Viquez, E., Esquivel-Alvarado, D., Madrigal-Carballo, S., Krueger, C., & Reed, J. (2018). Cranberry proanthocyanidin-chitosan hybrid nanoparticles as a potential inhibitor of extra-intestinal pathogenic *Escherichia coli* invasion of gut epithelial cells. *International Journal of Biological Macromolecules*, 415-420. doi:10.1016/j.ijbiomac.2018.01.033.

Alfaro-Viquez, E., Esquivel-Alvarado, D., Madrigal-Carballo, S., Krueger, C., & Reed, J. (2019). Proanthocyanidin-chitosan composite nanoparticles prevent bacterial invasion and colonization of gut epithelial cells by extra-intestinal pathogenic *Escherichia coli*. *International Journal of Biological Macromolecules*, 630-636. doi:10.1016/j.ijbiomac.2019.04.170.

Barbosa, S., Pardo-Mates, N., Hidalgo-Serrano, M., Saurina, J., Puignou, L., & Núñez, O. (2018). Detection and Quantitation of Frauds in the Authentication of Cranberry-Based Extracts by UHPLC-HRMS (Orbitrap) Polyphenolic Profiling and Multivariate Calibration Methods. *Journal of Agricultural and Food Chemistry, 66*(35), 9353-9365. doi:10.1021/acs.jafc.8b02855.

Birmingham, A. D., Esquivel-Alvarado, D., Maranan, M., Krueger, C. G., & Reed, J. D. (2020). Inter-laboratory validation of 4-(dimethylamino) cinnamaldehyde (DMAC) assay using cranberry proanthocyanidin standard for quantification of soluble proanthocyanidins in cranberry foods and dietary supplements, First Action Method: 2019.06. *Journal of AOAC International*. doi:10.1093/jaoacint/qsaa084.

Callao, P., & Ruisánchez, I. (2018). An overview of multivariate qualitative methods for food fraud detection. *Food Control, 86*, 283-293. doi:10.1016/j.foodcont.2017.11.034.

Cheynier, V., & Ricardo-da-Silva, J. (1991). Oxidation of grape procyanidins in model solutions containing trans-caffeoyltartaric acid and polyphenol oxidase. *Journal of Agricultural and Food Chemistry, 39*(6), 1047-1049. doi:10.1021/jf00006a008.

Dias, L., Fernandes, A., Veloso, A., Machado, A., Pereira, J., & Peres, A. (2014). Single-cultivar extra virgin olive oil classification using a potentiometric electronic tongue. *Food Chemistry, 160*, 321-329. doi:10.1016/j.foodchem.2014.03.072.

Esquivel-Alvarado, D., Alfaro-Viquez, E., Krueger, C., Vestling, M., & Reed, J. (2020). Identification of A-type proanthocyanidins in cranberry-based foods and dietary supplements by matrix-assisted laser desorption/ionization time-of-flight mass spectrometry, First Action Method: 2019.05. *Journal of AOAC International*. doi:10.1093/jaoacint/qsaa106

Esquivel-Alvarado, D., Muñoz-Arrieta, R., Alfaro-Viquez, E., Madrigal-Carballo, S., Krueger, C., & Reed, J. (2020). Composition of anthocyanins and proanthocyanidins in three tropical *Vaccinium* species from Costa Rica. *Journal of Agricultural and Food Chemistry, 68*(10), 2872-2879. doi:10.1021/acs.jafc.9b01451.

Feliciano, R., Krueger, C., & Reed, J. (2015). Methods to determine effects of cranberry proanthocyanidins on extraintestinal infections: relevance for urinary tract health. *Molecular Nutrition & Food Research, 59*(7), 1292-1306. doi:10.1002/mnfr.201500108.

Feliciano, R., Krueger, C., Shanmuganayagam, D., Vestling, M., & Reed, J. (2012). Deconvolution of matrix-assisted laser desorption/ionization time-of-flight mass spectrometry isotope patterns to determine ratios of A-type to B-type interflavan bonds in cranberry proanthocyanidins. *Food Chemistry, 135*(3), 1485-1493. doi:10.1016/j.foodchem.2012.05.102.

Feliciano, R., Meudt, J., Shanmuganayagam, D., Krueger, C., & Reed, J. (2014). Ratio of "A-type" to "B-type" proanthocyanidin interflavan bonds affects extra-intestinal pathogenic *Escherichia coli* invasion of gut epithelial cells. *Journal of Agricultural and Food Chemistry, 62*(18), 3919-3925. doi:10.1021/jf403839a.

Feliciano, R., Shea, M., Shanmuganayagam, D., Krueger, C., Howell, A., & Reed, J. (2012). Comparison of isolated cranberry (*Vaccinium macrocarpon* Ait.) proanthocyanidins to catechin and procyanidins A2 and B2 for use as standards in the 4-(dimethylamino)cinnamaldehyde assay. *Journal of Agricultural and Food Chemistry, 60*(18), 4578-4585. doi:10.1021/jf3007213.

Foo, L., Lu, Y., Howell, A., & Vorsa, N. (2000). The structure of cranberry proanthocyanidins which inhibit adherence of uropathogenic P-fimbriated *Escherichia coli in vitro*. *Phytochemistry, 54*(2), 173-181. doi:10.1016/S0031-9422(99)00573-7.

Kondo, K., Kurihara, M., Fukuhara, K., Tanaka, T., Suzuki, T., Miyata, N., & Toyoda, M. (2000). Conversion of procyanidin B-type (catechin dimer) to A-type: evidence for abstraction of C-2

hydrogen in catechin during radical oxidation. *Tetrahedron Letters, 41*(4), 485-488. doi:10.1016/S0040-4039(99)02097-3.

Krueger, C., Reed, J., Feliciano, R., & Howell, A. (2013). Quantifying and characterizing proanthocyanidins in cranberries in relation to urinary tract health. *Analytical and Bioanalytical Chemistry, 405*(13), 4385-4395. doi:10.1007/s00216-013-6750-3.

Leclair, M. (2016). Fruits & Vegetable Markets in the US. *IBSWorld Industry Report*, IBISWorld.

Neto, C., Krueger, C., Lamoureaux, T., Kondo, M., Vaisberg, A., Hurta, R., Curtis, S., Matchett, M., Yeung, H., Sweeney, M., & Reed, J. (2006). MALDI-TOF MS characterization of proanthocyanidins from cranberry fruit (*Vaccinium macrocarpon*) that inhibit tumor cell growth and matrix metalloproteinase expression *in vitro*. *Journal of the Science of Food and Agriculture, 86*(1), 18-25. doi:10.1002/jsfa.2347.

Osman, A., & Wong, K. (2007). Laccase (EC 1.10. 3.2) catalyses the conversion of procyanidin B-2 (epicatechin dimer) to type A-2. *Tetrahedron Letters, 48*(7), 1163-1167. doi:10.1016/j.tetlet.2006.12.075.

Pardo-Mates, N., Vera, A., Barbosa, S., Hidalgo-Serrano, M., Nunez, O., Saurina, J., Hernandez-Cassou, S., & Puignou, L. (2017). Characterization, classification and authentication of fruit-based extracts by means of HPLC-UV chromatographic fingerprints, polyphenolic profiles and chemometric methods. *Food Chemistry, 221*, 29-38. doi:10.1016/j.foodchem.2016.10.033.

Poupard, P., Sanoner, P., Baron, A., Renard, C. M., & Guyot, S. (2011). Characterization of procyanidin B2 oxidation products in an apple juice model solution and confirmation of their presence in apple juice by high-performance liquid chromatography coupled to electrospray ion trap mass spectrometry. *Journal of Mass Spectrometry, 46*(11), 1186-1197. doi:10.1002/jms.2007.

Reed, J., Krueger, C., & Vestling, M. (2005). MALDI-TOF mass spectrometry of oligomeric food polyphenols. *Phytochemistry, 66*(18), 2248-2263. doi:10.1016/j.phytochem.2005.05.015

Sobolev, V., & Cole, R. (2004). Note on utilisation of peanut seed testa. *Journal of the Science of Food and Agriculture, 84*(1), 105-111. doi:10.1002/jsfa.1593.

van Boxtel, E., van den Broek, L., Koppelman, S., Vincken, J., & Gruppen, H. (2007). Peanut allergen Ara h 1 interacts with proanthocyanidins into higher molecular weight complexes. *Journal of Agricultural and Food Chemistry, 55*(21), 8772-8778. doi:10.1021/jf071585k.

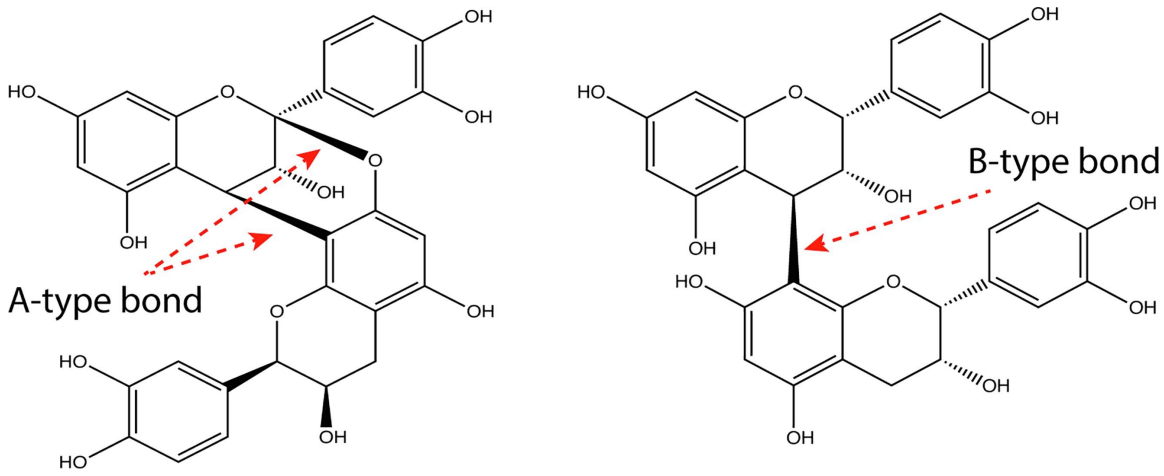

Figure 1. Representative structures of A-type and B-type interflavan bond dimers.

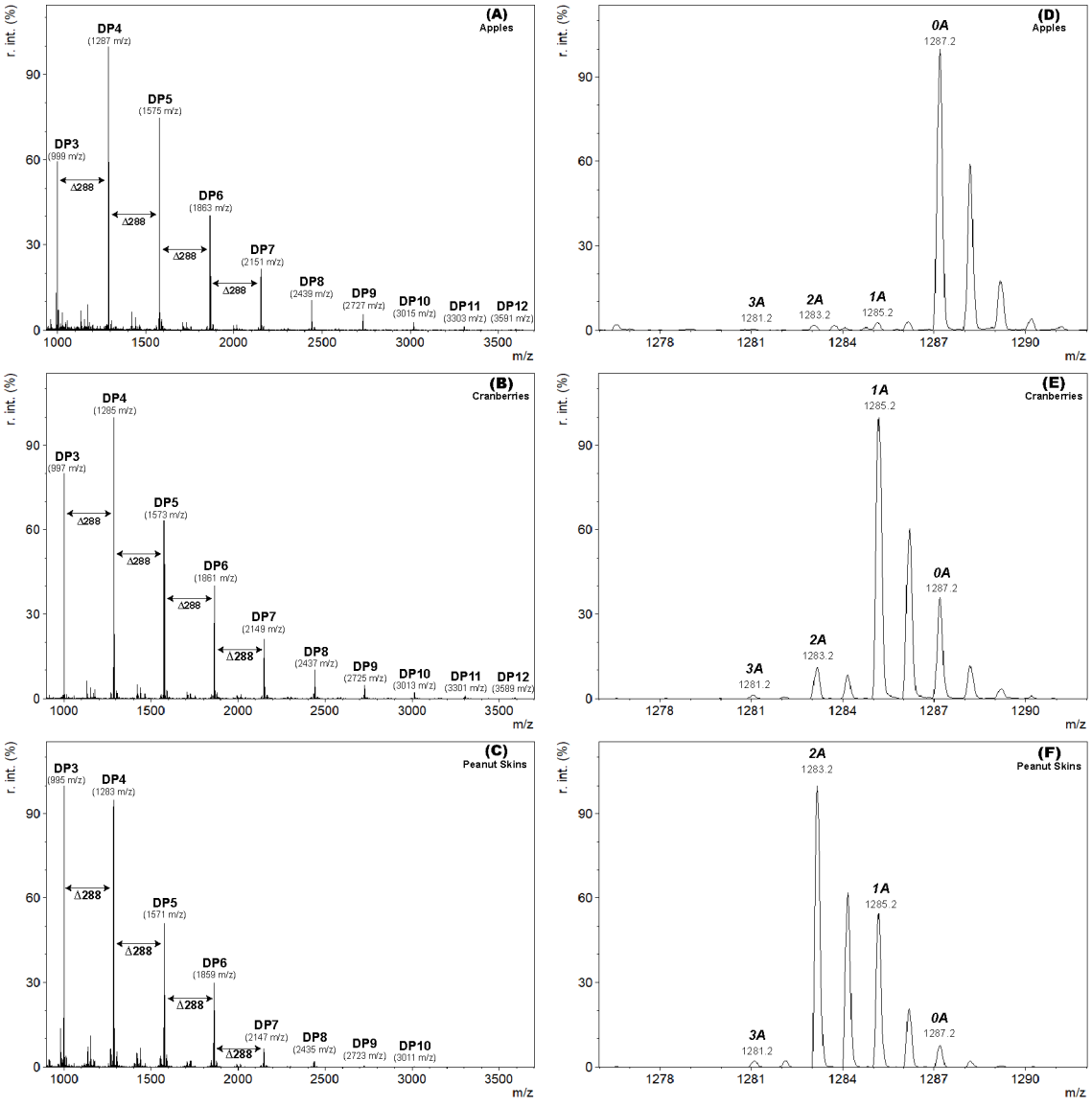

Figure 2. MALDI-TOF MS spectra in positive reflectron mode for apples (A), cranberries (B), and peanut skins (C) PAC.Isotopic patterns obtained from MALDI-TOF MS spectra in positive reflectron mode for apples (D), cranberries (E), and peanut skins (F) PAC tetramers displaying cesium adducts.

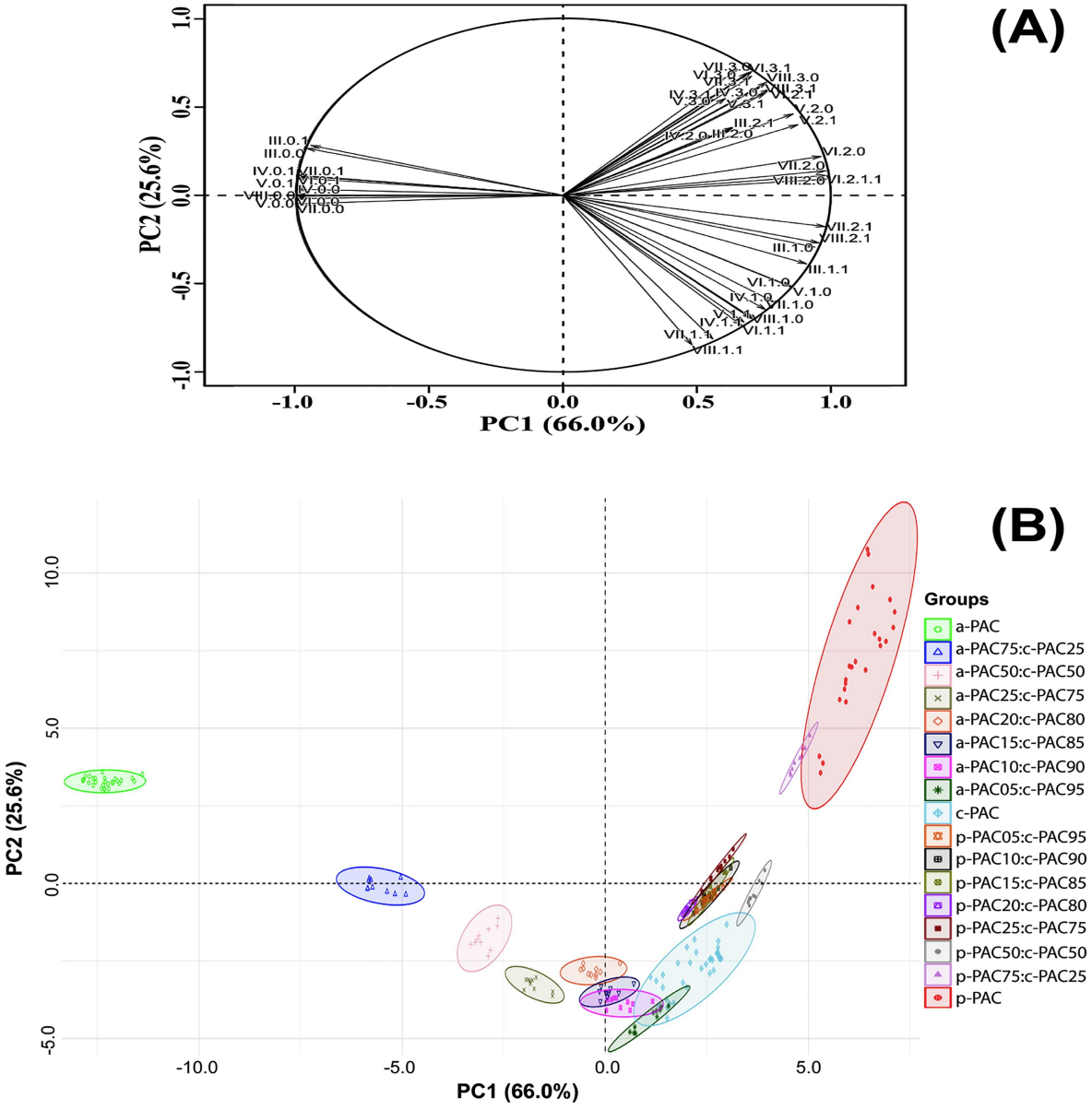

Figure 3. PCA loading (A) and score (B) plots based on the auto-scaled MALDI-TOF MS spectra data. PC1 (x-axis) and PC2 (y-axis) account for 91.6% of the total variance. The roman numeral identifies the DP (DP3 to DP8). The first number after the roman numeral identifies the number of A-type interflavan bonds (0, 1, 2 or 3- A-type) in each DP. The second number after the roman numeral identifies the mass of the interflavan bond (0) or its subsequent peaks (1).

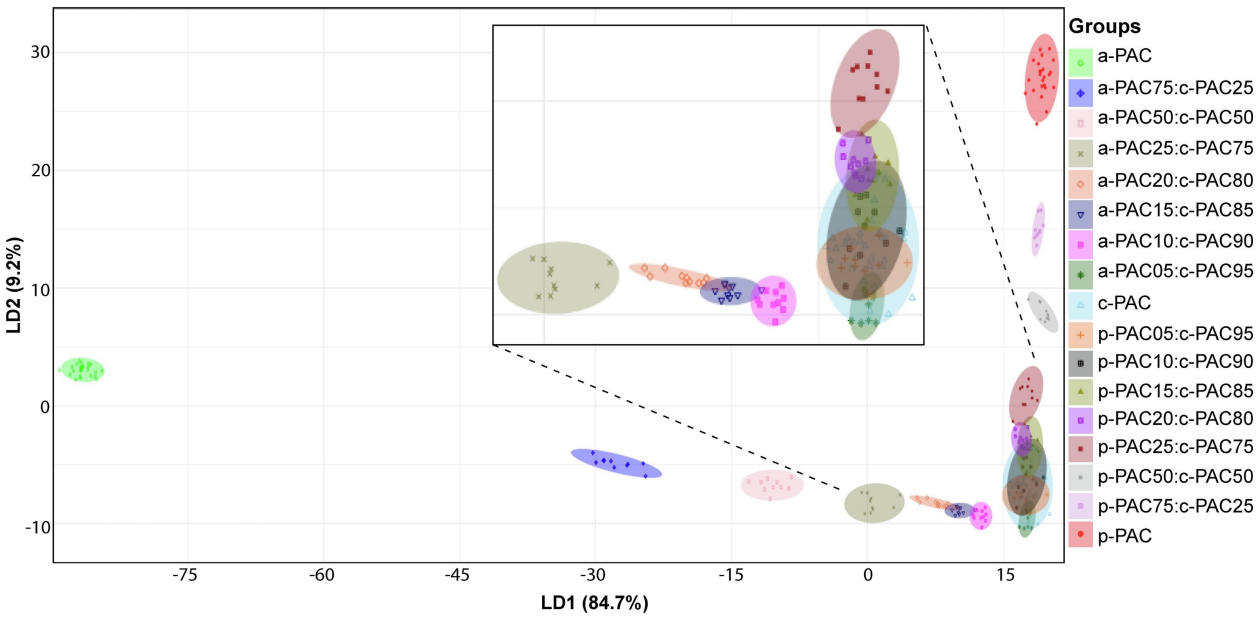

Figure 4. LDA score plot based on the auto-scaled MALDI-TOF MS spectra data, which show the LD1 (x-axis) and LD2 (y-axis) that accounted for 93.9% of the total variance.

Table 1. Representative percentages of A-type interflavan bonds from trimers to octamers in proanthocyanidins that were isolated from apples (a-PAC; n=28), cranberries (c-PAC; n=34), and peanut skins (p-PAC; n=24).

Sample	Degree of Polymerization	3A-type: 0B-type	2A-type: 0B-type	1A-type: 1B-type	0A-type: 2B-type
a-PAC	**Trimers**	n.a*	0.25 ± 0.51	4.14 ± 2.74	95.61 ± 2.58
	Tetramers	0.02 ± 0.06	0.76 ± 0.52	2.49 ± 0.74	96.73 ± 0.88
	Pentamers	0.03 ± 0.06	1.35 ± 0.65	3.09 ± 0.74	95.54 ± 1.03
	Hexamers	0.05 ± 0.17	1.29 ± 0.77	3.27 ± 0.67	95.39 ± 1.12
	Heptamers	0.00 ± 0.00	1.25 ± 1.24	4.14 ± 1.36	94.60 ± 1.94
	Octamers	0.03 ± 0.17	1.07 ± 1.43	6.31 ± 2.73	92.58 ± 2.81
c-PAC	**Trimers**	n.a	3.16 ± 2.47	92.58 ± 3.46	4.26 ± 3.71
	Tetramers	1.69 ± 1.23	15.51 ± 5.36	78.17 ± 3.89	4.64 ± 3.87
	Pentamers	2.18 ± 1.26	27.57 ± 4.06	66.00 ± 3.38	4.24 ± 2.85
	Hexamers	2.63 ± 1.42	49.00 ± 3.63	45.04 ± 3.38	3.33 ± 1.59
	Heptamers	8.42 ± 2.83	51.66 ± 3.81	35.51 ± 4.12	4.42 ± 2.00
	Octamers	16.64 ± 3.35	49.29 ± 6.33	28.16 ± 5.28	5.91 ± 3.39
p-PAC	**Trimers**	n.a	12.62 ± 7.97	79.12 ± 14.35	8.26 ± 8.17
	Tetramers	4.08 ± 3.65	67.07 ± 15.42	27.38 ± 12.36	1.47 ± 0.84
	Pentamers	10.16 ± 6.98	63.56 ± 11.17	23.37 ± 6.74	2.91 ± 0.96
	Hexamers	19.69 ± 5.75	70.55 ± 8.49	7.95 ± 4.14	1.81 ± 0.80
	Heptamers	45.59 ± 5.71	44.91 ± 8.03	6.59 ± 3.32	2.92 ± 2.10
	Octamers	57.37 ± 9.66	26.99 ± 9.35	9.61 ± 3.40	6.03 ± 2.27

The results are expressed as the mean of three independent replicates ± standard deviation. *n.a: not applicable.

Table 2. Results of the classification performance for the training, testing, and validation set.

Classification criterion	Classification	Number of Samples	Correct / Total	Accuracy (%)	Specificity (%)	Sensitivity (%)
Groups	Training set	159 (70%)	158 / 159	99.4	99.9	99.4
	Testing set	67 (30%)	67 / 67	100	100	100
	Validation	226 (100%)	213 / 226	94.2	99.7	94.5

Table 1S. Cranberries and apples employed to prepare the mixed c-PAC at ratios of 5, 10, 15, 20, 25, 50, and 75% (w/w) with a-PAC.

Cranberries	**Apples**
Ben Lear A2	Cameo
Scarlet Knight	Ambrosia
G1-A57	Kanzi
G2-A20	Jazz
Steven A10	Red Delicious
Ben Lear A2	Golden Delicious
Scarlet Knight	Braeburn
G1-A57	Pink Lady
G2-A20	Fuji
Steven A10	Granny Smith

Table 2S. Cranberries and peanut skins employed to prepare the mixed c-PAC at ratios of 5, 10, 15, 20, 25, 50, and 75% (w/w) with p-PAC.

Cranberries	**Peanut Skins**
Ben Lear A2	Virginia
Scarlet Knight	Runner
G1-A57	Valencia
G2-A20	Spanish
Steven A10	Virginia
Ben Lear A2	Runner
Scarlet Knight	Valencia
G1-A57	Spanish
G2-A20	Virginia
Steven A10	Runner

Table 3S. Results of the LDA model using the training set.

	a-PAC	a-PAC:c-PAC (5:95 w/w)	a-PAC:c-PAC (10:90 w/w)	a-PAC:c-PAC (15:85 w/w)	a-PAC:c-PAC (20:80 w/w)	a-PAC:c-PAC (25:75 w/w)	a-PAC:c-PAC (50:50 w/w)	a-PAC:c-PAC (75:25 w/w)	p-PAC	c-PAC	p-PAC:c-PAC (5:95 w/w)	p-PAC:c-PAC (10:90 w/w)	p-PAC:c-PAC (15:85 w/w)	p-PAC:c-PAC (20:80 w/w)	p-PAC:c-PAC (25:75 w/w)	p-PAC:c-PAC (50:50 w/w)	p-PAC:c-PAC (75:25 w/w)	Specificity (%)	Sensitivity (%)
a-PAC	**20**	0	0	0	0	0	0	0	0	0	0	0	0	0	0	0	0	**100.0**	**100.0**
a-PAC:c-PAC (5:95 w/w)	0	**7**	0	0	0	0	0	0	0	0	0	0	0	0	0	0	0	**100.0**	**100.0**
a-PAC:c-PAC (10:90 w/w)	0	0	**7**	0	0	0	0	0	0	0	0	0	0	0	0	0	0	**100.0**	**100.0**
a-PAC:c-PAC (15:85 w/w)	0	0	0	**7**	0	0	0	0	0	0	0	0	0	0	0	0	0	**100.0**	**100.0**
a-PAC:c-PAC (20:80 w/w)	0	0	0	0	**7**	0	0	0	0	0	0	0	0	0	0	0	0	**100.0**	**100.0**
a-PAC:c-PAC (25:75 w/w)	0	0	0	0	0	**7**	0	0	0	0	0	0	0	0	0	0	0	**100.0**	**100.0**
a-PAC:c-PAC (50:50 w/w)	0	0	0	0	0	0	**7**	0	0	0	0	0	0	0	0	0	0	**100.0**	**100.0**
a-PAC:c-PAC (75:25 w/w)	0	0	0	0	0	0	0	**7**	0	0	0	0	0	0	0	0	0	**100.0**	**100.0**
p-PAC	0	0	0	0	0	0	0	0	**17**	0	0	0	0	0	0	0	0	**100.0**	**100.0**
c-PAC	0	0	0	0	0	0	0	0	0	**24**	0	0	0	0	0	0	0	**100.0**	**100.0**
p-PAC:c-PAC (5:95 w/w)	0	0	0	0	0	0	0	0	0	0	**7**	0	0	0	0	0	0	**100.0**	**100.0**
p-PAC:c-PAC (10:90 w/w)	0	0	0	0	0	0	0	0	0	0	0	**6**	0	0	0	0	0	**100.0**	**85.7**
p-PAC:c-PAC (15:85 w/w)	0	0	0	0	0	0	0	0	0	0	0	**1**	**7**	0	0	0	0	**99.3**	**100.0**
p-PAC:c-PAC (20:80 w/w)	0	0	0	0	0	0	0	0	0	0	0	0	0	**7**	0	0	0	**100.0**	**100.0**
p-PAC:c-PAC (25:75 w/w)	0	0	0	0	0	0	0	0	0	0	0	0	0	0	**7**	0	0	**100.0**	**100.0**
p-PAC:c-PAC (50:50 w/w)	0	0	0	0	0	0	0	0	0	0	0	0	0	0	0	**7**	0	**100.0**	**100.0**
p-PAC:c-PAC (75:25 w/w)	0	0	0	0	0	0	0	0	0	0	0	0	0	0	0	0	**7**	**100.0**	**100.0**

Table 4S. Results of the LDA model using the testing set.

	a-PAC	a-PAC:c-PAC (5:95 w/w)	a-PAC:c-PAC (10:90 w/w)	a-PAC:c-PAC (15:85 w/w)	a-PAC:c-PAC (20:80 w/w)	a-PAC:c-PAC (25:75 w/w)	a-PAC:c-PAC (50:50 w/w)	a-PAC:c-PAC (75:25 w/w)	p-PAC	c-PAC	p-PAC:c-PAC (5:95 w/w)	p-PAC:c-PAC (10:90 w/w)	p-PAC:c-PAC (15:85 w/w)	p-PAC:c-PAC (20:80 w/w)	p-PAC:c-PAC (25:75 w/w)	p-PAC:c-PAC (50:50 w/w)	p-PAC:c-PAC (75:25 w/w)	**Specificity (%)**	**Sensitivity (%)**
a-PAC	**8**	0	0	0	0	0	0	0	0	0	0	0	0	0	0	0	0	**100.0**	**100.0**
a-PAC:c-PAC (5:95 w/w)	0	**3**	0	0	0	0	0	0	0	0	0	0	0	0	0	0	0	**100.0**	**100.0**
a-PAC:c-PAC (10:90 w/w)	0	0	**3**	**0**	0	0	0	0	0	0	0	0	0	0	0	0	0	**100.0**	**100.0**
a-PAC:c-PAC (15:85 w/w)	0	0	0	**3**	0	0	0	0	0	0	0	0	0	0	0	0	0	**100.0**	**100.0**
a-PAC:c-PAC (20:80 w/w)	0	0	0	**0**	**3**	0	0	0	0	0	0	0	0	0	0	0	0	**100.0**	**100.0**
a-PAC:c-PAC (25:75 w/w)	0	0	0	0	0	**3**	0	0	0	0	0	0	0	0	0	0	0	**100.0**	**100.0**
a-PAC:c-PAC (50:50 w/w)	0	0	0	0	0	0	**3**	0	0	0	0	0	0	0	0	0	0	**100.0**	**100.0**
a-PAC:c-PAC (75:25 w/w)	0	0	0	0	0	0	0	**3**	0	0	0	0	0	0	0	0	0	**100.0**	**100.0**
p-PAC	0	0	0	0	0	0	0	0	**7**	0	0	0	0	0	0	0	0	**100.0**	**100.0**
c-PAC	0	0	0	0	0	0	0	0	0	**10**	0	0	0	0	0	0	0	**100.0**	**100.0**
p-PAC:c-PAC (5:95 w/w)	0	0	0	0	0	0	0	0	0	0	**3**	0	0	0	0	0	0	**100.0**	**100.0**
p-PAC:c-PAC (10:90 w/w)	0	0	0	0	0	0	0	0	0	0	0	**3**	0	0	0	0	0	**100.0**	**100.0**
p-PAC:c-PAC (15:85 w/w)	0	0	0	0	0	0	0	0	0	0	0	0	**3**	0	0	0	0	**100.0**	**100.0**
p-PAC:c-PAC (20:80 w/w)	0	0	0	0	0	0	0	0	0	0	0	0	0	**3**	0	0	0	**100.0**	**100.0**
p-PAC:c-PAC (25:75 w/w)	0	0	0	0	0	0	0	0	0	0	0	0	0	0	**3**	0	0	**100.0**	**100.0**
p-PAC:c-PAC (50:50 w/w)	0	0	0	0	0	0	0	0	0	0	0	0	0	0	0	**3**	0	**100.0**	**100.0**
p-PAC:c-PAC (75:25 w/w)	0	0	0	0	0	0	0	0	0	0	0	0	0	0	0	0	**3**	**100.0**	**100.0**

Table 5S. Results of the LDA model using the validation set.

	a-PAC	a-PAC:c-PAC (5:95 w/w)	a-PAC:c-PAC (10:90 w/w)	a-PAC:c-PAC (15:85 w/w)	a-PAC:c-PAC (20:80 w/w)	a-PAC:c-PAC (25:75 w/w)	a-PAC:c-PAC (50:50 w/w)	a-PAC:c-PAC (75:25 w/w)	p-PAC	c-PAC	p-PAC:c-PAC (5:95 w/w)	p-PAC:c-PAC (10:90 w/w)	p-PAC:c-PAC (15:85 w/w)	p-PAC:c-PAC (20:80 w/w)	p-PAC:c-PAC (25:75 w/w)	p-PAC:c-PAC (50:50 w/w)	p-PAC:c-PAC (75:25 w/w)	Specificity (%)	Sensitivity (%)
a-PAC	**28**	0	0	0	0	0	0	0	0	0	0	0	0	0	0	0	0	**100.0**	**100.0**
a-PAC:c-PAC (5:95 w/w)	0	**10**	0	0	0	0	0	0	0	0	0	0	0	0	0	0	0	**100.0**	**90.9**
a-PAC:c-PAC (10:90 w/w)	0	0	**9**	**1**	0	0	0	0	0	0	0	0	0	0	0	0	0	**99.5**	**100.0**
a-PAC:c-PAC (15:85 w/w)	0	0	0	**10**	0	0	0	0	0	0	0	0	0	0	0	0	0	**100.0**	**83.3**
a-PAC:c-PAC (20:80 w/w)	0	0	0	**1**	**9**	0	0	0	0	0	0	0	0	0	0	0	0	**99.5**	**100.0**
a-PAC:c-PAC (25:75 w/w)	0	0	0	0	0	**10**	0	0	0	0	0	0	0	0	0	0	0	**100.0**	**100.0**
a-PAC:c-PAC (50:50 w/w)	0	0	0	0	0	0	**10**	0	0	0	0	0	0	0	0	0	0	**100.0**	**100.0**
a-PAC:c-PAC (75:25 w/w)	0	0	0	0	0	0	0	**10**	0	0	0	0	0	0	0	0	0	**100.0**	**100.0**
p-PAC	0	0	0	0	0	0	0	0	**24**	0	0	0	0	0	0	0	0	**100.0**	**100.0**
c-PAC	0	**1**	0	0	0	0	0	0	0	**33**	0	0	0	0	0	0	0	**99.5**	**100.0**
p-PAC:c-PAC (5:95 w/w)	0	0	0	0	0	0	0	0	0	0	**8**	**2**	0	0	0	0	0	**99.1**	**80.0**
p-PAC:c-PAC (10:90 w/w)	0	0	0	0	0	0	0	0	0	0	**2**	**6**	**2**	0	0	0	0	**98.1**	**60.0**
p-PAC:c-PAC (15:85 w/w)	0	0	0	0	0	0	0	0	0	0	0	**2**	**7**	**1**	0	0	0	**98.6**	**77.8**
p-PAC:c-PAC (20:80 w/w)	0	0	0	0	0	0	0	0	0	0	0	0	0	**10**	0	0	0	**100.0**	**83.3**
p-PAC:c-PAC (25:75 w/w)	0	0	0	0	0	0	0	0	0	0	0	0	0	**1**	**9**	0	0	**99.5**	**100.0**
p-PAC:c-PAC (50:50 w/w)	0	0	0	0	0	0	0	0	0	0	0	0	0	0	0	**10**	0	**100.0**	**100.0**
p-PAC:c-PAC (75:25 w/w)	0	0	0	0	0	0	0	0	0	0	0	0	0	0	0	0	**10**	**100.0**	**100.0**

CHAPTER 4: Composition of anthocyanins and proanthocyanidins in three tropical *Vaccinium* species from Costa Rica

Daniel Esquivel-Alvarado[§], Rodrigo Muñoz-Arrieta[‡], Emilia Alfaro-Viquez[§], Sergio Madrigal-Carballo[§], Christian G. Krueger[§,†], Jess D. Reed[§,†]

[§] University of Wisconsin-Madison, Dept. Animal Sciences, Reed Research Group, 1675 Observatory Drive, Madison, WI 53706, USA.

[‡] National Center for Biotechnological Innovations of Costa Rica - CENIBiot, 1174-1200, San José, Costa Rica.

[†] Complete Phytochemical Solutions, LLC, 317 South Street, Cambridge, WI 53523, USA.

This chapter is published as-is in the *Journal of Agricultural and Food Chemistry*

https://10.1021/acs.jafc.9b01451

ABSTRACT

Total polyphenol content (TPC), flavonoid content (TFC), anthocyanin content (TAC), and proanthocyanidin (PAC) content were determined in fruit from three tropical *Vaccinium* species (*V. consanguineum*, *V. floribundum*, and *V. poasanum*) from Costa Rica sampled at three stages of fruit development. Results show that TAC content increased as the fruit developed, while TPC, TFC, and PAC content decreased. Anthocyanin profiles were evaluated using ESI-MS/MS. Cyanidin and delphinidin glycosides were the predominant anthocyanins for the three tropical *Vaccinium* species. Proanthocyanidins were characterized using ATR-FTIR, NMR, and MALDI-TOF MS. Presence of procyanidin structures with B-type interflavan bonds were observed, but deconvolution of MS isotope patterns indicated that PACs with one or more A-type interflavan bonds accounted for more than 74% of the oligomers at each degree of polymerization.

Keywords: proanthocyanidins; anthocyanin; A-type interflavan bonds; MALDI-TOF MS.

INTRODUCTION

Vaccinium consanguineum Klotzsch*, V. floribundum* Kunth, and *V. poasanum* Donn. Sm., are the most common tropical *Vaccinium* species (TVS) that grow in the highlands of Costa Rica (1500-3500 m) (Jiménez-Bonilla & Abdelnour-Esquivel, 2016). *V. consanguineum and V. floribundum* have a similar physical appearance, characterized by pinnately nerved and serrulate-margined leaf-blades, racemose inflorescenses with small white to pink flowers, and glaucous berries (Montiel, 1991; Wilbur & Luteyn, 2008). However, these species differ from each other in height, flower structure, branch density and distribution of growth. *V. consanguineum* are shrubs between 1-3 m tall, with flowers that have spurred connectives, and grows only in the mountains of Costa Rica and western of Panama. Whereas, *V. floribundum* are densely branched shrubs between 2-8 m tall with spurless flowers, and grows from Costa Rica to the south America Andes (Wilbur & Luteyn, 2008). On the other hand, *V. poasanum*, are shrubs between 2-5 m tall and grows from Guatemala to Panama. This species is characterized by leaves with acute to broadly cuneate blade base, acute to acuminate apices, and racemose inflorescence with small yellowish to greenish-white flowers (Montiel, 1991; Wilbur & Luteyn, 2008).

TVS begin flowering in the rainy season (May-November) and bear fruit in the dry season (December-May)(Jiménez-Bonilla & Abdelnour-Esquivel, 2013). Berries from *Vaccinium* species are sources of polyphenols which are widely researched in the field of nutrition because of putative health benefits that are associated with polyphenols (Shahidi & Ambigaipalan, 2015; Alfaro-Viquez, Esquivel-Alvarado, Madrigal-Carballo, Krueger, & Reed, 2019). Berry consumption in Costa Rica has increased since 2012 and importation of berries from North and South America to Costa Rica increased 320%. (PROCOMER, 2018) In order to satisfy the national market,

initiatives to promote local cultivation of TVS have been launched as part of the National Fruit Growing Program by the Costa Rican Department of Agriculture (Brenes Angulo, Castillo Matamoros, & Gómez-Alpízar, 2015; Jiménez-Bonilla & Abdelnour-Esquivel, 2013, 2016).

Polyphenols found in *Vaccinium* species such as cranberry contain hydroxycinnamic acids, flavonols, anthocyanins, and proanthocyanidins, among others (Krueger, Reed, Feliciano, & Howell, 2013; Vvedenskaya & Vorsa, 2004). Anthocyanins are water-soluble pigments that vary by the number of methyl, methoxy, or hydroxyl groups, the nature and number of sugars attached to the molecule, and the nature and number of aliphatic or aromatic acids attached to sugars in the molecule (Kong, Chia, Goh, Chia, & Brouillard, 2003; J. Lee, Durst, & Wrolstad, 2005). Proanthocyanidins (PAC) are oligomers of flavan-3-ols. PAC structures vary by the nature of the monomer unit, interflavan linkage, and degree of polymerization (DP) (Wang, Singh, Hurst, Glinski, Koo, & Vorsa, 2016). PAC are classified by the type of flavan-3-ol monomers such as properlagonidins which are oligomers of (epi)afzelechin, procyanidins which are oligomers of (epi)catechin, and prodelphinidins which are oligomers of (epi)gallocatechin (Hellström, Sinkkonen, Karonen, & Mattila, 2007). However, many types of PAC contain more than one type of monomeric flavan-3-ols such as PAC in grape seeds. PAC can have B-type and A-type bonds. B-type bonds are defined by the presence of C_4-C_8 or C_4-C_6 interflavan bonds, whereas A-type bonds have C_4-C_8 bonds, but also have an additional interflavan bond between C_2-O-C_7 or C_2-O-C_5 (Kimura, Ogawa, Akihiro, & Yokota, 2011; Krueger, Reed, Feliciano, & Howell, 2013; Wang, Singh, Hurst, Glinski, Koo, & Vorsa, 2016).

Since other *Vaccinium* species contain a variety of polyphenols, the goal of this study was to characterize the polyphenol content and the anthocyanin and proanthocyanidin profiles of TVS collected in the Costa Rican highlands. The polyphenol contents at the three stages of fruit development have different potential economic values regarding their polyphenol composition. This information may be used to improve the market for *Vaccinium* berries that may provide sustainable economic opportunities for farmers.

MATERIAL AND METHODS

Chemicals and materials

Folin-Ciocalteu reagent, sodium carbonate, gallic acid, aluminium chloride, quercetin, potassium chloride, sodium acetate, cyanidin-3-glucoside, formic acid, bradykinin, glucagon, 4-(dimethylamino)cinnamaldehyde, and 2,5-dihydroxybenzoic acid (DHB) were obtained from Sigma-Aldrich (Milwaukee, WI, USA). Methanol and acetone were purchased from Fischer Scientific (Fair Lawn, NJ, USA). Methanol-d4 with TMS (0.03%) was obtained from Acros Organics (Fair Lawn, NJ, USA). Ethanol (100%) was obtained from Decon's lab (King of Prussia, PA, USA). Sephadex LH-20® was purchased from GE Healthcare (Uppsala, Sweden).

Sample collection and extraction

TVS were collected bi-monthly starting in August 2014 and classified into three stages of maturation (early, middle, and late stage) according to color development (Figure 1). Berries from *V. poasanum* were collected at 3,000 m (latitude 009°36'41.6"N and longitude 083°51'11.6" W), whereas berries from *V. consanguineum* and *V. floribundum* were collected at 3,200 m (latitude 009°34'21.7"N and longitude 083°45'28.8"W and latitude 009°34'24.0"N and longitude 083°45'28.2"W, respectively). Species identification was carried out by botanist Luis Poveda from the National University of Costa Rica and confirmed by comparison of branches, flowers, and fruits by botanist Joaquin Sanchez from the National Herbarium of Costa Rica. Samples were cleaned, freeze-dried, milled, passed through a sieve (18 mesh), and stored at -80°C for further analysis. One hundred milligrams of TVS were extracted with 3 mL of acetone (70% v/v) in an ultrasonic bath for 30 min at 25°C and then centrifuged at 1,800 g for 15 min. The supernatant was

collected, and the extraction was repeated two additional times. The supernatants were pooled and concentrated by rotary evaporation to dryness and then brought to 10 mL volume with methanol.

Polyphenol contents

Quantification of total polyphenol content

The total phenolic content (TPC) was determined using the Folin-Ciocalteu assay with some modifications (Singleton, Orthofer, & Lamuela-Raventós, 1999). Two hundred microliters of ultrapure water, 15 µL of Folin-Ciocalteu reagent, 30 µL of sample, and 50 µL of sodium carbonate (20% w/v) were added to a microplate and incubated at 40°C for 20 min. Absorbance was measured at 765 nm. The results were expressed as mg gallic acid equivalent per gram of sample dry matter (mg GAE/g DM).

Determination of total flavonoid content

The total flavonoid content (TFC) was determined using the Dowd method with slight modifications (Pękal & Pyrzynska, 2014). One hundred microliters of aluminium chloride (2% w/v) in methanol was mixed with 100 µL of sample and incubated at room temperature for 10 min. Absorbance was read at 415 nm using a microplate reader. A standard solution of quercetin from 30 to 100 µg/µL was prepared in methanol. TFC were expressed as mg quercetin equivalent per gram of sample on a dry matter (mg QE/g DM).

Quantification of total anthocyanin content

The total anthocyanin content (TAC) was determined using the differential pH method (J. Lee, Durst, & Wrolstad, 2005). Absorbance of the samples was measured at 520 and 700 nm using potassium chloride buffer (pH 1.0, 25 mM) and sodium acetate buffer (pH 4.5, 0.4 M), respectively. Samples and buffers were mixed in 1:4 volume ratios, respectively. TAC was expressed as cyanidin-3-glucoside per gram of dry matter (mg C3G/g DM), using $A = (A_{520nm} - A_{700nm})_{pH1.0} - (A_{520nm} - A_{700nm})_{pH4.5}$.

Determination of soluble proanthocyanidins

Quantification of soluble proanthocyanidins (s-PAC) was determined using the 4-(dimethylamino)cinnamaldehyde (DMAC) assay (Feliciano, Shea, Shanmuganayagam, Krueger, Howell, & Reed, 2012). Two hundred ten microliters of DMAC (1 mg/mL) were dissolved in a buffer solution (75:12.5:12.5 EtOH:HCl:H_2O), which was then mixed with 70 µL of the sample. Absorbance readings at 640 nm were taken every 8 s for 30 min using a microplate reader. Proanthocyanidins that were isolated from cranberries (c-PAC) were used as a standard and results were expressed as mg proanthocyanidin (c-PAC) equivalents per gram of dry matter (mg c-PAC/g DM) (Krueger, Reed, Feliciano, & Howell, 2013).

Characterization of anthocyanin by ESI-MS/MS

Characterization of anthocyanins was performed on an Agilent 1200 series system (Agilent Technologies, Santa Clara, CA) equipped with an API 4000QTrap® triple quadrupole mass spectrometer (Applied Biosystems, Foster City, CA). Prior to injection, the fraction was filtered through a PTFE membrane (0.22 µm, diam. 17 mm). Eight microliters were injected into a Zorbax-

SB C18 column (4.6 x 250 mm x 10 μm) set at 35°C. The mobile phase consisted of 5% (v/v) formic acid in water (solvent A) and 5% (v/v) formic acid in methanol (solvent B) at a flow rate of 0.4 mL/min. The gradient elution program was as follows: the first 6 min isocratic at 10% B; 6-17 min, B increased linearly from 10 to 40%; 17-30 min, B increased linearly from 40 to 70%; followed by reconditioning of the column. The flow generated by the chromatographic system was introduced directly into the ESI source. The following parameters were employed: positive ionization mode, curtain gas (CUR 30), ion spray (IS 4000 V), turbo gas temperature (TEM 375°C), nebulizer gas pressure (GS1 25 psi), and gas turbo (GS2 18 psi). Identification of individual compounds was based on MS/MS spectral data, which matched the data reported in the existing literature.

Purification of proanthocyanidins

The crude extract, at a concentration of 40 mg/mL of c-PAC (as suggested by the previous DMAC assay), was evaporated to dryness by rotary evaporation, re-solubilized in ethanol, and loaded onto a glass column (2.5 x 20 cm, Kontes, Chromaflex) packed with Sephadex LH-20® resin (which had been previously swollen and washed in water). The resin bed was subsequently eluted with 150 mL of ethanol, 150 mL of ethanol:methanol (1:1 v/v), and 300 mL of acetone (80% v/v). The acetone fraction was evaporated to dryness by rotary evaporation under vacuum at 40 °C, reconstituted in 1.5 mL of methanol 100% (v/v), and quantified according to the previously described DMAC method.

RP-HPLC-DAD analysis

The HPLC analyses of the extracts of PAC were conducted using a Waters system equipped with two pumps (model 501), a Rheodyne manual injector model 7125, and an automated gradient controller. The effluent was monitored with a Waters 2998 photodiode array detector. One hundred microliters at 20 mg/mL of PAC equivalent were injected onto a Waters Spherisorb 10 μm ODS2 RP-18 column (4.6 × 250 mm) with the flow rate maintained at 2 mL/min. The solvents were (0.1% v/v) trifluoroacetic acid/water (solvent A) and (0.1% v/v) methanol (solvent B). The HPLC elution program was as follows: 10 min isocratic at 10% B; 10−25 min, B linear increase from 10 to 28%; 25−45 min, B linear increase from 28 to 55%; 45−50 min; B linear increase from 55 to 99%; and isocratic at 99% B for 5 min; followed by reconditioning of the column. Waters Empower Pro 2 software was used for data acquisition and data processing.

Attenuated total reflectance fourier transform infrared (ATR-FTIR) spectroscopy

The spectra of the extracts of PAC were obtained using a FTIR spectrometer Bruker Tensor 27 (Billerica, MA, USA), with a horizontal attenuated total reflectance (ATR) accessory with a diamond/ZnSe crystal. The spectra were scanned between 4000 and 600 cm^{-1} at a resolution of 4 cm^{-1} averaged over 64 scans.

Nuclear magnetic resonance (NMR) spectroscopy experiments

PAC were dissolved in approximately 0.75 mL of methanol-d4 with 0.03% tetramethylsilane (TMS). Experiments were carried out on a Bruker AVANCE 500 MHz spectrometer equipped with a DCH cryoprobe. Experiments used standard ^{1}H NMR parameters: pulse program (zg30), acquisition time = 6.6 s, number of scans = 256, and D1 = 1 s. Experiments used standard ^{13}C

NMR parameters: pulse program (zgpg30), acquisition time = 3.1 s, number of scans = 2048, and D1 = 1 s. Chemical shifts were referenced to TMS at 0 ppm. The processing of spectra was finished using MestResNova software (*v*12.0.4-22023).

MALDI-TOF MS analysis

Matrix-Assisted Laser Desorption/Ionization Time-of-Flight Mass Spectrometry (MALDI-TOF MS) spectra were collected on a Bruker UltraFlex III mass spectrometer (Billerica, MA, USA) (Alfaro-Viquez, Esquivel-Alvarado, Madrigal-Carballo, Krueger, & Reed, 2018). All analyses were performed in positive reflectron mode. Deflection was set at 800 Da. Samples at 1 mg/mL of procyanidin A2 and DHB (0.973 mM in methanol) were mixed in a 1:1 ratio and spotted on the MALDI-TOF MS stainless steel target (0.3 μL). Spectra were calibrated with bradykinin (1060.6 Da) and glucagon (3483.8 Da) as external standards.

Deconvolution of MALDI-TOF MS to determine percentages of A- to B-type interflavan bonds

The algebraic matrix for overlapping isotopic peaks in MALDI-TOF mass spectra was calculated for all the samples to determine the percentage of A- to B-type interflavan bonds (Feliciano, Krueger, Shanmuganayagam, Vestling, & Reed, 2012). The percentage of A- to B-type interflavan bonds were calculated using the matrix form $A^{-1} \times b = c$, where A^{-1} represents the inverse coefficient matrix of the relative intensity (ri) of the isotope patterns, b represents the constant matrix of absolute intensity from the spectrum, and c represents the variable matrix of linear combinations that solve the simultaneous equation. The linear combinations obtained from $A^{-1} \times b$ were divided by the sum of all the possible iterations and multiplied by 100 to obtain the

percentage of A- to B-type interflavan bonds. An additional row and column were added to the matrix for each additional degree of polymerization (DP). Monoisotopic mass determinations and a calculation of absolute intensity were collected using mMass software (version 5.5.0). Peaks in the data were excluded from analysis if the peaks included in the deconvolution of the isotope pattern had a signal to noise (S/N) ratio less than 3.

Statistical analysis

Results were expressed as mean ± standard deviation. Tukey-Kramer HSD was used to compare the means ($p < 0.05$). These statistics were calculated using JMP® Pro 14.0.0.

RESULTS AND DISCUSSION

The results for TPC, TFC, TAC, and s-PAC content in three TVS at three fruit development stages are summarized in Table 1. TPC values ranged from 13.89 to 22.42 mg GAE/g DM in TVS. Moreover, the highest values for TPC were found in *V. consanguineum*, followed by *V. poasanum*, and then *V. floribundum*. TPC decreased during fruit development by 0.70-fold for *V. consanguineum*, 0.72-fold for *V. poasanum*, and 0.81-fold for *V. floribundum*. Similar to the trends found for TPC, TFC had higher values in early stages compared to fruit at late stages of development. TFC ranged from 2.00 to 3.08 mg QE/g DM. Likewise, the highest values for TFC were found in *V. consanguineum*, followed by *V. poasanum*, and then *V. floribundum*. During fruit development TFC decreased by 0.80-fold for *V. consanguineum*, 0.73-fold for *V. poasanum*, and 0.78-fold for *V. floribundum*. On the other hand, TAC at late fruit development in TVS had the highest values in comparison to fruit at early stages of development. The levels of anthocyanins over the development and ripening period varied by 34-fold for *V. consanguineum*, 36-fold for *V. poasanum*, and 43-fold for *V. floribundum*. Overall, as the fruit ripens, TPC and TFC decrease while TAC increases. This suggests that the increase of anthocyanin at late fruit development has been produced in the epicarp, whereas the decrease of the other polyphenols occurs in the rest of the fruit (mesocarp and endocarp) because of fruit enlargement, thus producing a dilution effect.

Quantification of soluble PAC was carried out with the DMAC assay, using the c-PAC standard (Krueger, Reed, Feliciano, & Howell, 2013). The use of a c-PAC standard allows a more accurate quantification of PAC content because the c-PAC standard reflects the structural heterogeneity of PAC with higher DP (Feliciano, Shea, Shanmuganayagam, Krueger, Howell, & Reed, 2012).

Thus, the resulting molar absorption coefficient is minimized when c-PAC is used instead of catechins or commercially available dimers (Wang, Singh, Hurst, Glinski, Koo, & Vorsa, 2016). s-PAC content of the three TVS is shown in Table 1. Values ranged from 27.89 to 70.26 mg c-PAC/g DM. In addition, soluble proanthocyanidins followed the same trends as TPC and TFC over the course of fruit development. During fruit development, soluble PAC decreased by 0.53-fold for *V. consanguineum*, 0.43-fold for *V. poasanum*, and 0.47-fold for *V. floribundum*. This trend has been observed in cranberries and it is believed that PAC at early fruit development provides protection against premature feeding and fungal pathogens (Vvedenskaya & Vorsa, 2004).

The presumptive identification of anthocyanins using ESI-MS/MS at late fruit development for the three TVS is shown in Table 2. The presumptive identification of anthocyanins was determined only in the late fruit development to ensure the highest expression of this class of polyphenols. The same five anthocyanins were detected in *V. consanguineum* and *V. floribundum,* albeit in different proportion, whereas in *V. poasanum* ten anthocyanins were detected. Aglycone forms of anthocyanins were not detected in TVS. Cyanidin-3-O-hexoside, cyanidin-3-O-pentoside, and delphinidin-3-O-hexoside were the predominant anthocyanins in TVS. Delphinin-3-O-(6'-O-coumaryl)hexoside was present in *V. consanguineum* and *V. floribundum,* but not in *V. poasanum*. In contrast, methylated anthocyanins (malvidin, peonidin, and petunidin) were present in *V. poasanum*, but not in *V. consanguineum* and *V. floribundum*.

Phenolic compounds can be classified using the maximum wavelength (λ_{max}) when HPLC is used. The complex structural heterogeneity of the PAC fractions that were isolated from TVS displayed

complex HPLC chromatograms with two unresolved humps with λ_{max} at 280 nm (Figure 2). The polyphenols PAC, hydroxycinnamic acid, flavonol, and anthocyanin exhibit λ_{max} at approximately 280, 320, 370, and 520 nm respectively. Hydroxycinnamic acids, flavonols, and anthocyanins have other absorption bands at UV/visible wavelengths. However, these compounds typically do not have much absorbance at 280 nm compared to the PAC, whereas PAC only exhibit a higher absorption band at 280 nm. The presence of the λ_{max} at 280 nm and the reduction of the other absorbance wavelengths characteristic of the other polyphenols is a good indicator of the relative purity of the PAC fraction (Feliciano, Shea, Shanmuganayagam, Krueger, Howell, & Reed, 2012).

PAC were also analyzed using ATR-FTIR. Bands at 3379, 2934, 1604, 1518, 1438, 1358, 1274, 1198, 1100, 1056, 1006, 869, 816, and 777 cm^{-1} were observed (Figure 3). The broadband over the spectral region from 3600 to 3000 cm^{-1} corresponds to the hydroxy stretching vibration of the flavan-3-ol monomers (Grasel Fdos, Ferrão, & Wolf, 2016). The weak shoulder peak at 2934 cm^{-1} is due to the methine stretching region for aromatic compounds. The region between 1604 to 1438 cm^{-1} of strong to medium peaks corresponds to the stretching vibration of the aromatic ring (Falcão & Araújo, 2013). Consistent with Foo (1981), the single peaks at 1518 and 777 cm^{-1} are mainly indicative of procyanidin units with *cis* configuration (Lai Y Foo, 1981). The peak at 1198 cm^{-1} is attributed to C-O-H aliphatic stretching. Asymmetric stretching of C-O bonds at 1358 and 1274 cm^{-1} and symmetric motions at 1100 and 1006 cm^{-1} correspond to the elongation of the etheric group in the pyran ring (Gonultas & Ucar, 2012; Laghi, Parpinello, Del Rio, Calani, Mattioli, & Versari, 2010). The peaks at 869 and 816 cm^{-1} correspond to the out-of-plane

deformations of the hydrogen. Thus, the IR spectra of PAC obtained from TVS suggest that PAC are mainly composed of procyanidins with a *cis* configuration.

PAC extracts were further analyzed via liquid state ^{1}H and ^{13}C spectroscopy. Despite PAC complexity and heterogeneity, the interpretation of the signal assignments is consistent with the literature (Czochanska, Foo, Newman, & Porter, 1980; L. Y. Foo, Lu, Howell, & Vorsa, 2000). The ^{1}H spectrum is shown in Figure 4. The characteristic signals at δ 2.5-3.1, 3.7-4.4, and 5.1-5.5 ppm are consistent with the H-4 of terminal units, H-3, and H-2 on the C-ring, respectively. The signals at δ 5.8-6.3 ppm indicate the H-6 and H-8 on the A-ring. The signals at δ 6.5-7.5 ppm reflect the H2', H5', and H6' on the B-ring. The ^{13}C is shown in Figure 4. The characteristic peaks in the ^{13}C spectra of procyanidins units were observed. The peaks at δ 115-116.5 ppm (C2', C5'), 119-120 ppm (C6'), δ 133-134 ppm (C1'), and 145.3-145.9 ppm (C3', C4') are attributed to (epi)catechin units with dihydroxyl groups in the B-ring. The peaks at δ 65-70 ppm and δ 70-75 ppm are assignable to the C3 top, extender, and terminal units. The peaks at δ 75-80 ppm are attributed to C2. The stereochemistry of the C-ring was determined from the region between δ□65-80 ppm. The results indicate the presence of procyanidins with (-)-epicatechin (2*R*,3*R*) as the main constitutive monomers (Jiang, Liu, Wu, Tan, Meng, Wang, et al., 2015). The peaks at δ 154-158 ppm are assigned to C5, C7, and C8q, whereas peaks at δ 95-99 ppm correspond to the extender units of C6 and C8 of the A-ring, as well as the absence of C4-C6 interflavan bonds (Navarrete, Pizzi, Pasch, Rode, & Delmotte, 2010). The presence of the C4-C8 linkages are attributed to the extender flavanol units at δ□106.8 ppm (C8) and 37 ppm (C4). The presence of A-type interflavan bonds is deduced by the occurrence of additional peaks at δ 148-153 ppm (C8a) and a quaternary

carbon peak at δ 104.9 ppm (C2q). The peaks at δ 29-30 ppm are ascribed to the terminal units of C4. Finally, peaks at 102.5 ppm correspond to C4q.

Mass spectrometry analysis of the TVS were conducted by MALDI-TOF MS. Masses that correspond to sodium adducts based on repeating (epi)catechin (Δ288 amu) monomers were observed (Figure 5). TVS showed different isotopic patterns compared to the American cranberry (*V. macrocarpon*) and apple fruits (*Malus pumila* 'Golden Delicious') (Feliciano, Meudt, Shanmuganayagam, Krueger, & Reed, 2014). The percentage of A- to B-type interflavan bonds of TVS were determined using the deconvolution method (Table 3, Figure 5) (Feliciano, Krueger, Shanmuganayagam, Vestling, & Reed, 2012). Results indicate that B-type, not A-type, interflavan bonds are the predominant bonds in PAC, but greater than 74% of the oligomers contain one or more A-type interflavan bonds. Additionally, when the deconvolution data of TVS were compared with cranberries and apple fruits, different trends were observed (Feliciano, Meudt, Shanmuganayagam, Krueger, & Reed, 2014). For instance, as the DP of *V. macrocarpon* increased, the percentage of procyanidins with 2 or 3 A-type interflavan bonds increased, and the percentage with 0 A-type interflavan bonds remained constant. A contrary trend is observed for TVS, namely that as the DP increased, the percentage of PAC oligomers with no A-type bonds increased. However, procyanidin oligomers with one or more A-type interflavan bonds continued to have a higher percentage.

CONCLUSIONS

Results indicate that TAC content increased as the fruit developed, while TPC, TFC, and PAC contents decreased. In addition, the anthocyanin profiles for TVS differ from cranberries because only cyanidin and peonidin glycosides are present in cranberries, whereas for TVS cyanidin, delphinidin glycosides are the predominant anthocyanins (Jungmin Lee, 2016). Specifically, *V. consanguineum* and *V. floribundum* have anthocyanin profiles similar to evergreen huckleberries, while *V. poasanum* has anthocyanin profiles similar to blueberries (Kalt, McDonald, Ricker, & Lu, 1999; Jungmin Lee, 2016; Jungmin Lee, Finn, & Wrolstad, 2004). The similarities in anthocyanin profiles are related to the phylogenetic dendrogram by Kron *et al*. (2002), where the hierarchical cluster analysis places *V. consanguineum* and *V. floribundum* in an unique clade, which is one removed from cranberries (*Vaccinium* clade), whereas the unique clade containing *V. consanguineum* and *V. floribundum* is two removed from the clade that contain *V. poasanum* (Meso-American/Caribbean clade) (Kron, Powell, & Luteyn, 2002). Results also indicate that the majority of PAC in TVS have at least 1 A-type interflavan bond. This finding suggests that PAC in the TVS analyzed in this study are similar to cranberry PAC rather than blueberry (*V. angustifolium* Aiton) and evergreen huckleberry (*V. ovatum* Pursh) PAC because the majority of PAC in cranberries have at least 1 A-type interflavan bond, whereas the majority of PAC oligomers in blueberries and huckleberries have all B-type interflavan bonds (Feliciano, Meudt, Shanmuganayagam, Krueger, & Reed, 2014; Kimura, Ogawa, Akihiro, & Yokota, 2011).

In the United States, consumer demand for cranberries and blueberries is increasing partly because anthocyanins and PAC are associated with health benefits. Our results show that PAC in TVS are

similar to cranberries and anthocyanins in TVS are similar to blueberries and may be used to promote the development of new markets for Costa Rica *Vaccinium* species.

ACKNOWLEDGMENTS

The authors acknowledge financial support from the Ministry of Science, Technology and Telecommunications (MICITT), Innovation and Human Capital Program for Competitiveness (PINN), and the National Council for Scientific and Technology Research (CONICIT) (Grant number PED-056-2015-I) at Costa Rica.

AUTHORSHIP CONTRIBUTION STATEMENT

Daniel Esquivel-Alvarado: Conceptualization, Methodology, Formal analysis, Investigation, Data curation, Writing - original draft, Writing - review & editing, Visualization. **Rodrigo Muñoz-Arrieta:** Investigation **Emilia Alfaro-Viquez:** Conceptualization, Writing - review & editing, Visualization. **Sergio Madrigal-Carballo:** Writing - review & editing. **Christian G. Krueger:** Conceptualization, Writing - review & editing, Funding acquisition. **Jess D. Reed:** Conceptualization, Writing - review & editing, Supervision, Funding acquisition.

REFERENCES

Alfaro-Viquez, E., Esquivel-Alvarado, D., Madrigal-Carballo, S., Krueger, C., & Reed, J. (2018). Cranberry proanthocyanidin-chitosan hybrid nanoparticles as a potential inhibitor of extra-intestinal pathogenic *Escherichia coli* invasion of gut epithelial cells. *International Journal of Biological Macromolecules*. doi:10.1016/j.ijbiomac.2018.01.033

Alfaro-Viquez, E., Esquivel-Alvarado, D., Madrigal-Carballo, S., Krueger, C., & Reed, J. (2019). Proanthocyanidin-chitosan composite nanoparticles prevent bacterial invasion and colonization of gut epithelial cells by extra-intestinal pathogenic *Escherichia coli*. *International Journal of Biological Macromolecules*. doi:10.1016/j.ijbiomac.2019.04.170

Brenes Angulo, A., Castillo Matamoros, R., & Gómez-Alpízar, L. (2015). Micropropagation of four blueberry cultivars. *Agronomía Costarricense, 39*(1), 7-23.

Czochanska, Z., Foo, L. Y., Newman, R. H., & Porter, L. J. (1980). Polymeric proanthocyanidins. Stereochemistry, structural units, and molecular weight. *Journal of the Chemical Society Perkin Transactions 1*, 2278-2286. doi:10.1039/p19800002278

Falcão, L., & Araújo, M. (2013). Tannins characterization in historic leathers by complementary analytical techniques ATR-FTIR, UV-Vis and chemical tests. *Journal of Cultural Heritage, 14*(6), 499-508. doi:10.1016/j.culher.2012.11.003

Feliciano, R., Krueger, C., Shanmuganayagam, D., Vestling, M., & Reed, J. (2012). Deconvolution of matrix-assisted laser desorption/ionization time-of-flight mass spectrometry isotope patterns to determine ratios of A-type to B-type interflavan bonds in cranberry proanthocyanidins. *Food Chemistry, 135*(3), 1485-1493. doi: 10.1016/j.foodchem.2012.05.102

Feliciano, R., Meudt, J., Shanmuganayagam, D., Krueger, C., & Reed, J. (2014). Ratio of "A-type" to "B-type" proanthocyanidin interflavan bonds affects extra-intestinal pathogenic *Escherichia coli* invasion of gut epithelial cells. *Journal of Agricultural and Food Chemistry, 62*(18), 3919-3925. doi:10.1021/jf403839a

Feliciano, R., Shea, M., Shanmuganayagam, D., Krueger, C., Howell, A., & Reed, J. (2012). Comparison of isolated cranberry (*Vaccinium macrocarpon* Ait.) proanthocyanidins to catechin and procyanidins A2 and B2 for use as standards in the 4-(dimethylamino)cinnamaldehyde assay. *Journal of Agricultural and Food Chemistry, 60*(18), 4578-4585. doi:10.1021/jf3007213

Foo, L. (1981). Proanthocyanidins: gross chemical structures by infrared spectra. *Phytochemistry, 20*(6), 1397-1402. doi:10.1016/0031-9422(81)80047-7

Foo, L., Lu, Y., Howell, A., & Vorsa, N. (2000). The structure of cranberry proanthocyanidins which inhibit adherence of uropathogenic P-fimbriated *Escherichia coli in vitro*. *Phytochemistry, 54*(2), 173-181. doi:10.1016/s0031-9422(99)00573-7

Gonultas, O., & Ucar, M. B. (2012). Chemical composition of some commercial tannins produced in Turkey. *Proceedings of the 55th International Convention of Society of Wood Science and Technology*, (pp. 1-9).

Grasel Fdos, S., Ferrão, M., & Wolf, C. (2016). Development of methodology for identification the nature of the polyphenolic extracts by FTIR associated with multivariate analysis. *Spectrochimica Acta A: Molecular Biomolecular Spectroscopy, 153*, 94-101. doi:10.1016/j.saa.2015.08.020

Hellström, J., Sinkkonen, J., Karonen, M., & Mattila, P. (2007). Isolation and Structure Elucidation of Procyanidin Oligomers from Saskatoon Berries (*Amelanchier alnifolia*). *Journal of Agricultural and Food Chemistry, 55*(1), 157-164. doi:10.1021/jf062441t

Jiang, X., Liu, Y., Wu, Y., Tan, H., Meng, F., Wang, Y. S., Li, M., Zhao, L., Liu, L., Qian, Y., Gao, L., & Xia, T. (2015). Analysis of accumulation patterns and preliminary study on the condensation mechanism of proanthocyanidins in the tea plant [*Camellia sinensis*]. *Scientific Reports, 5*, 8742. doi:10.1038/srep08742

Jiménez-Bonilla, V., & Abdelnour-Esquivel, A. (2013). Identificación y valor nutricional de algunos materiales nativos de arándano (*Vaccinium* spp). *Tecnología en Marcha, 26*(2), 3-8. doi:10.18845/tm.v26i2.1398

Jiménez-Bonilla, V., & Abdelnour-Esquivel, A. (2016). Establecimiento in vitro de (*Vaccinium consanguineum*), un arándano nativo de Costa Rica. *Tecnología en Marcha, 29*(2), 77-84. doi:10.18845/tm.v29i2.2692

Kalt, W., McDonald, J., Ricker, R., & Lu, X. (1999). Anthocyanin content and profile within and among blueberry species. *Canadian Journal of Plant Science, 79*(4), 617-623. doi:10.4141/p99-009

Kimura, H., Ogawa, S., Akihiro, T., & Yokota, K. (2011). Structural analysis of A-type or B-type highly polymeric proanthocyanidins by thiolytic degradation and the implication in their inhibitory effects on pancreatic lipase. *Journal of Chromatography A, 1218*(42), 7704-7712. doi:10.1016/j.chroma.2011.07.024

Kong, J., Chia, L., Goh, N., Chia, T., & Brouillard, R. (2003). Analysis and biological activities of anthocyanins. *Phytochemistry, 64*(5), 923-933. doi:10.1016/S0031-9422(03)00438-2

Kron, K., Powell, E., & Luteyn, J. (2002). Phylogenetic relationships within the blueberry tribe (Vaccinieae, Ericaceae) based on sequence data from matK and nuclear ribosomal ITS regions, with comments on the placement of Satyria. *American Journal of Botany, 89*(2), 327-336. doi:10.3732/ajb.89.2.327

Krueger, C., Reed, J., Feliciano, R., & Howell, A. (2013). Quantifying and characterizing proanthocyanidins in cranberries in relation to urinary tract health. *Anal Bioanal Chem, 405*(13), 4385-4395. doi:10.1007/s00216-013-6750-3

Laghi, L., Parpinello, G., Del Rio, D., Calani, L., Mattioli, A., & Versari, A. (2010). Fingerprint of enological tannins by multiple techniques approach. *Food Chemistry, 121*(3), 783-788. doi:10.1016/j.foodchem.2010.01.002

Lee, J. (2016). Anthocyanin analyses of *Vaccinium* fruit dietary supplements. *Food Science & Nutrition, 4*(5), 742-752. doi:10.1002/fsn3.339

Lee, J., Durst, R. W., & Wrolstad, R. (2005). Determination of total monomeric anthocyanin pigment content of fruit juices, beverages, natural colorants, and wines by the pH differential method: collaborative study. *Journal AOAC International, 88*(5), 1269-1278. doi:10.1093/jaoac/88.5.1269

Lee, J., Finn, C., & Wrolstad, R. (2004). Comparison of anthocyanin pigment and other phenolic compounds of *Vaccinium membranaceum* and *Vaccinium ovatum* native to the Pacific Northwest of North America. *Journal of Agricultural and Food Chemistry, 52*(23), 7039-7044. doi:10.1021/jf049108e

Montiel, M. (1991). *Introducción a la flora de Costa Rica*: Editorial Universidad de Costa Rica.

Navarrete, P., Pizzi, A., Pasch, H., Rode, K., & Delmotte, L. (2010). MALDI-TOF and ^{13}C NMR characterization of maritime pine industrial tannin extract. *Industrial Crops and Products, 32*(2), 105-110. doi:10.1016/j.indcrop.2010.03.010

Pękal, A., & Pyrzynska, K. (2014). Evaluation of aluminium complexation reaction for flavonoid content assay. *Food Analytical Methods, 7*(9), 1776-1782. doi:10.1007/s12161-014-9814-x

PROCOMER. (2018). Portal Estadistico de Comercio Exterior. volumen 2018.

Shahidi, F., & Ambigaipalan, P. (2015). Phenolics and polyphenolics in foods, beverages and spices: Antioxidant activity and health effects–A review. *Journal Functional Foods, 18*, 820-897. doi:10.1016/j.jff.2015.06.018

Singleton, V., Orthofer, R., & Lamuela-Raventós, R. (1999). Analysis of total phenols and other oxidation substrates and antioxidants by means of Folin-Ciocalteu reagent. *Methods in Enzymology*, 299, 152-178. doi:10.1016/S0076-6879(99)99017-1

Vvedenskaya, I., & Vorsa, N. (2004). Flavonoid composition over fruit development and maturation in American cranberry, *Vaccinium macrocarpon* Ait. *Plant Science, 167*(5), 1043-1054. doi:10.1016/j.plantsci.2004.06.001

Wang, Y., Singh, A. P., Hurst, W. J., Glinski, J. A., Koo, H., & Vorsa, N. (2016). Influence of Degree-of-Polymerization and Linkage on the Quantification of Proanthocyanidins using 4-Dimethylaminocinnamaldehyde (DMAC) Assay. *Journal of Agricultural and Food Chemistry, 64*(11), 2190-2199. doi:10.1021/acs.jafc.5b05408

Wilbur, R. L., & Luteyn, J. L. (2008). A synopsis of the Mexican and Central American species of *Vaccinium* (Ericaceae). *Journal of the Botanical Research Institute of Texas*, 207-241.

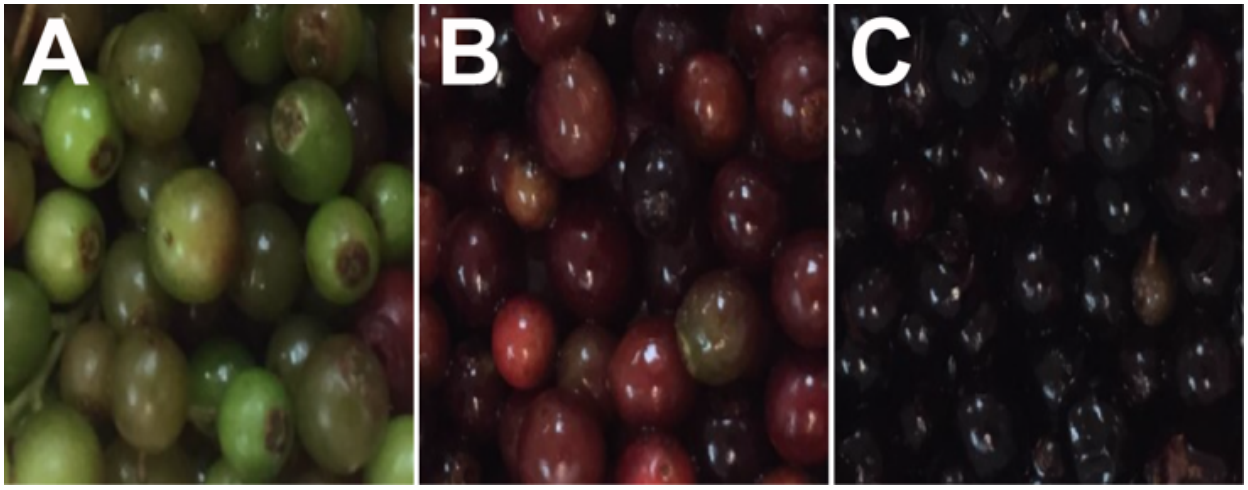

Figure 1. Fruits of *Vaccinium consanguineum* at early (A), middle (B), and late (C) fruit development.

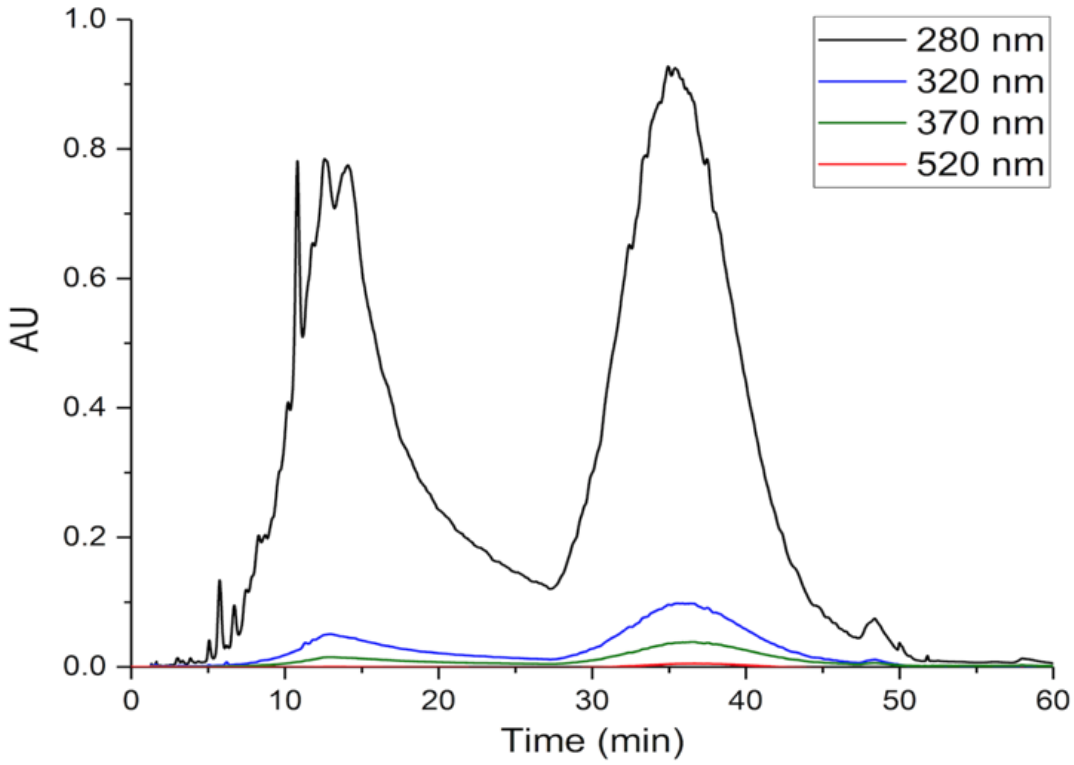

Figure 2. HPLC chromatogram for PAC from *V. consanguineum* at late fruit development, collected at different wavelengths (280, 320, 370, and 520 nm). The chromatogram is similar for the three TVS at the three fruit development stages.

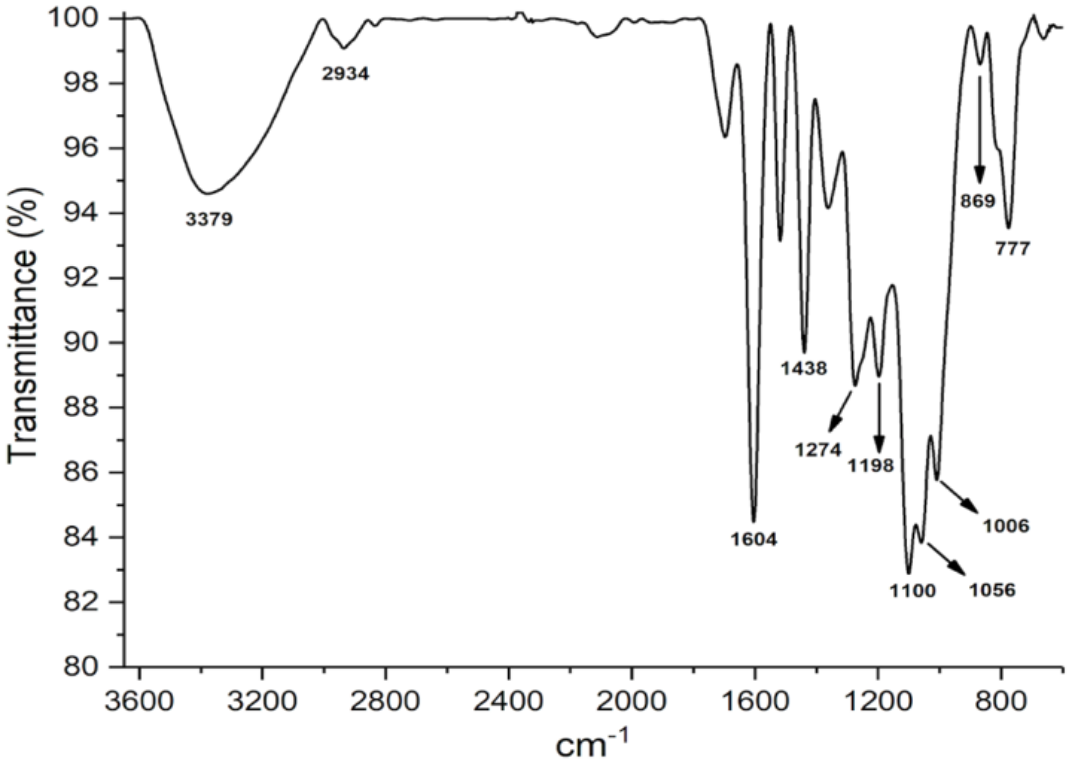

Figure 3. ATR-FTIR spectrum for PAC from *V. consanguineum* at late fruit development. The spectrum is similar for the three TVS at the three fruit development stages.

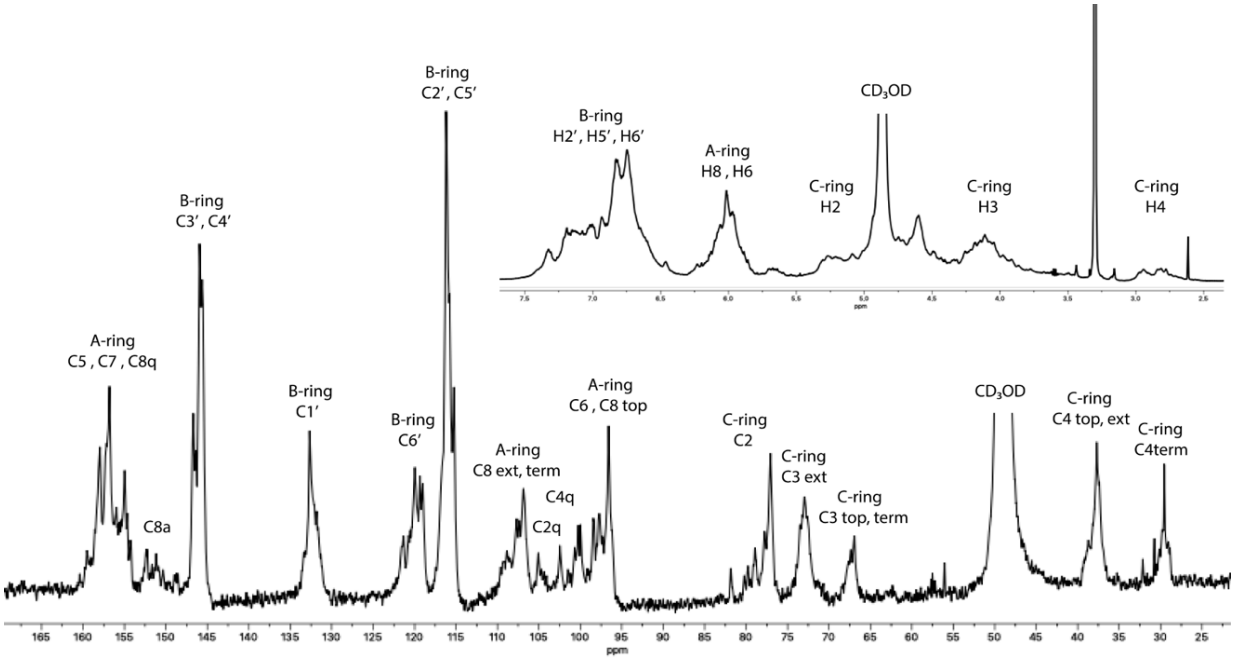

Figure 4. ^{13}C-NMR spectrum for PAC from *V. consanguineum* at late fruit development in methanol-d4. The graph inserted above is the ^{1}H-NMR spectrum for PAC from *V. consanguineum* at early fruit development in methanol-d4.

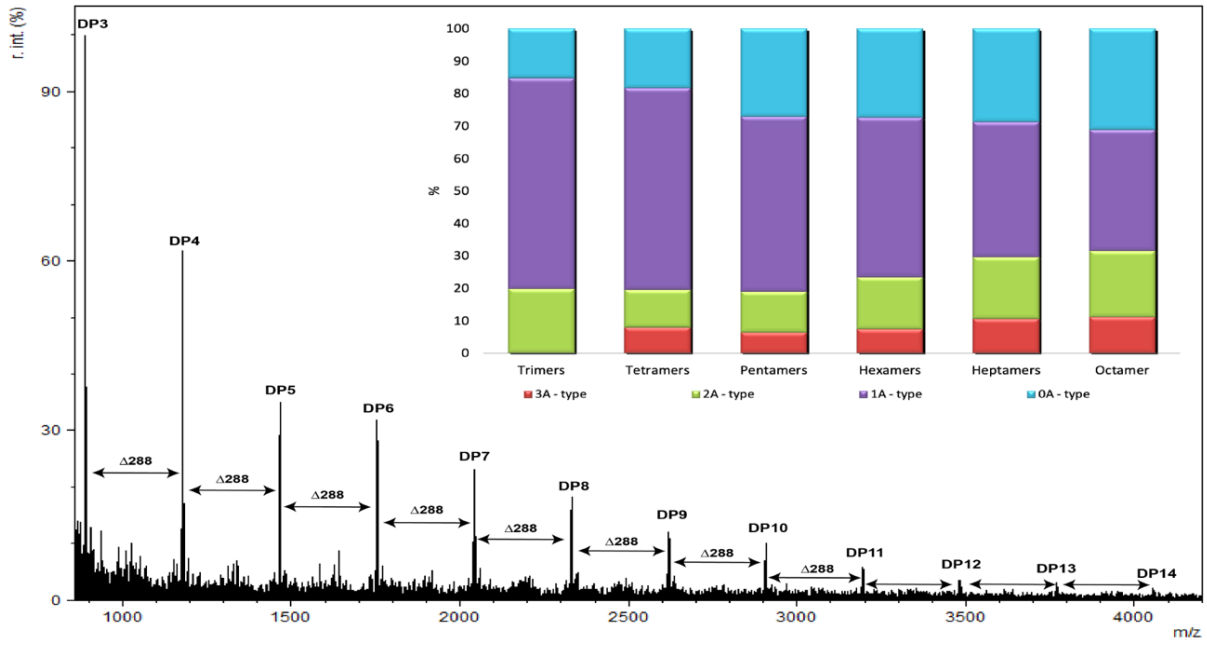

Figure 5. MALDI-TOF mass spectrum for PAC from *V. consanguineum* at late fruit development in positive reflectron mode, showing a procyanidin series [M + Na^+] from trimers to tetradecamers. The inserted bar chart is the percentage of A- and B-type interflavan bonds for PAC from *V. consanguineum* at late fruit development from trimers to octamers using the deconvolution method after MALDI-TOF MS analysis.

CHAPTER 5: Synthesis of fluorescent proanthocyanidin-cinnamaldehydes pyrylium products for microscopic detection of interactions with extra-intestinal pathogenic *Escherichia coli*

Daniel Esquivel-Alvarado[§], Emilia Alfaro-Viquez[§], Michael A. Polewski[§], Christian G. Krueger[§,†], Martha M. Vestling[π], Jess D. Reed[§,†]

[§] University of Wisconsin-Madison, Department of Animal Sciences, Reed Research Group,1675 Observatory Drive, Madison, WI 53706, USA.

[†] Complete Phytochemical Solutions, LLC, 275 Rodney Road, Cambridge, WI 53523, USA.

[π] University of Wisconsin-Madison, Department of Chemistry, 1101 University Avenue, Madison, WI 53706, USA.

ABSTRACT

The synthesis of proanthocyanidin-cinnamaldehydes pyrylium products (PCPP) was achieved by the condensation reaction of proanthocyanidins (PAC) with cinnamaldehyde and four cinnamaldehyde derivatives, 4-methylcinnamaldehyde, 4-(dimethylamino)cinnamaldehyde, 4-hydroxy-3,5-dimethoxycinnamaldehyde, and 4-hydroxy-3-methoxycinnamaldehyde. Matrix-assisted laser desorption/ionization time-of-flight mass spectrometry spectra of PCPP show masses that correspond to (epi)catechin oligomers attached to single, double, or triple moieties of cinnamaldehydes. Synthesized PCPP exhibited fluorescence at higher excitation and emission wavelengths than PAC and each cinnamaldehyde condensation product exhibited different fluorescent properties. PCPP were evaluated for their ability to agglutinate extra-intestinal pathogenic *Escherichia coli* (ExPEC). Results indicate that PCPP were significantly more bioactive (p-value < 0.05) for agglutinating ExPEC compared to PAC. Scanning electron microscopy indicates that PCPP interacts with ExPEC surface structures and suggests that PCPP have higher affinity with the fimbriae-like structures on the surface of ExPEC in comparison to PAC. In addition, fluorescent microscopy performed on *in vitro* and *in vivo* agglutination assays show that PCPP were entrapping ExPEC in a web-like network, thus demonstrating agglutination of ExPEC. This study demonstrated the potential of PCPP to improve our understanding of the temporal and dynamic interactions of PAC in *in-vitro* and *in-vivo* studies.

Keywords**:** proanthocyanidins; A-type interflavan bonds; B-type interflavan bonds; cinnamaldehydes; MALDI-TOF MS; fluorescence; microscopy; agglutination assay; extra-intestinal pathogenic *Escherichia coli*.

INTRODUCTION

Proanthocyanidins (PAC) are oligomers of flavan-3-ol units, which are associated with health benefits (Feliciano, Meudt, Shanmuganayagam, Krueger, & Reed, 2014). PAC are linked by A- and B-type interflavan bonds. In A-type interflavan bonds, the flavan-3-ols form two bonds between C_4-C_8 and C_2-O-C_7, whereas in B-type interflavan bonds, the flavan-3-ols form only one bond between C_4-C_8. The structural heterogeneity of PAC is caused by their degree of polymerization (DP), the nature of their interflavan bonds (A- and B-type), the pattern of hydroxylation of their flavan units (B-ring), and their stereochemistry (Foo, Lu, Howell, & Vorsa, 2000; Reed, Krueger, & Vestling, 2005).

Visualization of temporal and dynamic interactions of PAC with bacteria using fluorescent microscopy would be a useful tool to test hypotheses regarding structure/function relationships in antimicrobial activity. However, the fluorescent properties of PAC are not useful for microscopy because excitation and emission wavelengths are located in the ultraviolet region (Feliciano, Heintz, Krueger, Vestling, & Reed, 2015). Our laboratory has previously published the use of 5-([4,6-dichlorotriazin-2-yl]amino)fluorescein (DTAF) to tag PAC (Feliciano, Heintz, Krueger, Vestling, & Reed, 2015). Unfortunately auto-fluorescence at the excitation wavelength of fluorescein creates difficulties in distinguishing signal from noise in fluorescent microscopy using DTAF tagged PAC.

Cinnamaldehydes, such as cinnamaldehyde (CIN), 4-methylcinnamaldehyde (TOL), 4-(dimethylamino)cinnamaldehyde (DMAC), 4-hydroxy-3,5-dimethoxycinnamaldehyde (SIN), and 4-hydroxy-3-methoxycinnamaldehyde (CON) react with flavan-3-ols and PAC to form new compounds (de Freitas, Sousa, Silva, Santos-Buelga, & Mateus, 2004; Sousa, Mateus, Perez-Alonso, Santos-Buelga, & de Freitas, 2005; Tanaka, Matsuo, Yamada, & Kouno, 2008). We hypothesized that the proanthocyanidin-cinnamaldehydes pyrylium products (PCPP) may have useful fluorescent properties, i.e. higher excitation and emission wavelength than PAC, for use in microscopy of PAC interactions with bacteria, mammalian cells, and tissues. Although the DMAC assay has been used as a colorimetric method for quantifying PAC content (Feliciano, Shea, Shanmuganayagam, Krueger, Howell, & Reed, 2012; Birmingham, Esquivel-Alvarado, Maranan, Krueger, & Reed, 2020), the existing literature has not described the synthesis of these cinnamaldehyde compounds with PAC for use as fluorophores.

The goals of this study were: (1) to characterize the synthesis of PCPP based on the reactions of PAC with cinnamaldehydes; (2) to evaluate the ability of PCPP to exhibit fluorescence; (3) to evaluate the bioactivity of PCPP to agglutinate extra-intestinal pathogenic *Escherichia coli* (ExPEC) in an *in-vitro* model; and (4) use fluorescent microscopy to visualize the interactions between PAC and ExPEC during *in-vitro* and *in-vivo* agglutination. These PCPP may be used to improve our understanding of the temporal and dynamic interactions of PAC in *in-vitro* and *in-vivo* studies. In addition, the use of these PCPP with fluorescent microscopy is an alternative to complex and expensive techniques such as ^{14}C radio-labeling of PAC.

MATERIAL AND METHODS

Chemical and materials

Cinnamaldehyde (CIN), 4-methylcinnamaldehyde (TOL), 4-(dimethylamino)cinnamaldehyde (DMAC), 4-hydroxy-3,5-dimethoxycinnamaldehyde (SIN), 4-hydroxy-3-methoxycinnamaldehyde (CON), 2,5-dihydroxybenzoic acid (DHB), magnesium chloride, bradykinin, glucagon, chitosan, sodium triphosphate, and Triton X-100 were obtained from Sigma-Aldrich (Milwaukee, WI, USA). Methanol, acetone, water, sodium hydroxide, hydrochloric acid, Dulbecco's phosphate buffered saline solution 10X with calcium and magnesium (PBS Ca^{+2}/Mg^{+2}), Fluoromount-G, and HyperSep C_{18} cartridges (5 g bed weight, 25 mL column volume, 40-60 μm particle size, 60 Å pore size) were purchased from Fisher Scientific (Fair Lawn, NJ, USA). Dulbecco's phosphate buffered saline solution (PBS) was diluted to 1X concentration before use. Ethanol (100%) was obtained from Decon's lab (King of Prussia, PA, USA). Sephadex LH-20® (18-111 μm particle size) was purchased from GE Healthcare (Uppsala, Sweden). Cranberry fruits were obtained from Habelman Bros. Company (Tomah, WI, USA)

Extraction of proanthocyanidins

Whole frozen cranberries were placed in liquid nitrogen and blended into a powder. Two liters of acetone 70% (v/v) were added to 1 kg of frozen cranberry powder and sonicated for 30 minutes. The acetone was removed using rotary evaporation. The aqueous extract (~500 mL) was filtered with Whatman 1, Whatman 50, and a Corning funnel with pores of 0.22 μm. The filtered aqueous cranberry extract was loaded onto an FPX-66 resin that was previously washed with ethanol and

water. Polyphenols were purified by sequential elution with water and ethanol (Liu, Liu, Wang, Khoo, Taylor, & Gu, 2011; Alfaro-Viquez, Roling, Krueger, Rainey, Reed, & Ricketts, 2018). The ethanol fraction was concentrated (~25 mL) using a rotary evaporator and loaded onto a Sephadex LH-20 resin that was previously swollen in water and equilibrated with ethanol for 45 min at 4 mL/min. PAC were purified by sequential elution with ethanol, ethanol/methanol (1:1), and acetone 80% (v/v) (Feliciano, Shea, Shanmuganayagam, Krueger, Howell, & Reed, 2012). The acetone fraction contained PAC. The acetone was removed by rotary evaporation, lyophilized, and stored at -20°C.

Synthesis of proanthocyanidin-cinnamaldehydes pyrylium products

Proanthocyanidins (50 mg) were dissolved in 2 mL of methanol and mixed with 5 mg of magnesium chloride. Each cinnamaldehyde compounds (6 mg) were added, followed by 250 μL of HCl (0.3 M). After 60 minutes of incubation at 25°C, the reaction was quenched by adding 250 μL of NaOH (0.3 M). The pH of the quenched reaction was checked using pH strips until a neutral pH was obtained. Then, 6 mL of water were added to each neutralized solutions prior to isolation of products.

Purification of proanthocyanidin-cinnamaldehydes pyrylium products

The purification of PCPP was achieved using two procedures. The first procedure to purify PAC-CIN, PAC-TOL, PAC-CON, and PAC-SIN was carried out using Sephadex LH-20®, whereas the second procedure to purify PAC-DMAC was carried out using a C_{18} cartridge. For the first

procedure: the neutralized solutions (PAC-CIN, PAC-TOL, PAC-CON and PAC-SIN) were loaded onto a glass column (Kontes, 2.5 cm internal diameter x 20 cm length) packed with Sephadex LH-20® that was previously conditioned with water and equilibrated with ethanol. Unreacted cinnamaldehydes were eluted with ethanol, and the PCPP were eluted with acetone 80% (v/v). The fractions of PCPP were concentrated by evaporating the acetone and lyophilizing. For the second procedure, the neutralized sample of PAC-DMAC was loaded onto a C_{18} cartridge that was previously conditioned with methanol followed by double distilled water. Unreacted DMAC was eluted with water, and the PAC-DMAC fraction was eluted with methanol 45% (v/v). The PAC-DMAC products were obtained by evaporation of the methanol followed by lyophilization.

Matrix-assisted laser desorption/ionization time-of-flight mass spectrometry

Matrix-assisted laser desorption/ionization time-of-flight mass spectrometry (MALDI-TOF MS) spectra were collected on a Bruker UltraFlex III mass spectrometer (Billerica, MA, USA). All analyses were performed in positive reflectron mode. Deflection was set at 800 Da. Samples (2 mg/L of PAC equivalent in methanol) and matrix (DHB; 0.973 mM in methanol) were mixed at a 1:1 volume ratio and spotted on the MALDI-TOF MS stainless steel target (0.3 μL). Spectra were calibrated with bradykinin (1060.6 Da) and glucagon (3483.8 Da) as external standards. PCPP were detected as pyrylium ions $[M]^+$, whereas non-charged conjugates of cinnamaldehydes and PAC were detected as sodium adducts $[M+Na]^+$. FlexControl and FlexAnalysis (Bruker Daltonik GmbH, Bremen, Germany) were used for data acquisition and data processing, respectively (Esquivel-Alvarado, Muñoz-Arrieta, Alfaro-Viquez, Madrigal-Carballo, Krueger, & Reed, 2020).

Absorption and emission spectra of proanthocyanidin-cinnamaldehyde pyrylium products

The absorption spectra for PAC and PCPP were acquired using a UV/Visible spectrometer (Varian Cary50) in the spectral range 250-700 nm by dissolving the samples in methanol. The concentrations were adjusted so that the absorption intensities of the samples were similar. The fluorescence emission spectra were acquired using a spectrofluorimeter (Hitachi f-4500) at the previously determined maximum wavelength (λ) absorption. The slits for excitation and emission were both set at 5 nm and the excitation voltage at 700 V.

Bioactivity assays

***In vitro* agglutination assay**

ExPEC strain CFT073, transformed to expresses green fluorescent protein (GFP), was cultured under static conditions in tryptose broth for 48 h at 37°C. After the incubation time, 1 mL of the culture was taken from the surface of the culture to inoculate a new culture under static conditions for 24 h at 37°C. On the day of assay, the culture was centrifuged at 1800g for 10 min to obtain a bacterial pellet. The pellet was washed twice with PBS by centrifugation at 1840g for 10 min and then resuspended in 1 mL PBS to obtain the bacterial stock solution. Optical density was used to adjust the bacterial cell density with a previously established bacterial density-absorbance curve (Feliciano, Meudt, Shanmuganayagam, Krueger, & Reed, 2014). The assay was conducted in 3.0 mL microcuvettes using 1.0 mL total reaction volume. Nine hundred and forty microliters of PBS were added to each microcuvette. This was followed by 10 μL of PAC and PCPP at a concentration of 20 mg/mL of PAC equivalent, and 50 μL of ExPEC stock solution at $1.0e^{\wedge 10}$ CFU/mL.

Transmittance was read at 600 nm every 1 min for 4 hours on a UV/Visible spectrometer (Evolution 201, Thermo Scientific). The area under the curve for each sample was calculated as a function of the ability of PAC and PCPP to agglutinate ExPEC (Alfaro-Viquez, Esquivel-Alvarado, Madrigal-Carballo, Krueger, & Reed, 2019).

Scanning electron microscopy

The agglutinated ExPEC obtained from the *in vitro* agglutination assay was passed through a 0.45 μm silver membrane filter (Steritech #45329), followed by treatment with1 mL of glutaraldehyde (3% v/v) to fix the bacteria. The silver membrane filter was left in glutaraldehyde (3% v/v) overnight. The filter was then dehydrated with 15-minute treatments with a series of increasing ethanol concentrations in doubly distilled water (v/v): 30, 50, 70, 80, 90, 95, and two-times with absolute ethanol. Then, the filter was dried via the critical point procedure (10 minutes × 3 soaks) and adhered to aluminum SEM specimen stubs with double-sided carbon sticky tabs. The filter was then sputter coated with a ~5 nm layer of gold. Scanning electron microscopy images were acquired with a Zeiss LEO-1550 VP (Zeiss, Oberkochen, Germany) using an accelerating voltage at 6 kV (Alfaro-Viquez, Esquivel-Alvarado, Madrigal-Carballo, Krueger, & Reed, 2018).

***In vivo* urine agglutination experiment**

Sprague-Dawley rats (Charles River Laboratories, Wilmington, MA) weighing 220 to 240 g (10-weeks old) were separated into three groups and acclimated for 10 days prior to the day of the experiment. Rats were kept under circadian rhythm with unlimited access to water and chow and

monitored daily for symptoms of stress and discomfort. The first group was treated with ExPEC solution at a final concentration of 1.0e^8 CFU/mL. The second group was treated with PAC-DMAC at a final concentration of 750 μg. The third group was treated with PAC-DMAC at a final concentration of 750 μg and ExPEC solution at a final concentration of 1.0e^8 CFU/mL. On the day of the experiment, rats were anesthetized with isoflurane (4%) and oxygen in a closed box and maintained on isoflurane (1-2.5%) and oxygen administered by nose-cone. After anesthesia, rats were subjected to one of the three treatments (ExPEC, PAC-DMAC, and PAC-DMAC with ExPEC) by intra-vesicular bladder administration via a catheter. The catheter remained in place for the duration of the experiment (90 min) to prevent voiding of the bladder. After 90 min of incubation, urine from each rat was collected via the catheter and place into a collection tube. This experimental procedure was approved by the Institutional Animal Care and Use Committee (IACUC) at the University of Wisconsin-Madison (Protocol #A005854-A03).

Agglutination fluorescent images

Samples from the *in vitro* and *in vivo* agglutination assays were centrifuged at 1800g for 10 min. The supernatants were discarded, and the pellets were suspended in 1 mL of neutral buffered formalin and stored for 1h at 4°C. Next, 50 μL of the suspensions were spotted onto glass slides that were previously spotted with 50 μL of Fluoromount-G solution and then covered with coverslips. For the *in vitro* agglutination assays, the slides evaluated were the treatments containing ExPEC, PAC with ExPEC, and PAC-DMAC with ExPEC. For the *in vivo* agglutination assay, the slides evaluated were the treatments containing ExPEC, PAC-DMAC, and PAC-DMAC with ExPEC. Both *in vitro* and *in vivo* agglutination images were acquired under a Zeiss Axio Imager

M2 Microscope using the differential interference contrast (DIC), and green fluorescent protein (GFP) and Texas red filters. In addition, 3D-images of PAC-DMAC with ExPEC solution was acquired using a Nikon A1R-SI+ confocal microscope at a magnification of 100X.

Statistical analysis

Data were analyzed using RStudio (version 1.2.1335) by the ‘car’ and ‘agricolae’ packages. One-way analysis of variance with least significant difference (LSD) post-test were used for multiple comparisons with a probability of less than 0.05 considered to be statistically significant.

RESULTS AND DISCUSSION

Synthesis and characterization of proanthocyanidin-cinnamaldehydes pyrylium products

Similar to the mechanism described in the existing literature to explain the formation of catechin-pyrylium and procyanidin-pyrylium products (de Freitas, Sousa, Silva, Santos-Buelga, & Mateus, 2004; Sousa, Mateus, Perez-Alonso, Santos-Buelga, & de Freitas, 2005), we found that PAC react with cinnamaldehydes in acidic conditions to form PCPP, which in turn produce fluorescence. **Figure 1** shows the hypothetical structures of single and double cinnamaldehyde moieties of PCPP trimers resulting from the reaction between PAC and CIN.

The synthesis of PCPP produced a dark-amber color for PAC-CIN, a light-amber color for PAC-TOL, a purple color for PAC-DMAC, a red color for PAC-CON, and a red-brick color for PAC-SIN. Based on the ratio of weight of the isolated PCPP to the sum of the reactants (PAC and cinnamaldehydes). The yield obtained for PAC-CIN was 69% (w/w), 80% (w/w) for PAC-TOL, 64% (w/w) for PAC-DMAC, 75% (w/w) for PAC-CON, and 76% (w/w) for PAC-SIN.

MALDI-TOF MS spectra were used to characterize PAC extracted from cranberry, PCPP, and non-charged conjugates of PCPP. The MALDI-TOF MS spectrum of PAC detected oligomeric (epi)catechin units in positive reflectron mode from trimers to nonamers with structural variation in the nature of the interflavan bonds (A- and B-type) (**Figure 2**). The isotope patterns of MALDI-TOF MS for the oligomeric (epi)catechin units revealed that masses corresponding to PAC with one A-type interflavan bond had the highest intensity. The masses of oligomeric (epi)catechin units

are predicted by the equation m/z = 290 + 288*d* - 2*A* + *b*, where 290 represents the molecular weight of the terminal (epi)catechin unit, *d* is the number of (epi)catechin extension units, *A* is the number of A-type interflavan linkages, and *b* is the atomic weight of sodium cations (23 Da) (Krueger, Vestling, & Reed, 2003).

The MALDI-TOF MS spectra of PCPP show masses that correspond to (epi)catechin oligomers attached to one, two, or three DMAC (**Figure 3)**, CIN, TOL, CON, or SIN moieties (**Figure 1-4S**). The isotope patterns of MALDI-TOF MS for PCPP with single CIN, TOL, DMAC, CON, or SIN moieties revealed that PCPP with one A-type interflavan bond had the highest intensity. PCPP masses detected as pyrylium ions $[M]^+$ with single CIN, TOL, DMAC, CON, or SIN moieties are predicted by the equation m/z = 290 + 288*d* -2*A* + *X* - H_2O - *H*, where 290 represents the molecular weight of the terminal (epi)catechin unit, *d* is the number of (epi)catechin extension units, *A* is the number of A-type interflavan bonds, *X* represent the molecular weight of the cinnamaldehydes [(CIN=132 Da), (TOL=146 Da), (DMAC=175 Da), (CON=178 Da), and (SIN=208 Da)], H_2O represents the molecular weight of water (18 Da), and *H* is the hydrogen atom (1 Da). H_2O and *H* are lost during the condensation reaction.

The isotope patterns of MALDI-TOF MS for PCPP with two or three CIN, TOL, DMAC, CON, or SIN moieties revealed that PCPP with zero or two A-type interflavan bonds had the highest intensity. PCPP masses detected as pyrylium ions with two or three CIN, TOL, DMAC, CON, or SIN moieties with zero A-type interflavan bonds are predicted by the equation m/z = 290 + 288*d* + *nX* - nH_2O - *H*, whereas with two A-type interflavan bonds are predicted by the equation m/z =

290 + 288*d* – 2*A* + *nX* - *nH₂O* – *H,* where 290 represents the molecular weight of the terminal (epi)catechin unit, *d* is the number of (epi)catechin extension units, *A* is the number of A-type interflavan bonds, *n* is the number of cinnamaldehydes moieties, *X* represent the molecular weight of the cinnamaldehydes [(CIN=132 Da), (TOL=146 Da), (DMAC=175 Da), (CON=178 Da), and (SIN=208 Da)], *H₂O* represent the molecular weight of water (18 Da), and *H* is the hydrogen atom (1 Da) lost during the condensation reaction. In addition, signals with mass differences of 23 Da higher to PCPP with one, two or three CIN, TOL, DMAC, CON, or SIN moieties were observed. Usually, in MALDI-TOF MS, mass differences of 23 Da correspond to sodium adducts. Thus, signals with mass differences of 23 Da higher to PCPP with CIN, TOL, DMAC, CON, or SIN moieties correspond to non-charged conjugates of PCPP, which are detected as sodium adducts. **Figure 3** and **Figure 2-5S** show that the relative intensity of non-charged conjugates of PCPP was below 10%, which suggests that PCPP detected as pyrylium ions are predominant. The cation in the PCPP can resonate over the PCPP molecules, resulting in highly delocalized systems. These delocalized systems are often responsible for absorbing light in the visible region and producing colored compounds.

Ability of proanthocyanidin-cinnamaldehydes pyrylium products to exhibit fluorescence

The UV/Vis spectrum of PAC revealed one λ_{max} at 280 nm, whereas the UV/Vis spectra of PCPP revealed two absorption bands. The first λ_{max} was at 280 nm that corresponds to PAC, while the second λ_{max} of the PCPP were at higher wavelengths that differed among the cinnamaldehyde substitutions. The second λ_{max} absorption was at 404 nm for PAC-CIN, 416 nm for PAC-TOL, 559 nm for PAC-DMAC, 443 nm for PAC-CON, and 460 nm for PAC-SIN. Previous studies

indicate that the addition of electron-donating functional groups, which increases the electron density of the π system via resonance- or inductive-donating effects, alters absorption and emission spectra (Abou-Hatab, Spata, & Matsika, 2017). Thus, differences in the second λ_{max} absorptions, which result from the pyrylium substitutions could be explained by the ability of the functional groups of the cinnamaldehydes to contribute to the resonance structures of the conjugated system, driven by alkyl, methoxy, hydroxy, and tertiary amine groups (Bamfield, 2010). First, alkyl and methoxy groups differ in the electron density that each one donates to the conjugate π system via resonance- or inductive-donating effects. Alkyl groups are located in the inductive-donating effect, whereas the methoxy groups are located in the resonance-donating effect. The resonance-donating effect has lower ionization potential than the induction-donating effect. Second, both methoxy and hydroxy groups are located in the resonance-donating effect. However, the lone pair of electrons in the methoxy group is disturbed by hyperconjugation of the antibonding molecular orbital of the C-H bonds. This effect is absent in the hydroxy group. Third, both hydroxy and tertiary amine groups are located in the resonance-donating effect. However, the lower electronegativity of the N atom compared to the O atom makes the tertiary amine a better electron-donating group.

The fluorescence spectra of PAC and PCPP revealed λ_{max} emission for PAC at 320 nm, 473 nm for PAC-CIN, 480 nm for PAC-TOL, 613 nm for PAC-DMAC, 524 nm for PAC-CON, and 536 nm for PAC-SIN. The Stoke shifts value found for PAC was 40 nm, 69 nm for PAC-CIN, 64 nm for PAC-TOL, 54 nm for PAC-DMAC, 81 nm for PAC-CON, and 76 nm for PAC-SIN. The Stoke shifts are indicative of a change from the excited state to the ground state, which according to the Jablonski diagram, indicates strong excitation light separate from the weak emitted fluorescence.

Results indicate that each of the five PCPP exhibits unique and useful excitation and emission wavelengths. These characteristics demonstrate that PCPP are a new class of fluorescent probes. For instance, by complexing PCPP with proteins, glycoproteins, or polysaccharides the visualization of each complex by fluorescent microscopy may be achieved. However, because the fluorescence of PCPP may be affected by temperature, pH, metals ions, and solvent polarity/viscosity, future work with PCPP should evaluate the effect of intensity and fluorescence lifetime. For instance, previous studies indicate that the fluorescence intensity of rhodamine-B is temperature-dependent and that the fluorescence lifetime decrease as the polarity of the solvent increases (Zhang, Zhang, & Liu, 2014).

Bioactivity of proanthocyanidin-cinnamaldehyde pyrylium products to agglutinate extra-intestinal pathogenic *Escherichia coli*

PAC and PCPP were compared for their ability to agglutinate ExPEC (**Figure 4**). Results of the agglutination assay indicate that, at a fixed concentration of 200 μg/mL of PAC equivalent, PAC and PCPP have the ability to agglutinate ExPEC. As the bacteria agglutinate and precipitate from suspension, an increase in transmittance (600 nm) occurs. Results suggest that PCPP were significantly more bioactive (p-value < 0.05) for agglutinating ExPEC compared to PAC at a fixed concentration of 200 μg/mL of PAC equivalent. These results suggest that the cinnamaldehydes attached to PAC were not detrimental to PAC agglutination activity. In addition, cinnamaldehydes (negative controls) showed no agglutination.

Scanning electron micrographs of ExPEC solution, PAC with ExPEC solution, and PAC-DMAC with ExPEC solution were used to visualize the interaction between PAC-DMAC and ExPEC after the agglutination assay. **Figure 5A** shows the normal physical structure of the fimbriae-like structures expressed by ExPEC. **Figure 5B** shows the interaction of PAC with ExPEC. This micrograph indicates that PAC interact with the fimbriae-like structures on the surface of the bacteria, which allows the formation of bacteria-to-bacteria agglomerates, thus causing agglutination and precipitation of the bacteria. **Figure 5C** shows the interaction of PAC-DMAC with ExPEC. This micrograph indicates that PAC-DMAC have higher affinity with the fimbriae-like structures on the surface of the bacteria, thus causing higher agglutination and precipitation of the bacteria as was demonstrated previously by the agglutination assay.

Visualization of the interaction between proanthocyanidin and extra-intestinal pathogenic *Escherichia coli* during *in-vitro* and *in-vivo* agglutination by fluorescent microscopy

Fluorescent and differential interference contrast (DIC) microscopy was performed on the precipitated material of ExPEC, PAC with ExPEC, and PAC-DMAC with ExPEC from the *in vitro* agglutination assay. **Figure 5S-A** show that ExPEC were detected using the GFP filter and were visible by DIC microscopy but were not detected with the Texas Red filter. The overlay of GFP, Texas Red, and DIC micrographs only demonstrated GFP expression from ExPEC, which were dispersed across the field of view. **Figure 5S-B** show that PAC were not detected with the GFP and Texas Red filters, but ExPEC were detected with the GFP filter and were visible by DIC microscopy. The overlay of GFP, Texas Red, and DIC micrographs only demonstrated GFP fluorescence from ExPEC. Unlike **figure 5S-A** in which ExPEC alone were dispersed across the

field of view, **figure 5S-B** shows that when ExPEC are instilled with PAC the ExPEC are located in clumps on the slide because the ExPEC are closely associated with PAC. However, the PAC are not visible by fluorescent microscopy because PAC were not fluorescently tagged. **Figure 5S-C** show that PAC-DMAC were detected with the Texas Red filter and that ExPEC were detected with the GFP filter and with DIC microscopy. The overlay of GFP, Texas Red, and DIC micrographs demonstrated GFP expression from ExPEC and fluorescence of PAC-DMAC with the Texas Red filter. Micrograph suggests that PAC-DMAC were entrapping ExPEC in a web-like network, thus demonstrating agglutination of ExPEC by PAC-DMAC. Evidence of colocalization can be observed by the yellow color produced upon overlaying the red (Texas Red) and green (GFP) filters.

Similarly, fluorescent and DIC microscopy was performed on the urine samples of rats that were subjected to intra-vesicular bladder administration of ExPEC, PAC-DMAC, and PAC-DMAC with ExPEC. **Figure 6A** show that ExPEC were detected with the GFP filter and were visible by DIC microscopy. The ExPEC were not detected with the Texas Red filter. **Figure 6B** show that PAC-DMAC were not detected with the GFP filter but are detected with the Texas Red filter. While no ExPEC were instilled in this treatment, the DIC microscopy shows a number of distinct white spots that could be bacteria that were native to the rat urine/bladder. In previous experiments (unpublished data) we have observed that rats have an endogenous bacterial population in their urine/bladder. The overlay of GFP, Texas Red, and DIC micrographs indicate that PAC-DMAC are closely associated with the suspected endogenous bacteria, indicating that PAC may be entrapping endogenous bacteria. **Figure 6C** show that ExPEC were detected with the GFP filter

and PAC-DMAC were detected with the Texas Red filter. The overlay of GFP, Texas Red, and DIC micrographs indicate that PAC-DMAC were entrapping ExPEC. The slide containing PAC-DMAC with ExPEC solution was later observed using fluorescent confocal microscopy (**Figure 6D**). Confocal microscopy captures 2D-images at different depths allowing the reconstruction of 3D-images. The micrograph of PAC-DMAC with ExPEC supports our finding that PAC-DMAC (red color) entangle ExPEC (green color). This is distinctly evident where yellow color was detected, which is produced by the overlapping of the Texas red and GFP filters. The laser scanning confocal micrograph illustrates that PAC-DMAC is localized where ExPEC are localized. This co-localization is the result of the bacterial agglutination, which corresponds to an increase in concentration of bacteria in a limited area of the micrograph. This phenomenon may inhibit bacterial growth, cause structural damage to bacteria, and increase bacterial clearance by macrophages and other phagocytic cells. In addition, the bacterial agglutination leads to a decrease in enterocyte invasion by ExPEC (Feliciano, Heintz, Krueger, Vestling, & Reed, 2015; Rodrigo Feliciano, Krueger, & Reed, 2015).

CONCLUSION

In this work, we describe the condensation reactions between PAC with cinnamaldehydes to obtain PCPP. MALDI-TOF MS, used to characterized PCPP, showed that PAC and cinnamaldehydes were covalently linked. Spectrophotometric analyzes indicate that PCPP exhibit fluorescence at useful wavelengths for use in fluorescent microscopy. PCPP were used to visualize PAC bioactivity. Our results suggested that PCPP did not affect PAC agglutination activity. On the contrary, PCPP were significantly more bioactive (p-value < 0.05) for agglutinating ExPEC compared to PAC at a fixed concentration of 200 μg/mL of PAC equivalent. Fluorescent micrographs of PAC-DMAC demonstrated the ability of PCPP to visualize the *in-vitro* agglutination of ExPEC. These results suggest that PCPP is a more cost-effective alternative for visualizing the temporal interaction of PAC as compared to the complex and expensive technique of ^{14}C radio-labeling of PAC. Future work should include the use of PCPP to study the *in situ* and *in vivo* interaction of PAC with endogenous bacteria and in the development of a diagnostic tool for determining bacteriuria and urinary tract infections (UTIs) in real-time. Currently, the diagnosis of bacteriuria and UTIs are performed using urinalysis and culture test, which can take up to two days to reveal infection status.

CONFLICT OF INTEREST

The authors declare the following competing financial interest(s): Christian G. Krueger and Jess D. Reed have ownership interest in Complete Phytochemical Solution, LLC., and acknowledge their affiliation with this company.

ACKNOWLEDGMENTS

The authors acknowledge financial support from the Ministry of Science, Technology and Telecommunications (MICITT), the Innovation and Human Capital Program for Competitiveness (PINN), and the National Council for Scientific and Technology Research (CONICIT, Grant PED-056-2015-I) from Costa Rica. We are grateful to UroPharma, Inc (Minneapolis, MN, USA) for providing funding. Additionally, the authors gratefully acknowledge use of the Bruker ULTRAFLEX III supported by NIH thought the University of Wisconsin, Department of Chemistry, Mass Spectrometry facility (NCRR 1S10RR024601-01). We thank the Welch Laboratory from the Department of Medical Microbiology and Immunology at UW-Madison for providing *E.coli* strain CFT073-GFP.

AUTHORSHIP CONTRIBUTION STATEMENT

Daniel Esquivel-Alvarado: Conceptualization, Methodology, Formal analysis, Investigation, Data curation, Writing - original draft, Writing - review & editing, Visualization. **Emilia Alfaro-Viquez:** Conceptualization, Writing - review & editing, Visualization. **Michael A. Polewski:** Investigation. **Christian G. Krueger:** Conceptualization, Writing - review & editing, Funding acquisition. **Martha M. Vestling:** Writing -review & editing. **Jess D. Reed:** Conceptualization, Writing - review & editing, Supervision, Funding acquisition.

REFERENCE

Abou-Hatab, S., Spata, V., & Matsika, S. (2017). Substituent effects on the absorption and fluorescence properties of anthracene. *Journal of Physical Chemistry A, 121*(6), 1213-1222. doi:10.1021/acs.jpca.6b12031

Alfaro-Viquez, E., Esquivel-Alvarado, D., Madrigal-Carballo, S., Krueger, C., & Reed, J. (2018). Cranberry proanthocyanidin-chitosan hybrid nanoparticles as a potential inhibitor of extra-intestinal pathogenic *Escherichia coli* invasion of gut epithelial cells. *International Journal of Biological Macromolecules*, 415-420. doi:10.1016/j.ijbiomac.2018.01.033

Alfaro-Viquez, E., Esquivel-Alvarado, D., Madrigal-Carballo, S., Krueger, C., & Reed, J. (2019). Proanthocyanidin-chitosan composite nanoparticles prevent bacterial invasion and colonization of gut epithelial cells by extra-intestinal pathogenic *Escherichia coli*. *International Journal of Biological Macromolecules*, 630-636. doi:10.1016/j.ijbiomac.2019.04.170

Alfaro-Viquez, E., Roling, B., Krueger, C., Rainey, C., Reed, J., & Ricketts, M. (2018). An extract from date palm fruit (*Phoenix dactylifera*) acts as a co-agonist ligand for the nuclear receptor FXR and differentially modulates FXR target-gene expression *in vitro*. *PloS One, 13*(1), e0190210. doi:10.1371/journal.pone.0190210

Bamfield, P. (2010). *Chromic phenomena: technological applications of colour chemistry*: Royal Society of Chemistry.

Birmingham, A. , Esquivel-Alvarado, D., Maranan, M., Krueger, C., & Reed, J. (2020). Inter-laboratory validation of 4-(dimethylamino) cinnamaldehyde (DMAC) assay using cranberry proanthocyanidin standard for quantification of soluble proanthocyanidins in cranberry foods and dietary supplements, First Action Method: 2019.06. *Journal of AOAC International*. doi:10.1093/jaoacint/qsaa084

de Freitas, V., Sousa, C., Silva, A. M., Santos-Buelga, C., & Mateus, N. (2004). Synthesis of a new catechin-pyrylium derived pigment. *Tetrahedron letters, 45*(51), 9349-9352. doi:10.1016/j.tetlet.2004.10.132

Esquivel-Alvarado, D., Muñoz-Arrieta, R., Alfaro-Viquez, E., Madrigal-Carballo, S., Krueger, C., & Reed, J. (2020). Composition of anthocyanins and proanthocyanidins in three tropical *Vaccinium* species from Costa Rica. *Journal of Agricultural and Food Chemistry, 68*(10), 2872-2879. doi:10.1021/acs.jafc.9b01451

Feliciano, R., Heintz, J., Krueger, C., Vestling, M., & Reed, J. (2015). Fluorescent labeling of cranberry proanthocyanidins with 5-([4,6-dichlorotriazin-2-yl]amino)fluorescein (DTAF). *Food Chemistry, 166*, 337-345. doi:10.1016/j.foodchem.2014.06.031

Feliciano, R., Krueger, C., & Reed, J. (2015). Methods to determine effects of cranberry proanthocyanidins on extraintestinal infections: relevance for urinary tract health. *Molecular Nutrition & Food Research, 59*(7), 1292-1306. doi:10.1002/mnfr.201500108

Feliciano, R., Meudt, J., Shanmuganayagam, D., Krueger, C., & Reed, J. (2014). Ratio of "A-type" to "B-type" proanthocyanidin interflavan bonds affects extra-intestinal pathogenic *Escherichia coli* invasion of gut epithelial cells. *Journal of Agricultural and Food Chemistry, 62*(18), 3919-3925. doi:10.1021/jf403839a

Feliciano, R., Shea, M., Shanmuganayagam, D., Krueger, C., Howell, A., & Reed, J. (2012). Comparison of isolated cranberry (*Vaccinium macrocarpon* Ait.) proanthocyanidins to catechin and procyanidins A2 and B2 for use as standards in the 4-(dimethylamino)cinnamaldehyde assay. *Journal of Agricultural and Food Chemistry, 60*(18), 4578-4585. doi:10.1021/jf3007213

Foo, L., Lu, Y., Howell, A., & Vorsa, N. (2000). The structure of cranberry proanthocyanidins which inhibit adherence of uropathogenic P-fimbriated *Escherichia coli in vitro*. *Phytochemistry, 54*(2), 173-181. doi:10.1016/s0031-9422(99)00573-7

Krueger, C., Vestling, M., & Reed, J. (2003). Matrix-assisted laser desorption/ionization time-of-flight mass spectrometry of heteropolyflavan-3-ols and glucosylated heteropolyflavans in sorghum [Sorghum bicolor (L.) Moench]. *Journal of Agricultural and Food Chemistry, 51*(3), 538-543. doi:10.1021/jf020746b

Liu, H., Liu, H., Wang, W., Khoo, C., Taylor, J., & Gu, L. (2011). Cranberry phytochemicals inhibit glycation of human hemoglobin and serum albumin by scavenging reactive carbonyls. *Food & Function, 2*(8), 475-482. doi:10.1039/c1fo10087d

Reed, J., Krueger, C., & Vestling, M. (2005). MALDI-TOF mass spectrometry of oligomeric food polyphenols. *Phytochemistry, 66*(18), 2248-2263. doi:10.1016/j.phytochem.2005.05.015

Sousa, C., Mateus, N., Perez-Alonso, J., Santos-Buelga, C., & de Freitas, V. (2005). Preliminary study of oaklins, a new class of brick-red catechinpyrylium pigments resulting from the reaction between catechin and wood aldehydes. *Journal of Agricultural and Food Chemistry, 53*(23), 9249-9256. doi:10.1021/jf051970e

Tanaka, T., Matsuo, Y., Yamada, Y., & Kouno, I. (2008). Structure of polymeric polyphenols of cinnamon bark deduced from condensation products of cinnamaldehyde with catechin and procyanidins. *Journal of Agricultural and Food Chemistry, 56*(14), 5864-5870. doi:10.1021/jf800921r

Zhang, X., Zhang, Y., & Liu, L. (2014). Fluorescence lifetimes and quantum yields of ten rhodamine derivatives: Structural effect on emission mechanism in different solvents. *Journal of Luminescence, 145*, 448-453. doi:10.1016/j.jlumin.2013.07.066

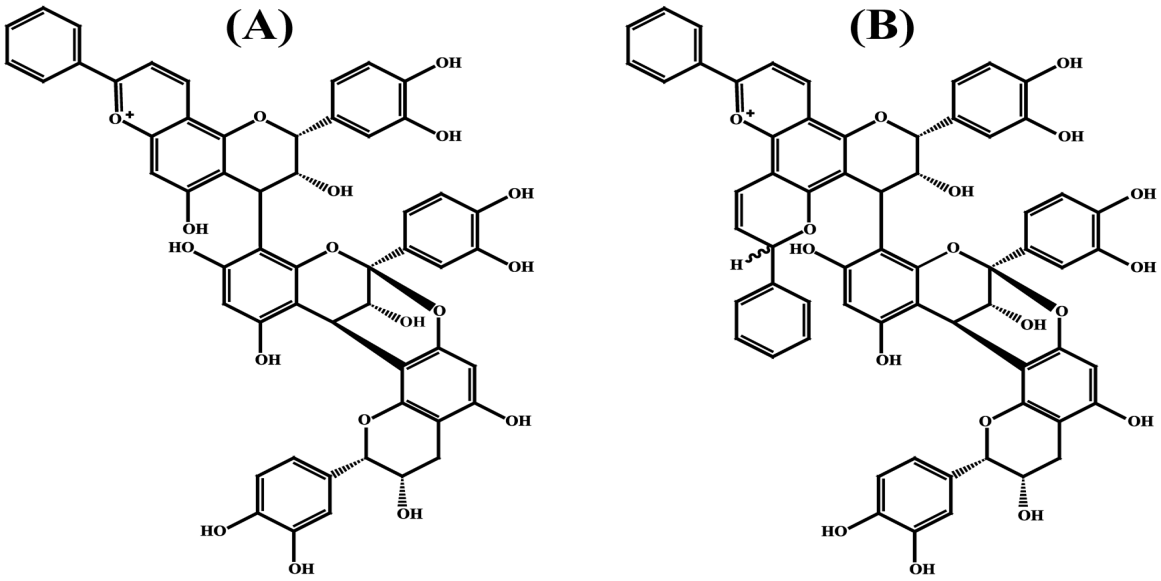

Figure 1. Hypothetical structures of proanthocyanidin trimers with one A-type interflavan bond covalently linked to a single (A) and double (B) cinnamaldehyde moieties.

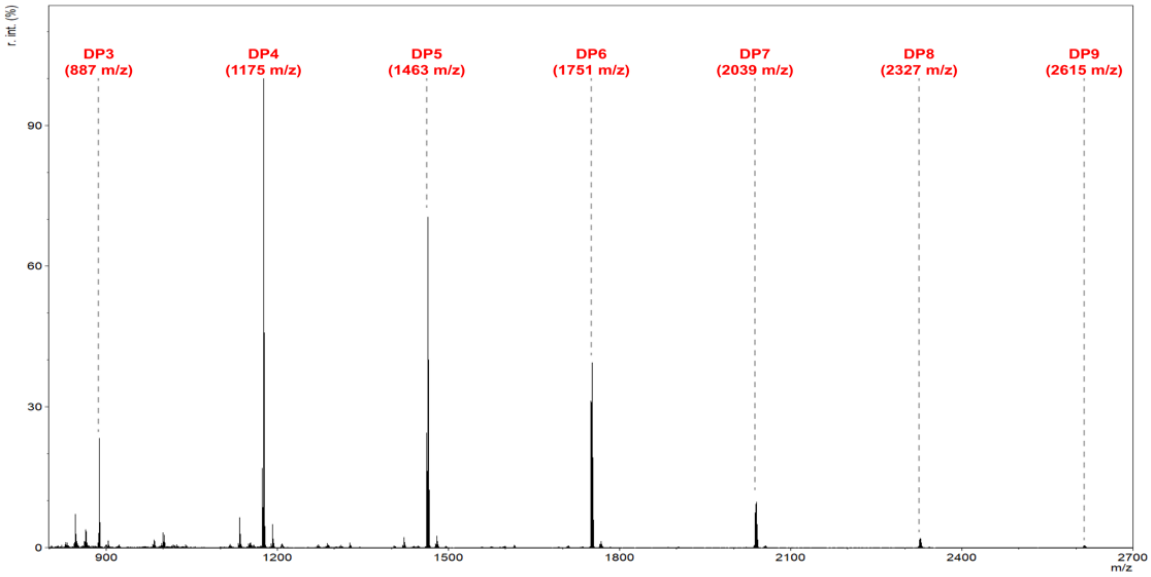

Figure 2. MALDI-TOF MS spectra in positive reflectron mode for PAC, which show PAC oligomers from trimers to nonamers detected as sodium adducts $[M+Na]^+$.

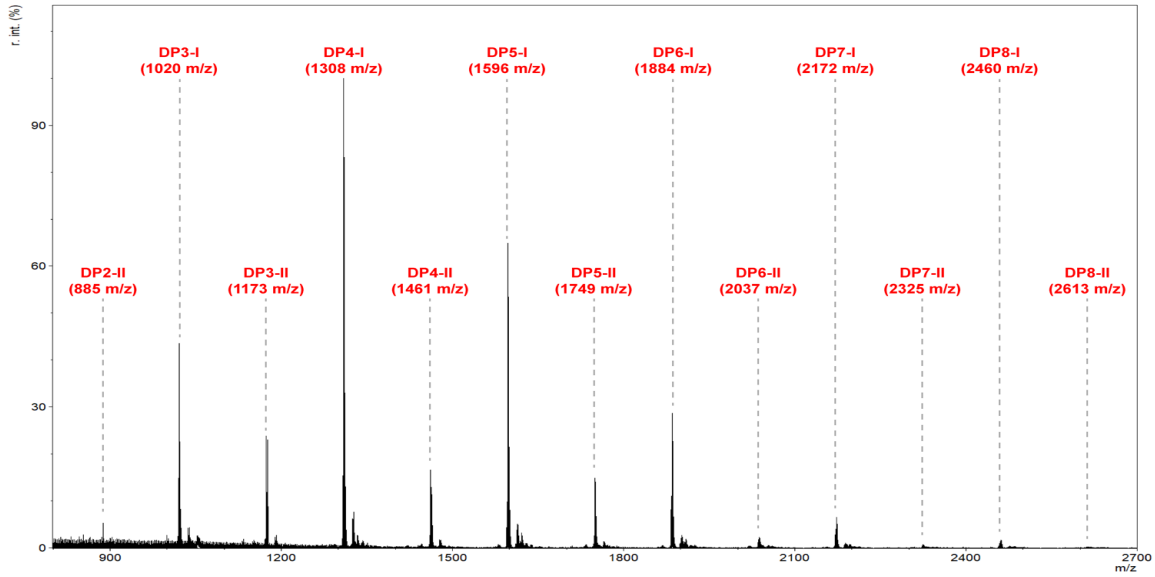

Figure 3. MALDI-TOF MS spectra in positive reflectron mode for PAC-DMAC, which show PAC oligomers from trimers to octamers. Roman numerals followed by the DP represent the numbers of DMAC moieties attached.

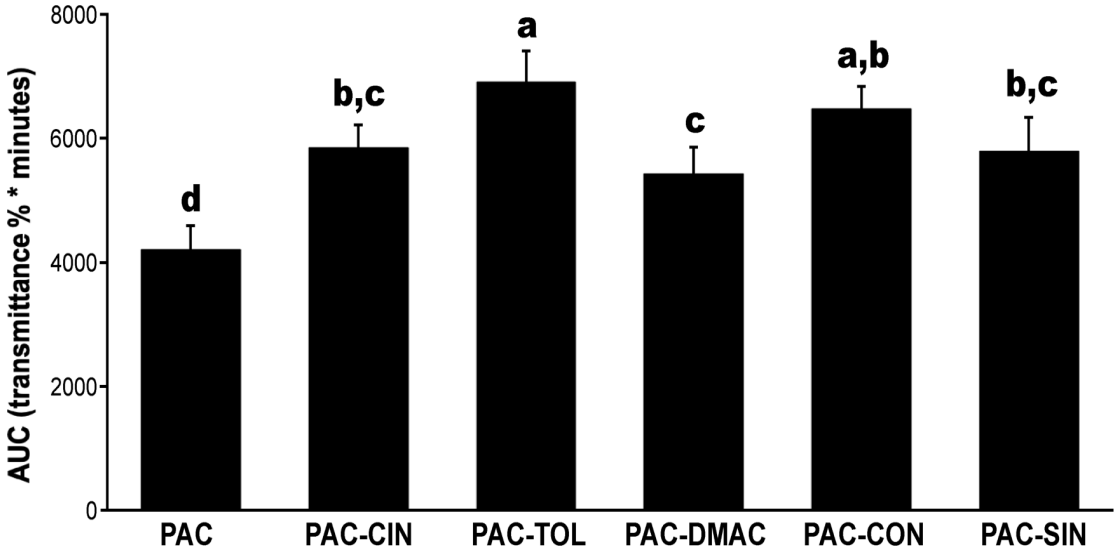

Figure 4. Area under the curve (AUC) obtained for the agglutination assay with ExPEC in PBS 1x (Ca^{2+}/Mg^{2+}) at a fixed concentration of 200 μg/mL of PAC equivalent for PAC and PCPP. The results represent the average of five independent replicates ± standard deviation. Different letters correspond to significant differences at *p*-value < 0.05.

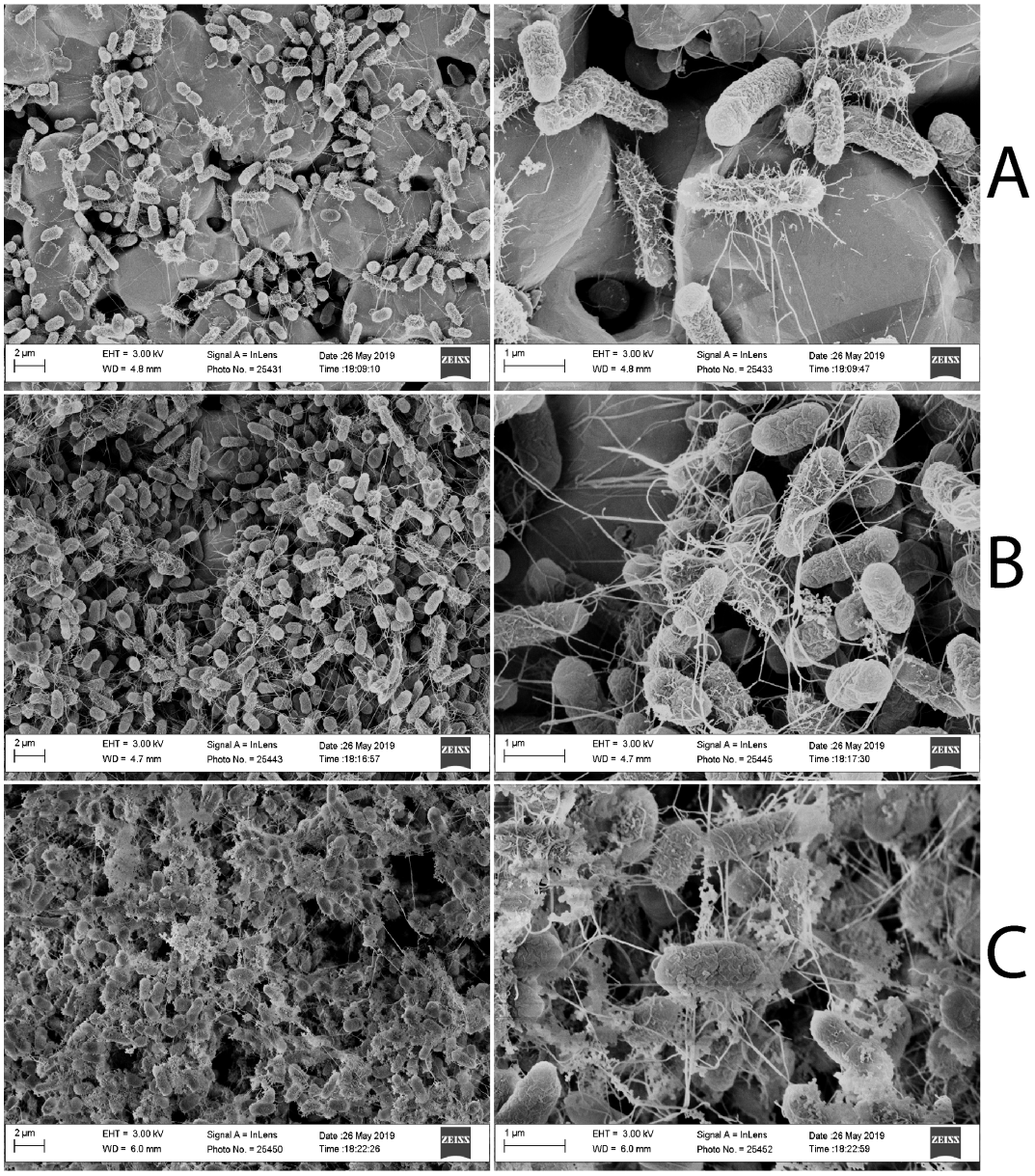

Figure 5. Scanning electron micrographs showing the effect of ExPEC solution (A), PAC with ExPEC solution (B), and PAC-DMAC with ExPEC solution (C) after the agglutination assay.

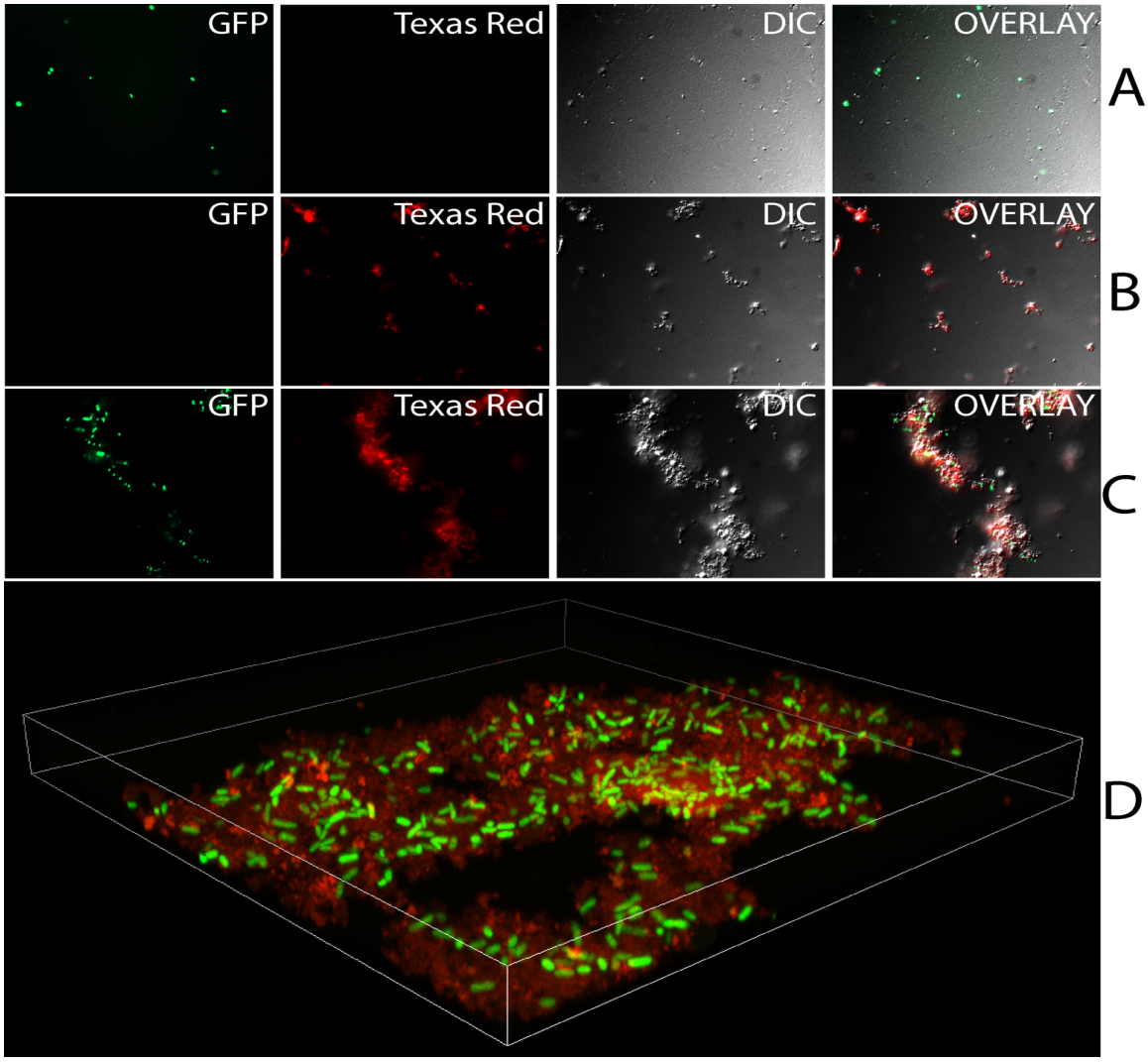

Figure 6. Micrographs of rat urine containing the ExPEC (A), PAC-DMAC (B), and PAC-DMAC with ExPEC (C) under a magnification of 40x. Micrographs were obtained using the green fluorescent protein (GFP) and Texas Red filters, and the differential interference contrast (DIC) microscopy. Laser scanning confocal micrograph of rat urine containing PAC-DMAC with ExPEC solution (D) under a magnification of 100x.

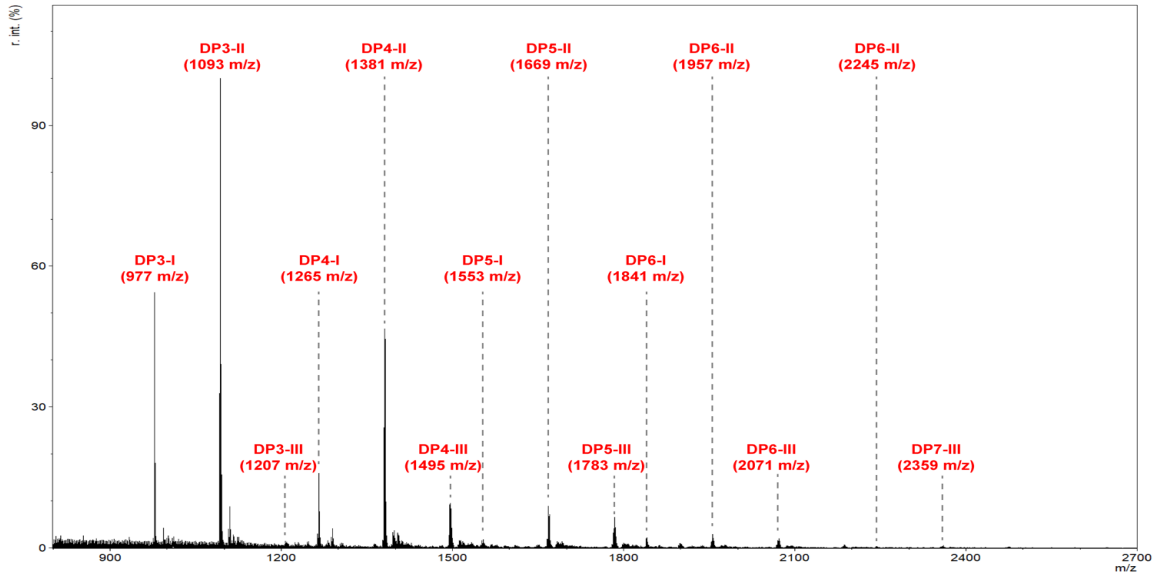

Figure 1S. MALDI-TOF MS spectra in positive reflectron mode for PAC-CIN, which show PAC oligomers from trimers to hexamers. Roman numerals followed by the DP represent the numbers of CIN moieties attached.

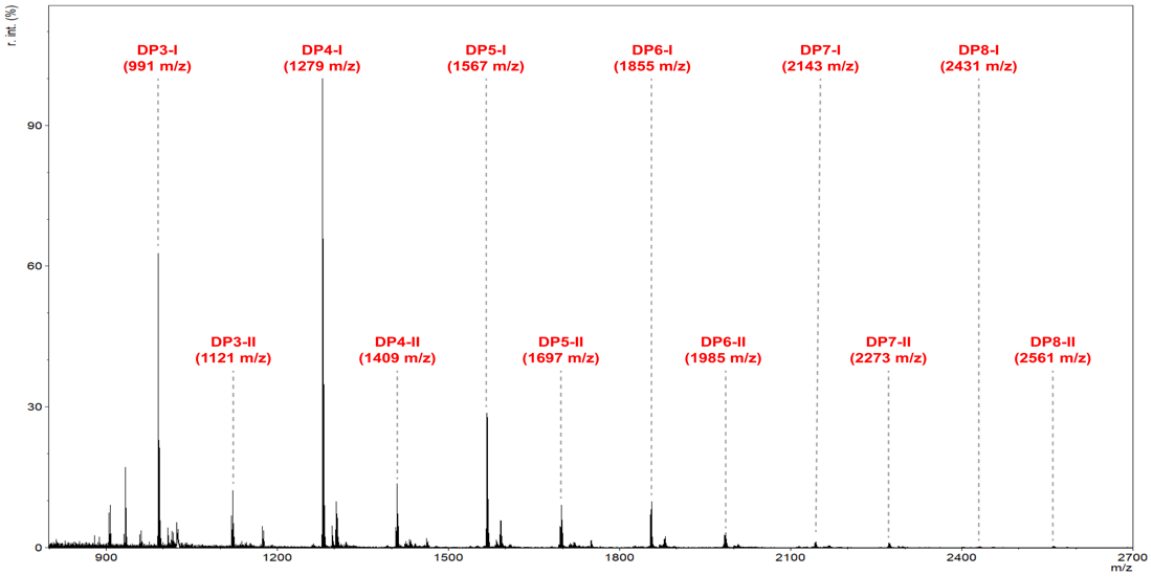

Figure 2S. MALDI-TOF MS spectra in positive reflectron mode for PAC-TOL, which show PAC oligomers from trimers to octamers. Roman numerals followed by the DP represent the numbers of TOL moieties attached.

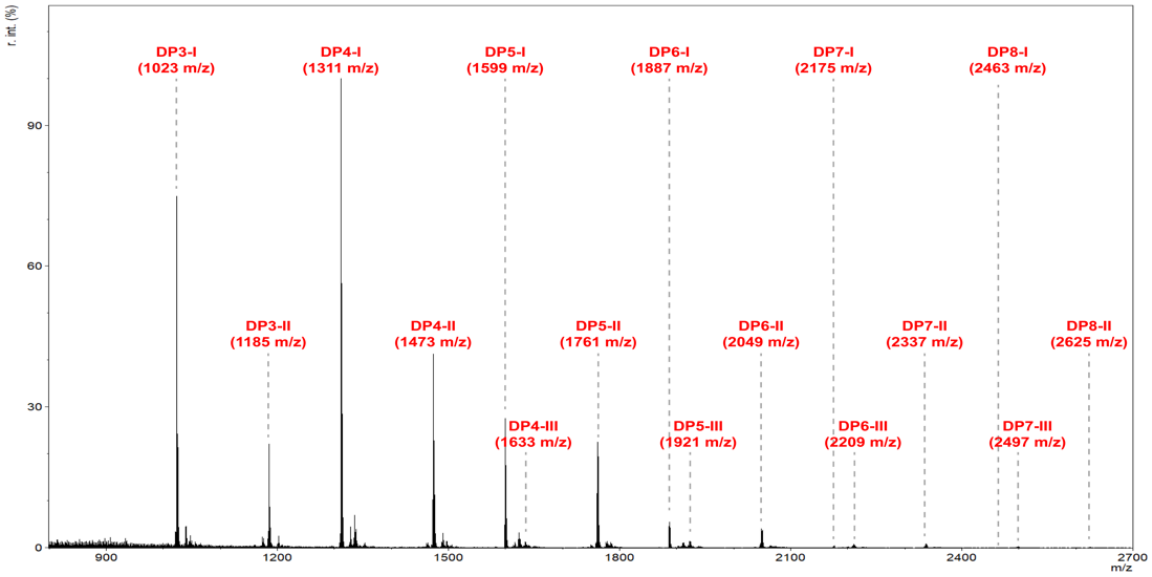

Figure 3S. MALDI-TOF MS spectra in positive reflectron mode for PAC-CON, which show PAC oligomers from trimers to octamers. Roman numerals followed by the DP represent the numbers of CON moieties attached.

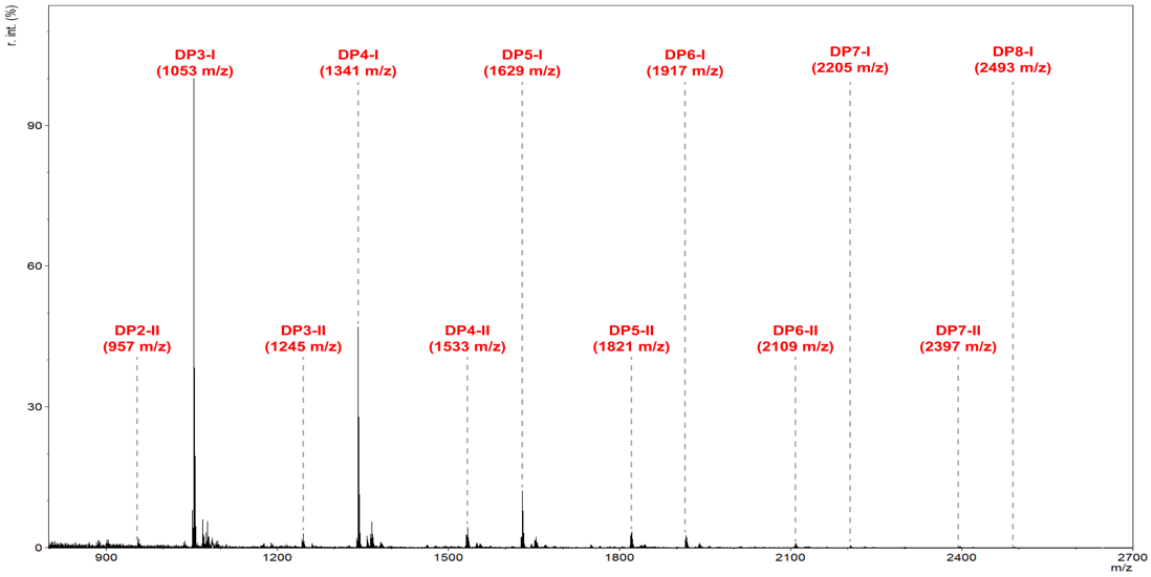

Figure 4S. MALDI-TOF MS spectra in positive reflectron mode for PAC-SIN, which show PAC oligomers from trimers to octamers. Roman numerals followed by the DP represent the numbers of SIN moieties attached.

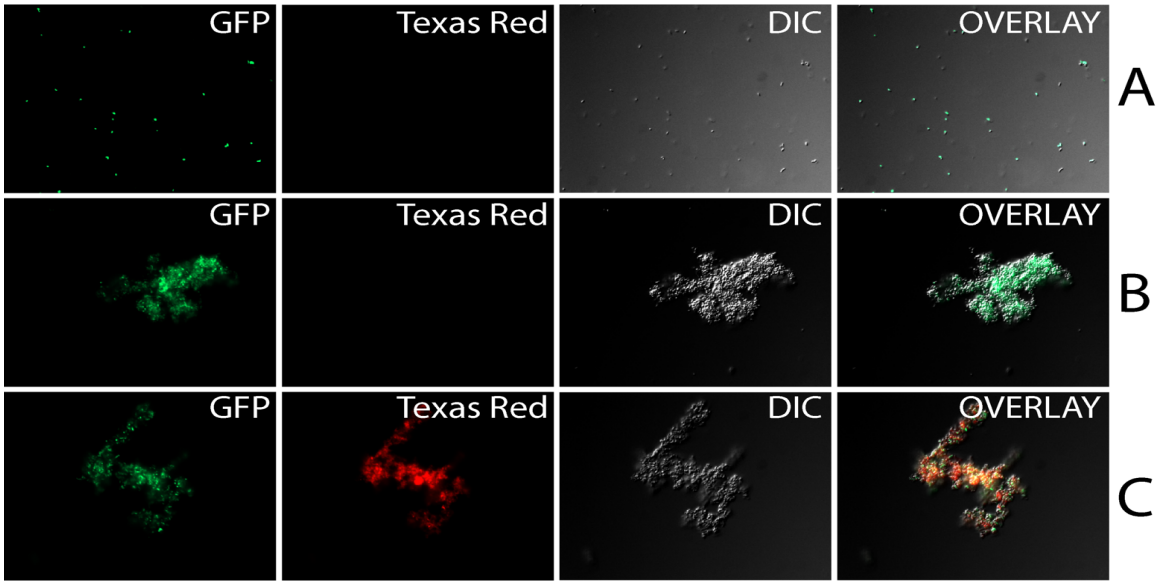

Figure 5S. Micrographs of the *in vitro* agglutination assay containing the ExPEC solution (A), PAC and ExPEC solution (B), and PAC-DMAC with ExPEC solution (C) under a magnification of 40x. Micrographs were obtained using the green fluorescent protein (GFP) and Texas Red filters, and the differential interference contrast (DIC) microscopy.

SUMMARY AND FUTURE DIRECTION

During the last 15 years, research laboratories have strived to develop more robust and accurate analytical tools for quantifying and characterizing PAC. However, the heterogeneity and complexity of PAC have meant that even today there is no consensus amongst laboratories on which methodology is adequate for quantifying and characterizing PAC. In this dissertation, we validated the use of a customized PAC standard isolated from cranberry fruits for quantifying soluble PAC in cranberry foods and dietary supplements following the AOAC requirements (Chapter 1). We developed a MALDI-TOF MS methodology to identify A-type PAC in cranberry foods and dietary supplements following the AOAC requirements (Chapter 2). We evaluated the MALDI-TOF MS methodology combined with multivariate analysis to build classification models which are able to predict the mixing of c-PAC either with a-PAC or p-PAC (Chapter 3). We determined the composition of anthocyanins and PAC from three tropical *Vaccinium* species from Costa Rica (Chapter 4). Finally, we synthesized PCPP, which can be used to improve our understanding of the temporal and dynamic interaction of PAC in *in vitro* and *in vivo* studies as they exhibit fluorescence (Chapter 5). In summary, the development of this dissertation could serve as a starting point for the development of standardize methods for quantitative and qualitative analysis of PAC in research and commercial laboratories. The lack of analytical methods to standardize and authenticate cranberry products, which are associated with putative health benefits, undermines consumer perception**,** because the use of non-standardized cranberry products may result in sub-effective doses and absence of A-type PAC.

In Chapter 1, we conducted an inter-laboratory validation of the DMAC assay for quantifying soluble PAC in cranberry foods and dietary supplements and compared both ProA2 and c-PAC standards by using a 96-well microplate reader. Four test materials were analyzed: cranberry fiber powder [ranged, 0.03-15% (w/v)], cranberry extract powder [ranged, 0.03-15% (w/v)], concentrated cranberry juice [ranged, 0.03-15% (w/v)], and a solution of cranberry PAC [at 30% w/w]. Results indicated that the use of both ProA2 and c-PAC standards meet the SMPR 2017.003 acceptance criteria (linearity, repeatability precision, inter-laboratory precision, and limit of quantification). However, the use of c-PAC resulted in values that were 3.3 fold higher than those of ProA2, which suggests that ProA2 standard leads to an underestimation of PAC content from samples containing higher molecular weight PAC. Overall, the accurate quantification of soluble PAC using the c-PAC standard would allow to design clinical studies that support the putative health benefits of PAC.

In Chapter 2, we developed a MALDI-TOF MS method for obtaining high-resolution spectra to identify A-type PAC in cranberry-foods and dietary supplements to meet specifications as proposed by AOAC SMPR 2017.004. Furthermore, we described the deconvolution method, which was used to differentiate A-type PAC from other botanical sources containing mostly B-type PAC. Seventy-one test materials were analyzed: 35 samples reported to contain A-type PAC and 36 samples reported to contain B-type PAC. Results indicated that by modifying five parameters (matrix selection, sample to matrix ratio, cationization agent, pulsed ion extraction, and laser power), high-resolution MALDI-TOF MS spectra were obtained. MALDI-TOF MS and deconvolution of overlapping isotope patterns were able to identify the A-type PAC with a

probability greater than 90% and a confidence of 95%. Overall, this study showed that MALDI-TOF MS is capable of identifying PAC and determining its structural characteristics (A- and B-type interflavan bonds, substituents, among others).

In Chapter 3, we characterized the PAC profiles of apples (a-PAC), cranberries (c-PAC), and peanut skins (p-PAC) by MALDI-TOF MS. Furthermore, MALDI-TOF MS spectra data were differentiated and discriminatd by principal component analysis (PCA) and linear discriminant analysis (LDA), respectively. MALDI-TOF MS spectra combined with multivariate analysis was used to build classification models capable of determining mixtures of c-PAC with either a-PAC or p-PAC at different w/w ratios. Two hundred twenty-six test materials were analyzed: 28 unmixed a-PAC samples, 34 unmixed c-PAC samples, 24 unmixed p-PAC samples, 70 samples of c-PAC mixed with a-PAC, and 70 samples c-PAC mixed with p-PAC. Results indicated the feasibility of MALDI-TOF MS to characterize the PAC profile of apples, cranberries, and peanut skins. PCA classified the different mixed and unmixed PAC profiles into seventeen groups according to their percentage. LDA models correctly classified 99.4% of the training set, 100% the testing set, and 94.2% of the validation set. In addition, results suggest that our method may determine the adulteration of c-PAC with either a-PAC or p-PAC, within 5% (w/w) with a confidence level of 95% across the seventeen groups. Overall, MALDI-TOF MS spectra data combined with multivariate analysis were able to classify mixtures of c-PAC with either a-PAC or p-PAC, based on the percentage (w/w) of the adulterant. This suggests that the classification model may be used as a routine method in quality control laboratories for detecting adulteration of PAC in cranberry products.

In Chapter 4, we determined the composition of anthocyanins and proanthocyanidins in three tropical *Vaccinium* species (TVS) from Costa Rica. Anthocyanin profiles were determined using ESI-MS/MS, while PAC profiles were determined using ATR-FTIR, NMR, and MALDI-TOF MS. Results indicated that the aglycone forms of anthocyanins were not detected in the three TVS (*V. consanguineum*, *V. floribundum*, and *V. poasanum*). Cyanidin- and delphinidin-glycosides were the predominant anthocyanins in TVS. Malvidin-, peonidin-, and petunidin-glycosides were present in *V. poasanum* but not in *V. consanguineum* and *V. floribundum*. In addition, TVS are composed mainly of (-)-epicatechin (2*R*,3*R*). Deconvolution of overlapping isotope pattern of MALDI-TOF MS spectra indicated that PAC with one or more A-type interflavan bonds accounted for more than 74% of the oligomer at each DP. Overall, the anthocyanin profiles of *V. consanguineum* and *V. floribundum* are similar to evergreen huckleberries (*V. ovatum* Pursh), whereas anthocyanin profile of *V. poasanum* is similar to blueberries (*V. angustifolium* Aiton). PAC profiles in TVS are similar to cranberry PAC rather than blueberry and evergreen huckleberry.

In Chapter 5, we synthesized proanthocyanidin-cinnamaldehydes pyrylium products (PCPP) by the condensation reaction of PAC with cinnamaldehyde and four cinnamaldehyde derivatives. PCPP were characterized by MALDI-TOF MS, while their capacity to exhibit fluorescence and agglutinate extra-intestinal pathogenic *Escherichia coli* (ExPEC) were evaluated. MALDI-TOF MS showed masses that correspond to (epi)catechin oligomers attached to single, double, or triple moieties of cinnamaldehydes. Synthesized PCPP exhibited fluorescence at higher excitation and emission wavelengths than PAC, and each cinnamaldehyde condensation product exhibited

different fluorescent properties. In addition, PCPP were significantly more bioactive ($P<0.05$) for agglutinating ExPEC compared to PAC. Fluorescent microscopy performed on *in vitro* and *in vivo* agglutination assays showed that PCPP were entrapping ExPEC in a web-like network. Overall, this study demonstrated the potential of PCPP to improve our understanding of the temporal and dynamic interactions of PAC in *in vitro* and *in vivo* studies.

Future work should focus on promoting the use of customized PAC standards isolated from each fruit, which reflect the structural complexity and heterogeneity of PAC. As shown in Chapter 1, PAC content depends on the standard used for the DMAC assay. The development of customized PAC standards would allow us to gain a better understanding of the influence of PAC degree of polymerization on kinetics of the DMAC reaction. Proper characterization of customized PAC standards is crucial for comparing efficacy in clinical trials. In addition, more research needs to be done on how PAC react with the DMAC reagent at the current acid conditions [10.7% (v/v) concentrated hydrochloric acid of total volume]. Unpublished data obtained using MALDI-TOF MS showed that DP of PAC oligomers decreases as the reaction takes place. This suggests that the DMAC assay is affected by the normality of the acid. Thus, the stoichiometry of the reaction is not one molecule of DMAC per each molecule of PAC.

Additionally, future work should take advantage of the fluorescence produced by the condensation reaction between PAC with DMAC and develop a fluorescence method to quantify soluble PAC. The development of a fluorescence method could be more sensitive and specific than current absorption methods to quantify PAC.

Our results using MALDI-TOF MS and deconvolution method indicates that the overlapping isotope patterns for each botanical source are repeatable at each DP, which suggest that each botanical source has a unique PAC fingerprint. In addition, we showed that classification models can be built based on the nature of the interflavan bond. Taken together, future work should focus on developing MALDI-TOF MS spectral libraries from samples of authentic dietary supplements to build classification models, which could work as predictive models for standardization, authenticity, and efficacy.

Overall, this dissertation expanded our knowledge in PAC characterization and its importance for revealing other aspects of authenticity (e.g. A- and B-type interflavan bonds, galloyl units) when MALDI-TOF MS was used. It also opens an exciting research field such as pattern recognition and machine learning of MALDI-TOF MS spectral data able to exceed recognition performed using visual inspection by experts in the field.

APPENDIX 1: Matrix-Assisted Laser Desorption/Ionization Time-of-Flight Mass Spectrometry (MALDI-TOF MS) of Proanthocyanidins to Determine Authenticity of Functional Foods and Dietary Supplements

Daniel Esquivel-Alvarado[§], Jess D. Reed[§,†], and Christian G. Krueger[§,†]

[§] Department of Animal Sciences, University of Wisconsin-Madison, Madison, USA

[†] Complete Phytochemical Solutions LLC, Cambridge, Wisconsin, USA

This chapter is published as-is in the *Recent Advances in Polyphenol Research Book, Vol 7*

ABSTRACT

The lack of analytical methods to determine authenticity of proanthocyanidins (PAC) in functional foods and dietary supplements is a problem in market regulation and development of efficacious products. Matrix-assisted laser desorption/ionization time-of-flight mass spectrometry (MALDI-TOF MS) of PAC structure offers good potential for rapid analysis in authenticity research. We used MALDI-TOF MS and deconvolution to determine the percentage of A- and B-type interflavan bonds in PAC oligomers. Deconvolution works because isotope patterns are repeatable and accurate. Multivariate analysis using relative ratios of A- to B- type interflavan bonds as determined by deconvolution or autoscaled spectra was used to classify and differentiate plant species based on PAC spectral data. Principal component analysis (PCA) of PAC spectra data was able to differentiate botanical sources and linear discriminant analysis (LDA) correctly classified botanical sources, indicating that MALDI-TOF MS combined with multivariate analysis is an effective tool to determine PAC authenticity.

Keywords: Deconvolution, interflavan bonds, isotope patterns, linear discriminant analysis, MALDI-TOF MS, multivariate analysis, principal component analysis, and proanthocyanidins.

INTRODUCTION

There is a significant need within the functional food and dietary supplement industries and regulatory agencies for rapid, accurate, and reliable analytical methods to authenticate bioactive ingredients (Clydesdale, 2004). The health benefits conferred by the bioactive compounds found within many functional foods (e.g. fruits, juices, purees, and dried fruits/vegetables) depend on the quantity, type, source, and ratio of bioactive ingredients within these products. The functional food market is substantial; in the United States fruits and vegetables are an $80.2B/year market, and botanicals represent an ~$37B/year market (LeClair, 2016). Cranberries alone, for example, are the second most consumed supplement in the US herbal ingredient industry, with a $800M/year market, and cranberry value-added products are a $54M/year market (Polito, 2015; Smith, Lynch, Johnson, Kawa, Bauman, & Blumenthal, 2015).

Attempts have been made to characterize and authenticate the presence and type(s) of PAC within natural products and dietary supplements. However, current methods that are used by the industry are obsolete and do not rapidly identify, characterize, and distinguish PAC. For instance, high-performance thin layer chromatography (HPTLC) and high-performance liquid chromatography (HPLC) can identify and quantify individual, low molecular weight compounds, and distinguish genuine compounds from adulterants (Rumalla, Avula, Wang, Smillie, & Khan, 2012; Craciun, Cretu, Mirea, Tanczos, Popa, & Miron, 2015). However, they are incapable of characterizing complex classes of oligomeric polyphenolic compounds, such as PAC or hydrolysable tannins. Genomic methods can identify the presence of plant species and distinguish genuine plant materials from some types of adulterants (Wallace, Boilard, Eagle, Spall, Shokralla, & Hajibabaei,

2012). However, nucleic acids are not the bioactive compounds within natural products. The simple detection of a species' DNA within a sample does not indicate whether the bioactive compound from that species is present within the product, nor does it rule out the presence of other compounds (bioactive or otherwise) within the product. For example, roots and leaves could test positive for the plant of interest, but could fail to contain the bioactive components of interest if those compounds were found primarily in the fruit. These shortcomings have not prevented DNA testing from being promoted and adopted by some in the industry as a standard method for the authentication of natural products (Twilley, 2015).

A lack of standardized data and information on bioactive ingredients, coupled with an inability to quickly and accurately characterize and quantify the bioactive ingredients within functional foods, undermines the market because these problems prevent verification of authenticity. As a result, many products are improperly labeled, contain adulterants (including allergens), or lack the bioactive ingredients of interest. This hinders: (i) research on their health benefits and the establishment of dosage and/or dietary guidelines; (ii) the ability of the industry (growers, processors, distributors, and sellers) to improve crops and food products based on bioactive compounds, and; (iii) the ability of consumers to gauge which functional foods are most effective when used to improve their health.

The United States Department of Agriculture (USDA) Economic Research Service report on Food and Drug Administration (FDA) refusals of imported food products from 2005 through 2013 indicated that 41% of the 142,679 total violations reported were for misbranding, which may

include untruthful or misleading labels (Bovay, 2016). As stated in the report, “Although adulteration generally poses a greater risk to human health than misbranding, improper labeling, such as failure to identify an allergen, may lead to illness and fatalities in some cases” (Bovay, 2016). Bioactive ingredients may degrade or be lost as the result of processing or improper handling. Regulatory bodies are unable to assess whether a product is properly labeled or if it complies with FDA regulations, such as the Food Modernization Safety Act (FMSA), current Good Manufacturing Practices (cGMP), Generally Recognized As Safe (GRAS), and the New Dietary Ingredient (NDI) requirements (Congress, 1938, 2011).

Thus, many products currently being marketed to consumers as dietary supplements may lack the bioactive ingredients of interest, contain subclinical quantities, or contain unsafe adulterants, such as allergens and toxins. For example, some unethical manufacturers substitute peanut skins as an inexpensive source of PAC in products purported to contain cranberry or grape seed PAC (Kupina & Gafner, 2016), introducing the risk of unknowing consumption of peanut allergens by consumers (Villani, Reichert, Ferruzzi, Pasinetti, Simon, & Wu, 2015). Improper handling or processing may also degrade or eliminate the bioactive compounds within products. The lack of efficacy of the components in these products only serves to erode consumer confidence and the overall perception of the health benefits.

There are greater than 10000 phenolic compounds that have been identified in plants (Cheynier, Comte, Davies, Lattanzio, & Martens, 2013). The main classes found in fruits and fruit products are hydroxycinnamic acids, flavonoids (including flavonol glycosides, anthocyanins, and

proanthocyanidins), and hydrolysable tannins (gallotannins and ellagitannins). All species of plants contain a unique “fingerprint” of these polyphenolic compounds and research is required to demonstrate that technology to characterize the unique polyphenolic composition of plants may be used to determine authenticity. This “fingerprint” may be determined by liquid chromatography/mass spectrometry (LC/MS) methods to produce a data set (i.e. the "polyphenol fingerprint") that is unique to each species. This information may then be used to determine the presence or absence of the plant species through analysis of the mass spectral data sets. In the case of PAC and oligomeric ellagitannins, we have previously demonstrated that MALDI-TOF MS has good potential for rapid development of fingerprints for authentication of whole fruit and fruit products (Reed, Krueger, & Vestling, 2005; Feliciano, Meudt, Shanmuganayagam, Krueger, & Reed, 2014).

Introduction to Matrix-Assisted Laser Desorption/Ionization Time-of-Flight Mass Spectrometry (MALDI-TOF MS)

In MALDI-TOF MS (Figure 1), an analyte is combined with a matrix and placed on a target plate within the instrument. A pulsed laser irradiates and ablates the compounds, ionizing them in the process. The ionized particles are drawn into a vacuum tube to a detector. The molecules arrive in waves based on their transit time, which is determined by their molecular weight (MW). Lower MW particles arrive first, followed by higher MW particles. The detector’s response (output) is then converted to a mass spectrum with high mass resolution (1000 to 60000), which detects compounds that differ by one mass unit or less. Since elements have both relative abundances and specific isotopic masses, mass spectrometers are able to differentiate masses of less than one mass

unit because compounds with the same nominal masses have different proportions of elements. For instance, 4-methyl-1-pentene (C_6H_{12}), 2-methyl-2-butenal (C_5H_8O), and 3-(methylamino)propanenitrile ($C_4H_8N_2$) all have the same nominal mass of 84. However, C_6H_{12} has an exact mass of 84.0939, C_5H_8O has an exact mass of 84.0575, and $C_4H_8N_2$ has an exact mass of 84.0688.

MALDI-TOF MS was approved by the FDA in 2013 as "the first mass spectrometry system for automated identification of bacteria and yeasts that are known to cause serious illness in humans"; the method was approved for clinical applications (Laine, 2013). The method depends on matching peptide mass fingerprints (PMF) from direct MALDI-TOF MS analysis of complex mixtures of microorganisms with PMF databases (Singhal, Kumar, Kanaujia, & Virdi, 2015). Thus, MALDI-TOF MS offers the potential for rapid, inexpensive analysis that avoids complex chromatography, giving it a competitive advantage over other approaches when analyzing the presence and type of polyphenolic compounds to determine authenticity of functional foods.

Mass Spectrometry of Proanthocyanidins

Research on the application of MALDI-TOF MS for analysis of PAC oligomers in foods has been developed over the last 20 years (Ohnishi-Kameyama, Yanagida, Kanda, & Nagata, 1997; Foo, Lu, Howell, & Vorsa, 2000a, 2000b; Krueger, Dopke, Treichel, Folts, & Reed, 2000; Reed, Krueger, & Vestling, 2005). The first publication demonstrated that MALDI-TOF MS could determine the degree of polymerization (DP) of PAC oligomers in apples (Ohnishi-Kameyama, Yanagida, Kanda, & Nagata, 1997). Oligomers were detected from the dimer to the pentadecamer,

whereas previous research with fast atom bombardment (FAB) MS had only given a range up to the pentamer.

Krueger et al., (2000) used MALDI-TOF MS to characterize the structural heterogeneity of galloylated procyanidins from grape seed extract (GSE) and were able to detect a series of PAC oligomers up to the nonamer in the positive reflectron mode and up to the undecamer in the positive linear mode. Additional masses corresponding to a series of galloyl procyanidins were also detected; the highest degree of galloylation observed was six (Krueger, Dopke, Treichel, Folts, & Reed, 2000). Yang & Chien, (2000) subsequently published similar results and indicated that the method has potential as a sensitive and quantitative technique. Both electrospray ionization (ESI) and MALDI-TOF MS were used to characterize the DP and structure of PAC oligomers in cranberries that are associated with the *in vitro* inhibition of adhesion of *Escherichia coli* to uroepithelial cells (Foo, Lu, Howell, & Vorsa, 2000a, 2000b). The methods detected oligomers up to a DP of 7 in the PAC fraction that had the greatest antiadhesion activity. The application of MALDI-TOF MS clearly demonstrated the presence of A-type linkages in the tetramer through hexamer.

Porter et al., (2001) used MALDI-TOF MS to characterize the PAC oligomers that are associated with decreased susceptibility of human low density lipoproteins (LDL) to *in vitro* Cu^{2+} induced oxidation (Porter, Krueger, Wiebe, Cunningham, & Reed, 2001). The identified masses closely resembled the epicatechin structures reported by Foo et al., (2000b) to be present in cranberries. However, the spectra also had masses that were 16 Dalton (Da) greater than the masses previously

reported, that may correspond to oligomers with one epigallocatechin unit. Although Foo et al., (2000b) reported the presence of epigallocatechin subunits in their cranberry juice fraction, they did not detect heteropolymers with both epicatechin and epigallocatechin units by mass spectrometry. Differences in the detection of these heteropolymers may be a result of the types of instrumentation that were used and methods of isolating the PAC (Foo, Lu, Howell, & Vorsa, 2000b). MALDI-TOF MS results also showed the presence of more complex heteropolymers for PAC with a DP greater than four. These results indicated that cranberry PAC oligomers with a DP greater than four have more than one A-type interflavan bond. These pioneering results on the application of MALDI-TOF MS clearly demonstrate its value to characterize the nature of PAC oligomers in functional foods.

Rush et al., (2018) used MALDI-TOF MS in negative reflectron mode to characterize procyanidins from cocoa, peanut skins, cinnamon, and crab apples. The negative reflectron mode was preferred over the positive reflectron mode to avoid splitting the PAC signals between $[M+Na]^+$ and potassium $[M+K]^+$ ion adducts. Results indicate that MALDI-TOF MS in negative reflectron mode demonstrated the structural heterogeneity of procyanidins (Rush, Rue, Wong, Kowalski, Glinski, & van Breemen, 2018). Although Rush et al., (2018) described a rapid method to determine structures of procyanidins, this work used isolated procyanidins and not complex mixtures of PAC from botanical sources.

Recently, Esquivel-Alvarado et al., (2020) used MALDI-TOF MS in positive reflectron mode to characterize PAC in three *Vaccinium* species from Costa Rica. Masses that correspond to sodium

adducts $[M+Na]^+$ based on repeating (epi)catechin monomers from trimers to tetradecamers were observed. MALDI-TOF MS spectra indicated that the *Vaccinium* species from Costa Rica have different isotopic patterns compared to cranberry and blueberry. Results also indicated that the majority of PAC in these *Vaccinium* species from Costa Rica have at least one A-type interflavan bond, which suggest that PAC from these *Vaccinium* species are closer to cranberry PAC than blueberry PAC (Esquivel-Alvarado, Muñoz-Arrieta, Alfaro-Viquez, Madrigal-Carballo, Krueger, & Reed, 2020). Although (Esquivel-Alvarado et al., (2020) mentioned the ability of MALDI-TOF to show different isotopic patterns of PAC, this work split the PAC signals as both $[M+Na]^+$ and potassium $[M+K]^+$ ion adducts.

Currently, our laboratory uses a protocol to obtain high-resolution MALDI-TOF MS spectra in positive reflectron mode. This protocol eliminates the signal splitting between sodium $[M+Na]^+$ and potassium $[M+K]^+$ ion adducts by using cesium trifluoroacetate. As a result the PAC signal is detected only as $[M+Cs]^+$ ion adducts. In our protocol, 2,5-dihydroxybenzoic acid (DHB) at a concentration of 1.3 mol/L in methanol and samples at a concentration of 1.3 mg/mL in methanol are subjected to deionization using PureSpeed IEX strong cation resin tips. After deionization, cesium trifluoroacetate at a concentration of 0.01 mol/L in methanol and the deionized DHB are mixed at a ratio of 1:1 (v/v). Each deionized sample (0.5 μL) is spotted on the stainless-steel target, followed by the addition of the matrix (0.6 μL), which is pipetted a minimum of five times up and down in the pipette tip and allowed to dry on the target. The samples are analyzed in positive reflectron mode using a Bruker UltraFlex® III MALDI-TOF MS equipped with a SmartBeam

laser. The settings are modified to a pulsed ion extraction of 130 ns, detector gain of 2.64x and 1548kV, preamplifier filter bandwidth small, and digitizer sampling frequency of 100 Hz.

Deconvolution of Isotope Patterns of A- to B-type Interflavan Bonds in Proanthocyanidins

Deconvolution is defined as a process of resolving something into its constituent elements or removing complication in order to understand composition. MALDI-TOF MS analysis of PAC that contains both A- and B-type interflavan bonds results in mass spectra with complex overlapping isotope patterns. Based on the known structures of PAC and the known relative abundance of naturally occurring isotopes, equations can be written and solved by methods of matrix algebra to deconvolute the overlapping isotope patterns, resulting in the ability to quantify relative ratios of A- to B-type interflavan bonds within each DP of PAC (Feliciano, Krueger, Shanmuganayagam, Vestling, & Reed, 2012). The deconvolution data sets can be analyzed by multivariate analysis (see Section 5.5) and used to determine authenticity of PAC.

Previous research has shown that B-type interflavan bonds can be converted to A-type interflavan bonds as a result of oxidative intramolecular reactions (Kondo, Kurihara, Fukuhara, Tanaka, Suzuki, Miyata, et al., 2000; Poupard, Sanoner, Baron, Renard, & Guyot, 2011). These oxidative reactions lead to loss of two hydrogens and may be mistakenly identified as A-type interflavan bonds in the MS spectra. Kondo et al., (2000) demonstrated that procyanidins B1 and B2 were converted into procyanidin A1 and A2 by radical oxidation using 1,1-diphenyl-2-picrylhydrazyl at neutral pH. Similarly, (Poupard et al., 2011) described oxidation of procyanidin B2 in an apple

juice model solution using caffeoylquinic acid o-quinone. Results indicate that no extensive polymerization occurred when procyanidin B2 was oxidized with caffeoylquinic acid o-quinone. Moreover, procyanidin A2 did not accumulate, but rather continued to react and form dimer end-products with three linkages ($[M-H]^-$ at m/z 573). Previous results from our laboratory showed that when MALDI-TOF MS was performed on samples of apple juice, unexplained masses corresponding to trimers with more than two A-type interflavan bonds and tetramers with more than 3 A-type interflavan bonds were observed. These masses do not correspond to the suggested structures of trimers and tetramers with all A-type interflavan bonds because there would be more interflavan bonds present in the oligomer than what is possible. However, when MALDI-TOF was performed on apple, masses indicative of intramolecular oxidations were not detected. We hypothesize that intramolecular oxidation in PAC that are extracted from the apple fruit does not occur but oxidation occurs during the production of apple juice (Poupard, Sanoner, Baron, Renard, & Guyot, 2011). Currently, no evidence of intramolecular oxidation has been reported on cranberry PAC.

Isotope Distributions

Mass calculating programs such as IsoPro 3.0 can be used to predict the masses and abundance of the isotopes for a given formula and allow for comparison between predicted and observed isotopic distributions (Senko, 2002). For example; the predicted monoisotope of procyanidin A2 dimer is $m/z = 599$ (Figure 2a), detected as a sodium ion adduct $[M+Na]^+$, which represents the contribution of ^{12}C, ^{16}O, and ^{1}H, to the compound. The mass at $m/z = 600$ represents one ^{13}C, or one ^{17}O, or one ^{2}H. The mass at $m/z = 601$ represents two ^{13}C, or one ^{13}C and one ^{2}H, or one ^{18}O, or two ^{2}H.

Similarly, the isotope distribution of procyanidin B2 can be predicted (Figure 2b). The monoisotopic mass of B2 is *m/z* = 601. The 2 atomic mass unit (amu) difference between the monoisotope of the B2 and A2 dimers is due to the loss of two H in the formation of the C-O-C bond that defines the A-type interflavan linkage in the procyanidin A2 dimer. A series of PAC, which vary only in the ratio of A- to B-type interflavan bonds, produces a mass spectrum with overlapping isotope patterns for each individual oligomer. As an example, a 1:1 (w/w) mixture of procyanidin A2 and B2 has predictable overlapping isotope patterns at *m/z* = 601 to *m/z* = 604 (Figure 2c). At *m/z* = 601, the monoisotopic mass of B2 overlaps with the mass of A2 that contains the third most abundant combination of heavier isotopes of C, O, and H that are 2 amu heavier than monoisotopic mass of A2. Thus, in a 1:1 (w/w) mixture of these dimers, the relative intensity (r_i = 0.3739) at *m/z* = 601 is higher than the r_i at m/z = 599 (r_i = 0.3474) because the third isotopic peak of A2 as well as the monoisotope of B2 contribute to the intensity of m/z = 601 (Figure 2c).

Precision and Accuracy Validation for Binary Mixtures of Procyanidin A2 and B2

Feliciano et al., (2012) used the MALDI-TOF MS spectra of procyanidin A2 and B2 dimers to deconvolute overlapping isotope patterns and determine relative ratios of A- to B-type interflavan bonds. In a binary system, 11 known ratios of procyanidin A2 and B2 were combined and subjected to positive reflectron mode MALDI-TOF MS. The data sets were then subjected to deconvolution. All observed ratios were within 3.6% of the predicted ratios for both compounds (Table 1), showing that the method is accurate (Feliciano, Krueger, Shanmuganayagam, Vestling, & Reed, 2012).

The standard deviation among each series of replicates was ≤3.5% and the standard error of the mean (SE) was <0.8%, which indicates that the method is also precise. The results using the A2 and B2 dimers indicated that the deconvolution method could be used to accurately and precisely predict ratios of A- to B-type bonds in PAC oligomers.

Deconvolution of Cranberry PAC Ratios of A- to B-type Bonds within Each Degree of Polymerization

Obviously, cranberry PAC have a greater diversity in polymer distribution than A- and B-type dimers and as the DP of PAC increases, complexity of overlapping isotope patterns increases. For example, cranberry PAC trimers contain three molecules that differ in the number of A-type interflavan bonds: two A-type and zero B-type (*m/z* = 885), one A-type and one B-type (*m/z* = 887), and zero A-type and two B-type (*m/z* = 889) (Figure 3) (Foo, Lu, Howell, & Vorsa, 2000b). The spectra in this mass range will have overlapping isotope patterns if trimers with one or two A-type interflavan bonds are present in the sample, as previously demonstrated for the A2 and B2 dimers. For example, the intensity of the signal at *m/z* = 889 is the combination of three PAC trimers: (i) the monoisotopic signal of the trimer with 2 B-type bonds, (ii) lower signals due to heavier isotopes present in the trimer with one A-type and one B-type interflavan bond, and (iii) the trimer with two A-type interflavan bonds. Again, matrix algebra (solving simultaneous unknown equations) enables deconvolution to be performed on increasingly complex overlapping isotope patterns at each DP within a PAC polymer distribution.

Procyanidin dimers showed high correlation between predicted natural isotope abundance and observed isotope distributions, suggesting good precision. By extension, positive reflectron mode MALDI-TOF MS spectra were collected on isolated purified cranberry PAC and subjected to deconvolution for PAC oligomers from DP3 to DP11 (Feliciano, Krueger, Shanmuganayagam, Vestling, & Reed, 2012). The relative ratios of A-type to B-type interflavan bonds was determined for each DP. Results showed that PAC oligomers with one or more A-type interflavan bonds occurred at higher proportion than PAC oligomers with all B-type interflavan bonds. Furthermore, >90% of the cranberry PAC were shown to contain at least one A-type interflavan bond and the number of A-type interflavan bonds within each oligomer increased as DP increased (Figure 4).

Deconvolution Application for PAC Structure in Studies of Bioactivity

The unique structural attributes of PAC (i.e. nature of interflavan bonds) are associated with bioactivity. Putative health benefits of PAC include a decreased risk of heart disease and dyslipidemia for PAC in grape seed extract or pine bark (Schoonees, Visser, Musekiwa, & Volmink, 2012; Sahebkar, 2014; Haili Zhang, Liu, Li, Liu, Liu, Mi, et al., 2016), and a decreased risk of urinary tract infections (UTIs) for PAC in cranberry. However, meta-analysis results of clinical trials on UTI prevention are often conflicted, with associations between PAC intake and health benefits in the trials being confounded due to use of unstandardized product forms that lack compositional analysis, doses that may be subefficacious, and little to no mechanistic guidance for selection of subjects and study design (Jepson & Craig, 2007; Jepson, Williams, & Craig, 2012). The MALDI-TOF MS may be used to correlate PAC structure to bioactivity.

Feliciano et al., (2014) demonstrated the utility of MALDI-TOF MS to determine the relative ratios of A- to B-type PAC in cranberry and apples and correlated PAC structure to the ability of PAC to agglutinate *E. coli,* and inhibit *E. coli* invasion of gut epithelial cells. Results from this work indicated that >94.5% of the isolated cranberry PAC oligomers had at least one A-type bond, while >88.3% of the isolated apple PAC oligomers had no A-type bonds (Figure 5). A-type bonds found in apple PAC are likely due to oxidative intramolecular linkages produced during the extraction, isolation, and characterization of PAC. Furthermore, the cranberry A-type PAC had greater bioactivity in *E. coli* agglutination and inhibition of *E. coli* invasion of epithelial cells in comparison to the apple B-type PAC (Feliciano, Meudt, Shanmuganayagam, Krueger, & Reed, 2014).

MALDI-TOF MS for Mixtures of Isolated Cranberry and Apple Proanthocyanidins

We used isolated cranberry and apple PAC to further validate the precision and accuracy for deconvolution of overlapping isotope patterns in complex mixtures across a wide range of PAC polymers (DP 3–7). In a binary system, 21 known ratios of isolated cranberry and apple PAC were combined and subjected to positive reflectron mode MALDI-TOF MS. The data sets were then subjected to deconvolution. Observed ratios were within 3.9% of the predicted ratios, showing that the method is accurate (Figure 6).

This research demonstrated that MALDI-TOF MS and deconvolution of overlapping isotope patterns may be used to determine the authenticity of PAC from a single source and to accurately determine the ratios at which two known PAC sources are combined. By extension, these methods

could be used to determine the source of PAC in blends of whole fruits, juices, and dietary ingredients and to confirm authenticity of the products.

Multivariate Analysis of MALDI-TOF MS Spectra Data

The rapid development of high-throughput analytical techniques such as MALDI-TOF MS allow generation of a large amount of data. Multivariate analysis is a useful tool to discover trends and reveal information that is not obvious through visual inspection of large data sets. MALDI-TOF spectral data combined with multivariate analysis can therefore be used to determine the authenticity of functional foods and dietary supplements that contain PAC.

Multivariate analysis may be divided into two categories: unsupervised and supervised. Unsupervised methods use unlabeled data and are categorized as exploratory techniques. Unsupervised methods include PCA, self-organizing maps (SOM), and hierarchical clustering analysis (HCA). Supervised methods use labeled data and are categorized as predictive techniques (Abney, 2007). Supervised methods include LDA, partial least squares discriminant analysis (PLSDA), k-nearest neighbor (KNN), and soft independent modeling of class analogy (SIMCA).

PCA uses an orthogonal transformation to convert a large number of correlated variables into a small number of uncorrelated variables called principal components (PCs), which are useful for data reduction and cluster visualization (Johnson, 1998). PCA is composed of matrices of direction (eigenvectors) and scale (eigenvalues). PCA may be represented by two plots: loading and score. The loading plot shows how strongly each variable influences a PC, whereas the score plot shows the clustering of samples based on their similarity (Lucci, Saurina, & Núñez, 2017).

Deconvoluted or autoscaled MALDI-TOF spectra data may be used to classify botanical sources of PAC. The deconvolution method only uses the monoisotopic peaks for each predicted A- or B-type interflavan bonds. Deconvoluted MALDI-TOF spectra data differ from the autoscaled MALDI-TOF spectra data because the latter divides the absolute intensity of each A- or B-type interflavan bond by the sum of all absolute intensities of each A- or B-type interflavan bond for each individual PAC oligomer.

Three approaches that use deconvoluted or autoscaled MALDI-TOF MS spectra data combined with PCA have been evaluated. In our first approach, MALDI-TOF MS spectra of 19 samples (5 blueberries and 14 cranberries) were subjected to PCA. PCA differentiated samples by the presence of A- or B-type interflavan bonds in PAC oligomers. Score plot based on the deconvoluted MALDI-TOF spectra data indicated that PC1 and PC2 explained 87.6% of the total variance (Figure 7). In addition, samples with all B-type interflavan bonds (blueberries) were located on the negative part of PC1, whereas samples with one A-type interflavan bond (cranberries) were located on the positive part of PC1. This preliminary result showed that PCA can differentiate botanical sources with different PAC profiles.

In our second approach, a more robust design was evaluated. MALDI-TOF spectra of 75 samples (30 cranberries, 5 cranberry supplements, 25 apples, 6 grape skins, 4 cocoa powders, and 5 blueberries) were subjected to deconvolution of PAC isotope patterns prior to performing PCA. Score plot based on the deconvoluted MALDI-TOF spectra data indicates that PC1 and PC2 explained 86.7% of the total variance (Figure 8). Furthermore, samples were grouped according their PAC profile. Samples in which the most abundant peak corresponds to a PAC structure with

all B-type interflavan bonds (apples, grape skins, cocoa powders, and blueberries) were located on the negative part of PC1, whereas samples in which the most abundant peak corresponds to a PAC structure with one A-type interflavan bond (cranberries and cranberry supplements) were located on the positive part of PC1. Results of this study indicate that the deconvolution method is robust, precise, and accurate and also contributes to a better understanding of differences in PAC structure when PCA is used.

Lastly, in our third approach, MALDI-TOF MS data of 86 samples (28 apples, 34 cranberries, and 24 peanut skins) were subjected to both data selection and autoscaling. As previously described by Feliciano et al., (2014), PAC were isolated from the botanical samples prior to MALDI-TOF MS analysis. Data selection was used instead of deconvolution to obtain more information from the MALDI-TOF spectra data. The deconvolution method only uses the relative intensity of the overlapping peaks for each predicted A- or B-type interflavan bond and ignores the signal of the intermediate isotope signals. Data selection uses these intermediate isotope signals. Therefore, the selection of all predicted isotope patterns of PAC from DP3 to DP8 were used. The isotope patterns of PAC were subjected to autoscaling. Autoscaling was chosen instead of other pretreatment methods to maintain equality amongst all the isotopic peaks (van den Berg, Hoefsloot, Westerhuis, Smilde, & van der Werf, 2006). Loading plot indicated that PC1 separated all the samples (apples) with no A-type interflavan bonds, which were located on the negative part of PC1, from all the samples (cranberries and peanut skins) with one, two, and three A-type interflavan bonds, which were located on the positive part of PC1. In addition, the loading plot indicated that PC2 separated all the samples (cranberries) with one A-type interflavan bond, which were located on the negative part of PC2, from all the samples (peanut skins) with two and three A-type interflavan bonds,

which were located on the positive part of PC2 (Figure 9a). Score plot based on the autoscaled MALDI-TOF spectra data indicated that PC1 and PC2 explained 92.0% of the total variance (Figure 9b). PCA was able to differentiate PAC from apples, cranberries, and peanut. This approach is an improvement over our previous studies because it introduces PAC from peanut skins, which also contains A-type interflavan bonds (Huiwen Zhang, Yang, & Ma, 2013). Cranberry and peanut skin PAC were differentiated from one another because the latter contained a higher percentage of PAC with two or three A-type interflavan bonds. The separation between cranberries and peanut skins was reflected in the higher percentage variation explained by PC2 (23.3%) compared to the two previous approaches. Results support our previous studies that showed that PCA can accurately predict the PAC profile of products that are used in dietary supplements. In addition, this latter approach allows the inclusion of other features that are present in samples such as the galloyl units in grape skins, the 3-deoxyproanthocyanidins in sorghum, and ellagitannins in pomegranate.

LDA is a reduction technique used to create prediction models to assign unknown samples to each class (Callao & Ruisánchez, 2018). LDA maximizes the ratio of between-class variance and minimizes the ratio of within-class variance (Berrueta, Alonso-Salces, & Heberger, 2007). LDA was used to evaluate the potential of the autoscaled MALDI-TOF MS data to correctly classify samples. LDA was evaluated using our previous data set (n = 86) of individual PAC samples, a data set (n = 70) in which 10 cranberry PAC samples were combined with 10 apple PAC samples at each of the following ratios [5, 10, 15, 20, 25, 50, and 75% (w/w)], and a data set (n = 70) in which 10 cranberry PAC samples were combined with 10 peanut skin PAC samples at each of the following ratios [5, 10, 15, 20, 25, 50, and 75% (w/w)]. The complete data set (n = 226) was split

into two subsets: training set and testing set. The training set composed of 159 samples (70% of the total samples) was used to build the predictive algorithm. The testing set composed of 67 samples (30% of the total samples) was used to provide an unbiased evaluation of the model on the training set. Score plot based on the autoscaled MALDI-TOF MS data indicated that LD1 and LD2 explained 93.9% of the total variance. The classification performance was determined using the training set, the testing set, and the leave-one-out cross validation (LOOCV) method. The LOOCV method uses one sample from the total samples as the testing data, and the remaining samples as the training data. This process is repeated such that each sample is used once as the validation data. Results indicated that the recognition ability (training set) was 99.4%, predictive ability (testing set) was 100%, and the LOOCV method was 94.2%. The high performance obtained by the LDA model indicated that autoscaled MALDI-TOF spectral data were able to correctly classify unknown samples based on PAC structure.

In conclusion, the use of MALDI-TOF MS analysis of PAC has potential as a method to determine authenticity of functional food and dietary supplements such as cranberries, grape seed extracts, and many other ingredients. In this study, we demonstrate that MALDI-TOF MS accurately distinguishes PAC from different foods and ingredients that are used in dietary supplements. We also demonstrated that MALDI-TOF MS accurately determines the relative proportion of PAC in mixtures of PAC from different plant species. However, more research is needed to develop MALDI-TOF MS as a practical tool for authenticity. For instance, the impact of oxidation on the robustness of the method and its validation when applied to food samples prone to oxidation needs to be studied. The most challenging task will be the development of spectral libraries from samples of authentic dietary supplements and functional foods for use in building predictive capabilities of

multivariate analysis.

REFERENCES

Abney, S. (2007). *Semisupervised learning for computational linguistics*: Chapman and Hall/CRC.

Berrueta, L., Alonso-Salces, R., & Heberger, K. (2007). Supervised pattern recognition in food analysis. *Journal of Chromatography A, 1158*(1-2), 196-214. doi:10.1016/j.chroma.2007.05.024

Bovay, J. (2016). FDA refusals of imported food products by country and category, 2005-2013.

Callao, P., & Ruisánchez, I. (2018). An overview of multivariate qualitative methods for food fraud detection. *Food Control, 86*, 283-293. doi:10.1016/jfoodcont.2017.11.034

Cheynier, V., Comte, G., Davies, K., Lattanzio, V., & Martens, S. (2013). Plant phenolics: recent advances on their biosynthesis, genetics, and ecophysiology. *Plant Physiology and Biochemistry, 72*, 1-20. doi:10.1016/j.plaphy.2013.05.009

Clydesdale, F. (2004). Functional foods: opportunities & challenges. *Food Technology*.

Congress. (1938). Drug, and Cosmetic Act (FD&C Act). Chapter V § 351Adulterated drugs and devices [S/OL].

Congress. (2011). Food Safety Modernization Act (FSMA).

Craciun, M., Cretu, G., Mirea, C., Tanczos, S., Popa, A., & Miron, A. (2015). Anthocyanins identification, separation and measurement from cranberry, blueberry, bilberry, chokeberry and acai berry extracts by HPTLC. *Revista de Chimie, 66*(7), 929-936.

Esquivel-Alvarado, D., Muñoz-Arrieta, R., Alfaro-Viquez, E., Madrigal-Carballo, S., Krueger, C., & Reed, J. (2020). Composition of anthocyanins and proanthocyanidins in three tropical *Vaccinium* species from Costa Rica. *Journal of Agricultural and Food Chemistry*. *68*(10), 2872-2879. doi:10.1021/acs.jafc.9b01451

Feliciano, R., Krueger, C., Shanmuganayagam, D., Vestling, M., & Reed, J. (2012). Deconvolution of matrix-assisted laser desorption/ionization time-of-flight mass spectrometry isotope patterns to determine ratios of A-type to B-type interflavan bonds in cranberry proanthocyanidins. *Food Chemistry, 135*(3), 1485-1493. doi:10.1016/j.foodchem.2012.05.102

Feliciano, R., Meudt, J., Shanmuganayagam, D., Krueger, C., & Reed, J. (2014). Ratio of "A-type" to "B-type" proanthocyanidin interflavan bonds affects extra-intestinal pathogenic *Escherichia coli* invasion of gut epithelial cells. *Journal of Agricultural and Food Chemistry, 62*(18), 3919-3925. doi:10.1021/jf403839a

Foo, L., Lu, Y., Howell, A., & Vorsa, N. (2000a). The structure of cranberry proanthocyanidins which inhibit adherence of uropathogenic P-fimbriated *Escherichia coli in vitro*. *Phytochemistry, 54*(2), 173-181. doi:10.1016/s0031-9422(99)00573-7

Foo, L., Lu, Y., Howell, A., & Vorsa, N. (2000b). A-Type proanthocyanidin trimers from cranberry that inhibit adherence of uropathogenic P-fimbriated *Escherichia coli*. *Journal of Natural Products, 63*(9), 1225-1228. doi:10.1021/np000128u

Jepson, R., & Craig, J. (2007). A systematic review of the evidence for cranberries and blueberries in UTI prevention. *Molecular Nutrition & Food Research, 51*(6), 738-745. doi:10.1002/mnfr.200600275

Jepson, R., Williams, G., & Craig, J. (2012). Cranberries for preventing urinary tract infections. *Cochrane Database of Systematic Reviews*. doi:10.1002/14651858.CD001321.pub5

Johnson, D. (1998). *Applied multivariate methods for data analysts* (Vol. 48): Duxbury Press Pacific Grove, CA.

Kondo, K., Kurihara, M., Fukuhara, K., Tanaka, T., Suzuki, T., Miyata, N., & Toyoda, M. (2000). Conversion of procyanidin B-type (catechin dimer) to A-type: evidence for abstraction of C-2 hydrogen in catechin during radical oxidation. *Tetrahedron Letters, 41*(4), 485-488. doi:10.1016/S0040-4039(99)02097-3

Krueger, C., Dopke, N., Treichel, P., Folts, J., & Reed, J. (2000). Matrix-assisted laser desorption/ionization time-of-flight mass spectrometry of polygalloyl polyflavan-3-ols in grape seed extract. *Journal of Agricultural and Food Chemistry, 48*(5), 1663-1667. doi:10.1021/jf990534n

Kupina, S., & Gafner, S. (2016). Adulteration of grape seed extract. *Botanical Adulterants Bulletin*.

Laine. (2013). New test system identifies 193 different yeasts and bacteria known to cause illnes. *Infection Control Today*.

LeClair, M. (2016). Fruit & Vegetable Markets in the US. *IBSWorld Industry Report*. IBISWorld.

Lucci, P., Saurina, J., & Núñez, O. (2017). Trends in LC-MS and LC-HRMS analysis and characterization of polyphenols in food. *Trends in Analytical Chemistry, 88*, 1-24. doi:10.1016/j.trac.2016.12.006

Ohnishi-Kameyama, M., Yanagida, A., Kanda, T., & Nagata, T. (1997). Identification of catechin oligomers from apple (Malus pumila cv. Fuji) in matrix-assisted laser desorption/ionization time-of-flight mass spectrometry and fast-atom bombardment mass spectrometry. *Rapid Communications in Mass Spectrometry, 11*(1), 31-36. doi:10.1002/(SICI)1097-0231(19970115)11:1<31::AID-RCM784>3.0.CO;2-T

Polito, R. (2015). The regulatory shakeup. *Nutritional Business Journal*.

Porter, M., Krueger, C., Wiebe, D., Cunningham, D., & Reed, J. (2001). Cranberry proanthocyanidins associate with low-density lipoprotein and inhibit in vitro Cu^{2+}-induced oxidation. *Journal of the Science of Food and Agriculture, 81*(14), 1306-1313. doi:10.1002/jsfa.940

Poupard, P., Sanoner, P., Baron, A., Renard, C. M., & Guyot, S. (2011). Characterization of procyanidin B2 oxidation products in an apple juice model solution and confirmation of their presence in apple juice by high-performance liquid chromatography coupled to electrospray

ion trap mass spectrometry. *Journal of Mass Spectrometry, 46*(11), 1186-1197. doi:10.1002/jms.2007

Reed, J., Krueger, C., & Vestling, M. (2005). MALDI-TOF mass spectrometry of oligomeric food polyphenols. *Phytochemistry, 66*(18), 2248-2263. doi:10.1016/j.phytochem.2005.05.015

Rumalla, C., Avula, B., Wang, Y., Smillie, T., & Khan, I. (2012). Densitometric-HPTLC method development and analysis of anthocyanins from acai (*Euterpe oleracea* Mart.) berries and commercial products. *Journal of Planar Chromatography, 25*(5), 409-414. doi:10.1556/JPC.25.2012.5.4

Rush, M., Rue, E., Wong, A., Kowalski, P., Glinski, J., & van Breemen, R. (2018). Rapid determination of procyanidins using MALDI-ToF/ToF mass spectrometry. *Journal of Agricultural and Food Chemistry, 66*(43), 11355-11361. doi:10.1021/acs.jafc.8b04258

Sahebkar, A. (2014). A systematic review and meta-analysis of the effects of pycnogenol on plasma lipids. *Journal of Cardiovascular Pharmacology and Therapeutics, 19*(3), 244-255. doi:10.1177/1074248413511691

Schoonees, A., Visser, J., Musekiwa, A., & Volmink, J. (2012). Pycnogenol® for the treatment of chronic disorders. *Cochrane Database of Systematic Reviews*. doi:10.1002/14651858.CD008294.pub3

Senko, M. (2002). IsoPro 3.0 MS/MS software. *Isotopic abundance simulator version, 3*.

Singhal, N., Kumar, M., Kanaujia, P., & Virdi, J. (2015). MALDI-TOF mass spectrometry: an emerging technology for microbial identification and diagnosis. *Frontiers in Microbiology, 6*, 791. doi:10.3389/fmicb.2015.00791

Smith, T., Lynch, M., Johnson, J., Kawa, K., Bauman, H., & Blumenthal, M. (2015). Herbal dietary supplement sales in US increases 6.8 in 2014. *The Journal of the American Botanical Council,* 107, 52-59.

Twilley, N. (2015). How not to test a dietary supplement. *New Yorker*.

van den Berg, R., Hoefsloot, H., Westerhuis, J., Smilde, A., & van der Werf, M. (2006). Centering, scaling, and transformations: improving the biological information content of metabolomics data. *BMC Genomics, 7*, 142. doi:10.1186/1471-2164-7-142

Villani, T., Reichert, W., Ferruzzi, M., Pasinetti, G., Simon, J., & Wu, Q. (2015). Chemical investigation of commercial grape seed derived products to assess quality and detect adulteration. *Food Chemistry, 170*, 271-280. doi:10.1016/j.foodchem.2014.08.084

Wallace, L., Boilard, S., Eagle, S., Spall, J., Shokralla, S., & Hajibabaei, M. (2012). DNA barcodes for everyday life: routine authentication of natural health products. *Food Research International, 49*(1), 446-452. doi:10.1016/j.foodres.2012.07.048

Yang, Y., & Chien, M. (2000). Characterization of grape procyanidins using high-performance liquid chromatography/mass spectrometry and matrix-assisted laser desorption/ionization time-of-flight mass spectrometry. *Journal of Agricultural and Food Chemistry, 48*(9), 3990-3996. doi:10.1021/jf000316q

Zhang, H., Liu, S., Li, L., Liu, S., Liu, S., Mi, J., & Tian, G. (2016). The impact of grape seed extract treatment on blood pressure changes: A meta-analysis of 16 randomized controlled trials. *Medicine, 95*(33), e4247. doi:10.1097/MD.0000000000004247

Zhang, H., Yang, Y., & Ma, C. (2013). Structures and antioxidant and intestinal disaccharidase inhibitory activities of A-type proanthocyanidins from peanut skin. *Journal of Agricultural and Food Chemistry, 61*(37), 8814-8820. doi:10.1021/jf402518k

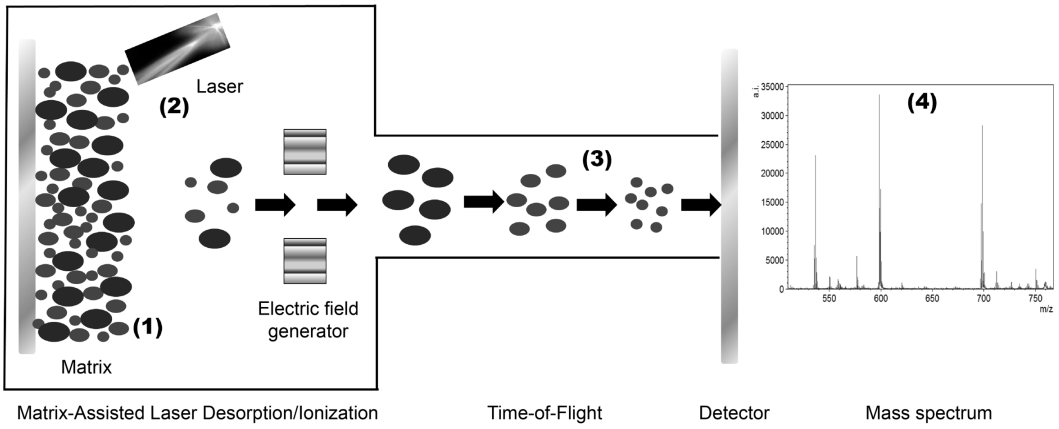

Figure 1. Representative schematic of the MALDI-TOF MS process. From left to right: (a) matrix and analyte are deposited on a target; (b) a laser beam irradiates the target, desorbing and ionizing the compounds; (c) compounds are separated by molecular weight (MW) in response to their transit time (time of flight) down a vacuum tube, with lower MWs arriving at the detector before heavier MWs; and (d) the detector response is converted to a mass spectrum with unit mass resolution.

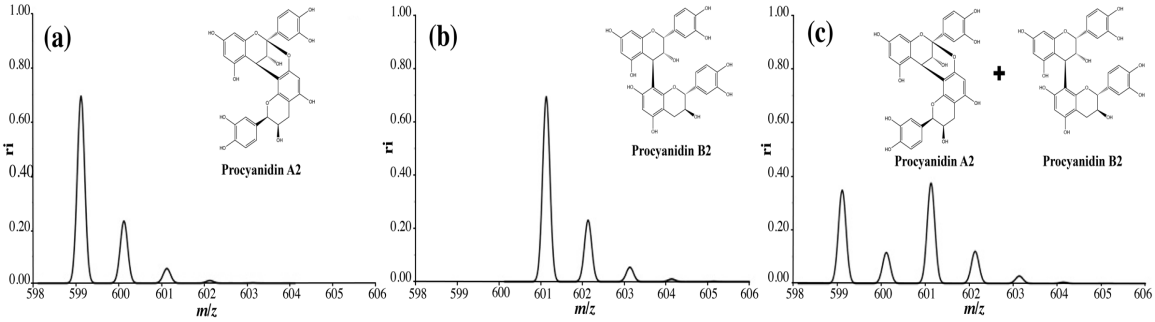

Figure 2. Natural isotope distribution of procyanidin A2 (a) and procyanidin B2 (b). Complex overlapping isotope patterns of procyanidin A2 and B2 mixed at a 1:1 (w/w) ratio (c).

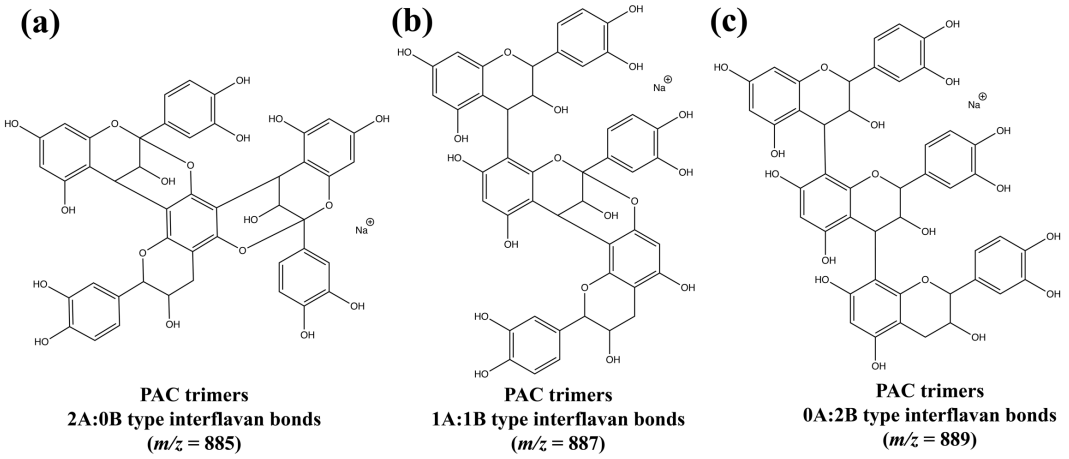

Figure 3. Chemical structures of PAC trimers, which show 2A:0B-type interflavan bonds (a), 1A:1B-type interflavan bonds (b), and 0A:2B-type interflavan bonds (c).

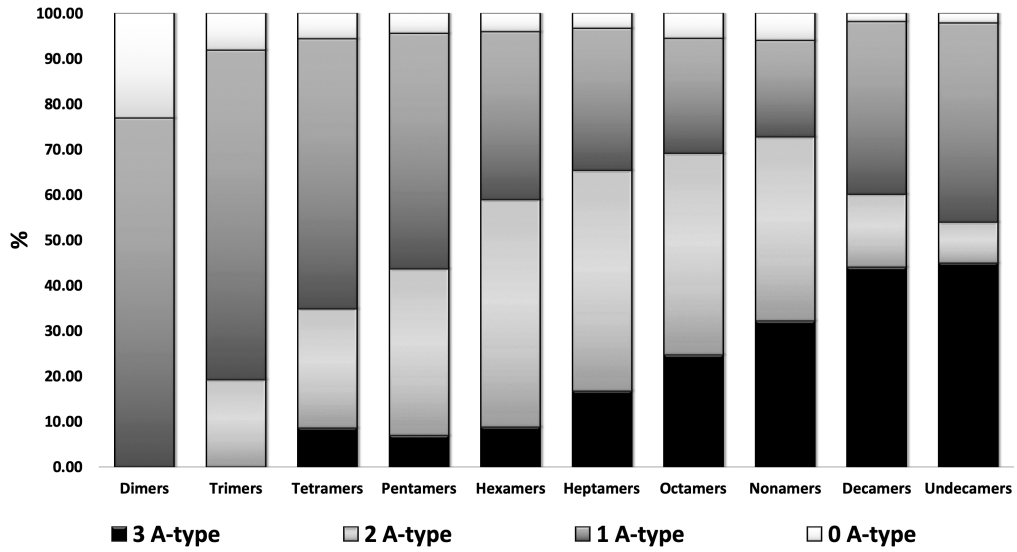

Figure 4. Percentage of A-type interflavan bonds in cranberry PAC oligomers from dimers to undecamers analyzed by deconvolution for isotope patterns in MALDI-TOF MS.

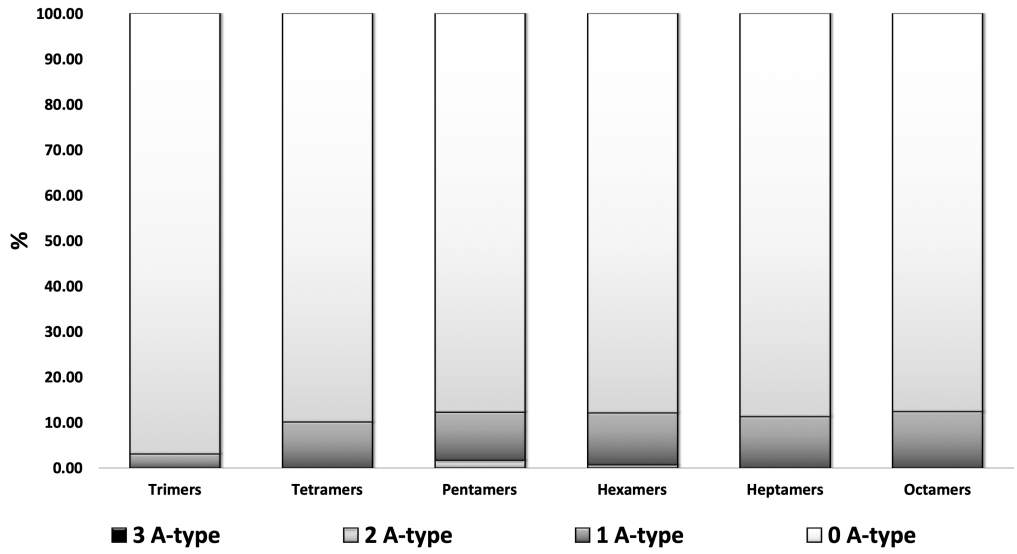

Figure 5. Percentage of A-type interflavan bonds in apple PAC oligomers from trimers to octamers analyzed by deconvolution of isotope patterns in MALDI-TOF MS.

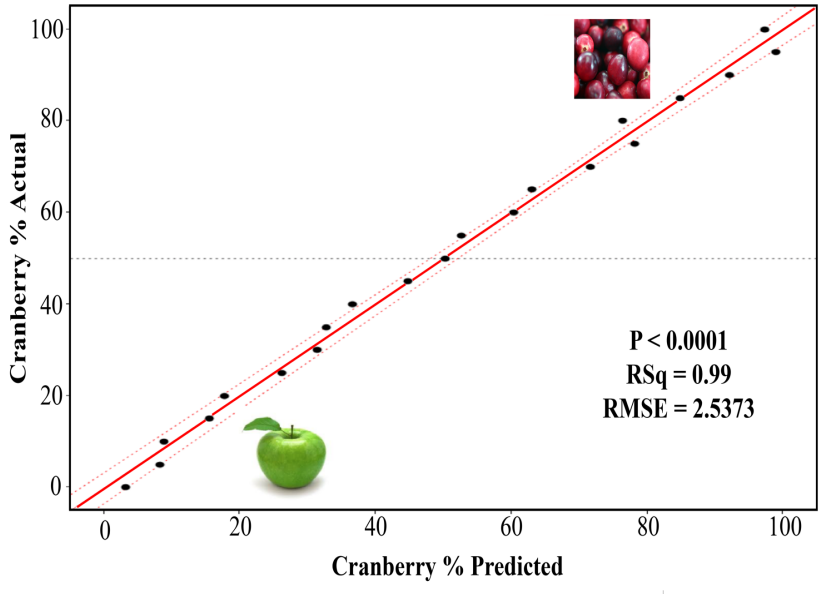

Figure 6. Deconvolution of MALDI-TOF MS of 21 different ratios of isolated cranberry and apple PAC shows predicted percentage cranberry PAC is within 3.9% of actual mixed ratios.

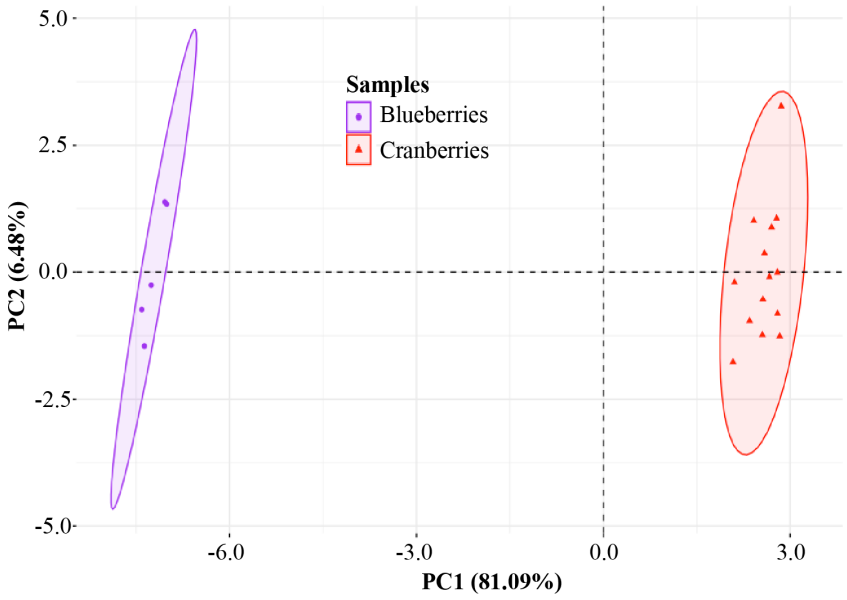

Figure 7. Principal component analysis score plot of proanthocyanidins from blueberries and cranberries based on the deconvoluted MALDI-TOF MS spectra. PC1 (x-axis) and PC2 (y-axis) accounts for 87.6% of the total variance. The colored shadows correspond to the 95% confidence ellipse, based on the distribution of A-type interflavan bonds in the PAC oligomers.

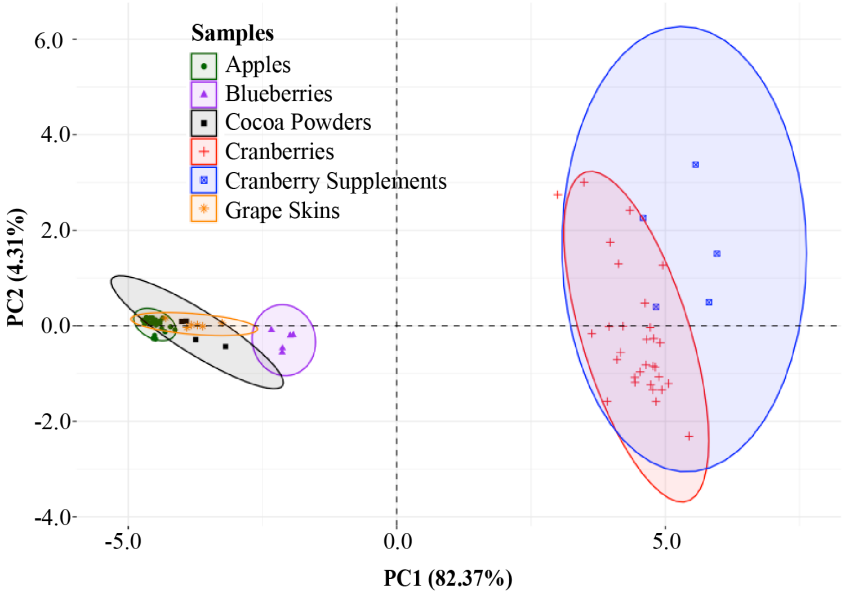

Figure 8. Principal component analysis score plot of proanthocyanidins from apples, blueberries, cocoa, powders, cranberries, cranberry supplements, and grape skins based on the deconvoluted MALDI-TOF MS spectra. PC1 (x-axis) and PC2 (y-axis) accounts for 86.7% of the total variance. The colored shadows correspond to the 95% confidence ellipse, based on the distribution of A-type interflavan bonds in the PAC oligomers.

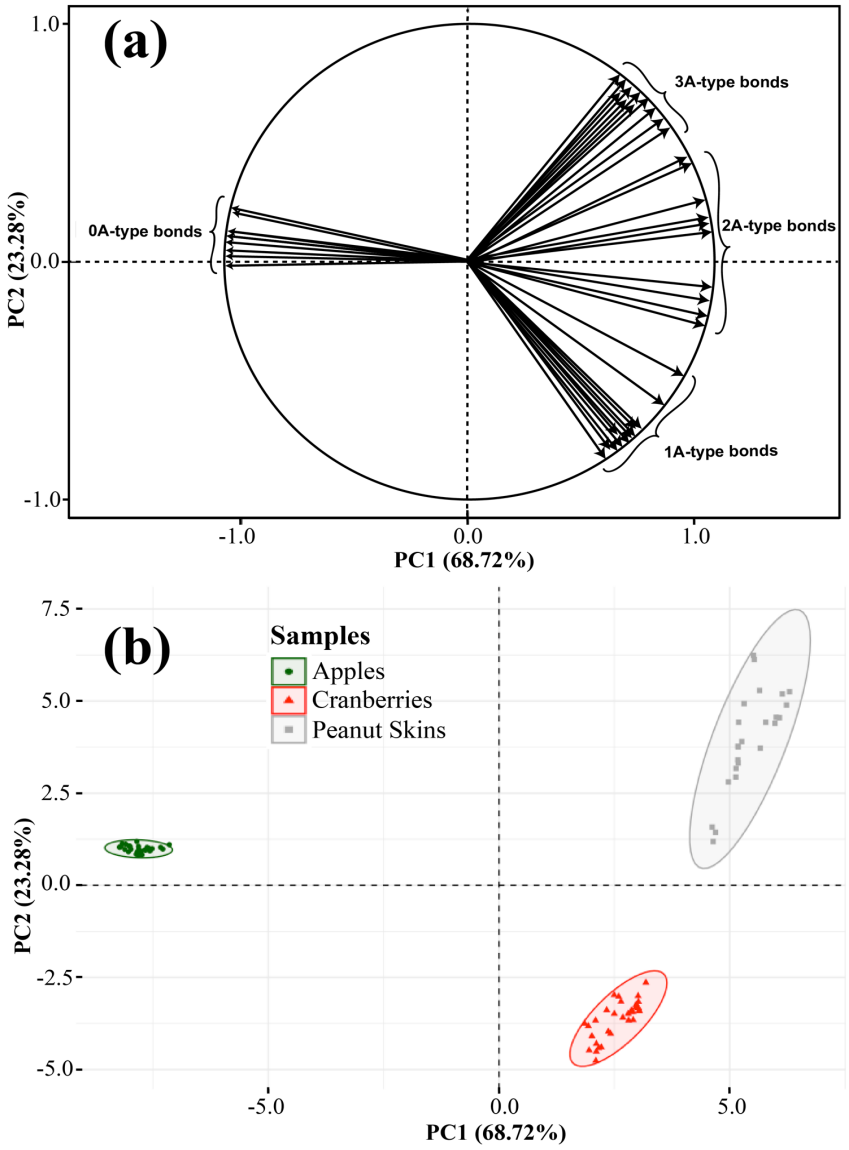

Figure 9. Principal component analysis of proanthocyanidins from apples, cranberries, and peanut skins based on the autoscaled MALDI-TOF MS spectral data. PC1 (x-axis) and PC2 (y-axis) accounts for 92.0% of the total variance. (a) PCA loading plot. The arrows indicate the location of all the PAC oligomers with the number of A-type interflavan bonds, as represented by the brackets, for oligomers from DP3 to DP8. (b) PCA score plot. The colored shadows correspond to the 95% confidence ellipse, based on the distribution of A-type interflavan bonds in the PAC oligomers.

Table 1. Predicted and observed percentages of binary mixtures of procyanidins A2 and B2 after deconvolution.

Procyanidin B2		**Procyanidin A2**	
Predicted	**Observed**	**Predicted**	**Observed**
95.0	93.3	5.0	6.7
90.0	88.2	10.0	11.8
80.0	79.0	20.0	21.0
70.0	67.5	30.0	32.5
60.0	56.9	40.0	43.1
50.0	49.0	50.0	51.0
40.0	39.9	60.0	60.1
30.0	28.8	70.0	71.2
20.0	16.5	80.0	83.6
10.0	8.6	90.0	91.4
5.0	5.1	95.2	94.9

APPENDIX 2: Additional Publications

1. Ureña-Saborio, H., Alfaro-Viquez, E., **Esquivel-Alvarado, D**., Esquivel, M., Madrigal-Carballo, S. (**2018**). Collagen/chitosan hybrid 3D-scaffolds as potential biomaterials for tissue engineering. *International Journal of Nano and Biomaterials*. 7(3). 163-175. doi:10.1504/ijnbm.2018.094240

2. Alfaro-Viquez, E., **Esquivel-Alvarado, D**., Madrigal-Carballo, S., Krueger, C., Reed, J. (**2018**). Cranberry proanthocyanidin-chitosan hybrid nanoparticles as a potential inhibitor of extra-intestinal pathogenic *Escherichia coli* invasion of gut epithelial cells. *International Journal of Biological Macromolecules*. 111. 415-420. doi:10.1016/j.ijbiomac.2018.01.033

3. Ureña-Saborio, H., Alfaro-Viquez, E., **Esquivel-Alvarado, D**., Madrigal-Carballo, S., Gunasekaram, S., (**2018**). Electrospun plant mucilage nanofibers as biocompatible scaffolds for cell proliferation. *International Journal of Biological Macromolecules.* 115. 1218-1224. doi: 10.1016/j.ijbiomac.2018.04.129

4. Alfaro-Viquez, E., **Esquivel-Alvarado, D**., Madrigal-Carballo, S., Krueger, C., Reed, J. (**2019**). Proanthocyanidin-chitosan composite nanoparticles prevent bacterial invasion and colonization of gut epithelial cells by extra-intestinal pathogenic *Escherichia coli*. *International Journal of Biological Macromolecules.* 135. 630-636. doi: 10.1016/j.ijbiomac.2019.04.170

5. Polewski, M., **Esquivel-Alvarado, D**., Wedde, N., Krueger, C., Reed, J. (**2020**). Isolation and characterization of blueberry polyphenolic components and their effects on gut barrier

dysfunction. *Journal of Agricultural and Food Chemistry*. 68(10). 2940-2947. doi:10.1021/acs.jafc.9b01689

6. Alfaro-Viquez, E., **Esquivel-Alvarado, D**., Madrigal-Carballo, S., Krueger, C., Reed, J. (**2020**). Characterization of proanthocyanidin-chitosan interactions in the formulation of composite nanoparticles using surface plasmon resonance. *International Journal of Biological Macromolecules.* 152. 1068-1076. doi:10.1016/j.ijbiomac.2019.10.194

7. Alfaro-Viquez, E., **Esquivel-Alvarado, D**., Madrigal-Carballo, S., Krueger, C., Reed, J. (**2020**). Antimicrobial proanthocyanidin-chitosan composite nanoparticles loaded with gentamicin. *International Journal of Biological Macromolecules.* 162. 1500-1508. doi:10.1016/j.ijbiomac.2020.07.213